A MECHANO-PERFUSION BIOREACTOR FOR TISSUE ENGINEERING

Dino Miguel Fernandes Freitas

Universitat de Girona

DOCTORAL THESIS

A MECHANO-PERFUSION BIOREACTOR FOR TISSUE ENGINEERING

Dino Miguel Fernandes Freitas

2019

Universitat de Girona

DOCTORAL THESIS

A MECHANO-PERFUSION BIOREACTOR FOR TISSUE ENGINEERING

Dino Miguel Fernandes Freitas

2019

Doctoral Program in Technology

Supervised by:

Professor Paulo Jorge da Silva Bártolo, PhD

Professor Joaquim De Ciurana Gay, PhD

Presented to obtain the degree of PhD at the University of Girona

Professor Dr Paulo Jorge da Silva Bártolo, Department of Mechanical, Aerospace & Civil Engineering, School of Mechanical, Aerospace and Civil Engineering, University of Manchester – Supervisor

Professor Dr Joaquim de Ciurana Gay, Department of Mechanical Engineering and Industrial Construction, Polytechnic School, University of Girona – Co-Supervisor

WE DECLARE:

That the thesis titles "A Mechano-Perfusion Bioreactor for Tissue Engineering", presented by Dino Miguel Fernandes Freitas to obtain a doctoral degree, has been completed under my supervision/co-supervision and meets the requirements to opt for an International Doctorate.

For all intents and purposes, I hereby sign this document.

Professor Dr. Paulo Jorge da Silva Bártolo (Supervisor)

Professor Dr. Joaquim de Ciurana Gay (Co-Supervisor)

To my dear Wife,
Mom, Dad and Brother

"On the shoulders of giants."

Isaac Newton

ACKNOWLEDGEMENTS

Ao Professor Doutor Paulo Bártolo, meu Orientador, a quem profundamente agradeço, mais que a sua generosa paciência, exigência, ambição e orientação académica e científica, a sua inestimável amizade. O tempo pode passar, e passa, mas a sua persistência e, quase cega, confiança em mim tornam-no numa das pessoas mais queridas que, felizmente, tive o prazer de conhecer em todo o meu percurso académico. Poucas pessoas tomo como exemplo de vida, e, no Professor Paulo Bártolo, vejo um dos melhores.

Ao Professor Doutor Joaquim Ciurana, meu Co-Orientador e amigo, só posso agradecer profundamente todos os momentos de incentivo, de puxões de orelhas (bem merecidos) e pela incansável, ajuda ao longo de todo este trajecto.

Agradeço, também, a todos os meus amigos e familiares por todo o apoio, contributo e incentivo prestado. Por estarem sempre presentes quando mais preciso e principalmente por compreenderem os meus momentos de constante ausência. Agradeço especialmente ao André Vieira, Amorim, Catherine Grilo, Daniel Janeiro, David Bregieiro, Jair Cruz, Joana Maia, Rúben Santos, Nídia Benito, Vitor Hugo.

Um especial agradecimento à empresa S3D, na pessoa do Sr. João Ferreira, que me deu o suporte necessário para terminar esta dissertação.

Ao meu irmão Alexandre, por compreender a minha ausência, mesmo quando precisou de mim. Por nunca me pedir nada em troca e ser, só e simplesmente, o meu melhor amigo de sempre e para sempre. Meu mano, obrigado!

Aos meus Pais, Maria e Lino. À minha Mãe por, desde que nasci, dar-me tudo quanto têm. Por ter mostrado que na vida tudo é alcançável mesmo quando o mundo parece desabar. A minha amiga para a vida e, que, nunca desiste de mim! Que dá mais do que recebe. Ao meu Pai, por ser o meu suporte, a minha estrutura. Por ser o lutador que é, e consequentemente, me obrigar a lutar também. Por nem sempre me entender, mas por me compreender e apoiar incansavelmente. A ambos agradeço por nunca me terem deixado desistir, obrigado!

À Cinderela, minha amiga, namorada e esposa. A sua paciência que, apesar de não parecer, ser enorme. Agradeço todas as noites que, até neste momento em que escrevo, aguardou por mim no sofá enquanto trabalhava nesta dissertação. O apoio e encorajamento que sempre me deu e, as diversas formas, de motivação que me foi dando. Obrigado por seres a Mulher que és, por me teres poupado a tantos e tantos trabalhos e teres organizado tantas e tantas coisas da nossa vida. Por tornares o meu mundo, nosso. Obrigado!

DECLARATION

This dissertation is the result of my work and includes nothing, which is the outcome of work done in collaboration except where specifically indicated in the text. It has not been previously submitted, in part or whole, to any university or institution for any degree, diploma, or other qualification.

Signed:____

Date:____

Dino Miguel Fernandes Freitas

Girona

LIST OF TABLES

LIST OF FIGURES

LIST OF ABBREVIATIONS AND ACRONYMS

0-9

2D	Two-dimensional
3D	Three-dimensional

B

BME	Basal Medium Eagle
BMP	Bone morphogenetic protein

C

CAD	Computer-aided Design
CFD	Computational Fluid Dynamics
cm	centimetres

D

DMEM	Dulbecco's Modified Eagle's Medium
DNA	Deoxyribonucleic acid
dyn	Dyne (unit)

E

ECM	Extracellular Matrix
EMEM	Eagle's Minimal Essential Medium
EGF	Epidermal growth factor

F

FGF	Fibroblast growth factor
FTE	Functional Tissue Engineering

G

GAG	Glycosaminoglycans
GMEM	Glasgow Minimum Essential Medium

H

HARV	High Aspect Ratio Vessel
HEPES	4-(2-hydroxyethyl)-1-piperazineethanesulfonic acid
HFB	Hollow Fibre Bioreactor
Hz	Hertz

I

IGF	Insulin-like growth factor

K

kPa	kilopascal

L	
L-15	Leibovitz Medium

M	
min	minute
ml	millilitre
mm	millimetre

N	
NASA	National Aeronautics and Space Administration

P	
Pa	Pascal (unit)
PCL	Poly(ε-caprolactone)
PDGF	Platelet-derived growth factor

R	
rpm	Revolutions per minute
RPMI	Roswell Park Memorial Institute Medium
RSB	Rotating Shaft Bioreactor
RWPV	Rotating-wall Perfusion Vessel
RWV	Rotating-wall Vessel

S	
SMC	Smooth Muscle Cells
STLV	Slow Turning Lateral Vessel

T	
TCP	Tricalcium Phosphate
TE	Tissue Engineering
TKE	Turbulence Kinetic Turbulence
TGF-β	Transforming growth factor-β

U	
USA	United States of America

W	
WWB	Wavywalled Bioreactor

CONTENTS

ABSTRACT

Tissue Engineering plays a vital role in tissue construct to repair, maintain or replace tissues. Those tissues can be cultivated *in vivo* or *in vitro* using devices such as bioreactors. There are several approaches to create the necessary tissues, but one of the most popular and successful is by using scaffold constructs to provide the required stability and support. After the cells being implanted on the scaffolds, they are then inserted in the bioreactors.

Those bioreactors seek to mimic the conditions provided to cells by the human body. This issue by itself presents several challenges where it is required, to bioreactors, besides the optimum environment in terms of temperature, nutrients, the creation of the necessary *stimulus* to cells to differentiate and proliferate.

In this work, is presented a novel concept of bioreactor for Tissue Engineering that can provide multiples *stimulus* when cultivating the tissue. To achieve an optimised design was performed several numerical simulations to access the best design parameters. For this, it was taken into account several variables such as fluid velocity, the proximity of the inlet/outlet to the scaffold, directions of the fluid and the impact of the liquid on the scaffold and subsequently the cells by analysing the wall shear stress provoked by the fluid flow.

Keywords: Scaffold, Tissue Engineering, Bioreactors, Numerical Simulation, Cell Culture, Mechanical Stimulation, Perfusion Stimulation.

RESUM

L'enginyeria de teixits té un paper fonamental en la construcció de teixits per reparar, mantenir o substituir teixits. Aquests teixits es poden cultivar *in vivo* o *in vitro* mitjançant dispositius biomèdics com ara bioreactors. Hi ha diversos enfocaments per crear els teixits necessaris, però un dels més populars i amb èxit, és utilitzar construccions d'estructures semblants a les bastides, anomenats *scaffolds*, per proporcionar l'estabilitat i el suport necessaris a les cèl·lules. Després de la implantació de les cèl·lules a les bastides, es col·loquen a l'interior dels bioreactors.

Aquests bioreactors pretenen imitar les condicions que proporciona el cos humà a les cèl·lules. Aquesta qüestió per si mateixa presenta diversos reptes en què es requereix, als bioreactors, a més de l'ambient òptim en termes de temperatura i nutrients, la creació de l'estímul necessari perquè les cèl·lules es diferenciïn i proliferin.

En aquest treball, es presenta un concepte nou de bioreactor per a l'enginyeria de teixits que pot proporcionar estímuls múltiples al cultiu del teixit. Per aconseguir un disseny optimitzat s'han realitzat diverses simulacions numèriques per accedir als millors paràmetres de disseny. Per a això, es va tenir en compte diverses variables com la velocitat del fluid, la proximitat de l'entrada / sortida a la *scaffold*, les direccions del fluid i l'impacte del fluid sobre la *scaffold* i, posteriorment, sobre les cèl·lules mitjançant l'anàlisi de la tensió de cisalla provocada pel flux de fluids.

Paraules clau: *Scaffold*, Enginyeria de teixits, Bioreactors, Simulació numèrica, Cultiu cel·lular, Estimulació mecànica, Estimulació de perfusió.

RESUMEN

La ingeniería de tejidos juega un papel vital en la construcción de tejidos para reparar, mantener o reemplazar tejidos. Los tejidos pueden cultivarse *in vivo* o *in vitro* utilizando dispositivos biomédicos tales como biorreactores. Existen varios enfoques para crear los tejidos, pero uno de los más populares y exitosos es el uso de construcciones de estructuras como andamios, que reciben el nombre de *scaffolds*, para proporcionar la estabilidad y el soporte necesarios a las células. Después de que las células se implantan en los *scaffolds*, se insertan en los biorreactores.

Los biorreactores buscan imitar las condiciones proporcionadas a las células por el cuerpo humano. Este problema por sí mismo presenta varios desafíos donde se requiere, para los biorreactores, además del ambiente óptimo en términos de temperatura y nutrientes, la creación del estímulo necesario para que las células se diferencien y proliferen.

En este trabajo, se presenta un concepto novedoso de biorreactor para ingeniería de tejidos que puede proporcionar estímulos múltiples al cultivar el tejido. Para lograr un diseño optimizado se realizaron varias simulaciones numéricas para acceder a los mejores parámetros de diseño. Para esto, se tuvieron en cuenta varias variables, como la velocidad del fluido, la proximidad de la entrada / salida al *scaffold*, las direcciones del fluido y el impacto del fluido sobre el *scaffold* y, posteriormente, sobre las células mediante el análisis de la tensión de corte provocada por el flujo del fluido.

Palabras clave: *Scaffold*, ingeniería de tejidos, biorreactores, simulación numérica, cultivo celular, estimulación mecánica, estimulación por perfusión.

Resumo

A engenharia de tecidos desempenha um papel vital na construção de tecidos para reparar, manter ou substituir tecidos. Esses tecidos podem ser cultivados *in vivo* ou *in vitro* utilizando dispositivos como os bioreactores. Existem várias abordagens para criar os tecidos necessários, mas um dos mais populares e bem-sucedidos é usando *scaffolds* que fornecem a estabilidade e o suporte necessários às células. Após as células serem implantadas nos *scaffolds*, este conjunto é então inserido num bioreactor.

Os bioreactores permitem simular, aproximadamente, as mesmas condições fornecidas pelo corpo humano às células. Esta questão por si só apresenta vários desafios onde é necessário, além do óptimo ambiente em termos de temperatura e nutrientes, a criação do estímulo necessário para as células se diferenciarem e proliferarem.

Neste trabalho, é apresentado um novo conceito de bioreactor para Engenharia de Tecidos que pode fornecer múltiplos estímulos simultaneamente ao cultivar o tecido. Por forma a obter um design optimizado, foram realizadas várias simulações numéricas para definir os melhores parâmetros. Para isso, foram levadas em consideração diversas variáveis como velocidade do fluido, proximidade da entrada/saída do *scaffold*, direção do fluído e impacto do fluído no *scaffold* e consequentemente das células através da análise das tensões de corte da parede pelo fluxo de fluído.

Palavras-chave: *Scaffold*, Engenharia de Tecidos, Bioreactores, Simulação Numérica, Cultura Celular, Estimulação Mecânica, Perfusão.

1 Introduction

This chapter will give a general overview of Tissue Engineering, presenting the current trends and difficulties of this field. Of the two main areas of tissue engineering, the discussion will focus more on the *in vitro* techniques. More specifically tissue engineering using Bioreactors. A brief explanation of this type of equipment will be given. This work goal will be described at the end of this chapter, along with the published research papers.

1.1 Tissue Engineering

Tissue Engineering (TE) is an emerging field that complies different areas of science focusing primarily on the use of cells, biomaterials, computational methods and fabrication processes (Figure 1.1), merging principles of different areas such as biology, engineering and medicine in order to create biological tissues to replace natural functionally damaged tissues (Bártolo *et al*., 2009a, 2009b, 2008; Eshraghi and Das, 2010; Gibson, 2005; Pati *et al*., 2016; Risbud, 2001; Shafiee and Atala, 2016; Tan *et al*., 2005; Vozzi *et al*., 2003). Skalak and Fox (1988), defined TE as the "application of the principles and methods of engineering and life sciences toward the fundamental understanding of structure-function relationships in normal and pathological mammalian tissues and the development of biological substitutes to restore, maintain, or improve tissue and organ functions" (Bártolo *et al*., 2008). Figure 1.2 represents key milestones in the field of TE.

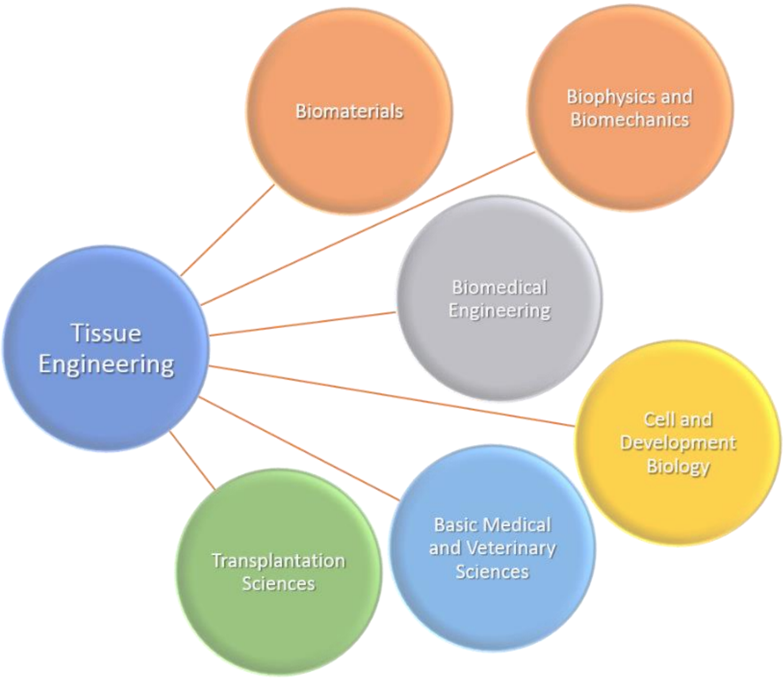

Figure 1.1 Multidisciplinary nature of tissue engineering.

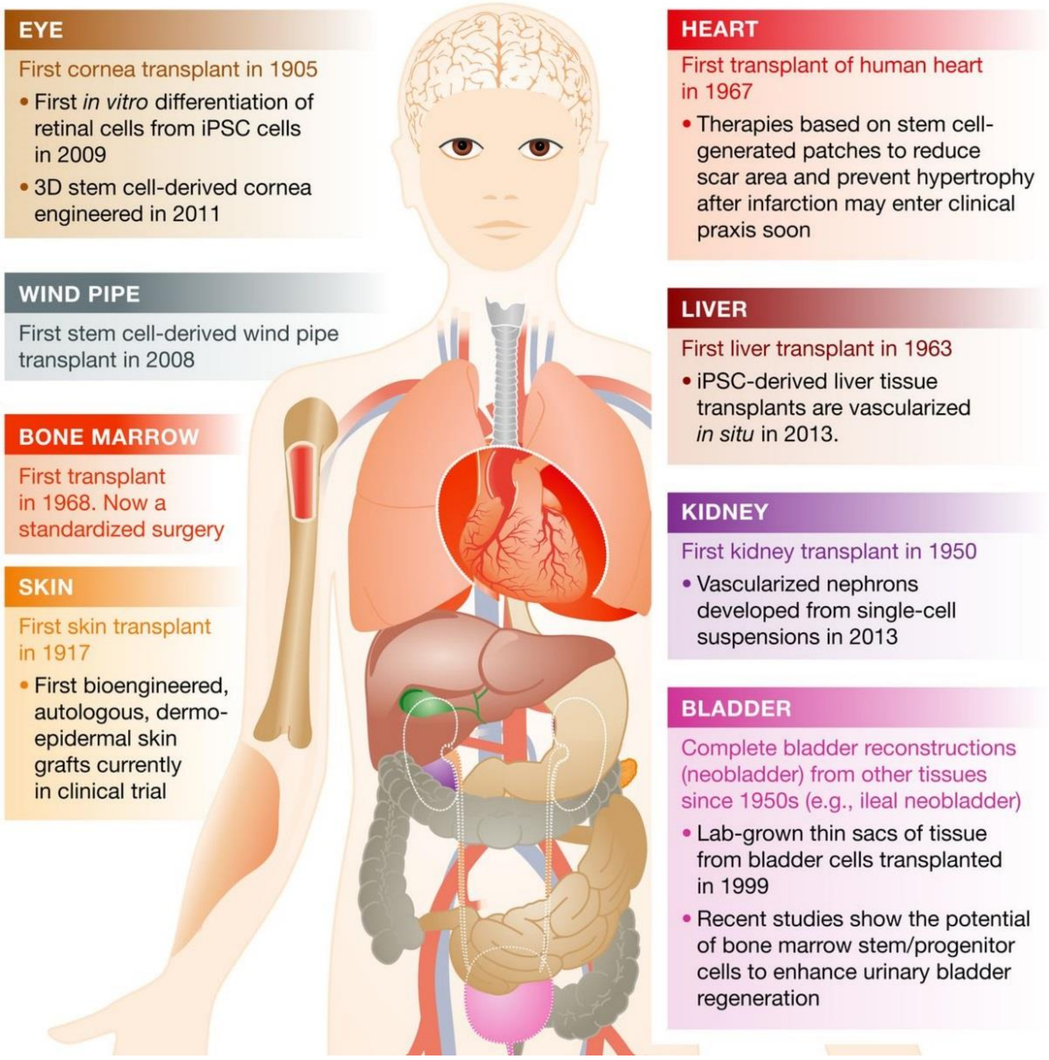

Figure 1.2 Organ transplantations and tissue and organ engineering (Hunter, 2014).

TE emerged to address the organ shortage problem and comprises organ substitution, tissue regeneration and gene therapy (Table 1.1). It also intends to develop cost-efficient, fast recover and personalised therapeutics targeting the main problems of the Health Services. Its relevance is notably higher in countries facing age-related issues such as new diseases (*e.g.* Parkinson and Alzheimer). Successful examples of tissue engineering include bone, skin, muscle, cartilage, craniofacial and cardiac regeneration (Fung and Skalak, 2009; García Cruz *et al*., 2012; Gaspar *et al*., 2012; Ladd *et al*., 2009; Nakamura *et al*., 2013; Niklason *et al*., 1999; Paez-Mayorga *et al*., 2018; Radisic *et al*., 2008; Visscher *et al*., 2016; Zhang *et al*., 2017).

According to Lysaght *et al*., 2008, 50 companies were working in the field of TE, employing 3,000 equivalent full-time positions. This number significantly increased to 391 in 2010 (Lewis, 2013). The global bone graft market, for example, was valued at $3 billion in 2010 and $4 billion in 2017. In the United States, the demand for orthopaedic biomaterials represented around $3.5 billion in 2012 (iData Research, 2013), while in Europe the market for spinal fusion constructs represented $177 million in 2010 and $461 million in 2016. In another area, skin burns and chronic wounds represent one of the most debilitating, painful, and costly health conditions. Typically, these wounds require extensive hospitalisation, labour intensive clinical procedures and expensive wound care products, representing a significant burden over total world healthcare expenditure. It is estimated that the cost of chronic wound care represents about 2% of the total EU financial resources. A total of 120 companies are operating in the field of skin treatment, including major corporations such as Advanced Dermatology Corporation, Bayer and Beiersdorf. TE is an area with significant growth in Portugal and Spain. Several spin-off companies emerged from Universities and Research Institutes and are now operating at a global level. Examples include REGEMAT3D (Granada, Spain) a company developing a wide range of relatively low-cost 3D bioprinting systems, actively competing with established companies like Envisiontec (Germany) and RegenHU (Switzerland). Another example is CERAMED (Lisbon, Portugal) developing synthetic ceramic grafts for dental and bone regeneration applications.

Table 1.1 Core areas within Tissue Engineering, adapted from Jeong *et al*., 2007; Kuppan *et al*., 2012; Tabata, 2001.

	Purpose	**Techniques/Methodology**
Tissue Regeneration	*In vitro* production of tissue constructs	Cell scaffolding, bioreactor, microgravity
	In vivo natural healing process	Cell scaffolding, controlled release, physical barrier
	Ischemia therapy	Angiogenesis
Organ Substitution	Immunoisolation	Biological Barrier
	Nutrition and oxygen supply	Angiogenesis
	Temporary assistance for organ function	Extracorporeal system
Gene therapy	Inhibiting induction of a specific gene, or by editing undesirable genomic mutations	Intracellular transfer of nucleic acid drugs to modulate cellular functions and responses by expressing exogenous proteins

Clinical approaches to repair and restore the function of damaged tissues usually require the use of allografts, autografts and xenografts. Autografts, defined as tissue that is transplanted from one part of the body to another part in the same individual, is the “gold standard”. as it does not induce rejection and the best clinical results can be obtained. They are osteoconductive, osteoinductive, promote osteogenesis, and do not present risk of immune system rejection or disease transmission. Main complications are related to pain and morbidity in the donor site, limited quantity and availability, prolonged hospitalisation time, the need for general sedation or anaesthesia and risk of deep infection and haematoma. Allografts are harvested from one individual and implanted into another individual of the same species. They can be obtained from cadavers or living donors. Significant limitations are associated with the risk of rejection, transmission of diseases and infections from donor to recipient, limited supply, loss of biological and mechanical properties due to its processing and cost. Xenografts are harvested from one individual and transplanted into another individual of a different species. They are low cost and highly available grafts. Major limitations are related to the risk of transmission of infections and diseases and poor clinical outcome. Ethical concerns have also arisen from the use of animals (Abousleiman and Sikavitsas, 2007; Ariadna *et al*., 2016; Bártolo *et al*., 2008; Fuchs *et al*., 2001; Grayson *et al*., 2008; Kuppan *et al*., 2012; Matsumoto and Mooney, 2006; Mistry and Mikos, 2005; Rabionet *et al*., 2018).

All of these biological grafts present significant limitations. TE addressed these issues through three different approaches (Figure 1.3). The first approach corresponds to the use of cell therapies. Cells are harvested usually from the patient and are cultured and expanded *in vitro* and then injected into the damaged site. This is a straightforward approach, but it is challenging to keep cells in the desired position during clinical relevant times. The second approach uses advanced fabrication techniques (*e.g.* additive manufacturing) to produced optimised designed scaffolds, which can be directly implanted into the damaged site or seeded with cells, pre-cultured in a bioreactor before their *in vivo* implantation. The third approach is based on the use of specific bioinks (hydrogels containing cells and growth factors) for the fabrication of cell-laden constructs, which can be directly implanted or pre-cultured in a bioreactor before implantation. Among all these strategies the scaffold-based ones are the most commonly used (Bártolo *et al.*, 2008; Bhumiratana and Vunjak-Novakovic, 2012; Fuchs *et al.*, 2001; Langer, 1997; Langer and Vacanti, 1993; Matsumoto and Mooney, 2006; Mistry and Mikos, 2005; Norotte *et al.*, 2009; Pereira and Bartolo, 2015).

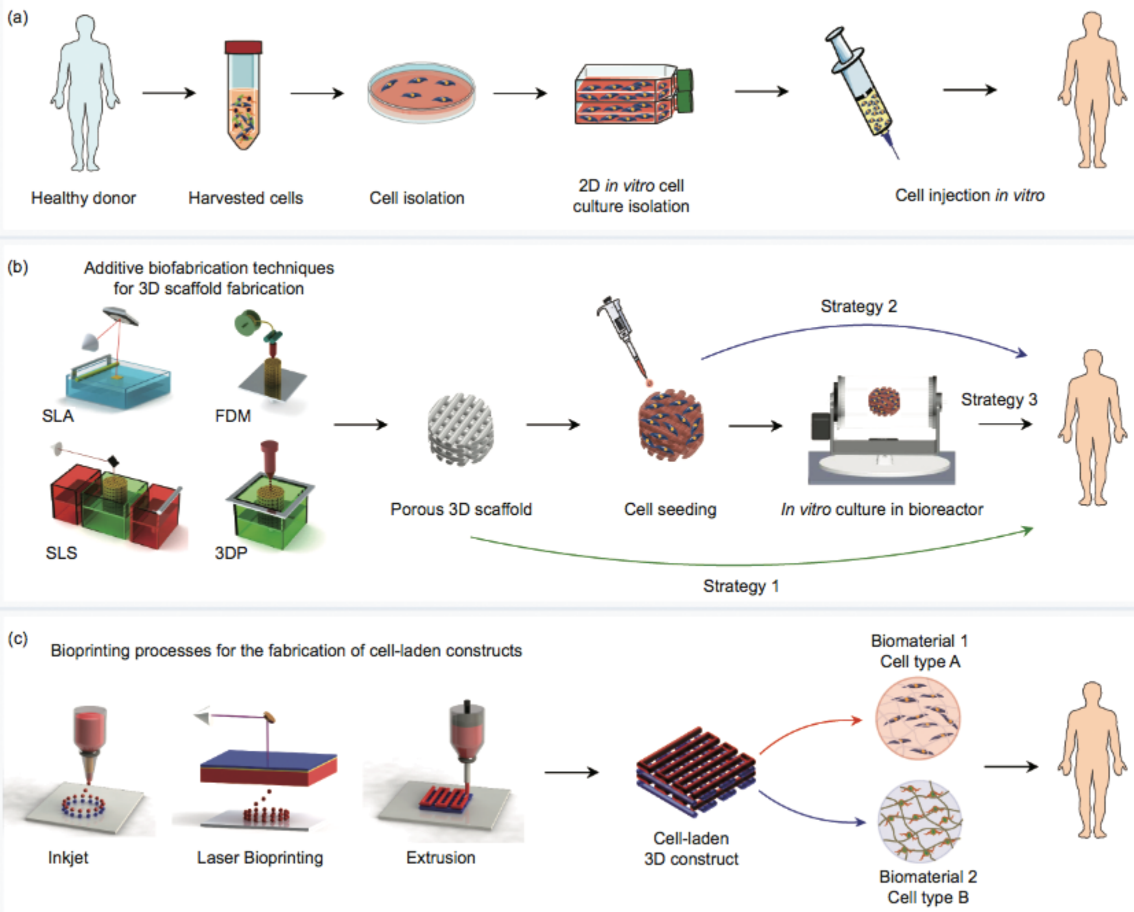

Figure 1.3 Main therapies for tissue engineering. (a) Cell-based therapy; (b) scaffold-based therapy; (c) therapy based on the implantation of cell-laden 3D constructs. In scaffold-based therapy, scaffolds can be implanted without cells (Strategy 1), after cell seeding (Strategy 2), or upon *in vitro* culture (Strategy 3) (Pereira and Bartolo, 2015).

Scaffold-based approaches require the use of biocompatible and biodegradable materials, growth-factors, cells, advanced fabrication techniques and bioreactors. A wide range of biomaterial have been explored including natural polymers (*e.g.* gelatine, collagen, dextrane, pectine, alginate and chitosan), synthetic polymers (*e.g.* poly(α-hydroxy acids), poly(urethane), poly(anhydride) and poly(orthoester)), inorganic materials (*e.g.* calcium phosphates, bioglasses, carbon nanotubes and graphene) and composites Table 1.2. (Bedian *et al*., 2017; Chen and Rosi, 2010; Fu *et al*., 2018, 2013; Hao *et al*., 2017; Huang *et al*., 2018; Janoušková, 2018; Kang *et al*., 2017; Place *et al*., 2009; Rijal *et al*., 2017; Terzaki *et al*., 2013; Thanaphat and Thunyakitpisal, 2008).

Table 1.2 Biomaterials used in the production of scaffolds used for TE (Bedian *et al*., 2017; Chen and Rosi, 2010; Fu *et al*., 2018, 2013; Hao *et al*., 2017; Huang *et al*., 2018; Janoušková, 2018; Kang *et al*., 2017; Place *et al*., 2009; Rijal *et al*., 2017; Terzaki *et al*., 2013; Thanaphat and Thunyakitpisal, 2008).

Manufacturing Material	Benefits	Potential Limitations
Hydrogels	High water content/growth media inclusion allows for cell encapsulation and growth	Mechanical properties limit use in load-bearing constructs
	Mechanical properties can be modified through crosslinking	Optimising printing conditions for individual hydrogels can be time-consuming
	Controlled drug/growth factor release possible	Physical manipulation of constructs can be difficult
	Ease of patterning via 3D printing to mimic tissue microarchitectures	Loading evenly with cells can be challenging
Polymers	Natural polymers can be derived from the extracellular matrix, ensuring high biocompatibility and low toxicity	Natural and synthetic polymers generally lack mechanical properties for load-bearing
	Biodegradable	Pathological impurities such as endotoxin may be present in natural polymers
	Often contain biofunctional molecules on their surface	Synthetic polymers are usually hydrophobic and lack cell recognition sites
	Synthetic polymers offer improved control over physical properties	
Ceramics	Osteoconductive and osteoinductive properties allow strong integration with host tissue	Hard and brittle when used alone
	A similar composition to host bone mineral content	May display inappropriate degradation/resorption rates, with a decline in mechanical properties as a result
	Can be delivered as granules, paste or in an injectable format	
Inorganic	Osteoconductive, osteoinductive properties	Inherent brittleness
		Difficult to tune resorption rate
	Adapted into clinical prosthesis already	Manipulation of constructs into 3D shapes to treat specific defects challenging
		Potential for release of toxic metal ions

Depending on the applications, scaffolds should incorporate different growth-factors, as shown in Table 1.3. Growth factors are proteins that are produced by cells functioning as signalling molecules. With these proteins, it is possible to promote cell adhesion, proliferation, migration and differentiation of the cultured cells (Boontheekul and Mooney, 2003; Rose and Oreffo, 2002; Tessmar and Göpferich, 2007). Cells include specific differentiated cell lines (*e.g.* osteoblasts, chondrocytes, fibroblasts, keratinocytes) or mesenchymal stem cells mainly derived from bone marrow, adipose tissue and umbilical cord.

Table 1.3 Most relevant growth factors for tissue engineering applications (Boontheekul and Mooney, 2003; Rose and Oreffo, 2002; Tessmar and Göpferich, 2007).

Bone Regeneration	
Growth factor	*Relevant activities*
Transforming growth factor-β (TGF-β)	Proliferation and differentiation of bone
Bone morphogenetic protein (BMP)	Differentiation of bone-forming cells
Insulin-like growth factor (IGF)	Stimulates proliferation of osteoblasts and the synthesis of bone matrix
Fibroblast growth factor (FGF)	Proliferation of osteoblasts
Platelet-derived growth factor (PDGF)	Proliferation of osteoblasts
Wound Healing	
Growth factor	*Relevant activities*
Platelet-derived growth factor (PDGF)	Active in all stages of the healing process
Epidermal growth factor (EGF)	Mitogenic for keratinocytes
Transforming growth factor-β (TGF-β)	Promotes keratinocyte migration, ECM synthesis and remodelling, and differentiation of epithelial cells
Fibroblast growth factor (FGF)	General stimulant for wound healing

Scaffolds are 3D biocompatible and biodegradable structures that provide a substrate for the implanted cells to attach, proliferate and grow, producing their Extra-Cellular Matrix (ECM) and stimulate new tissue formation (Bartolo *et al*., 2012). Besides providing the initial biochemical and biophysical substrate to improve the cell growth, scaffolds also serve as a temporary template to accommodate and aid in the definition, formation and orientation of the new tissue throughout the 3D space (Bartolo *et al*., 2012). Scaffolds must be designed to deliver and retain cells and growth factors and to enable the diffusion of cell nutrients and oxygen. They must provide an adequate temporary mechanical and biological environment enabling tissue regeneration in an organized way (Bártolo and Bidanda, 2008; Bártolo *et al*., 2009a, 2009b; Billiet *et al*., 2012; Gomes and Reis, 2004; Gross and Rodríguez-Lorenzo, 2004; Guillotin and Guillemot, 2011; Hutmacher, 2001; Kim and Mooney, 1998; Kreke *et al*., 2005; Langer and Vacanti, 1993; Leong *et al*., 2008; Liu and Czernuszka, 2007; Tan *et al*., 2005; Tan and Teoh, 2007; Truscello *et al*., 2012). In order to accomplish all of these goals, scaffolds must fulfil several biological and physical requirements (Figure 1.4 and Table 1.4) that will affect cell survival, signalling, growth, propagation and reorganization and also cell shape modelling and gene expression (Bartolo *et al*., 2012; Bártolo and Bidanda, 2008; Bártolo *et al*., 2009b, 2009a; Billiet *et al*., 2012; Chen *et al*., 1997; Leong *et al*., 2008; Mooney *et al*., 1991; Reverchon and Cardea, 2012; Sanz-Herrera *et al*., 2009; Shafiee and Atala, 2016; Vasanthan *et al*., 2012). The ability of additive manufacturing to pattern various materials, cell types and biomolecules provides a unique tool to create tissue constructs closely resembling the composition, architecture and function of biological tissues. Advances in printable biomaterials and 3D printing strategies allow the fabrication of vascularised tissue constructs composed of multiple cells embedded within suitable extracellular matrix components and supplied by functional vasculature (Huang *et al*., 2018; Vyas *et al*., 2017). Thick and perfusable vascular tissue constructs can now be designed, printed and *in vitro* cultured for relevant periods, offering a promising alternative to traditional vascularisation strategies (Figure 1.5) (Huang *et al*., 2018; Vyas *et al*., 2017).

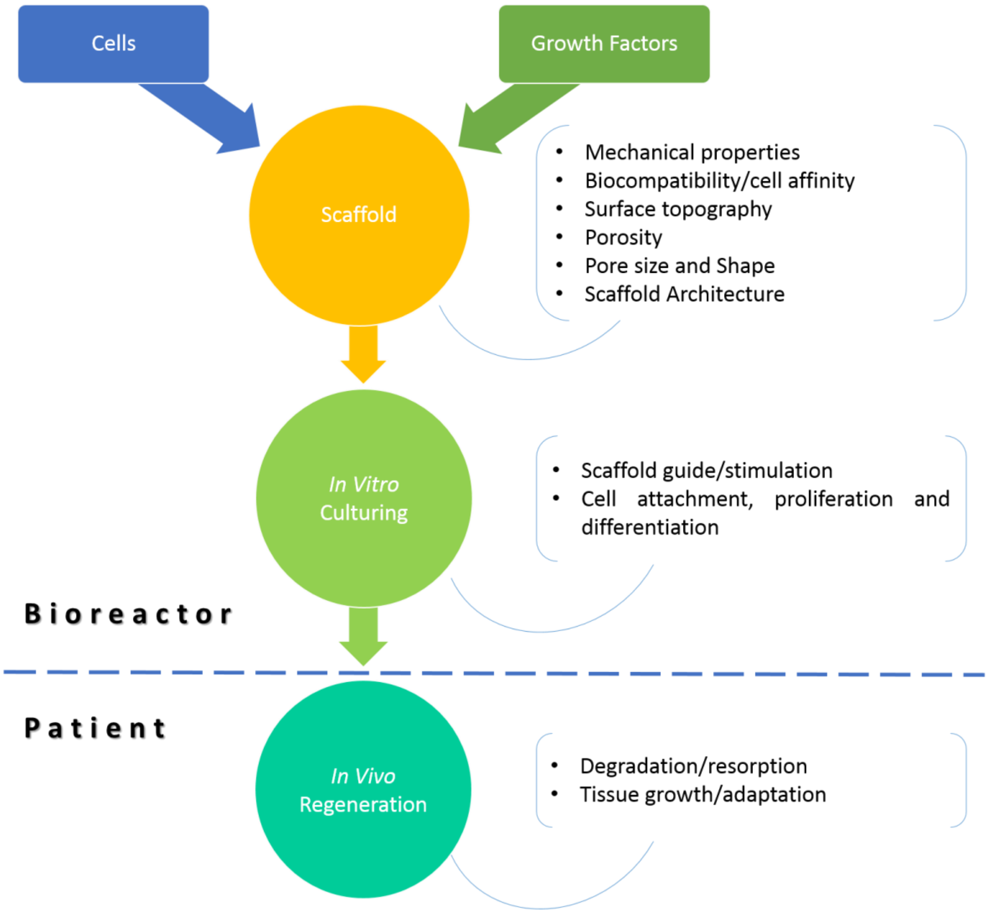

Figure 1.4 Tissue engineering process involving the cell seeding on scaffolds, *in vitro* culturing and patient implantation (Bartolo *et al*., 2012; Liu and Czernuszka, 2007).

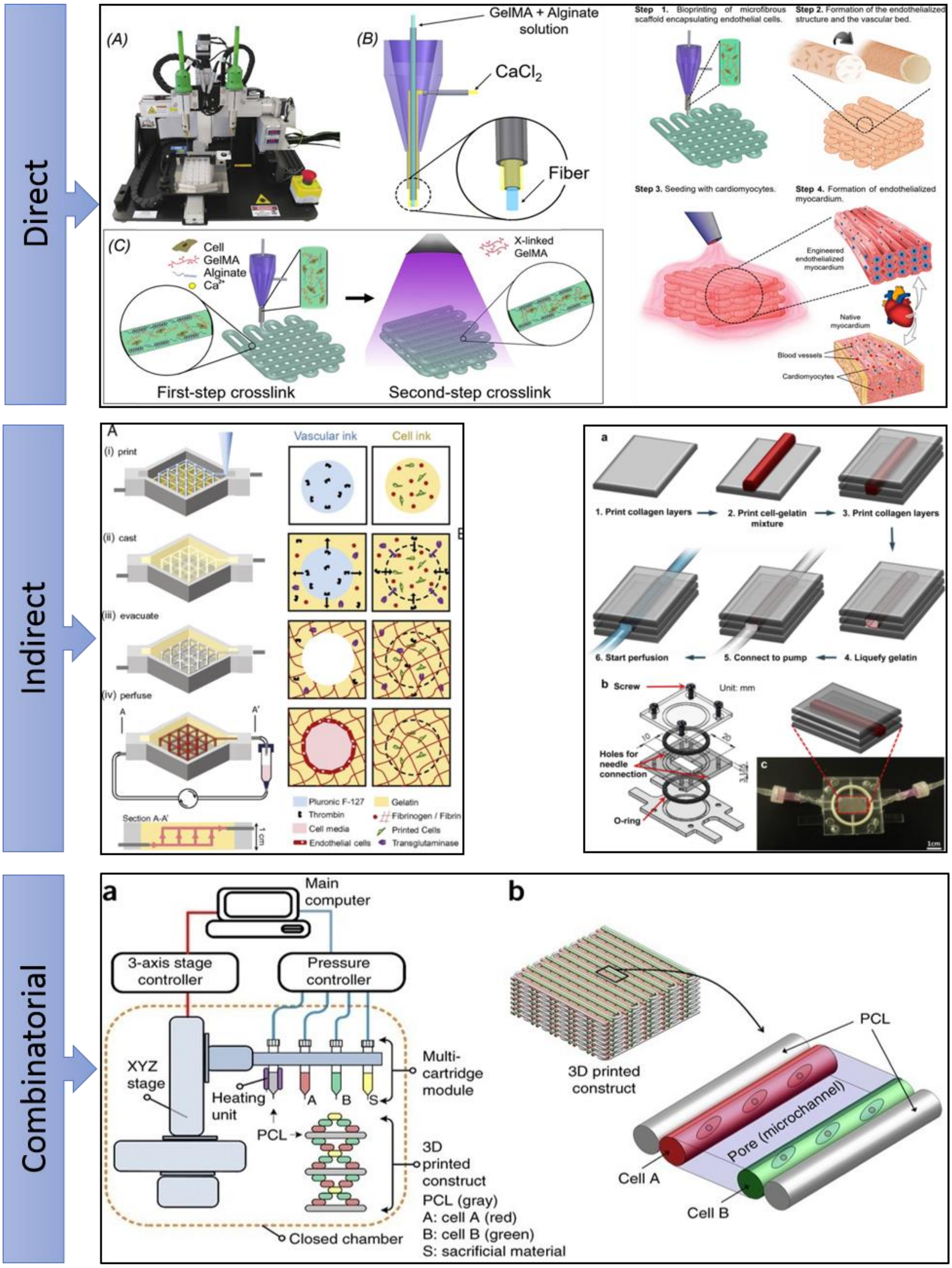

Figure 1.5 Examples of extrusion-based processes applied to create vascular networks in 3D tissue constructs through three significant approaches (Vyas *et al*., 2017).

Table 1.4 Relationship between scaffold characteristics and the corresponding biological effect (Mahajan, 2005).

Scaffold Characteristics	Biological Effects
Biocompatibility	Cell viability and tissue response
Biodegradability	Aids tissue remodelling
Porosity	Cell migration inside the scaffold - Vascularisation
Chemical properties of the material	Aids in cell attachment and signalling in the cell environment. Allows release of bioactive substances
Mechanical properties	Affects cell growth and proliferation response

1.2 Cell Culture and Bioreactors

In Tissue Engineering, cell culture plays a crucial role in the construction of tissue replacement. Therefore, bioreactors are vital elements in a tissue engineering approach. A tissue engineering bioreactor can be defined as a "device that uses mechanical means to influence biological processes" (Plunkett and O'Brien, 2010). Bioreactors (Figure 1.6) can be used to assist the *in vitro* development of new tissue by offering physical and biochemical regulatory signals to cells, stimulating and encouraging them to differentiate and/or to produce ECM prior to *in vivo* implantation (Pörtner *et al*., 2005). They are devices where biochemical or biological processes develop under a tightly controlled and closely monitored environment. The primary roles of a tissue engineering bioreactor are to guarantee (Wang *et al*., 2005; Wendt *et al*., 2008; Xie and Lu, 2016):

- A favourable environment for cell proliferation and differentiation;
- Homogeneous distribution of cells in the scaffold;
- Constant nutrient concentration supply;
- Efficient mass transfer;
- Physical stimuli.

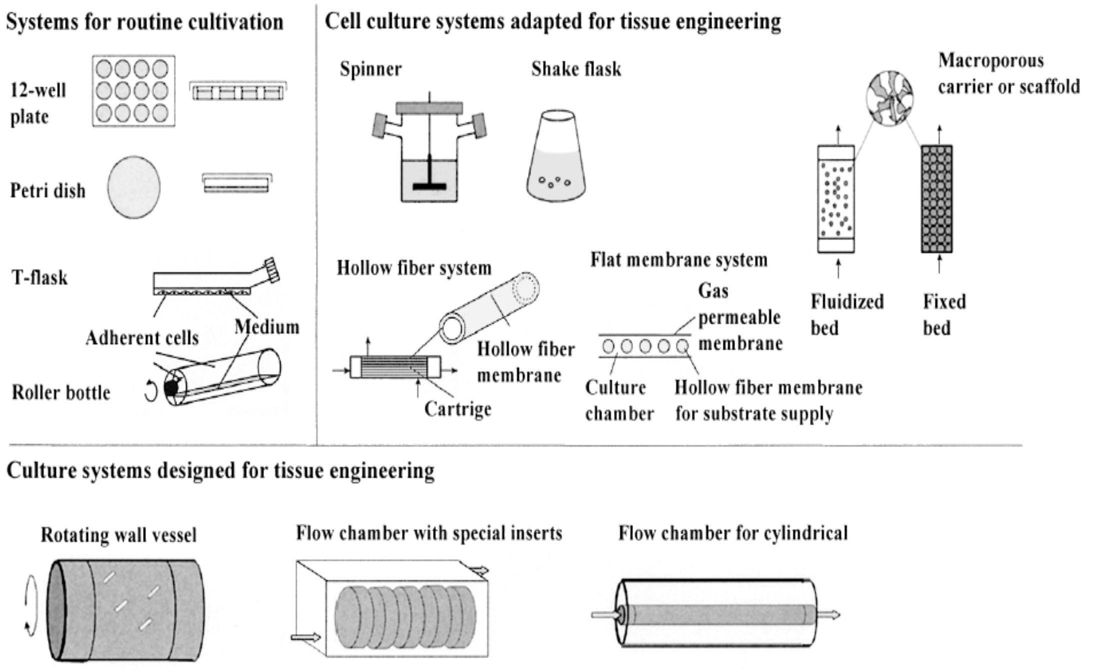

Figure 1.6 Static and dynamic cell culture systems used in TE (Pörtner *et al*., 2005).

Due to the specificity of each type of cell and the tissue that will be created, there was a need to develop various kinds of bioreactors with more focus on their operational aspects and ability to apply *stimulus*. These bioreactors are divided into two major groups: static culture bioreactors and dynamic culture bioreactors (Figure 1.7). Static culture systems are the simplest to operate only required to control the environmental conditions (*e.g.* petri dish, t-flask, culture bag) while dynamic systems apply stronger *stimulus* to the cells, either directly or indirectly. Dynamic cultures comprise agitation systems like spinner flask, Wavywalled Bioreactor (WWB), stirred vessel bioreactors and the rotational bioreactors (Bernhard Rieder, 2018; Gelinsky *et al*., 2015; Obregón *et al*., 2017; Rauh *et al*., 2011).

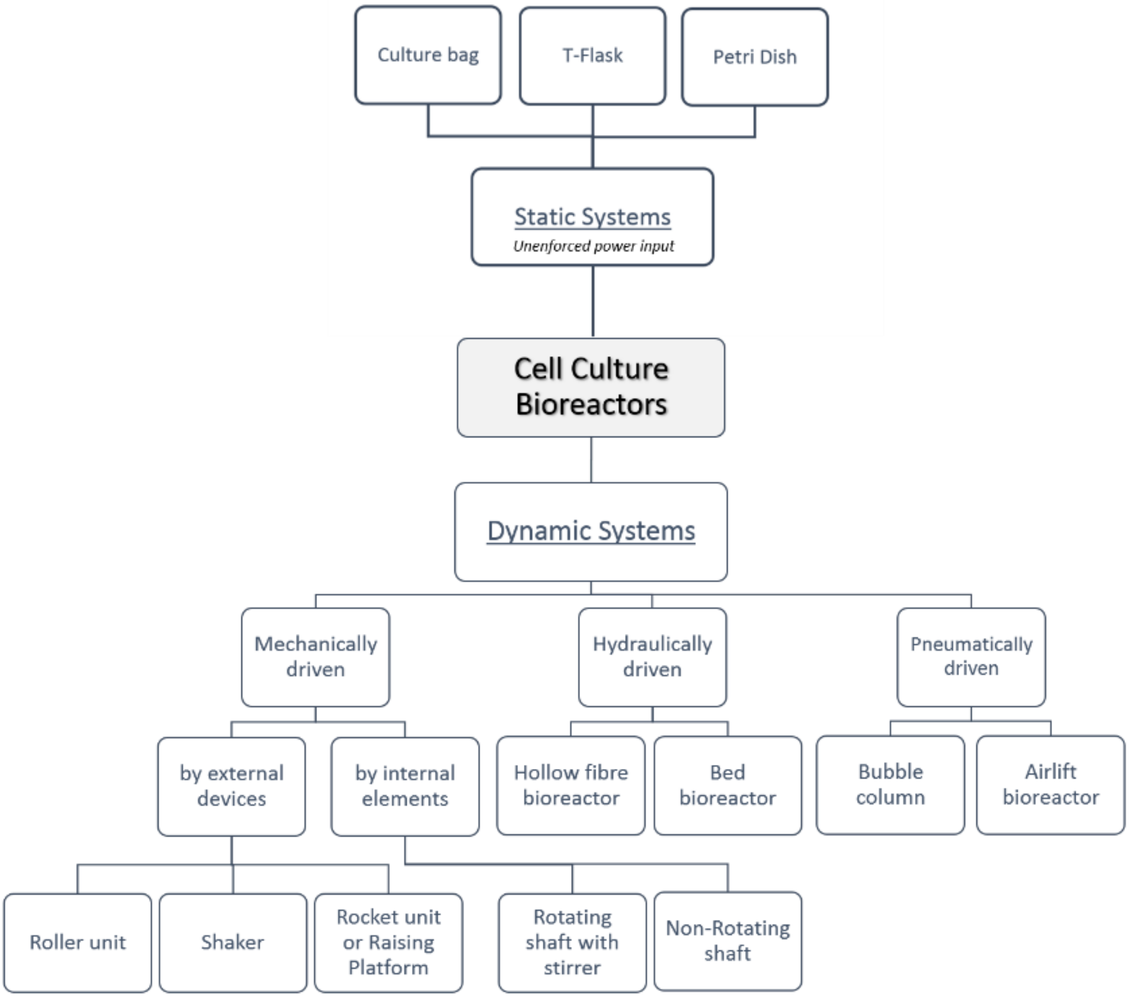

Figure 1.7 Bioreactors classification.

The operation of a bioreactor requires an optimal control on the oxygen concentration, temperature, pH, shear stresses, mechanical forces and aseptic conditions. These parameters are strongly dependent on the scaffold topology, scaffold material and cells, are pre-defined based on the user experience or empirical models. For example, if the shear stresses on the scaffolds are excessive, they can induce cell death (Table 1.5). Moreover, depending on the shear stresses, cell permeability can raise the liberation of extracellular proteins. However, despite the complexity in defining optimal processing conditions, and eventually the need for real-time modification of operating parameters (*e.g.* to accommodate scaffold degradation) wasn't found computational tools available to support the definition of optimised parameters.

Table 1.5 Example of limit and optimal stresses of several types of cells.

Cell Type	Shear Stress	Reference
	Osteogenesis	
Osteoblasts	$5x10^{-5}$ Pa (optimal stress)	Cartmell *et al.*, 2003
	$5,7x10^{-2}$ Pa (cell death)	Porter *et al.*, 2005
Osteocytes	0,5 to 1,5 Pa (optimal stress)	Godara *et al.*, 2008
	Chondrogenesis	
Chondrocytes	0,1 Pa (normal stress)	Schinagi *et al.*, 1999
	Myogenesis	
Smooth Muscle Cells	0,5 to 2,5 (optimal stress)	Martin and Vermette, 2005
Cardiomyocytes	0,24 Pa (cell death)	Radisic *et al.*, 2008
	Others	
Hepatocytes	0,033 Pa (optimal stress)	Park *et al.*, 2008
	0,5 Pa (critical stress)	
Heart Valves Cells	2,2 Pa (optimal stress)	Martin and Vermette, 2005

1.3 Research aims

Designing a new perfusion bioreactor for TE applications is the main topic of this research. Problems in this type of culture arise mainly because of the enhanced mass transfer within the bioreactor due to convection and diffusion of the fluid, increasing this way the shear stress levels on the scaffold surface. These critical tensions will damage the cells. So, it is imperative the optimisation and prediction of the fluid behaviour around and within the scaffold, allowing further improvements of scaffolds design to maintain excellent mechanical properties during the culturing stage.

Taking into account the different problems that are inherent to cell culturing in TE, this research work must consider the following main objectives:

- The design optimisation of a perfusion bioreactor;
- The evaluation of a new inlet fluid flow concept within the chamber;
- Analysis of the critical tensions that are admissible in cell culturing and in the scaffold;
- The heterogeneity of tissue culture by means of different *stimulus* applied on the scaffold surface.

1.4 Publications

The following publications were the direct results of the research performed for this PhD. These publications can also be consulted in the appendices.

Almeida SR, Freitas D, Almeida HA, Bártolo PJ. Structural and vascular performance of biodegrading scaffolds within bioreactors. In: Natal Jorge R, Mascarenhas T, Duarte JA, Ramos I, Costa ME, Figueiral MH, *et al*., editors. Biomedwomen, vol. 2, London: CRC Press; 2016, p. 165–71. DOI:10.1201/9781315644622.

Freitas D, Almeida H, Bartolo PJ. Perfusion Bioreactor Fluid Flow Optimization. Procedia Technology 2014a; 16:1238–47. DOI: 10.1016/j.protcy.2014.10.139.

Freitas D, Almeida H, Bartolo PJ. Optimisation of a perfusion bioreactor for tissue engineering. In: Jorge R, Campos J, Vaz M, Santos S, Tavares J, editors. Biodental Engineering III, London: CRC Press; 2014b, p. 6. DOI:10.1201/b17071.

Freitas D, Almeida HA, Bártolo PJ. Permeability Evaluation of Flow Behaviors Within Perfusion Bioreactors. Mechanisms and Machine Science, vol. 24, 2015a, p. 761–8. DOI:10.1007/978-3-319-09411-3_80.

Freitas D, Ciurana J, Almeida HA, Bartolo PJ. Computational analysis of a perfusion bioreactor for Tissue Engineering. The Second CIRP Conference on Biomanufacturing, vol. 00, Elsevier; 2015b, p. 1–7.

Freitas DM, Tojeira AP, Pereira RF, Bártolo PJ, Alves NM, Mendes AL, *et al*. Bioreactor Multifuncional para a Engenharia de Tecidos. Patente de Invenção Nacional No. 105176, 2013.

Pereira RF, Freitas D, Tojeira A, Almeida HA, Alves N, Bártolo PJ. Computer modelling and simulation of a bioreactor for tissue engineering. International Journal of Computer Integrated Manufacturing 2014;27:946–59. DOI:10.1080/0951192X.2013.812244.

2 Bioreactors For Tissue Engineering

A more in-depth analysis of the state-of-the-art of the several types of bioreactors will be presented in this chapter, as also the environmental and operational conditions in which the cell culture occurs.

2.1 Bioreactors, concepts and definitions

Bioreactors have been used for several years in applications such as water treatment and purification, manufacture of pharmaceuticals, fermentation, food production and also in the production of recombinant proteins (*e.g.* growth factors, antibiotics and vaccines) (Korossis *et al*., 2005; Martin and Vermette, 2005; Pörtner *et al*., 2005; Rauh *et al*., 2011). Using the same principles, they were adapted to TE (Figure 2.1). Generally, they serve as locations, *i.e.* incubators, in which occurs the development of biological, biochemical and biophysical processes in controlled and monitored environmental conditions (*e.g.* pH, temperature, pressure and concentration of nutrients). The reproducibility, control and automation of the process are one of the critical aspects when culturing new tissues (Lyons and Pandit, 2005; Martin *et al*., 2004; Rauh *et al*., 2011) and for that reasons the design of a bioreactor should reflect the application-specific prerequisites (Korossis *et al*., 2005; Rauh *et al*., 2011; Zhao *et al*., 2016).

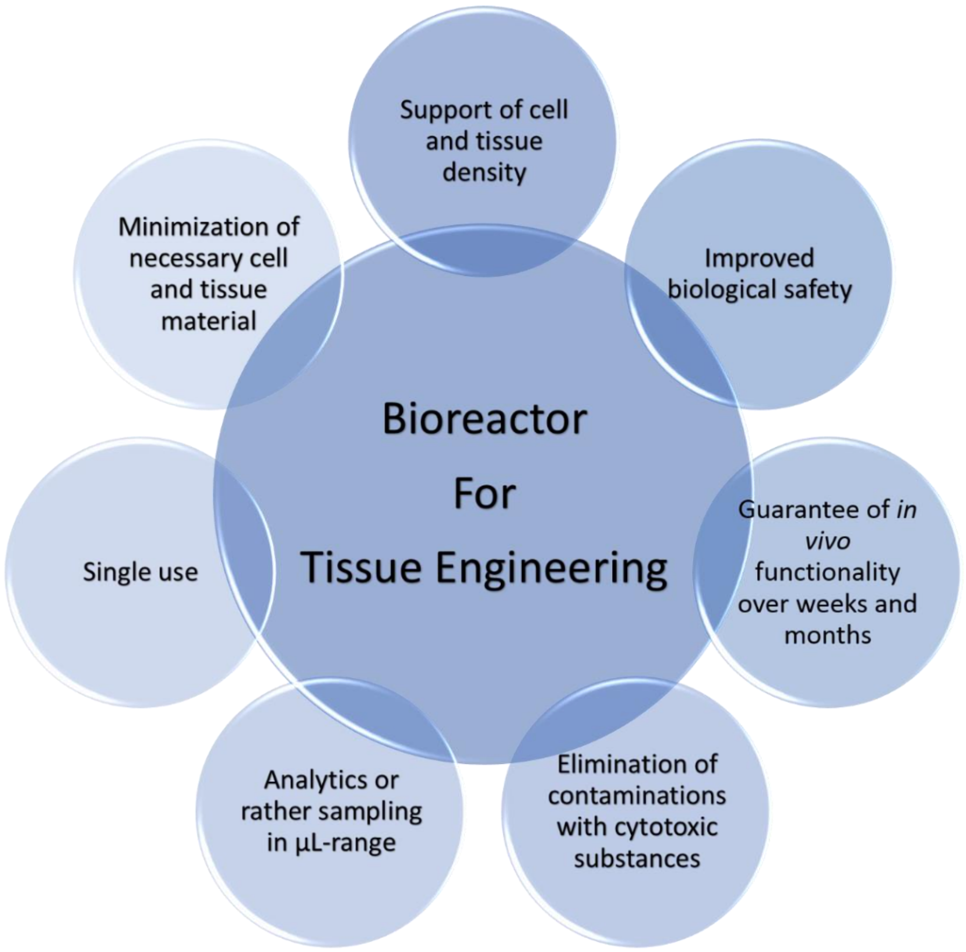

Figure 2.1 Properties of a bioreactor to use in TE.

The use of bioreactors in TE aims to provide an environment conducive to adhesion, proliferation and differentiation of living animal cells. Moreover, these devices provide the necessary conditions to perform *in vitro* studies about the effects of mechanical and biomechanical stimuli on cells. The most critical aspect in a bioreactor is related to the mass transfer (nutrients, gases and waste removal) (Martin and Vermette, 2005; Pörtner *et al.*, 2005), since *in vivo* cells benefit from their proximity to blood capillaries of 100-200µm (Rouwkema *et al.*, 2008), which is extremely difficult to replicate *in vitro*.

2.1.1 Importance of environmental and operational variables

Generically primary cells, which subsequently gives origin to a tissue, require a ribbed nutrient medium for the correct growth and proliferation. However, in specific environments, human cells need external control of conditions such as temperature, pH, product concentration of cell growth, among other parameters.

Temperature

The cell growth and development take place *in vivo* at a temperature of 37°C. *In vitro* conditions are ensured by incubator systems. However, the increase of an incubator throughout all the mechanical systems of the bioreactor limits the accessibility to the culture itself. More recently, have been suggested heated atmospheres systems using heating plates; another proposed solution is insertion of the heating units within the culture system, which can be monitored by computer using low-voltage circuits and circuit breakers which avoid the electric shock (Minuth *et al*., 2006; Pörtner, 2009; Ravichandran *et al*., 2018; Serra *et al*., 2009; Zhang *et al*., 2010).

pH

Human primary cells are susceptible to variations of pH. Therefore, the culture medium is controlled at this level by a buffer solution which maintains the pH between 7,0 and 7,3, these values are considered in the literature as optimum values (Pörtner, 2009; Ravichandran *et al*., 2018; Zhang *et al*., 2017). In several experiments, the solution of carbon dioxide-bicarbonate at 5% has been widely used since it resembles the solution existent in the blood, at *in vivo* conditions (Pörtner, 2009).

Under different conditions of 5% concentration of CO_2 the physiological pH becomes slightly alkaline (under normal atmospheric conditions – 0,3% CO_2 concentration) which can be countered by reducing the concentration of $NaHCO_3$ or by adding other buffer solutions such as sodium phosphate or HEPES, which can be monitored by the pH indicator phenol red (Minuth *et al*., 2006; Nazempour and Wie, 2018; Pörtner, 2009; Serra *et al*., 2009).

Medium Chemical composition

The cell activity *in vivo* is usually associated with the activity of sodium-potassium pump, whose function is to transport nutrients and other ions from the extracellular medium to the intra-cellular (Hoesli *et al*., 2009; Minuth *et al*., 2006). In addition to the necessary activity to standard cells ions are required to ensure power supply in the form of carbohydrates, is mostly reported, the glucose concentrations of 446 mg/dl. Besides, amino acids are also added (which are only precursors activity of protein synthesis), vitamins, minerals and other compounds (Eaker *et al*., 2017; Grayson *et al*., 2009; Minuth *et al*., 2006; Yeatts and Fisher, 2011).

In addition to all these components, it is also generally associated with a serum concentration ranging between 5 and 10%, and whose function is to provide specific growth and protect cells from shear stress. An example of such serum is the fetal of calf or horse. However, the addition of this component to the culture medium of cells entails some disadvantages, such as (1) the composition of the solution is not well defined; (2) the high cost of serum; (3) the difficult purification of the solution; (4) variation of loads in the solution; (5) the risk of contamination and spread of viruses.

However, the absence of this component in the growth medium and cell differentiation significantly delays the culture process (Butler *et al*., 2009; Eaker *et al*., 2017; Pati *et al*., 2016; Pörtner, 2009; Ravichandran *et al*., 2018).

Oxygenation

To achieve the aerobic metabolic cycles of the cells is necessary to take into account the distribution of gas in the culture medium, the transfer of nutrients and also the wastes of cellular reactions. Transferring a sufficient amount of oxygen to cells is difficult, mainly due to the low oxygen solubility in the culture medium (about 0,2 mmol/L). However, to have a viable cell culture is necessary to have an equal or approximated concentration of both O_2 and Glucose (Martin and Vermette, 2005; Salehi-Nik *et al*., 2013). In recent culture systems, the oxygen concentration is kept constant between 20% and 100% of air saturation that creates a balance between oxygen needs and tolerance to the formation of harmful free radicals that causes cytotoxic effects on cells (Cioffi *et al*., 2008; Patrachari *et al*., 2012; Salehi-Nik *et al*., 2013).

Oxygenation can be performed by two methods: (1) gas sparging and (2) without oxygen bubbles. The gas sparging process is often used since it proves to be simple to provide the oxygen to the bioreactor. This method allows a high oxygen transfer due to a high interfacial area per bubble. However, the bubbles can lead to failure in cell viability since the bubbles can damage the cells. The preferable process in bioreactor systems is the method without bubbles of the used gas that can be divided into two methods, the superficial gas sparging and the permeable membrane (porous or diffusion) (Bliem *et al*., 1991; Cioffi *et al*., 2008).

On the superficial gas sparging process, the culture medium is directly exposed to a controlled atmosphere rich in O_2 and 5% CO_2 regularly occurring diffusion of these gases and keeping them in the culture medium.

The permeable membranes transfer the gas to the culture medium, and they can be defined in two different types: porous or diffusion. In the first case, the culture medium is in continuous contact with the gas through pores arranged on the membrane (Cioffi *et al*., 2008; Curcio *et al*., 2017; Martin and Vermette, 2005). The interface created in the pores is controlled by pressure effects and hydrophobic forces. In the other end, the diffusion membranes diffuse the oxygen from the initial gas phase to a soluble membrane in oxygen and then into the culture medium. Although these two cases avoid the formation of bubbles, they are influenced by factors such as the concentration of oxygen, the porosity of the membrane and the surface area of the membrane. However, these processes of oxygenation present difficulties in their implementation, namely, the complexity of the process, control of intrinsic variables of the process, the need for high membrane area exposed to the gas phase, difficulties in maintenance and cleaning of the membrane. In addition, the deposition of proteins (derived from the culture medium) at the base of the membrane, modify its hydrophobic property (Curcio *et al*., 2017; Martin and Vermette, 2005; Ravichandran *et al*., 2018; X. Zhang *et al*., 2009).

2.1.2 Classification and design of bioreactors

Bioreactors may be classified according to many aspects, including:

- The environment in which unfolds the tissue culture - cell culture may be conducted in static or dynamic conditions;
- The type of *stimulus* involved - the bioreactor can apply several kinds of *stimuli* during cell culture or act in various ways to provide the same kind of *stimulus* (*e.g.* stirring action, infusion mechanical compression or rotation);
- The tissue in culture - each tissue requires different requirements from the bioreactor (the *stimulus* involved or the level design).

A bioreactor is designed according to the desired size, complexity and functionality. However, regardless of these considerations, a bioreactor must possess a number of essential requirements, as described in Table 2.1.

Table 2.1 Main requirements of a bioreactor for the use in TE (Chen and Hu, 2006; Hansmann *et al*., 2013; Korossis *et al*., 2005; Lei and Ferdous, 2016; Lyons and Pandit, 2005; Martin *et al*., 2004; Pörtner *et al*., 2005).

Bioreactor Main Requirements		
Adequacy of vascularity of the cells/tissue providing nutrients in the proper time and amount	Application of *stimuli* in order to increase the adhesion, proliferation and differentiation	Avoid flow turbulence and excessive pressure on the culture medium, which can damage cells and impair the formation of new tissue
Control of environmental, chemical and physical conditions of culture	Ensure aseptic and sterilised conditions	Ensure the biocompatibility of the building materials
Monitoring of cell growth and formation of new tissue	Allow removal of the waste generated by cells	Easily place the scaffold inside
Maintain a high degree of reproducibility	Allow the operation over long periods	Be simple and easy to sterilise, clean and perform the maintenance of the components

The general requirements listed above are determined by the needs of the mechanical, physical, biophysical and biomechanical level of the tissue in culture. For example, the use of pulsed mechanical/perfusion instead of continuous stimulation on tubular scaffolds with Smooth Muscle Cells (SMC) increases the structural organisation of blood vessels and their mechanical properties. While applying dynamic stresses to chondrocytes in an appropriate environment stimulates the synthesis of Glycosaminoglycans (GAG) and increases the mechanical properties of the formed cartilage (Chen and Hu, 2006; Mahajan, 2005; Wang *et al*., 2014). Studies on cell proliferation *in vitro* have shown that mechanical *stimuli* have a positive impact regarding the formation of new tissue, improving the acceleration of the processes of cell differentiation and proliferation (Chen and Hu, 2006; Mahajan, 2005; Martin *et al*., 2004; Obregón *et al*., 2017; Pörtner *et al*., 2005; Wang *et al*., 2014). This effect is particularly evident in the formation of cartilage, bone and cardiovascular tissue (Obregón *et al*., 2017; Pörtner and Giese, 2007). The most essential *stimulus* on cellular differentiation and proliferation are the shear forces resulting from the fluid passage from the surfaces and pores of the scaffold enabling signal transmission/stimulation of the cells (Chen and Hu, 2006; Cook *et al*., 2016; Freitas *et al*., 2014a; Obregón *et al*., 2017).

As a result of the specific needs of each type of cell in the culture process, various types of bioreactors were studied in particular on the level of operation and ability to apply *stimuli*.

a. Systems of static culture

The static culture systems are the simplest ones and include systems like T-flasks, Well Plates and Petri dishes (Figure 2.2), which are designed to culture cells in static conditions (Correia *et al*., 2012; Kumar *et al*., 2004; Mekala *et al*., 2011). The main characteristics of these devices include ease of use, low cost and the possibility of sterilisation. In return, these systems have several limitations such as (1) the weak agitation of the medium which translates into low nutrient concentrations in certain places; (2) poor reproducibility; (3) difficulty of changing the culture medium, and (4) low amount of cell numbers. Furthermore, the application of stimuli and the monitoring and control of environmental conditions, such as pH, moisture and CO_2 is practically impossible (Correia *et al*., 2012; Kumar *et al*., 2004; Lei and Ferdous, 2016; Mekala *et al*., 2011; Pörtner *et al*., 2005; Pörtner and Giese, 2007; Yeatts and Fisher, 2011).

These devices are widely used in cell culture for shorter periods of time being used mainly to increase the number of cells (Cabrita *et al*., 2003; Correia *et al*., 2012; Lei and Ferdous, 2016; Pörtner *et al*., 2005). After this period the cells are transferred to bioreactors in which will occur the development of the new tissue (Correia *et al*., 2012; Eaker *et al*., 2017; Kumar *et al*., 2004; Lyons and Pandit, 2005).

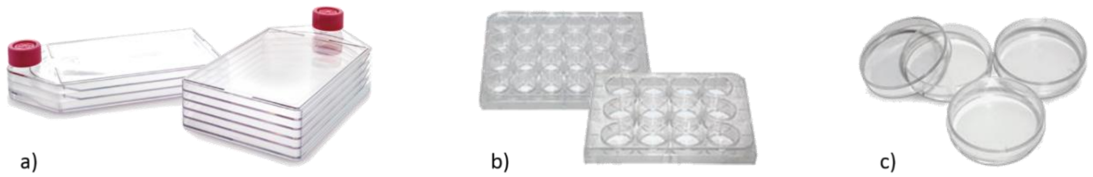

Figure 2.2 Example of static culture systems a) T-flasks, b) Well plates and c) Petri dishes.

Static culture in 3D scaffolds generally produces tissues with a small thickness and located at the periphery of the structure. The created tissue is characterised by its heterogeneity, a result of inadequate mass transfer (Cabrita *et al*., 2003; Correia *et al*., 2012; Eaker *et al*., 2017; Lei and Ferdous, 2016; Pörtner *et al*., 2005). In order to solve the mass transfer limitations of these simple culture systems other bioreactor systems were developed such as, spinner flasks, Rotating-Wall Vessel (RWV), perfusion bioreactors, mechanical compression bioreactors, among others (Bueno *et al*., 2004; Takebe *et al*., 2012; X. Zhang *et al*., 2009; Zhang *et al*., 2010).

b. Agitation Systems

The agitation bioreactors provide a homogeneous environment, presenting results that are superior to the static culture. The main purpose of these systems (*e.g.* Spinner flask, wavy-walled bioreactor (WWB) and Stirred vessel bioreactor), is the increase in mass transfer (Bilgen *et al*., 2006; Delafosse *et al*., 2014; Kumar *et al*., 2004; X. Zhang *et al*., 2009).

Spinner Flask

Spinner flask is the simplest type of bioreactor (Figure 2.3), in which the porous matrices containing the fixed cells are suspended on needles in the cap. Stirring of the medium is performed by using a magnetic bar, depending on its rotation, helps to induce the mixing of oxygen and nutrients to increase the homogeneity of the medium and consequently tissue growth (Chen and Hu, 2006; Yeatts and Fisher, 2011; Zhao *et al*., 2016). These devices can allow monitoring of variables such as pH and CO_2 (Kumar *et al*., 2004; Yeatts and Fisher, 2011; Zhao *et al*., 2016), the rotation speed of the medium between 50 and 80 rpm. The culture medium is renewed periodically (usually in periods of 2-3 days) to maintain or increase the concentration of nutrients. In this system, the bottle allows aeration of the culture medium and the resulting gas exchange. The nutrient delivery and waste removal occur by convection and by the fluid passage on the surface of the porous matrix. Their disadvantages are related to the agitation of the medium, which can generate high shear stress values and turbulent regimes harmful to the cell culture (Chen and Hu, 2006; Korossis *et al*., 2005; Lyons and Pandit, 2005; Martin *et al*., 2004; Seymour and M. Ecker, 2017; X. Zhang *et al*., 2009; Zhao *et al*., 2016).

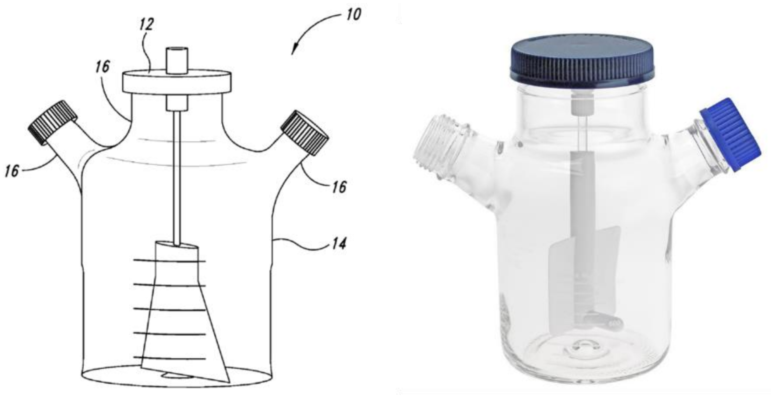

Figure 2.3 Patent schematic of a Spinner Flask from (Oldenburg *et al*., 2014) and a Spinner flask from Chemglass® (right).

Wavy-walled bioreactor

In order to overcome the limitations of the turbulence and shear stresses observed in Spinner flask systems, was developed a new bioreactor, the Wavy-Walled Bioreactor (WWB) (Figure 2.4). This machine has ribbed walls which allow reducing turbulence levels of the medium and its shear stresses (Bilgen *et al*., 2006; Bueno *et al*., 2004; Obregón *et al*., 2017). Studies conducted allowed to verify that this new system has an increase in cell proliferation and deposition/formation of extracellular matrix in polymeric scaffolds containing chondrocytes (Bilgen *et al*., 2006; Bueno *et al*., 2004; Chen and Hu, 2006; Obregón *et al*., 2017).

Bilgen *et al*., (2006) studied the hydrodynamic parameters involved in the bioreactor WWB, comparatively to the Spinner flask and its influence on the cartilage tissue engineering. This study concluded that the fluid flow is significantly different between them and it was also found that the position of the scaffold inside the bioreactor it is an important parameter because it alters the hydrodynamic behaviour of the fluid and the uniformity tensions on the scaffold.

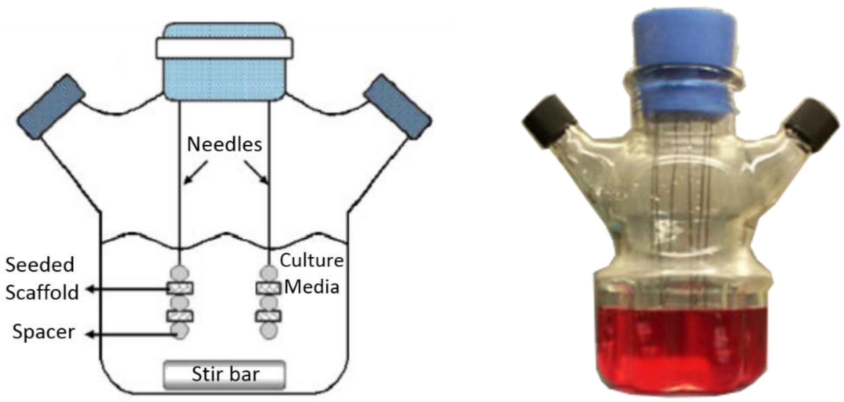

Figure 2.4 Wavy-walled bioreactor (Chen and Hu, 2006)

Stirred vessels bioreactors

This type of bioreactor (Figure 2.5) it's characterised by obtaining a homogeneous hydrodynamic environment and also because it is easy to operate. Generally, it comprises a container (where the cell culture takes place) pipes, sensors, valves, pumps and motor. This system is in motion, usually at a rotation speed of 50-80 rpm (Chen and Hu, 2006; Collins *et al*., 1998; Martin and Vermette, 2005; Obregón *et al*., 2017), while the sensors provide continuous monitoring of parameters such as temperature, pH, glucose, among others (Kumar *et al*., 2004; Nettleship, 2014; Obregón *et al*., 2017; Wang *et al*., 2005).

This system is similar to spinner flask glass however allows the control over a large number of variables, therefore presenting higher reproducibility. These bioreactors have been used in the culture and differentiation of various cells types of stem cells from human to rats (Cabrita *et al.*, 2003; Nettleship, 2014; Obregón *et al.*, 2017; Serra *et al.*, 2009). It is important to refer that the agitation of the medium can originate high shear stresses harmful to the cells which are a disadvantage of this type of equipment. One possible solution involves changing the shape and/or the diameter of the rotor blade (García Cruz *et al.*, 2012; Martin and Vermette, 2005; Wang *et al.*, 2005).

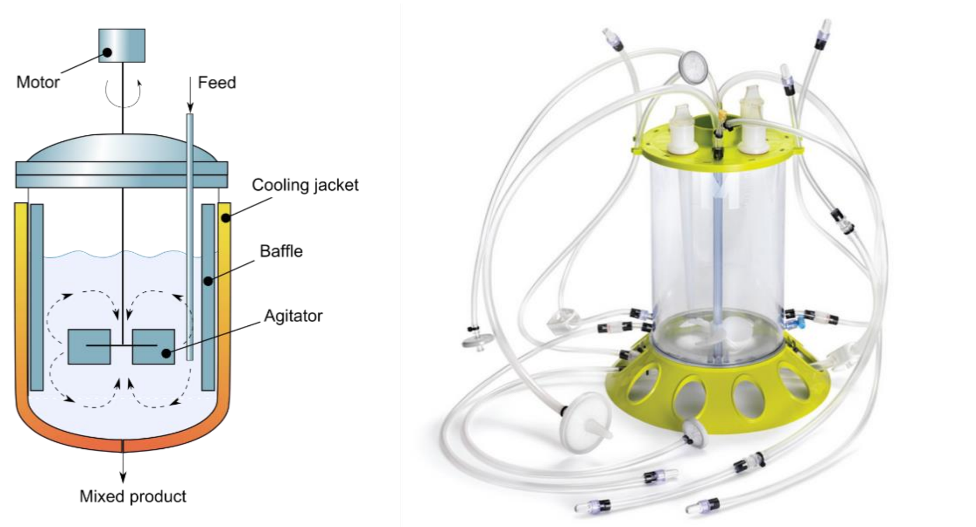

Figure 2.5 Schematic of a stirred vessel (left) (Redondo, 2014) and a stirred bioreactor from Merckmillipore® (right).

Serra *et al.*, (2009) used this bioreactor successfully to culture pancreatic stem cells from rats utilising a process of controlled expansion of the pancreatic stem cells to apply in the development of new cell therapies. In another study Martin and Vermette (2005b) mention the success of culturing cartilage with a thickness of 0.3-0.5 mm using this bioreactor, a value still far from clinical implant thickness (2-5 mm).

c. Rotation Systems

The rotation bioreactors base their operation on the application of rotation about one or more axes. This movement helps to increase the agitation of the culture medium and thus increase the mass transfer. Some bioreactor examples include Rotating-wall vessel bioreactor (RWV), Rotating Shaft bioreactor and biaxial rotating bioreactor.

Rotating-wall vessel

Despite the importance of shear forces in modelling the mechanical properties of new tissue, high shear stresses can lead to cell death (Chen and Hu, 2006; Hammond *et al*., 2016; Salehi-Nik *et al*., 2013; Yeatts and Fisher, 2011). Because of this, it was developed bioreactors that during its operation, can apply low shear stress values.

The RWV bioreactor (Figure 2.6) developed by the National Aeronautics and Space Administration (NASA) operates in a microgravity environment. This equipment was the first to combine the dynamic culture environment with low shear stress allowing a high mass transfer (Chen and Hu, 2006; Lyons and Pandit, 2005; Martin and Vermette, 2005; Pörtner *et al*., 2005; Takebe *et al*., 2012). In this bioreactor, the scaffold containing the cells is found floating in constant motion by the action of the forces involved (gravity, centrifugal and tangential force). The RWV bioreactor is presented as an alternative to overcome mass transfer limitations, typical of the bioreactors with low agitation (Martin *et al*., 2004). This equipment has been further modified to allow the fluid inlet at one end and its output through a filter located in the centre of the cylinder, originating the Rotating Wall Perfusion Vessel bioreactor (RWPV). The RWPV is used for cartilage engineering in a gravitic environment and was shown that the proliferation of cartilage tissue and heart tissue was superior at a structural and functional point of view to static culture and spinner flask (Chen and Hu, 2006; Hammond *et al*., 2016).

Figure 2.6 Rotating wall vessel (RWV) bioreactor from Synthecon®

Klement *et al*., (2004) used the bioreactor RWV to determine its influence on the number of processes involved in the formation of bone tissue. To do this, bone tissues have used embryonic rat at four different stages of differentiation. In the study carried out, it was found that tissues in the three advanced stages of differentiation, when placed in the bioreactor showed substantial growth, differentiation and mineralisation.

Other examples include crop rotation, the Slow Turning Lateral Vessel (STLV) and High Aspect Ratio Vessel (HARV). The STLV is a horizontal rotating bioreactor (Figure 2.7) consists of two concentric cylinders. The inner cylinder is stationary and consists of a silicone membrane that permits the exchange of gases, while the outer cylinder is of the rotary type and comprises a waterproof material. The rotation speed is variable and adjustable (between 15-40 rpm) allowing the scaffold remains suspended in the bioreactor stationary point due to the dynamic equilibrium of forces, avoiding and/or minimizing the shear stress from differential rotation (Chen and Hu, 2006; Hammond *et al*., 2016; Lyons and Pandit, 2005; Martin and Vermette, 2005; Salehi-Nik *et al*., 2013; Takebe *et al*., 2012). The HARV bioreactor is very similar to STLV and comprises two concentric cylinders, which have a membrane for gas exchange at the base. This equipment is characterised by having a large diameter, a small length and have low rotation velocities, about 12-15 rpm (Martin and Vermette, 2005; Mekala *et al*., 2011; Visscher *et al*., 2016). In this system the cylinders are connected to two independent motors allowing different rotation speeds and thus different levels of stress and turbulence (Lyons and Pandit, 2005; Visscher *et al*., 2016). The operation is carried out to a horizontal working volume of 100-110 ml, typically (Chen and Hu, 2006).

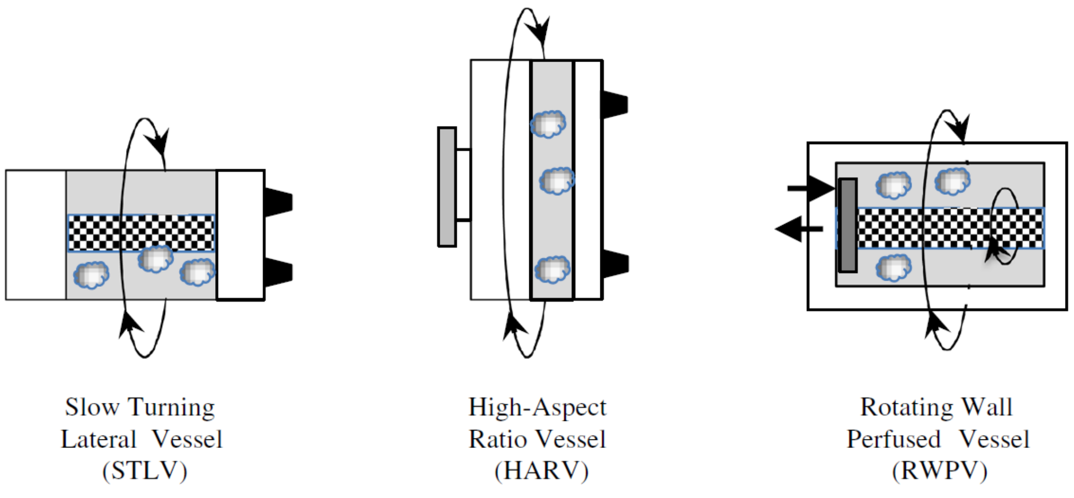

Figure 2.7 Illustration of a STLV, a HARV and a RWPV rotating bioreactor (Hammond *et al*., 2016).

The limitations associated with the above bioreactors include the possibility of a heterogeneous cell proliferation occur due to the low voltages involved and even possible damage due to collisions with the wall of the bioreactor (Chen and Hu, 2006; Hammond *et al*., 2016; Kang *et al*., 2015; X. Zhang *et al*., 2009). These bioreactors have also some limitations in culturing tissues with high mass (Martin and Vermette, 2005; Ravichandran *et al*., 2018; Salehi-Nik *et al*., 2013).

Rotating Shaft Bioreactor

To solve problems related to non-uniformity of the growth of tissues, Chen *et al*. (2004), developed a Rotating Shaft Bioreactor (RSB). This equipment consists of a central horizontal axis of stainless steel, which is coupled 22 support needles, as shown in Figure 2.8. This device has two distinct phases: a gas phase and a liquid phase (medium). Through a rotation provided by a motor, the assembly cells/scaffold is continuously transiting between phases at a given rotational speed, which helps to increase the efficiency of mass transfer (Chen *et al*., 2004; Chen and Hu, 2006; Eaker *et al*., 2017; Salehi-Nik *et al*., 2013; Zhao *et al*., 2016).

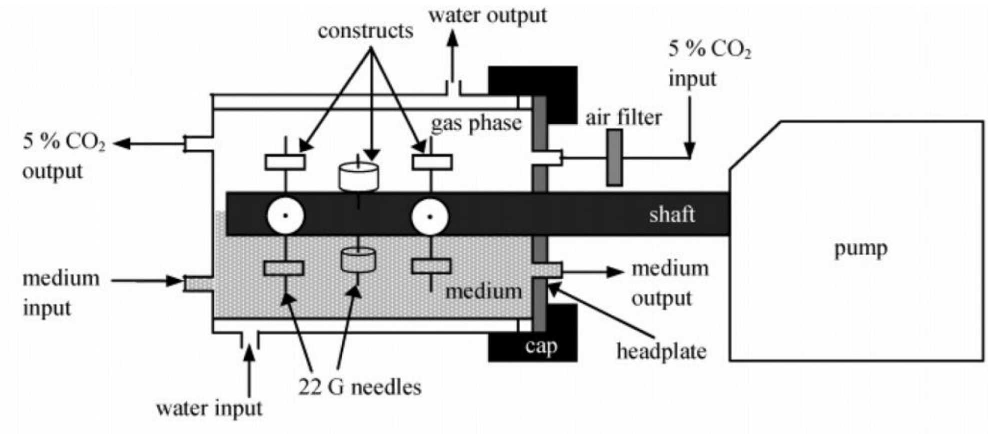

Figure 2.8 Schematic of a Rotating Shaft Bioreactor (Chen *et al*., 2004)

Biaxial rotation bioreactor

Hutmacher *et al*., (2006) developed a biaxial rotational bioreactor which allows a continuous movement of the culture medium and the control and monitoring in real time of key variables for the cell growth. This system allows the rotation of the culture chamber into two separate axes (x, z) and independent rotation speeds. Also, Ravichandran *et al*. (2018) developed a biaxial bioreactor that mimics the fetal rotation in the woman's womb in order to create bone tissue. The idea is to mimic the effect of the mechanical stresses and cyclic strains on cells in their early develop stage of the fetal growth (Figure 2.9). The container and the reservoir are connected, allowing the culture medium to circulate between them, resulting in a perfusion system. Thus, it is possible to maximise mass transfer across the scaffold and achieve greater uniformity in the new tissue (Hutmacher *et al*., 2006; Pereira *et al*., 2014; Salehi-Nik *et al*., 2013; Singh *et al*., 2007; Zhang *et al*., 2010).

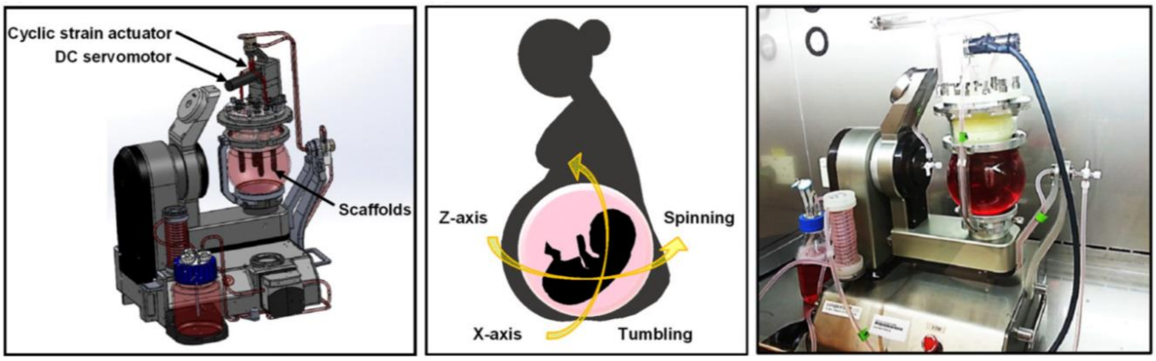

Figure 2.9 Biomimetic biaxial rotation bioreactor developed by Ravichandran *et al*., 2018.

Several studies have been conducted to evaluate the influence of the rotation on cell proliferation. Zhang *et al*. (2009) investigated the ability to form a bone graft using human mesenchymal stem cells contained in scaffolds of poly(ε-caprolactone)/tricalcium phosphate (PCL/TCP). This study compared the cell culture under static conditions and in a biaxial rotating bioreactor, performed tests *in vitro* and *in vivo*. Subsequently, they concluded that the static conditions are associated with lower cell proliferation and differentiation. Furthermore, the use of the bioreactor allowed to reduce the culture time *in vitro* and to obtain a better distribution of extracellular matrix and increased bone mineralisation (Bilgen *et al*., 2013; Hammond *et al*., 2016; Salehi-Nik *et al*., 2013).

Triaxial rotation bioreactor

Freitas *et al*. (2013) designed a novel bioreactor with three axes of rotation. With two, cylindrical or ellipsoid, chambers design, the bioreactor will maintain (or not) a steady fluid flow as a slow perfusion bioreactor, and it can rotate fully in two axes and in the third an oscillation movement as shown in the Figure 2.10.

With the extra axis movement, the mass transfer will increase and directly, the cell proliferation rate also increases due to a homogenization of the stress and strain levels on the surface of the scaffold (Freitas *et al*., 2013; Pereira *et al*., 2014; Tojeira *et al*., 2010)

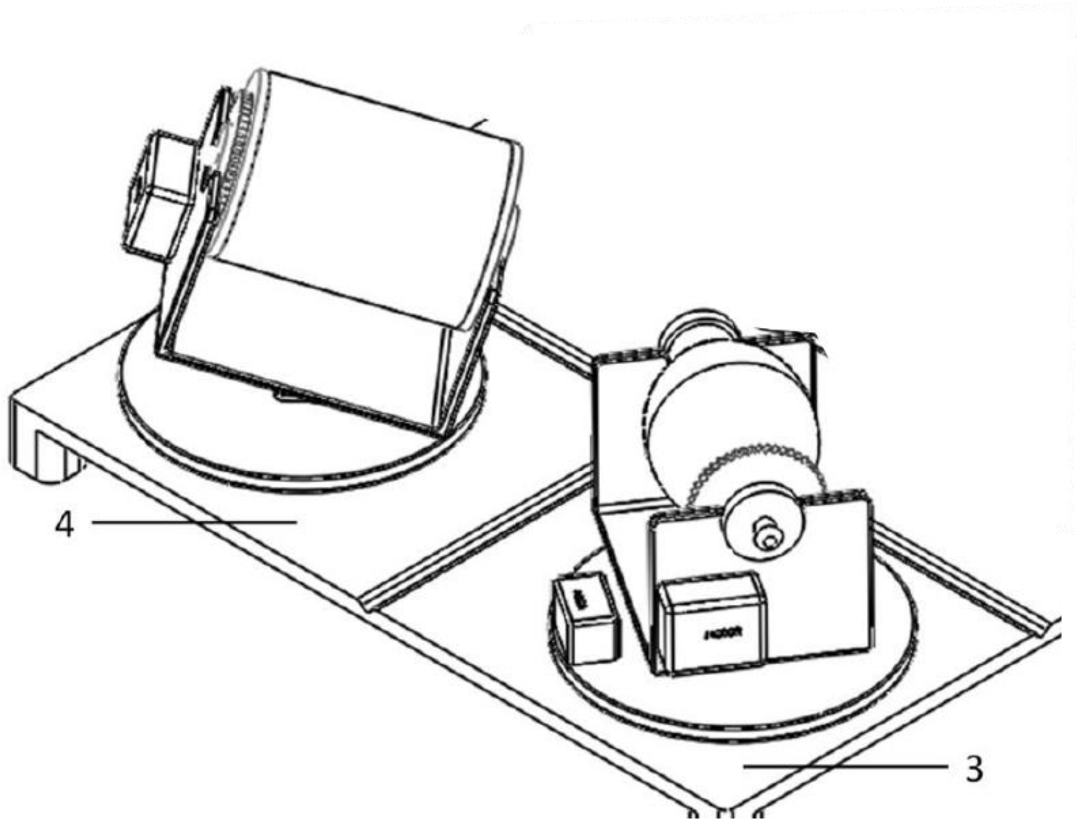

Figure 2.10 Cylindrical and ellipsoid culture chambers of the triaxial bioreactor developed by Freitas *et al*., 2013.

d. Mechanical stimulation systems

By applying mechanical *stimuli* to cells it will increase and aid the proliferation, differentiation and alignment of the cells (Altman *et al*., 2002; Halonen *et al*., 2014; Martin and Vermette, 2005; Obregón *et al*., 2017), taking into account that the maximum value of the applied stress depends on the cell type being used. For mammalian cell suspensions Martin and Vermette, (2005) report that for most cells, shear stresses of 0,1 Pa cause cellular damage being the ideal values around 0,01 Pa and also it was reported that stress values of 0,001 Pa are insufficient to promote the growth of tissue. Begley and Kleis, (2000) said that in mammalian cells the levels of shear stress between 0,3 and 1 Pa cause cellular damage and reduce viability while very low values such as 0,092 Pa, adversely affect the proliferation, morphology and cellular function. To stimulate the proliferation and growth of a 3D tissue shear stresses should be in the range of 0,01 Pa. To reach this goal, a laminar flow must avoid high shear stresses generated for example by turbulent flows.

The bioreactors that apply a mechanical *stimulus*, in particular, mechanical compression (Figure 2.11), allow the application of stress in cells with a given magnitude, frequency and duration. Thus, the performance can be of two types: static or dynamic mechanical compression (the first does not include the frequency). The application of the stress is controlled by an engine, and its intensity is regulated by a load cell (Cook *et al*., 2016; Martin *et al*., 2004; Rosser and Thomas, 2018). This type of stimulation has been applied in the culture of bone and cartilage (Altman *et al*., 2002; Bilgen *et al*., 2013) with a uniaxial compression considered the most crucial *stimulus* method that acts on cartilage *in vivo* (Schulz and Bader, 2007).

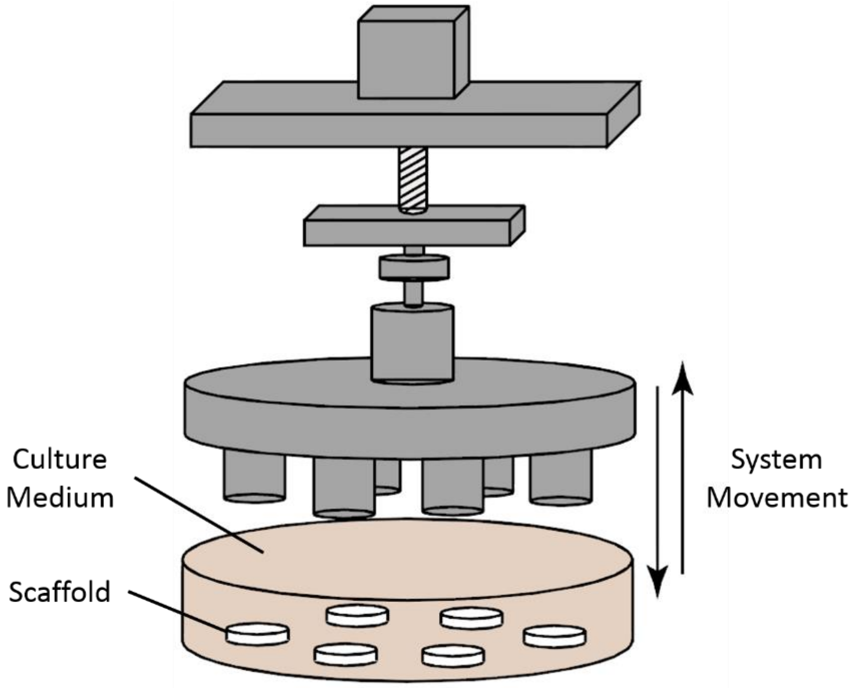

Figure 2.11 Schematic of a bioreactor that applies controlled mechanical forces (Martin *et al*., 2004).

Démarteau *et al*. (2003) developed a bioreactor and used it in the chondrocyte culture under the action of dynamic compression *stimulus*. This study concluded that the application of the *stimulus* for a period of time more than three days is associated with increased formation of GAG. (Orr and Burg, 2008) also developed a bioreactor (Figure 2.12) which combines the application of hydrostatic compression *stimuli* (about 300 kPa and frequency 0,5 Hz) and perfusion (shear stress of 0,07 Pa).

The hydrostatic pressure is applied on a diaphragm which compresses a volume of fluid contained at the culture zone. Preliminary tests showed cell viability using this type of bioreactor (Correia *et al*., 2012; Rosser and Thomas, 2018).

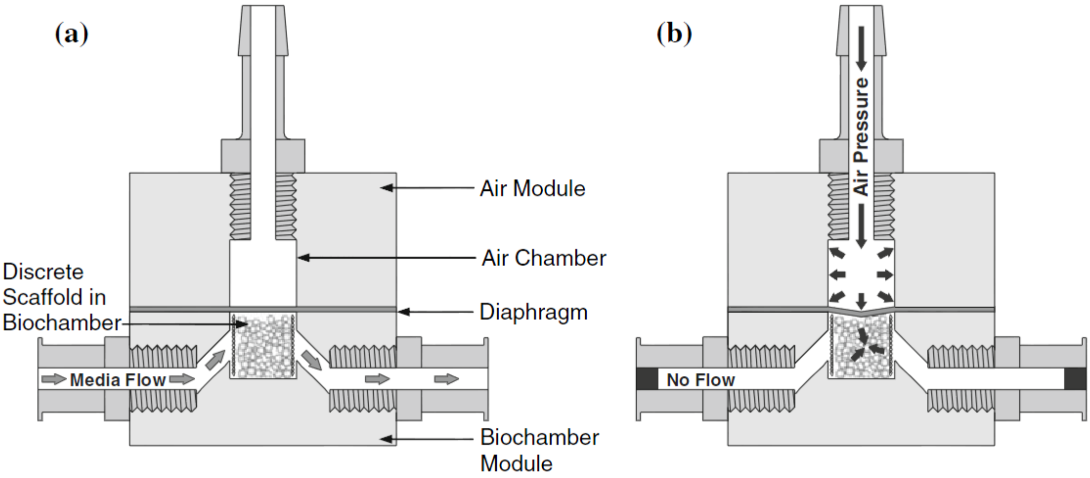

Figure 2.12 Schematic illustration of a bioreactor assembly that demonstrates (a) perfusion flow and (b) hydrostatic compression (Orr and Burg, 2008).

In tendon TE, mechanical stimulation plays a vital role. Paxton *et al*. (2013) mechanically constrained a collagen-based scaffold and therefore fabricated a highly aligned, compacted collagenous construct. With these conditions and applying the proper mechanical stimulations. Riley *et al*. (1994) found that fibroblasts can, using the previous fabrication method, generate contractile forces and increase the matrix production in collagen constructs. With the extensive research on tendon constructs, it was concluded that, when the mechanical stimulation is mimicked, *i.e.*, when the *in vivo* tendon activity is simulated *in vitro* (Figure 2.13) there is a direct improvement of the microstructure and mechanical properties of the constructed tissue (Lei and Ferdous, 2016; Youngstrom *et al*., 2015; Zhang *et al*., 2017).

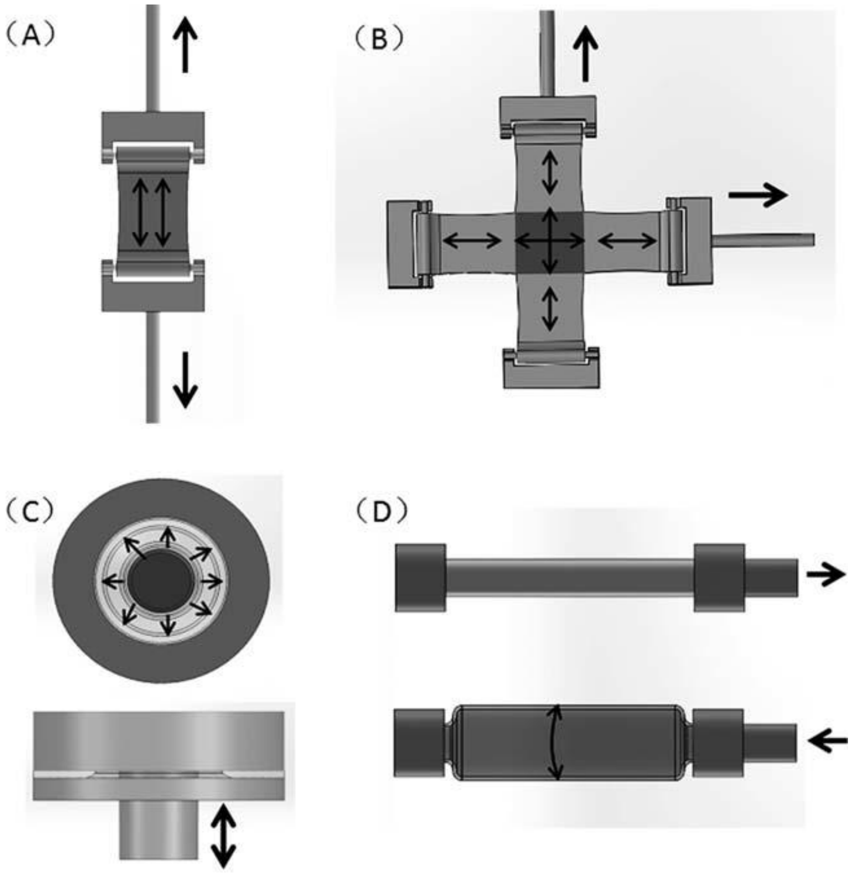

Figure 2.13 Different actuating units for stretch bioreactors: (A) Motor-driven clamps (Uniaxial); (B) Motor-driven clamps (Biaxial); (C) Moving plunger stretching a membrane; (D) Pressurized fluid or gas stretching a tube (Lei and Ferdous, 2016)

e. Perfusion Bioreactor

Perfusion systems aim to overcome the problems with non-uniform cell proliferation (Chen and Hu, 2006; Gelinsky *et al*., 2015; Nettleship, 2014; Ravichandran *et al*., 2018; Yeatts and Fisher, 2011) These devices draw their operation in the existence of a flow through the scaffold and cells while allowing simultaneously the constant renewal of the culture medium and cell retention. The applied flux can be continuous or discontinuous and can be applied at different frequencies and speeds. The existence of flow through the scaffold helps to increase the transfer of nutrients into the scaffold and remove the toxic waste produced by cellular respiration. Furthermore, cells are continuously subjected to hydrodynamic *stimuli* that have the ability to induce their alignment in the direction of the flow (Chen and Hu, 2006; Nazempour and Wie, 2018; Nettleship, 2014; Ravichandran *et al*., 2018).

The perfusion bioreactors (Figure 2.14) can operate in two distinct ways. In the first set, scaffold/cell is fixed in a column within the culture zone, while the second set has freedom of movement. Regardless the option made is necessary to ensure that the cells are not entrained by the flow of the culture medium (Gelinsky *et al*., 2015; Nazempour and Wie, 2018; Schulz and Bader, 2007).

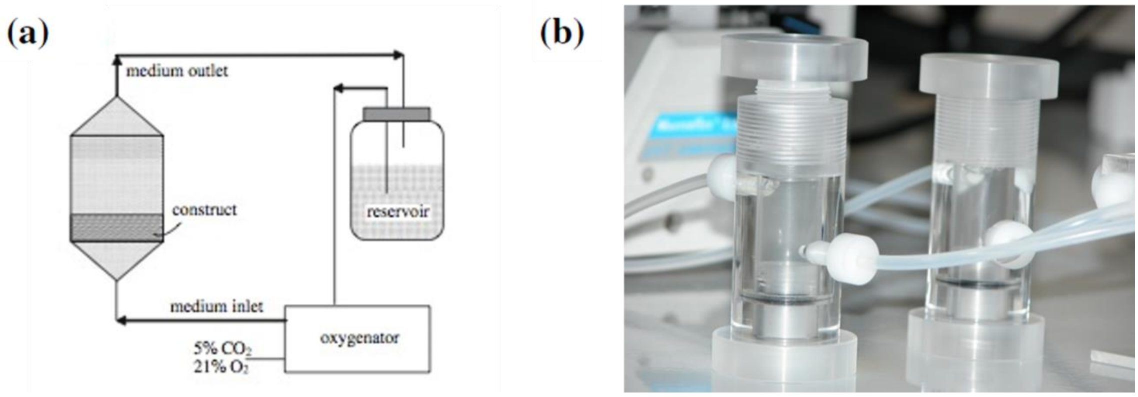

Figure 2.14 Illustration of an (a) perfusion bioreactor and (b) an example of a perfusion bioreactor (C.I.T., 2014; Chen and Hu, 2006).

In perfusion bioreactors nutrient delivery is not performed only on the periphery of the scaffold it also covers the internal zones (Chen and Hu, 2006; Gelinsky *et al*., 2015; Martin *et al*., 2004; Yeatts and Fisher, 2011). In addition, the continuous movement of the medium contributes to a more homogenous distribution of cells in the structure and also for greater homogenization of concentrations of gases, nutrients, metabolites and growth factors present in the medium (Gaspar *et al*., 2012; Korossis *et al*., 2005; Ravichandran *et al*., 2018). The success of this type of bioreactors depends on the following factors: (1) the relationship between the fluid velocity and the stage of cell maturation; (2) balance between the supply of nutrients and removing waste from the cells; (3) shear stresses exerted by the fluid passage and; (4) ability to retain the extra-cellular matrix (Diban *et al*., 2018; Egger *et al*., 2017; Martin *et al*., 2004). One of the limitations is the difference between stress and fluid speeds on the scaffold extremities compared with the inner part. This phenomenon can cause non-homogeneous distributions of cells or even cell drag if the fluid velocity is very high (X. Zhang *et al*., 2009).

Several studies have demonstrated the feasibility of perfusion in the bioreactor cell culture (Bancroft *et al*., 2002; Diban *et al*., 2018; Jaasma *et al*., 2008; Janssen *et al*., 2006; Lin *et al*., 2009; Nettleship, 2014; Pazzano *et al*., 2000; Sikavitsas *et al*., 2005). In these works, Pazzano *et al*. (2000) demonstrated the improved effectiveness of chondrocyte culture in the perfusion bioreactor comparatively to static culture. They have also observed an increase of 184% in the concentration of GAG, 118% in DNA content and 155% hydroxyproline.

Wendt *et al*. (2003) developed a bidirectional perfusion bioreactor which consists of two glass columns connected by a U tube (Figure 2.15). The equipment is composed of a set of sensors and actuators, and as a result of detecting a level of fluid (detected by the sensors), vacuum is applied, pressing it in the opposite direction.

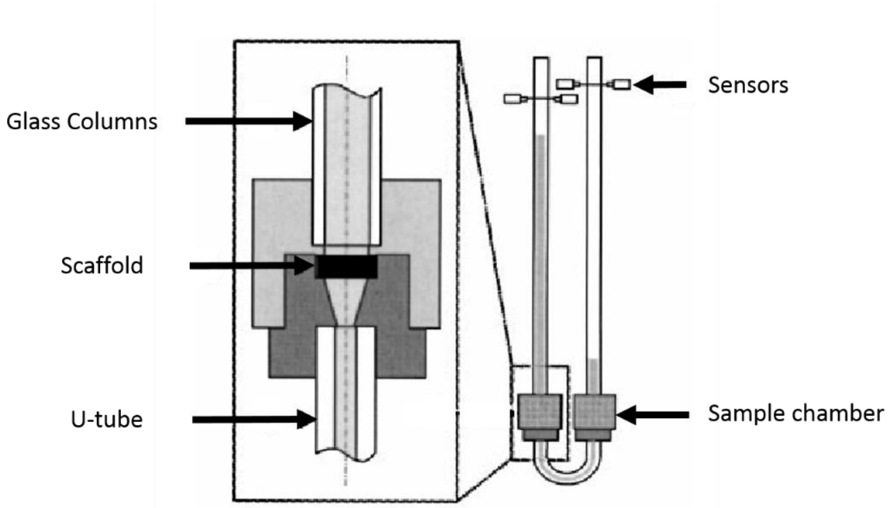

Figure 2.15 Bidirectional perfusion bioreactor in a U tube design (Wendt *et al*., 2003).

Hollow Fibre Bioreactor

These bioreactors were initially developed by Knazek *et al*. in 1972 (Curcio *et al*., 2017; Kumar *et al*., 2004) and consist of a cylinder containing bundles of parallel hollow fibres (Figure 2.16). This system includes a porous membrane that acts as a selective barrier to the transport of particles in the medium and has the ability to retain nutrients (*e.g.* high molecular weight proteins) from the cell, increasing its availability (Curcio *et al*., 2017; Hoesli *et al*., 2009; Kang *et al*., 2017; Martin and Vermette, 2005; Wang *et al*., 2005). In this type of bioreactor the primary method of mass transfer is the diffusion. However, the application of a pressure variation on the membrane surface can contribute to increasing the process, which increases the flow of nutrients in a given direction (Curcio *et al*., 2017; Wang *et al*., 2005). The cells are embedded in a gel inside the permeable membrane, and the perfusion occurs by pumping the culture medium from the outside of the permeable membrane. Applications using the Hollow Fibre Bioreactor (HFB) are carried out in cell culture with high and very sensitive metabolism, such as hepatocytes (Martin *et al*., 2004)or skin cells (Abousleiman and Sikavitsas, 2007; Curcio *et al*., 2017; Pörtner *et al*., 2005).

The significant advantage of these bioreactors is the ability to promote the delivery of nutrients to the centre of the growing tissue (Martin and Vermette, 2005). The main disadvantage includes the heterogeneity of culture, which is due to non-uniform gradients in the diffusion of oxygen and nutrients (Curcio *et al*., 2017; Martin and Vermette, 2005; Nguyen *et al*., 2005). This makes their use in the culture of animal cells a little limited (Wang *et al*., 2005).

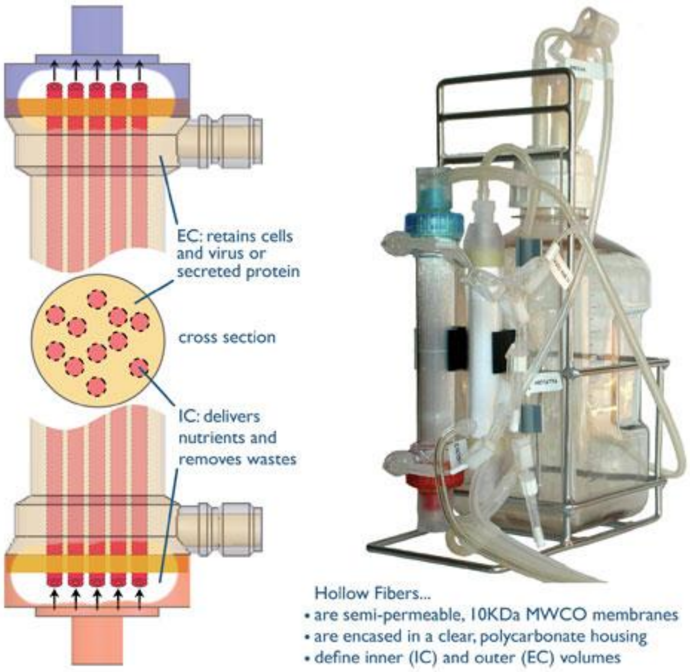

Figure 2.16 Basic hollow fibre bioreactor design and the HF Primer™ small-scale bioreactor (Hirschel *et al*., 2011).

Nguyen *et al*. (2005) presented a flow-type hollow fibre bioreactor with the aim of improving the delivery of nutrients. When studying the efficiency of the system in cultured hepatocytes concluded that with this strategy it is possible to increase the lifetime and the cell viability when compared to the same system without the introduction of a pulsed flow. Also, Hoesli *et al*. (2009) used this bioreactor in the encapsulation of mammalian cells in alginate process, obtaining good results.

Packed and Fluidised bed bioreactors

In this bioreactor (Figure 2.17) cells are immobilised in a column containing porous supports which are found fixed (packed bed) or floated (fluidised bed). This column is under continuous perfusion which causes the cells to suffer *stimuli* of hydrodynamic nature (Pörtner *et al.*, 2005; Ravichandran *et al.*, 2018; Zhang *et al.*, 2017). When comparing the fluidised bed bioreactor with the packed bed, it is found that the former allows greater productivity. However, their hydrodynamic complexity level is higher (Godia and Sola, 1995; Liu *et al.*, 2016; Zhang *et al.*, 2017). These bioreactors are used in the culture of mammalian cells, production of pharmaceuticals, cartilage cell culture, among others (Godia and Sola, 1995; Pörtner *et al.*, 2005; Ravichandran *et al.*, 2018; Skoneczny *et al.*, 2017).

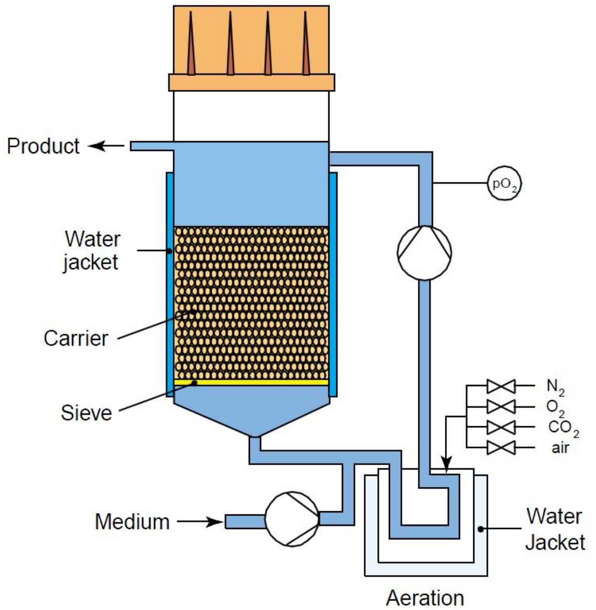

Figure 2.17 Schematic of the fluidised bed or packed bed bioreactor (Cabrita *et al.*, 2003).

Pulsatile flow bioreactor

The pulsatile flow bioreactor (Figure 2.18) is used primarily in cardiovascular tissue engineering and aims to simulate the conditions *in vivo* that these tissues are subjected. In these devices, the flow is pulsed through the cells and can have different frequencies and intensities; the fluid pressure is also similar to blood pressure in the human body. The pulsatile flow results from periodic inflation and deflation of a highly elastic membrane caused by an air pump (Aleksieva *et al.*, 2012; Brown *et al.*, 2008; Chen and Hu, 2006; Eaker *et al.*, 2017; Niklason *et al.*, 1999; Ravichandran *et al.*, 2018).

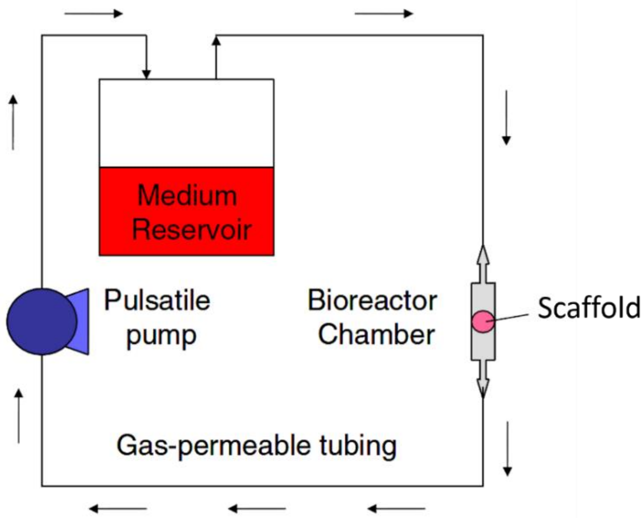

Figure 2.18 Schematic diagram of the pulsatile flow bioreactor system (Cooper *et al*., 2007).

Niklason *et al*. (1999) carried out the culture of smooth muscle cells using a pulsatile flow bioreactor for eight weeks. After this period, the appearance of the cultures blood vessels was similar to the original human arteries. Also, Brown *et al*. (2008) developed a perfusion bioreactor capable of applying pulsatile flows and allow the application of significant levels of shear stress. The system allows the regulation of the flow rate of the fluid carried by them, as well as their frequency of use. The same group of investigators tested in bioreactor culture of cardiac tissue and concluded that the pulsatile *stimulus* positively contributes to the contractile properties of the tissue originated.

The perfusion bioreactor, together with spinner flask and RWV are widely used in the tissue engineer of cartilage tissue, demonstrating successful *in vitro* culture of chondrocytes embedded in polymeric scaffolds (Aleksieva *et al*., 2012; Chen and Hu, 2006; Eaker *et al*., 2017; Ravichandran *et al*., 2018).

f. Mechano-Perfusion Bioreactors

In recent advances, a new type of bioreactors started gaining more interest due to their combination of several *stimuli* at the same time and in the same chamber (Koch *et al*., 2010; Nazempour and Wie, 2018; Pereira *et al*., 2014). Koch *et al*., (2010) using a perfusion bioreactor concluded that, by changing the fluid flow velocity and the perfusion cycle number, the cell-seeding efficiency was about 50%. There are several studies (Ishikawa *et al*., 2011; Liu *et al*., 2013; Sakai *et al*., 2009; Valmikinathan *et al*., 2011) demonstrating that tissue culture using dynamic bioreactors with improved fluid flow dynamics can improve cell seeding and also promote cell maturation. Also, the new bioreactors are biomimicking the physiological environment creating similar biological, physical, electrical or mechanical conditions in order to create new tissue (Koch *et al*., 2010; Pereira *et al*., 2014).

Nazempour and Wie, (2018), found a deficiency in current bioreactor models to simultaneously apply a different *stimulus* to cells, *i.e.*, applying a combination of shear stress and oscillating hydrostatic pressures. They built a new bioreactor for articular cartilage culturing that can provide both *stimuli* individually or combined (Figure 2.19).

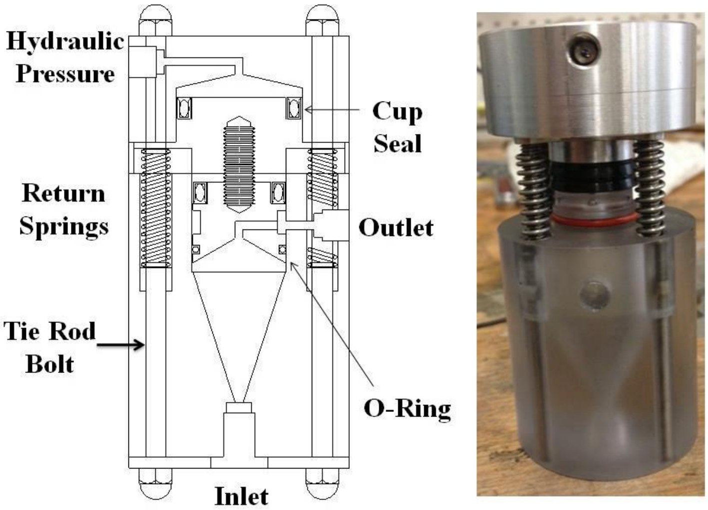

Figure 2.19 Double-piston bioreactor design (Nazempour and Wie, 2018).

2.2 Bioreactors – a brief comparison

As referred in the last chapter, the widely used bioreactors to culture tissues are the static and the functional tissue engineering (FTE) culture bioreactors that comprises all the bioreactors capable of providing dynamic stimulation. We are going to compare static culture to most used FTE bioreactors mentioned in the last chapter, *i.e.*, mixed flasks, rotating wall and perfusion bioreactor (Paez-Mayorga *et al*., 2018). These bioreactors provide different rates of nutrient supply to the tissue surface due to their distinctive flow conditions: static, turbulent and laminar (Malda *et al*., 2008; Paez-Mayorga *et al*., 2018; Rosser and Thomas, 2018; Zhao *et al*., 2016). The following table (Table 2.2) compares engineering parameters, advantages and limitations of these four types of bioreactors.

Table 2.2 Bioreactors comparison (Mekala *et al*., 2011; Salehi-Nik *et al*., 2013; Zhao *et al*., 2016).

Bioreactor Type	Description	Mass Transfer	Shear Stress	Special Usage	Tissue	Advantages	Limitations
Static Culture	Batch culture with no flow of nutrients	Diffusion (high)	Very Low	Cell proliferation	---	a. Favours cell adhesion, an optimum level of cell proliferation and produces better reproducible data.	a. Low seeding efficiency and a small number of cells can be maintained in culture due to the limited culture medium. b. Have presence of concentration gradients and also an oxygen inefficiency gas-liquid transfer.
Spinner Flask	Magnetically stirring of medium	Convection (high)	High	Dynamic seeding of scaffolds	Cartilage	a. Much easier to clean and sterilise the whole reactor setup. b. Through the transparent reactor vessel, it is very much possible to monitor every step in the reactor closely. c. Due to its small size (100ml-5L), media requirements and process cost can be minimised.	a. Recirculating flow patterns exert centrifugal force that drives the suspended cells against the vessel wall, and these hydrodynamic forces can damage the cells. b. Addition of gases (oxygen) is inevitable for large scale spinner flask, which can damage the cells due to cell bubble attachment.
Rotating Wall	Rotating at a speed, so the constructs in the reactor are maintained " stationary" in a state of continuous free fall	Convection (high)	Low	Tissue constructs which need dynamic laminar flow	Cartilage, bone and skin	a. Reduces the shear and turbulence generated by conventional stirred bioreactors. b. Effective for culturing difficult primary cell lines which are fragile. c. Culture cells in a more *in vivo* like environment.	a. The growth of heart and bone tissues found to be not uniform due to varying shear gradient across the rotating drum. b. Rotating-wall reactors need control systems to vary the rotation speed of the vessel in the function of the tissue size. c. Change in gravity also makes the term. Microgravity open to question. Since a rotating wall, bioreactor was designed to perform best in space.
Perfusion	The flow of medium over or through a cell population or bed of cells	Convection (moderate) and diffusion (high)	Moderate	Tissues physicochemical and environmentally relevant to human tissues	Epithelial cells, intestinal, bone, cartilage, and arteries	a. Perfusion bioreactor system is helpful for supporting the long-term development of 3D engineered tissue constructs using porous scaffolds. b. The perfusion bioreactor offers enhanced transport of nutrients, gases & metabolites due to effective media percolation through the interconnected pores of the scaffolds. c. The modular design of the perfusion system facilitates multiple tissue engineered construct production.	a. Though dynamic flow perfusion allows the media to percolate through the core of the construct. The cells on construct surface experience higher shear than the cells at inner core, creating a pressure gradient across the construct, which is typically not experienced by cells *in vivo*.

Other differences are the mass transfer rate and the shear stress during the cultivation process. Static culture presents limitations in the nutrient diffusion of large constructs because both external and internal mass transfer occurs by diffusion (Bueno *et al*., 2004; El Haj *et al*., 2005; Martin *et al*., 2004). Another significant limitation of this type of culture bioreactor is the deposition of waste materials as also the depletion of nutrients during the culturing process (Akter, 2016; Rolfe, 2006).

With the stirred flask the dynamic culturing of cells is possible due to the fact that the scaffolds will be attached to needles hanging from within this bioreactor which also will improve cell survival (Akter, 2016; Fernandes-Platzgummer *et al*., 2011; Khetani and Bhatia, 2006; Malda *et al*., 2005; Oragui *et al*., 2011; Yeatts and Fisher, 2011). Due to a convective flow created by a magnetic stirrer bar the construct is surrounded by the medium and compared to the static culture there will be an improvement of the nutrient diffusion and cell proliferation within the construct. The heterogeneity of the shear forces within this bioreactor as a downside of preventing the development of homogenous tissue (El Haj *et al*., 2005; Malda *et al*., 2008).

Rotating wall bioreactors, due to their dynamical laminar flow, promotes external mass transfer and also, improves typically the properties of the peripheral tissue layer (Akter, 2016; Belfiore *et al*., 2009; Oragui *et al*., 2011; Ravichandran *et al*., 2018; Salehi-Nik *et al*., 2013; X. Zhang *et al*., 2009). Comparing this bioreactors flow condition to the stirred flasks is easy to observe that this last has a higher shear stress level than the rotating wall bioreactor. With this low shear stress rate, the rotating wall bioreactor promotes the formation of cartilaginous tissues containing collagen and uniformly distributed glycosaminoglycans (GAG) (Hammond *et al*., 2016; Nesic *et al*., 2006; Rolfe, 2006; X. Yan *et al*., 2012).

A vital feature of the perfusion bioreactor as also, of the rotating wall bioreactor, is that the convective transfer within and around the scaffold at a proper flow rate will dissipate gradients of nutrients and aides to maintain the tissue mass (Khetani and Bhatia, 2006; Lin *et al*., 2009; Nettleship, 2014). Perfusion bioreactors are more known by forcing the culture medium through the pores of the scaffolds increasing the transport of nutrients and the necessary mechanical stimuli to cells (Abousleiman and Sikavitsas, 2007; Akter, 2016; Cimetta *et al*., 2007; Kim *et al*., 2007; Oragui *et al*., 2011; Plunkett and O’Brien, 2010; Sikavitsas *et al*., 2005). The nutrients and oxygenation of the culture are forced into the chamber and interior of the construct by diffusion and convection. It is of the most considerable importance to adjust the flow rate of the medium with respect to the limiting nutrient, frequently oxygen because of its low solubility (Malda *et al*., 2008; Martin and Vermette, 2005; Salehi-Nik *et al*., 2013). With a steady flow rate and a well-defined physicochemical culture environment the creation of homogenous tissue is possible, *e.g.* cartilage, vascular grafts or a uniform distribution of chondrocytes (Begley and Kleis, 2000; Démarteau *et al*., 2003; Lin *et al*., 2009; Nesic *et al*., 2006; Radisic *et al*., 2008; Song *et al*., 2012).

In short, Table 2.3 shows a comparison and the major differences of the culture conditions that static culture and FTE bioreactors can provide.

Table 2.3 Comparison of static culture versus FTE bioreactors (Paez-Mayorga *et al*., 2018).

Characteristics	**Static Culture**	**FTE**
Seeks architectural mimicry	V	V
Seeks functional mimicry	×	V
Culture conditions	Static	Mainly Dynamic
2D	V	V
3D	×	V
Biochemical stimulation	V	V
Mechanical and/or electrical stimulation	×	V
Compare results to native parameters	×	V

Table 2.4 shows the existing types of bioreactors developed until now, what kind of *stimulus* is applied and the corresponding tissue. Also, it is possible to observe the merits of each bioreactor study.

Table 2.4 Existent bioreactors and their characteristics, cultivated tissues and merits.

1st Author (year)	Bioreactor Characteristics/Type	Tissue	Merits
Lammi *et al.*, (1994)	Hydrostatic Static	Cartilage	High syntheses of proteoglycans
Vunjak-Novakovic *et al.*, (1998)	Shear Force/Spinner Flask	Cartilage	Enhanced kinetics
Prenosil and Kino-oka, (1999)	Automatic culture medium exchanger	Skin	Automated control of the culture
Mauck *et al.*, (2000)	Compression Dynamic	Cartilage	High increase in the equilibrium modulus
Altman *et al.*, (2002)	Perfusion/Strain based	hBMSCs	Cell density increase
Mizuno *et al.*, (2002)	Hydrostatic Pressure/Perfusion	Cartilage	High stimulation of aggrecans
Toyoda *et al.*, (2003)	Hydrostatic Pressure	Cartilage	Upregulation of mRNA
Yu *et al.*, (2004)	Shear Force/Rotating vessel	Bone	Enhanced bone cell phenotypic expression
Akmal *et al.*, (2006)	Shear Force/Rotating Vessel	Cartilage	Increase in staining intensity
Juncosa-Melvin *et al.*, (2006)	Mechanical stimulation	Collagen	Stiffness increase
Webb *et al.*, (2006)	Cyclic strain	Tendon	Stiffness increase
Androjna *et al.*, (2007)	Mechanical stimulation	Tendon	Cell density increase Stiffness increase
Mygind *et al.*, (2007)	Shear Force/Spinner Flask	Bone	Increased proliferation, differentiation and distribution
Shangkai *et al.*, (2007)	Stirred	Cartilage	Increase in DNA and GAG content
Candiani *et al.*, (2008)	Cyclic Hydrostatic Dynamic	Cartilage	2D to 3D guided cell differentiation
Grayson *et al.*, (2008)	Perfusion	Bone	Cell density increase
Sun *et al.*, (2008)	Aligned microfibres inserted in conduits	Nerve Conduit	Cellular adhesion and alignment
Nirmalanandhan *et al.*, (2008)	Mechanical stimulation	Tendon	Stiffness increase
Abousleiman *et al.*, (2009)	Mechanical stimulation	Tendon	Elastic modulus increase Cell proliferation
Butler *et al.*, (2009)	Mechanical stimulation	*N.A.*	Stiffness increase
Ladd *et al.*, (2009)	Uniaxial expansion	Skin	Increase in surface
Nguyen *et al.*, (2009)	Cyclic stretch	Tendons	Improved fibre orientation
Liu *et al.*, (2010)	Shear Force/Spinner Flask	Cartilage	Increase autologous tissue
Chen *et al.*, (2010)	Mechanical Stimulation	Tendon	Collagen increase Better cell alignment
Doroski *et al.*, (2010)	Cyclic stress	Human marrow	Collagen increase

Saber *et al.*, (2010)	Cyclic strain	Tendon	Stiffness increase
Santoro *et al.*, (2010)	Perfusion	Cartilage	Homogeneously tissue
Lei *et al.*, (2011)	Rotating cell with Microgravity	Skin	Multilayer epidermis structure
Woon *et al.*, (2011)	Cyclic axial loads	Tendon	Elastic modulus increase
Melchels *et al.*, (2011)	Perfusion	Cartilage	High cell deposition
Shahin and Doran, (2011)	Perfusion	Cartilage	Culture of larger constructs
Correia *et al.*, (2012)	Hydrostatic Dynamic/Pulsatile	Cartilage	High chondrogenic differentiation and matrix deposition
Takebe *et al.*, (2012)	Shear Force/Rotating Vessel	Cartilage	High cell proliferation
García Cruz *et al.*, (2012)	Shear Force/Stirred	Cartilage	Cell proliferation and differentiation
Aleksieva *et al.*, (2012)	Loop/Pulsatile flow	Heart Valves	Improvement of mechanical properties
Weinandy *et al.*, (2012)	Single loop circulation	Stents	Functional cell lining
Song *et al.*, (2012)	Vascular/Double Circulation Loop	Vascular Tissue	High cell proliferation. Large-scale vascular vessels
Yoon *et al.*, (2012)	Shear Force/Spinner Flask	Cartilage	Large-scale chondrogenic differentiation
Bilgen *et al.*, (2013)	Uniaxial/Biaxial mechanical strain	Stem cells	Elastic modulus increase Proteoglycan deposition
Chen *et al.*, (2013)	An integrated bioreactor that mimics the physiological pulsatile stimuli	Vascular Tissue	Simulation of circulatory hemodynamics
Wang *et al.*, (2013)	Mechanical stimulation	Tendon	Cell proliferation
Wang *et al.*, (2014)	Compression Dynamic	Cartilage	Cellular outgrowth and maturation
Laurent *et al.*, (2014)	Tension-Torsion Strain	Ligament	Cell proliferation
Goodhart *et al.*, (2014)	Cyclic Strain	GAG	Cell proliferation ECM production increase
Youngstrom *et al.*, (2015)	Cyclic mechanical stimuli	Tendon	Elastic modulus increase
Qin *et al.*, (2015)	Mechanical Strain	Tendon	Osteogenic differentiation Cell infiltration
Cook *et al.*, (2016)	Dynamic/uniaxial strain and electric *stimulus*	Several tissues	Cell proliferation
Wu *et al.*, (2017)	Mechanical stimuli	Tendon	Cell proliferation and infiltration Fibre alignment
Ravichandran *et al.*, (2018)	Biaxial rotation/Womb mimic	Bone	Higher maturation of cellular bone graft. Faster cell proliferation.

2.3 Scaffolds and cells

As mentioned in the first chapter, scaffolds need to meet several prerequisites in order to provide the necessary support to the cells. An adequate mechanical property is required to withstand the biodegradation, the shear stress and deformation before the tissue is fully grown. Also of extreme importance is adequate pore size, porosity and subsequently permeability to allow the cells to grow and increase their proliferation within the scaffold (Freitas *et al*., 2014b; Huang *et al*., 2018; Li and Cui, 2014; Tan *et al*., 2005; Truscello *et al*., 2012; Viana *et al*., 2013; Vyas *et al*., 2017). The material and the fabrication technique is of significant importance because it will shape not only the surface as the biocompatibility of the scaffold towards the cells (Huang *et al*., 2018; Porter *et al*., 2005; Sanz-Herrera *et al*., 2009; Tan *et al*., 2005; Viana *et al*., 2013). Table 2.5 shows the common properties of the scaffolds used in culture of several types of tissues in TE.

Table 2.5 Preferred scaffold properties for the different tissues (Zhang *et al*., 2018).

Tissue type	Pore size (um)	Porosity (%)	Elastic modulus
Cancellous bone	500-1000	50-90	0.1-0.5 GPa
Cortical bone	<500	3-12	3-30 GPa
Cartilage	400	80	0.7-15.3 MPa
Nerve	5-30	50-70	8-16 MPa
Subcutaneous adipose tissue	100	88-97	1.6-11.7 kPa
Skin	20-125	70-90	3-7 kPa
Liver	120-350	94	8-12 kPa
Kidney	100-300	---	5-10 kPa
Heart	40-160	---	10-15 kPa
Lung	100-300	---	3-6 kPa

3 Computational Simulation on Bioreactors

This third chapter will introduce several research works where simulation tools were used. Also, a brief theoretical explanation of fluids and mathematical modelling of fluids will be presented.

3.1 Mathematical modelling in TE

Mathematical modelling can be used to justify experimental results and help to decide future directions in TE (Chung *et al*., 2008, 2006; Gelinsky *et al*., 2015; Lewis *et al*., 2005; Malda *et al*., 2004; Zhou *et al*., 2011). Concerning the culture of cell-seeded porous structures for TE applications, there are just a few mathematical modelling studies which have focused on this thematic (O'Dea *et al*., 2008; Song *et al*., 2015; X Yan *et al*., 2012).

One of the most relevant roles of the numerical simulations is the prediction of the global dynamic responses in different areas of the bioreactor (Shi, 2008; Song *et al*., 2015; X Yan *et al*., 2012). Also, numerical analysis anticipates local hydrodynamic changes in tissue constructs within bioreactors (Jia *et al*., 2017; Shi, 2008; Song *et al*., 2015).

With recent computational tools, the estimation of variables such as flow fields within a new concept of bioreactor (Shakeel, 2011; Shakeel and Raza, 2014; Sucosky *et al*., 2004) or the shear stresses and mass transfer of scaffolds inside of a bioreactor (Salehi-Nik *et al*., 2013; Shakeel and Raza, 2014; Whittaker *et al*., 2009), the mechanics of certain scaffold biomaterials (Sengers *et al*., 2008), and the sufficiency of some bioreactor cultures (Chung *et al*., 2007; Coletti *et al*., 2006; Freitas *et al*., 2015b; Sucosky *et al*., 2004) can be easily predicted.

Park *et al*. (2018) study environmental conditions on which occurs the cell culture using Computational Fluid Dynamics (CFD) to study the behaviour of air bubbles in a microfluidic perfusion bioreactor. Air bubbles disturb the fluid flow which will cause instability on the cell culture conditions. Other studies also analyse both oxygen and shear stress conditions within the bioreactor. Regulating an optimum combination between the provided oxygen (that originate air bubbles) and the fluid flow velocity enhances cell proliferation and promotes a more homogeneous tissue (Cioffi *et al*., 2008; Grayson *et al*., 2011; Provin *et al*., 2008).

Initial studies using numerical simulation are often used to optimise bioreactors design. Santoro *et al*. (2010), used CFD to create a perfusion bioreactor capable of obtaining a uniform cell seeding distribution and create a homogeneous tissue. Figure 3.1 is possible to see on the right image the uniformity of the flow.

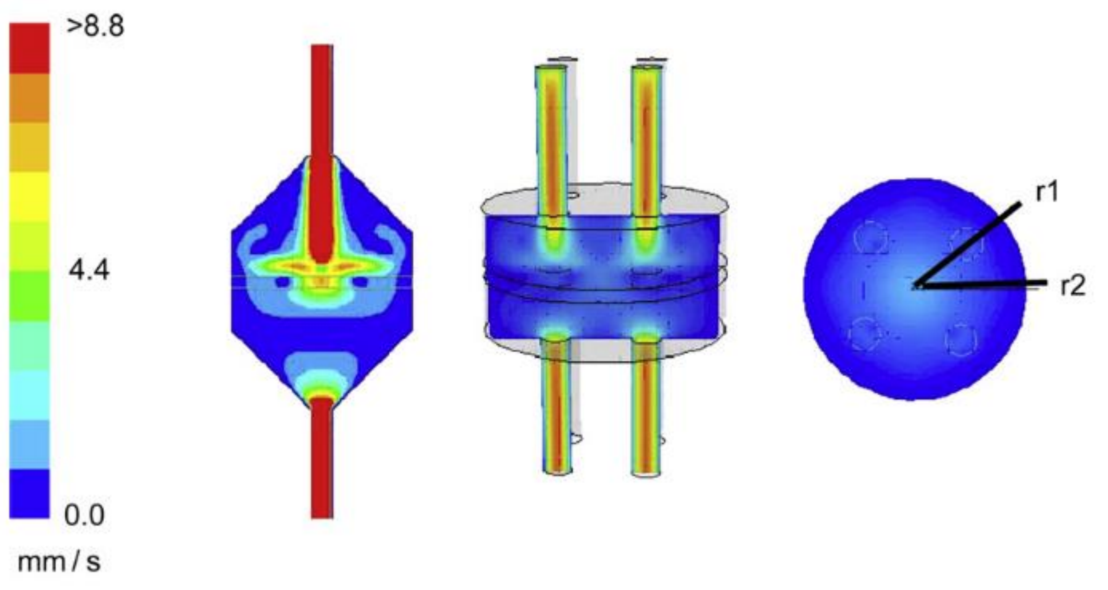

Figure 3.1 CFD analysis of two types of bioreactor. The left one is a single inlet/outlet chamber, and the middle and right image is the same four inlets/outlets bioreactor developed by Santoro *et al*, (2010).

Melchels *et al*. (2011) did a correlation between the numeric simulations and the distribution of cell densities. They analysed the influence of the fluid locally, around and within, on the scaffold in terms of shear stresses displayed on a colour map form and a microscopy image of the cell density after a perfusion culture process (Figure 3.2). It was concluded that the cell density was higher in the same areas wherein the colour mapping of the shear stress had the optimum values to enhance cell proliferation.

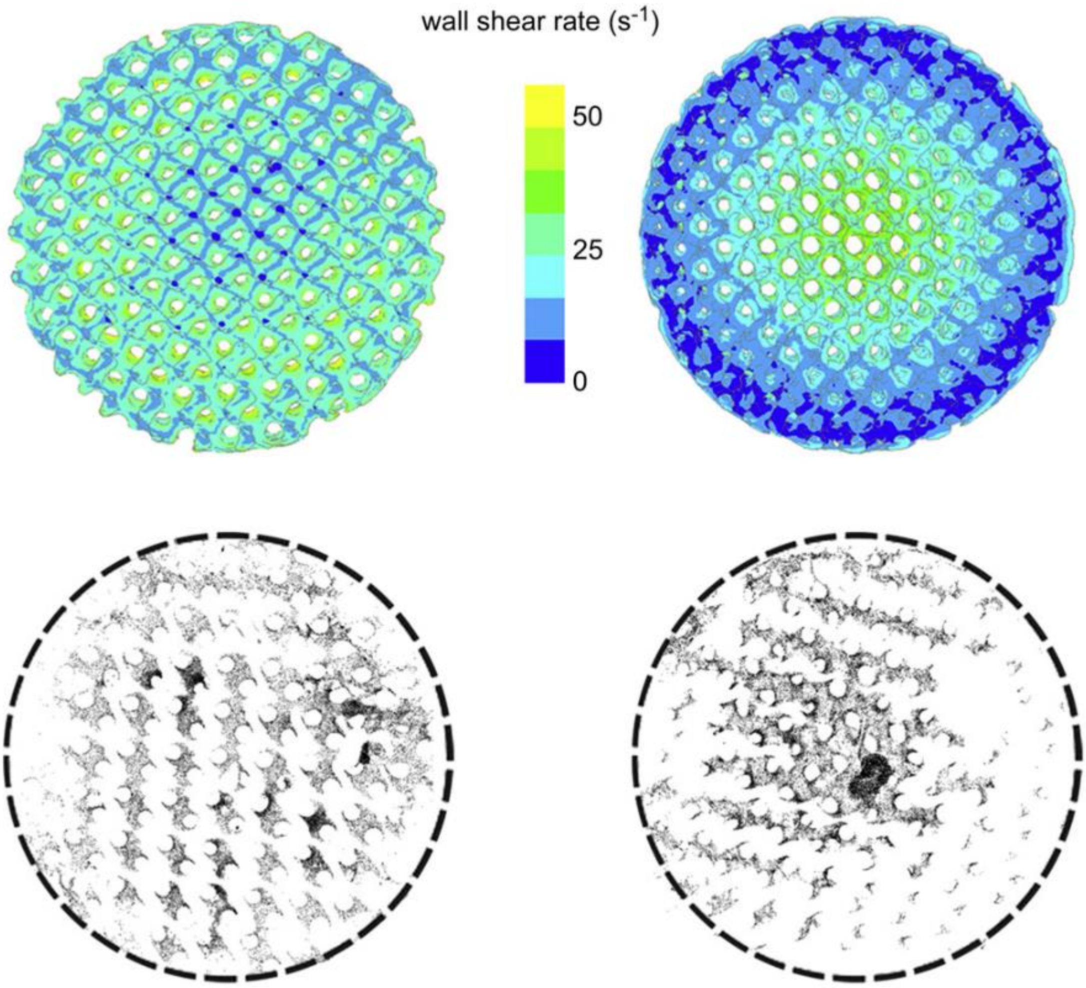

Figure 3.2 Comparison between the distribution of cell densities (bottom images) and the wall shear stress rates (top images) at the same cross-section. The left and right images differ on the scaffold homogeneity, where the right scaffold is heterogeneous (Melchels *et al*., 2011).

Pereira *et al*. (2014) studied the effect on the fluid flow and the shear stress on the the scaffold surface in a rotating bioreactor. Just by changing the length and diameter of the bioreactor chamber as also using three rotations (horizontal, vertical and the combination of both – biaxial). It was concluded that the distance of the inlet has a higher impact on the scaffold shear stress than the diameter and the biaxial rotation as more uniform behaviour with regard to the fluid flow and scaffold shear stress (Figure 3.3).

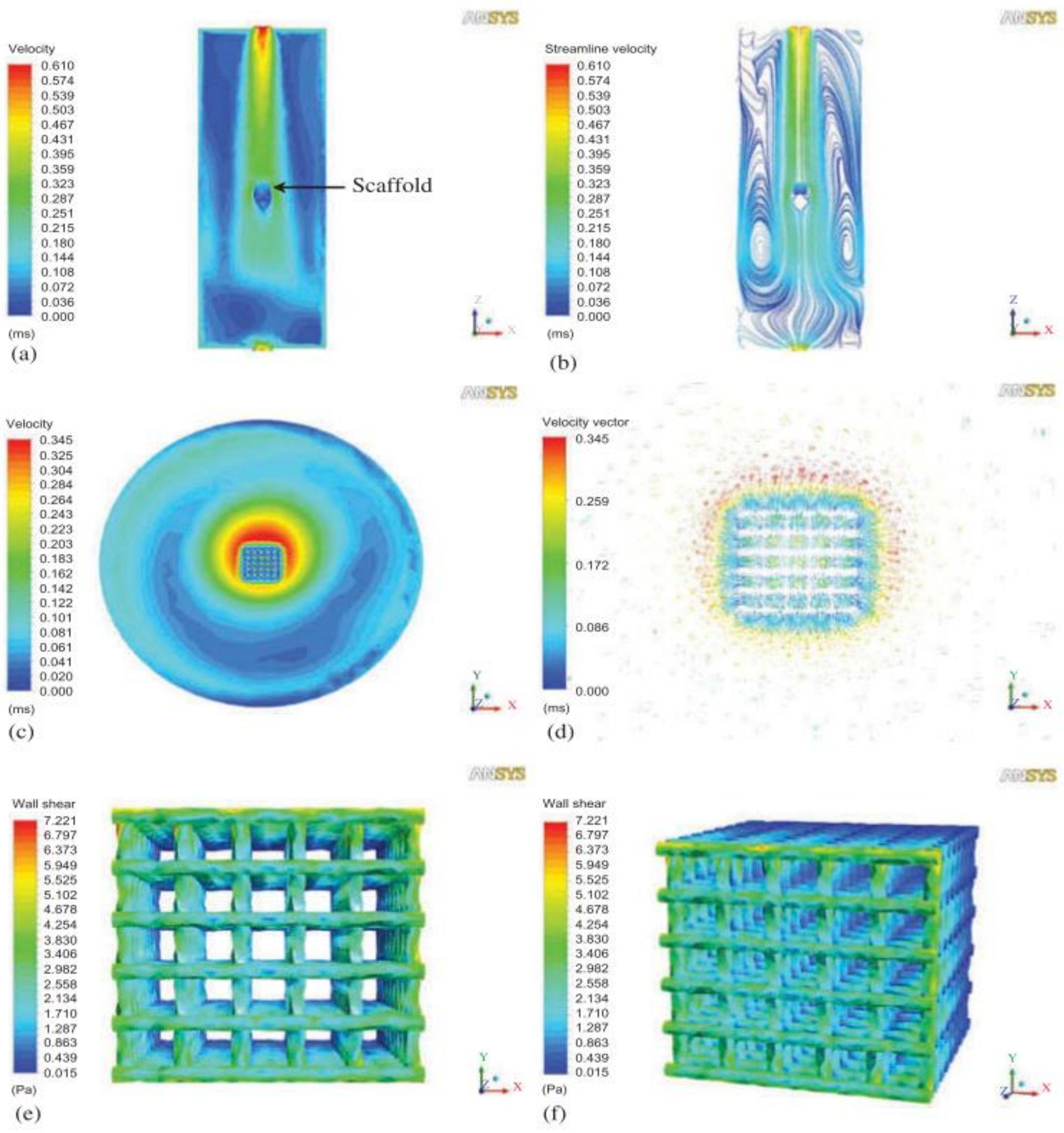

Figure 3.3 Biaxial rotation results regarding fluid velocity in the chamber and scaffold and scaffold shear stress (Pereira *et al*, 2014).

Almost all the studies in numerical simulations on bioreactors for TE focus on the optimization of the bioreactors design and mass transfer conditions as can be seen in the following studies (Cinbiz *et al.*, 2010; Egger *et al.*, 2017; Freitas *et al.*, 2014a; Hutmacher and Singh, 2008; Jungreuthmayer *et al.*, 2009; Kaul *et al.*, 2016; Lappa, 2005; Liu *et al.*, 2016; McCoy and O'Brien, 2010; Patrachari *et al.*, 2012; Porter *et al.*, 2005; Shakeel and Raza, 2014; Skoneczny *et al.*, 2017; Spencer *et al.*, 2013; X. Yan *et al.*, 2012; Zhang *et al.*, 2018)

3.2 Fluid Classification

The fluid is characterized by its inability to sustain deviatoric stresses when at rest and are classified into two major groups, the Newtonian and the non-Newtonian fluids. Essentially the difference between them depends strictly on the variation of the shear stress and the deformation ratio which can be represented by (Nguyen and Choi, 2012; Zienkiewicz *et al*., 2005):

$$\tau = \tau_y + \eta(\frac{du}{dy})^n \tag{3.1}$$

where τ is the shear stress, τ_y, η and n are constants, τ_y is the yield stress and is η the dynamic viscosity, du/dy is the deformation ratio. Figure 3.4 classifies the fluids according to their rheological properties. The viscosity of a Newtonian fluid is independent of time and shear rate and for that reason has an ideal behaviour (linear) as shown in Figure 3.4. Fluids are mention as plastic when the shear stress reaches a minimum value before it begins to flow. The non-Newtonian fluids are classified as plastic, Bingham plastic, pseudo-plastic and dilatant fluids (Douglas *et al*., 2005). The variation between the different classifications of non-Newtonian fluids varies with the constant n presented in Equation 3.1. If n is equal to one, the material is a Newtonian fluid but if the deformation rate does not reach a critical value of the shear stress the material is denominated as a Bingham plastic. If the dynamic viscosity decreases as the shear rate increases it is called a pseudo-plastic or shear-thinning fluid. If the opposite occurs, *i.e.*, the dynamic viscosity increases as the shear rate increases it is called a dilatant or shear-thickening fluid. In short, a dilatant fluid is represented by $n > 1$, a pseudo-plastic is represented by $n < 1$ and a Newtonian fluid is represented by $n = 1$ (Nguyen and Choi, 2012).

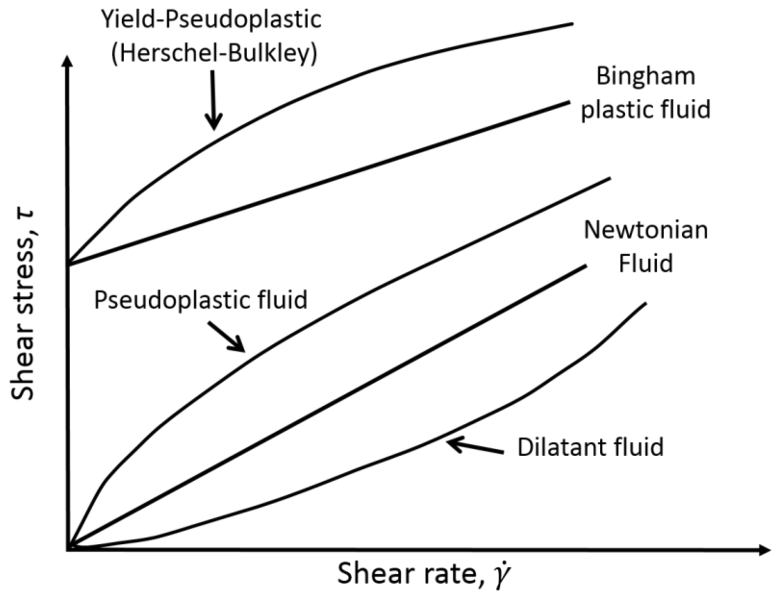

Figure 3.4 Classification of the rheological behaviour of fluids (adapted from Nguyen and Choi, 2012).

The materials can be yet characterised as thixotropic or rheopectic fluids depending on the variation of viscosity with the applied shear stress along time. If the viscosity decreases the fluid is called thixotropic if increases are called rheopectic (Derakhshandeh *et al.*, 2012).

3.3 Permeability Darcy's Law

In order to study the permeability of porous scaffolds, a method based on Darcy's Law seems to be an adequate approach. Darcy's law is a phenomenologically derived constitutive equation that describes the flow of a fluid through a porous medium (Dias *et al.*, 2012; Rahbari *et al.*, 2017; Viana *et al.*, 2013; Whittaker *et al.*, 2009).

Darcy's law is a simple proportional relationship between the instantaneous discharge rate through a porous medium, the viscosity of the fluid and the pressure drop over a given distance (Almeida and Bártolo, 2014; Dias *et al.*, 2012; Rahbari *et al.*, 2017).

$$Q = \frac{-kA}{\mu}\frac{(P_b - P_a)}{L} \tag{3.2}$$

The total discharge, Q (units of volume per time, *e.g.*, m^3/s) is equal to the product of the permeability of the medium, k (m^2), the cross-sectional area to flow, A (units of area, *e.g.*, m^2), and the pressure drop (P_b - P_a), all divided by the viscosity, μ (Pa·s) and the length over which the pressure drop is taking place (m). The negative sign is needed because fluid flows from high pressure to low pressure. If the change in pressure is negative (where $P_a > P_b$), then the flow will be in the positive '*x*' direction. Dividing both sides of the equation by the area and using more general notation leads to the following equation (Dias *et al*., 2012; Viana *et al*., 2013; Whittaker *et al*., 2009):

$$q = \frac{-k}{\mu} \nabla P \tag{3.3}$$

where q is the flux (discharge per unit area, with units of length per time, m/s) and ∇P is the pressure gradient vector (Pa/m). This value of flux, often referred to as the Darcy flux, is not the velocity which the water travelling through the pores is experiencing. The pore velocity (v) is related to the Darcy flux (q) by the porosity (n). The flux is divided by porosity to account for the fact that only a fraction of the total formation volume is available for flow. The pore velocity is the conservative velocity tracer would experience if carried by the fluid through the formation (Dias *et al*., 2012; Rahbari *et al*., 2017; Whittaker *et al*., 2009):

$$v = \frac{q}{n} \tag{3.4}$$

3.4 Computational Modelling

3.4.1 Navier-Stokes equation

The Navier-Stokes equations (Pozrikidis, 2009; Zienkiewicz *et al*., 2005) are differential equations that describe the flow of Newtonian fluids. These equations are partial derivatives for determining the velocity field and pressure in a flow. They were called after Claude-Louis Navier and George Gabriel Stokes that developed a set of equations that describe the motion of fluid substances such as liquids and gases.

The Navier-Stokes equation follows from the motion equation:

$$\rho \frac{du}{dt} = \nabla \cdot \sigma + \rho g \tag{3.5}$$

by substituting the constitutive equation for the stress tensor for an incompressible Newtonian fluid given by:

$$\sigma = -pI + 2\mu E \tag{3.6}$$

where σ is the stress, μ is the offset, t the time, ρ is the density, g is the gravitational acceleration, p is the pressure, μ is the fluid viscosity, I is the identity matrix, and E is the strain rate tensor.

For a fluid of uniform viscosity, the force of hydrodynamic volume is given by:

$$\sum \equiv \nabla \cdot \sigma = \nabla \cdot (-pI + \mu 2E) = -\nabla p + \mu 2\nabla \cdot E \tag{3.7}$$

In indicial notation, it is possible to observe that the default component of the second divergence tensor index of strain rate, E, is:

$$2\frac{\partial E_{ji}}{\partial x_j} = 2\frac{\partial}{\partial x_j}\left[\frac{1}{2}\left(\frac{\partial u_i}{\partial x_j} + \frac{\partial u_j}{\partial x_i}\right)\right] = \frac{\partial^2 u_i}{\partial_{x_j}\partial_{x_j}} + \frac{\partial^2 u_j}{\partial_{x_j}\partial_{x_i}} = \frac{\partial^2 u_i}{\partial_{x_j}\partial_{x_j}} + \frac{\partial}{\partial_{x_i}}\left(\frac{\partial_{u_j}}{\partial_{x_j}}\right) \tag{3.8}$$

Considering that the fluid is incompressible, the difference in velocity in the last term of Equation 3.8 enclosed in brackets is zero. In Equation 3.8, it is also possible to considerer:

$$\frac{\partial^2 u_i}{\partial_{x_j}\partial_{x_j}} = \frac{\partial^2 u_i}{\partial x^2} + \frac{\partial^2 u_i}{\partial y^2} + \frac{\partial^2 u_i}{\partial z^2} \equiv \nabla^2 \mathrm{u_i} \tag{3.9}$$

Using these results in order to simplify Equation 3.7 it is possible to verify that the force of hydrodynamic volume is given by:

$$\sum \equiv \nabla \cdot \sigma = -\nabla p + \mu \nabla^2 \mathrm{u} \tag{3.10}$$

Therefore, Equation 3.5 of movement is reduced to the Navier-Stokes equation.

$$\rho \frac{du}{dt} = -\nabla p + \mu \nabla^2 \mathrm{u} + \rho \mathrm{g} \tag{3.11}$$

that distinguishes from the Euler equation,

$$\rho \frac{Du}{Dt} = -\nabla p + \rho \mathrm{g} \tag{3.12}$$

by the presence of the viscous force represented by the product of the viscosity and the Laplacian of the velocity.

The Eulerian form of the Navier-Stokes equation involving the time and space derivatives is given by:

$$\rho\left(\frac{\partial u}{\partial t}+u\cdot\nabla u\right)=-\nabla p+\mu\nabla^2 u+\rho\mathrm{g} \tag{3.13}$$

The three main scalar Cartesian components of the Equation 3.23 are given by:

$$\begin{aligned}
\rho\left(\frac{\partial u_x}{\partial t}+u_x\frac{\partial u_x}{\partial_x}+u_y\frac{\partial u_x}{\partial_y}+u_z\frac{\partial u_x}{\partial_z}\right)&=-\frac{\partial p}{\partial x}+\mu\left(\frac{\partial^2 u_x}{\partial x^2}+\frac{\partial^2 u_x}{\partial y^2}+\frac{\partial^2 u_x}{\partial z^2}\right)+\rho g_x\\
\rho\left(\frac{\partial u_y}{\partial t}+u_x\frac{\partial u_y}{\partial_x}+u_y\frac{\partial u_y}{\partial_y}+u_z\frac{\partial u_y}{\partial_z}\right)&=-\frac{\partial p}{\partial y}+\mu\left(\frac{\partial^2 u_y}{\partial x^2}+\frac{\partial^2 u_y}{\partial y^2}+\frac{\partial^2 u_y}{\partial z^2}\right)+\rho g_y\\
\rho\left(\frac{\partial u_z}{\partial t}+u_x\frac{\partial u_z}{\partial_x}+u_y\frac{\partial u_z}{\partial_y}+u_z\frac{\partial u_z}{\partial_z}\right)&=-\frac{\partial p}{\partial x}+\mu\left(\frac{\partial^2 u_z}{\partial x^2}+\frac{\partial^2 u_z}{\partial y^2}+\frac{\partial^2 u_z}{\partial z^2}\right)+\rho g_z
\end{aligned} \tag{3.14}$$

3.4.2 Turbulence Kinetic Energy

One of the fundamental problems of Fluid Dynamics has been, and still is, the Turbulence. Taking that into account, there are several theoretical analysis and prediction models that are carried out in CFD simulations (Li *et al.*, 2013; Vickers and Thomas, 2013; Zienkiewicz *et al.*, 2005). The description of turbulent flow is so complex, and for that reason, the existing formulations may go from just simple definitions of skin friction or heat transfer coefficients, going up to a more specific energy spectra's and turbulence fluctuation magnitudes and scales (Celik, 1999; Liovic *et al.*, 2012; Xie *et al.*, 2016).

Several models can characterise fluid: there are the zero-equation models, one-equation models, two-equation models and there are more advanced models. To carry out the study of the turbulence within the chamber of this perfusion bioreactor, the Turbulence Kinetic Energy (TKE) model was used, and it is a one-equation model. It is an alternative to the algebraic model, and it predicts, by solving one additional transport equation, the turbulent flow. Despite the fact that common turbulent scales are often used as the variable in the transport equation, one of the most used methods is the calculation of the characteristic turbulent velocity scale proportional to the square root of the specific kinetic energy of turbulent fluctuations that is usually referred as turbulence kinetic energy, denoted by *k*. The variable *k* can be obtained by the mean of the turbulence normal stresses:

$$k = \frac{1}{2}\left(\overline{u'u'} + \overline{v'v'} + \overline{w'w'}\right) \tag{3.15}$$

where k is the turbulence kinetic energy; *u'*, *v'* and *w'* are the three fluctuating components of velocity. The full form of the TKE equation can be observed in the following equation:

$$\frac{\partial u}{\partial t} + \overline{u_j}\frac{\partial \mathrm{k}}{\partial x_j} = -\frac{1}{\rho}\frac{\overline{\partial u'_i p'}}{\partial x_i} - \frac{\overline{\partial k u'_i}}{\partial x_i} + v\frac{\overline{\partial^2 k}}{\partial x_j^2} - \overline{u'_i u'_j}\frac{\partial \overline{u_i}}{\partial x_j} - v\,\overline{\frac{\partial u'_i}{\partial x_j}\frac{\partial u'_i}{\partial x_j}} - \frac{g}{\rho_0} - \overline{\rho' \mathrm{u}'_i \delta_{i3}} \tag{3.16}$$

Where $\partial k/\partial t$ is the local derivative; $\overline{u}_j \partial k / \partial x_j$ is the advection value; $1/\rho_0\, \partial u'_i\, p' / \partial x_i$ is the pressure diffusion; $\partial k u'_i / \partial x_i$ is the turbulent transport (*T*); $v \partial^2 k / \partial x_j^2\, v$ is the molecular viscous transport value; $\overline{u'_i\, u'_j}\, \partial \overline{u_i} / \partial x_j$ is the production (*P*); $v \partial u'_i\, \partial u'_i / \partial x_j\, \partial x_j$ is the dissipation (ε_k); and the $g/\rho_0 - \overline{\rho' u'_i}\delta_{i3}$ is buoyancy flux (Baldocchi, 2005; Li *et al*., 2013; Zienkiewicz *et al*., 2005).

3.4.3 Reynolds Number

Reynolds number was coined by Arnold Sommerfeld in 1908 after Osborne Reynolds popularised the concept in 1883. It is dimensionless and can help predict flow patterns in different fluid flows. Reynolds number describes the fluid mechanics at a certain velocity in a determined interior of, *e.g.* pipe. The fluid flow can be characterised by laminar (a steady still flow) or turbulent (Celik, 1999; Singh *et al*., 2007; Zienkiewicz *et al*., 2005).

Moody (1944) studied the flow in a closed pipe that, analytically, can be studied using his chart (Figure 3.5) and determine the flow regime. The behaviour of the flow that can be described through the friction factor depends on the Reynolds number and in the relative roughness (Moody, 1944). The relative roughness indicates that there is a region that behaves differently because it is too close to the boundary. In the chart, fully turbulent flows are described in the right which will occur if Re is high and/or roughness values are also high. Laminar flow is linear and independent of the roughness, and it is reported on the left of the chart. The transition regime is described in the centre of the chart and where can be observed that the friction factor is heavily dependent on the relative roughness and also the on the Reynolds number (Moody, 1944; Stewart, 2016)

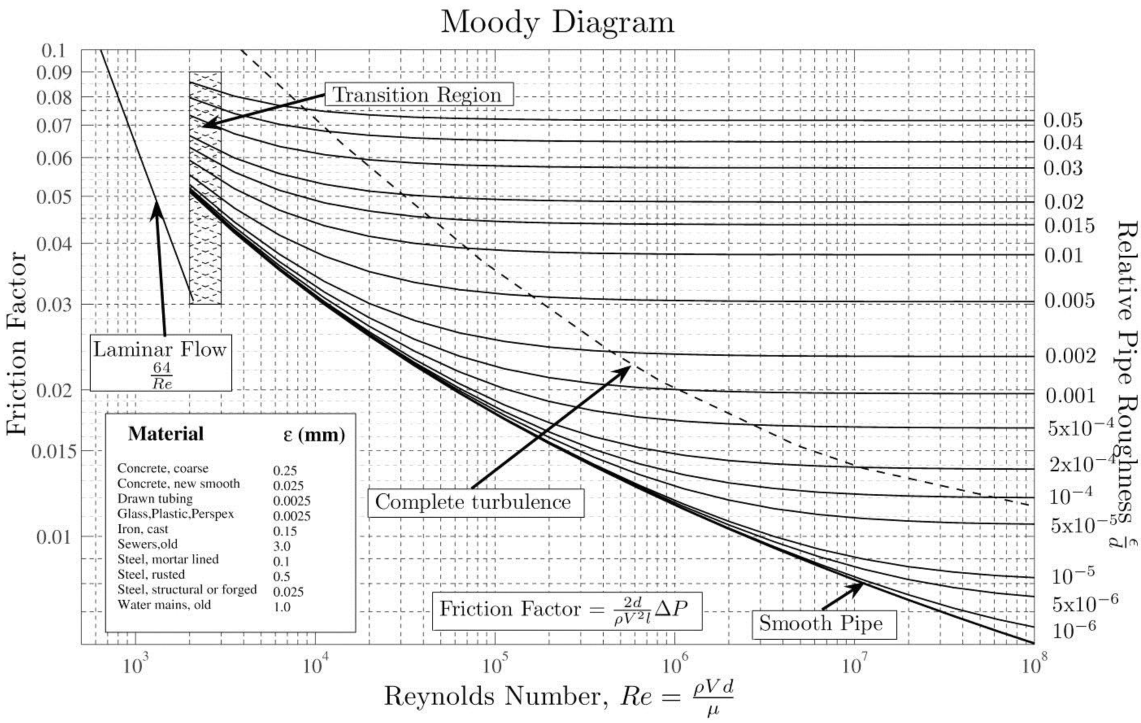

Figure 3.5 Moody's diagram where it is possible to observe the transition regime of the flow (Moody, 1944; Stewart, 2016)

The apparatus that Osbourne Reynolds developed enabled to study the transition of the fluid flow from laminar to turbulent. At low Reynolds numbers the fluid tends to be laminar, where viscous forces are dominant, and the fluid is smooth and constant, with higher Reynolds number the fluid tends to be turbulent and is dominated by inertial forces, provoking chaotic eddies, vortices and other flow variabilities (Celik, 1999; Zienkiewicz *et al.*, 2005).

The initial equation of Reynolds number can be obtained through the nondimensional form of the incompressible Navier-Stokes (Equation 3.17) and can be defined as

$$Re = \frac{\rho u L}{\mu} = \frac{uL}{\upsilon} \tag{3.17}$$

where, ρ is the density of the fluid; u is the velocity of the fluid considering the object; L is the characteristic linear dimension; μ is the dynamic viscosity of the fluid; and υ is the kinematic viscosity of the fluid.

Considering that the mechano-bioreactor presented in this study as the fluid flow passing to a pipe the Reynolds number must be defined as

$$Re = \frac{\rho u D_H}{\mu} = \frac{u D_H}{\upsilon} = \frac{Q D_H}{\upsilon A} \tag{3.18}$$

where, D_H defines the hydraulic diameter of the pipe; Q is the volumetric flow rate; A is the cross-section area of the pipe; ρ is the density of the fluid; u is the mean velocity of the fluid; μ is the dynamic viscosity; and υ is the kinematic viscosity both of the fluid.

To the fluid be considered fully developed flow and be considered laminar the Reynolds number must be $Re_D < 2300$ and to be considered turbulent $Re_D > 2900$ (Pok *et al*., 2013; Singh *et al*., 2007; Williams *et al*., 2002; Zienkiewicz *et al*., 2005).

3.4.4 Mesh Requirements

Finite element method (FEM) is the main part of the numerical simulations for solving mathematical problems computationally. FEM simplifies the interpretation of a geometry/object by the software and able the prediction of their behaviour. By dividing a geometry/object into several parts (mesh) this will enhance the representation of complex geometries, will simplify the representation of the total solution and also enables the capture of local effects (Reddy, 2006; Zienkiewicz *et al*., 2013).

A mesh is the discrete representation of the geometry. The mesh needs to take into account several parameters to increase its quality. Parameters as elements, size and shape, distribution, number of elements, among many others. Several shapes can be used to define the elements: tetrahedral, pyramid, triangular prism, hexahedron or polyhedron. To measure the quality of a mesh it is possible to use some indicators as the skewness and orthogonality of the elements. Depending on the value given it is possible to know if the mesh suits the needs of the calculation (Bakker, 2012; Reddy, 2006; Zhang *et al*., 2018; Zienkiewicz *et al*., 2013, 2005).

a. Skewness

Skewness is one of the primary quality indicators of mesh quality and suitability. Skewness determines how close to the ideal a face or cell is. Higher the value worse the quality of the mesh (Ansys, 2017; Bakker, 2012). Figure 3.6 shows the ideal shapes to consider the optimum cell quality and skewed cells with lousy quality.

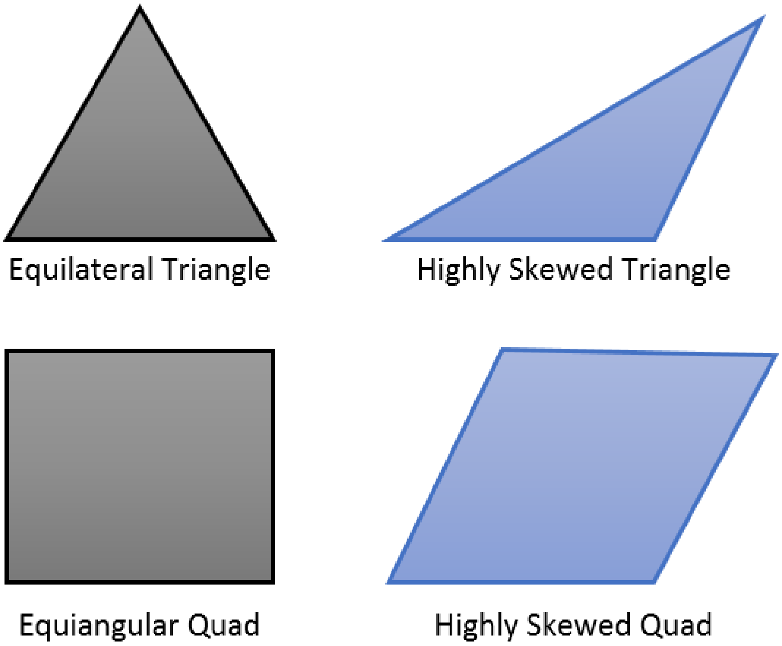

Figure 3.6 Ideal and Skewed geometries (Ansys, 2017; Bakker, 2012)

There are two methods to calculate Skewness. The first method is based on equilateral volume and is applied only to triangles and tetrahedrons. The second method is based on the deviation of the normalised equilateral angle and can be applied to all cell and face shapes like prisms or pyramids (Ansys, 2017; Bakker, 2012).

In the first method, the skewness is defined as

$$Skewness = \frac{Optimal\ cell\ size - Cell\ size}{Optimal\ cell\ size} \tag{3.19}$$

where, the optimal cell size is the size of an equilateral cell with the same circumradius.

The second method, based on the deviation of the angle of a normalised equiangular shape. In this method, skewness is generally defined as the maximum ratio of angular deviation from the ideal element. Can be calculated using the following equation

$$Skewness = max\left[\frac{\theta_{max}-\theta_e}{180-\theta_e}, \frac{\theta_e-\theta_{min}}{\theta_e}\right] \tag{3.20}$$

where, θ_{max} is the largest angle in the face or cell; the θ_{min} is the smallest angle in the face or cell; the θ_e it is the angle for an equiangular face or cell. If the shape is equilateral triangle $\theta_e = 60°$ and if it is a square $\theta_e = 90°$.

The first method is the most common for the calculation of the skewness. In Table 3.1, it is possible to see the range of skewness values and the corresponding quality.

Table 3.1 Range of values of skewness (Ansys, 2017).

Value of Skewness	Cell Quality
1	Degenerate
0.9 – <1	Bad
0.75 – 0.9	Poor
0.5 – 0.75	Fair
0.25 – 0.5	Good
>0 – 0.25	Excellent
0	Equilateral

A value of 0 indicates an equilateral cell, *i.e.*, the best quality of cell possible. If skewness is equal or higher than 1 the cell is in the worst quality and has to be re-meshed. Generally, cells that have a Bad (also known as Slivers) quality are characterised to have nodes that are nearly coplanar (Ansys, 2017).

The average quality of the meshes varies depending on if it is 2D (quality of 0.1) or 3D (quality of 0.4). For 2D, cells must have a Good or better-quality rating. Cells with Fair or worse indicates a poor boundary node. Concerning 3D cells, most of the cells can be Good or better, but it is admitted to have a small percentage in the Fair cell quality, and also it is admitted to have a few with Poor quality. Normally it is considered for 3D simulations to have a cell quality lower than 0.85 (Ansys, 2017; Bakker, 2012).

b. Orthogonality

While skewness indicates the distortion of an element shape in comparison to the respective ideal shape, orthogonality indicates how close the angles between adjacent element faces or edges are to some optimal angles (*e.g.* 90º for quadrilateral elements and

60º for the triangular faces). Figure 3.7 shows how the measurement of the orthogonality occurs. The angle between the vector that joins two mesh nodes – denominated by (s) in the figure – and the normal vector for each integration point associated with the related edge (n). Ip1 shows significant orthogonality while Ip2 reveals non-orthogonality (Ansys, 2017; Bakker, 2012; Zienkiewicz *et al.*, 2005).

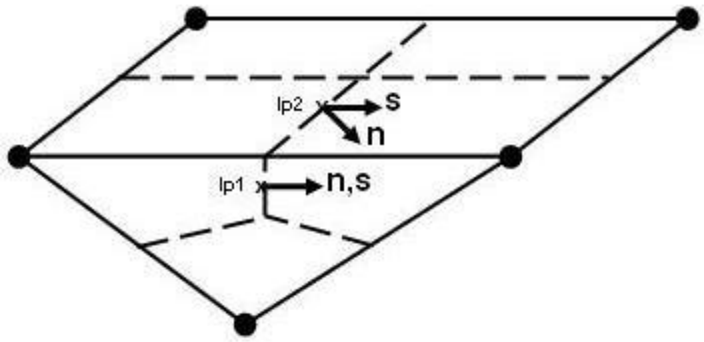

Figure 3.7 Measurement of the orthogonality (Ansys, 2017)

The acceptable range for the orthogonality angle has to be bigger than 20º (O_A>20º). This will indicate a robust and accurate general solution, values closer to zero (0º) will not produce reliable results because the cells do not have high quality (Ansys, 2017).

3.5 Mathematical Formulation of the Scaffold degradation

As mentioned in the previous chapter, polymeric scaffolds will be used for tissue culture *in vivo* or *in vitro*. Regardless of the method of tissue culture, the scaffold itself will be exposed to a diversity of biochemically and biophysically signals that will affect the scaffold in varied ways, namely:

i. Hydrolysis or other forms of chemical separation which produce oligomers and monomers in the polymer matrix;
ii. Mass transport within the polymer matrix and exchange of these products with the neighbourhood;
iii. Bioabsorption of compatible biodegradable products.

In this context, experimental studies were done in order to facilitate the understanding of the mechanisms of biodegradation in a complex process as described (Amass *et al.*, 1998).

Conceptually, degradation is defined as a set of molecular changes due to chain split within the polymer matrix, whereas surface erosion corresponds to structural and phenomenological changes due to the loss of mass of the degraded chains. Although detailed mechanisms have not yet been fully comprehended, extensive experimental studies have led to the exploration of degradation and erosion pathways (Chen *et al*., 2011). The split of the polymer matrix chains occurs when the adjacent water molecules attack the chemical bonds immediately after the surrounding solution begins to enter the matrix. As a result, both the penetration rate and the hydrolytic rate can determine the degradation pattern (Burkersroda *et al*., 2002; Hoque, 2017; Tamada and Langer, 1993).

If the rate of penetration of water exceeds the natural hydrolyzability of the polymer, degradation must occur on the polymer matrix as a whole, with uniform degradation, *i.e.*, degradation by mass. On the other hand, if the diffusion of the water molecules is relatively low, the hydrolysis will most likely occur in the form of surface erosion (Chen *et al*., 2011). However, these two extreme cases can co-occur for some materials with sophisticated configurations, which can significantly affect controlled release systems and tissue regeneration. The existence of models that correctly describe the different phenomena associated with the degradation process is, therefore fundamental. For this reason, the model of biodegradable mechanisms is a crucial step in controlling and regulating the degradation process (Amass *et al*., 1998; Han and Pan, 2011).

In the development of scaffolds for ET and controlled release systems, only simple degradation models are contemplated which do not contemplate, for example, aspects related to the effect of mechanical stresses under degradation. More recently, hybrid degradation mathematical models have been developed that combine stochastic hydrolysis and autocatalysis diffusion to simulate internal degradation and surface erosion (Chen *et al*., 2011).

Almeida *et al*. (2016) performed enzymatic degradation of a PCL (CAPA 6500) and obtained the results observed in Figure 3.8. On both graphics, it is possible to see the volume reduction of the scaffold on the left and on the right the variation of porosity both variables over time.

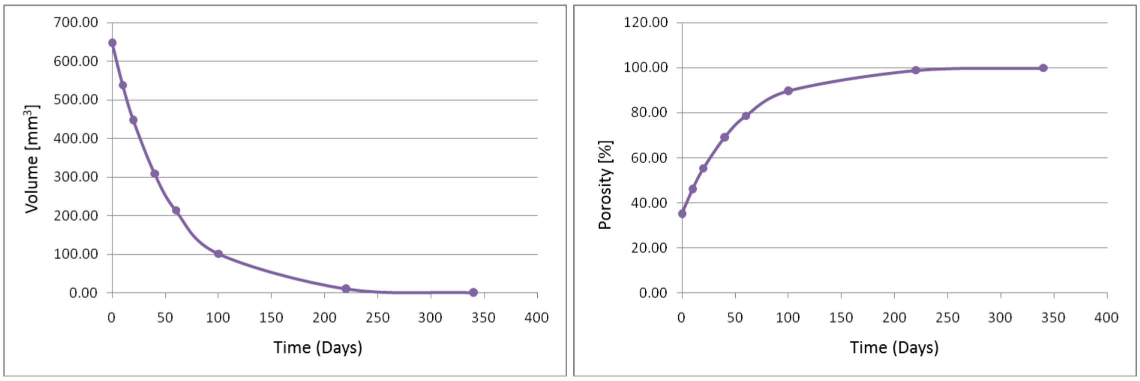

Figure 3.8 On the right the volume reduction of the scaffold and on the left the variation of porosity, both over time (Almeida *et al*., 2016).

<u>Initial considerations</u>

Consider a biodegradable polymer with a random configuration in a regular domain. In addition to the spatial variables, we also consider a variable x indicating two different states of degradation: "hydrolyzable" (x_h=1) and "hydrolyzed" (x_h = 0.001). For the sake of simplicity, also consider that the size distribution of the polymer chains and the initial density is uniform throughout the polymer matrix (Chen *et al*., 2011).

<u>Stochastic model of degradation</u>

In the hydrolytic reaction, the water molecules attack the bonds of the polymer chain, leading to a decrease in the average molecular weight of the polymer matrix (Burkersroda *et al*., 2002). According to experimental results, polymer degradation can be defined by first-order kinetic equations (Chen *et al*., 2011; Hoque, 2017):

$$M_a^t = M_a^0 e^{-\lambda t} \tag{3.21}$$

where M_a^0 and M_a^t are the average molecular weights at the initial time (t = 0) and at the instant of time, respectively, and λ is the rate of degradation constant (Chen *et al*., 2011). The molecular weight loss during degradation, M_a^l, is given by:

$$M_a^l = 1 - \frac{M_a^t}{M_a^0} = 1 - e^{-\lambda t} \tag{3.22}$$

According to the model developed by Göpferich (Göpferich, 1997), the degradation process can be considered as a stochastic event (process or random event that is time-dependent) for all hydrolyzable elements ($x_H = 1$). The mean molecular weight loss (Equation 3.22) corresponds to the first-order stochastic process of Erlang, where the density probability function, p, defines the probability of hydrolysis of a single hydrolyzable element and can be calculated from the following equation:

$$p(\lambda, t) = \lambda e^{-\lambda t} \tag{3.23}$$

the stochastic hydrolysis model described by Equation 3.23 contains some mathematical restrictions that need to be modified to describe the mechanism of degradation correctly. Firstly, it should be noted that the degradation kinetics described by Equation 3.21 is applicable when the initial polymer matrix has no surface irregularities. Thus, for a polymer with an initial porosity α, the probability density function defined in Equation 3.23 is imprecise. Since the probability of hydrolysis is identical for all the hydrolyzable elements at a specific time t, the degradation of the porous matrix can be considered from an initial state of low porosity and degraded gradually, as shown in Figure 3.9.

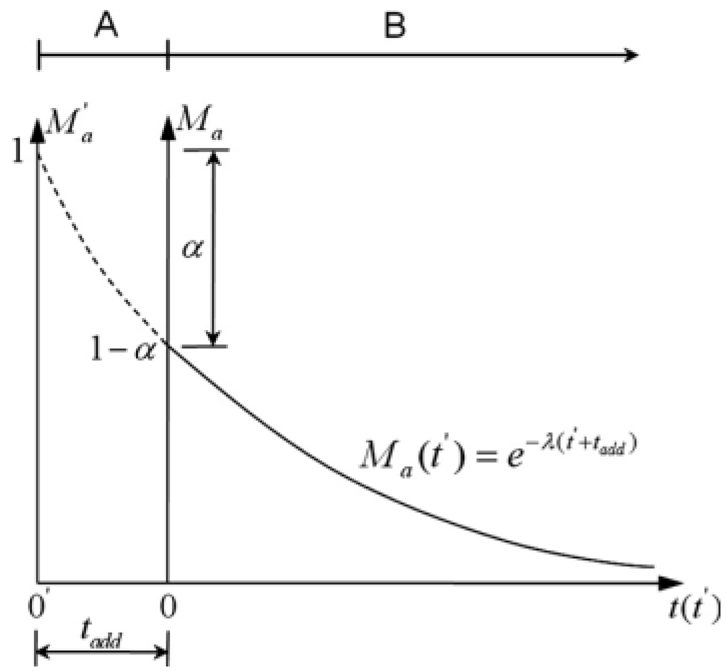

Figure 3.9 Schematic diagram to determine the hysteretic delay t_{add} for a polymer matrix with the initial porosity α.

As indicated in Figure 3.9, the hysteretic delay (the tendency of a material or system to conserve its properties in the absence of the *stimulus* that generated them), t_{add}, for a polymer matrix with initial porosity α, and considering Equation 3.2 can be calculated as:

$$t_{add} = -\frac{\ln{(M_a^t/M_a^0)}}{\lambda} = \frac{\ln{(1-\alpha)}}{\lambda} \tag{3.24}$$

In order to improve the computational efficiency, only the hydrolyzable elements (x_H=1) are considered in the stochastic model. In this way, it is possible to define a new density probability function *P* (*λ, t*), according to the following equation:

$$P(\lambda, t) = \frac{\lambda e^{-\lambda(t+t_{add})}}{V(t)} = \frac{\lambda e^{-\lambda t}}{V_0 V(t)} \tag{3.25}$$

where *V* (*t*) is the volume fraction of the polymer matrix at time *t* and V_0 is the initial volume fraction. Consequently, both the initial porosity and the porosity generated by the degradation can be considered proportionally by the increase of *P (λ, t)*.

Other studies present other degradation models that were carried out by (Han *et al*., 2010; Han and Pan, 2011). Han *et al*. (2010) presented a computational model of polyester biodegradation. This model comprises essential aspects such as molecular weight distribution, random split rates and the copolymer ratio as input data, being solved by the Monte Carlo method (MCM). In this case, the rate of the split of the nth ester-like bond is described by:

$$\frac{dR_i}{dt} = k_i C_i + k_i^a C_i C_{ol}^{0.5} \tag{3.26}$$

where R_i is the mole number of the total chain split of the nth ester-type bond per unit volume, *t* is the time, C_i is the mole concentration, C_{ol} is the molar concentration of oligomers and k_i^a represents the constants associated with the reactions of catalytic and autocatalytic hydrolytic processes. Chain split of the nth ester-type bond occurs if:

$$\sum_{j=1}^{i} \frac{dR_j}{dt} < \xi_1 \times \sum_{j=1}^{N} \frac{dR_j}{dt} < \sum_{j=1}^{i+1} \frac{dR_j}{dt} \tag{3.27}$$

where ξ1 Є (0,1) is a uniform random number and N is the total number of different types of ester bonds.

Han *et al*. (2010) presented a model based on the acceleration of tests at high temperatures, which has become an attractive but controversial technique, as an alternative to the high time (months to years) in which polymeric resorbable implants delay degrading. This study resulted in optimised formulas, which were based on the work of Han and Pan, (2011). Among all the optimised formulations, the following situation stands out:

$$\frac{M_n}{M_{n0}} = \frac{1 - tanh\left(\frac{t}{t\infty}\right)^2}{1 + \rho\ tanh\left(\frac{t}{t\infty}\right)^2} \quad (3.28)$$

where

$$t_\infty = \frac{2}{\propto k_2 \sqrt{C_{e0}}} \quad (3.29)$$

is the time characteristic for the hydrolytic reaction, and

$$\rho = \frac{C_{e0}}{N_{chain0}}\left(\frac{1}{\alpha} - \frac{1}{m}\right) \quad (3.30)$$

in which C_{e0} / N_{chain0} is the degree of polymerisation of the polymer. This equation was valid for the entire biodegradation process.

4 Novel Mechano-Perfusion Bioreactor Proposed

In this chapter, composed of two subchapters, it is presented the proposed design of a novel Mechano-Perfusion bioreactor and as also the goals of this research work in the first subchapter. The applied simulation parameters of scaffold, bioreactor and fluid are presented in the second subchapter.

4.1 Mechano-Perfusion Bioreactor proposed

Bioreactors, as demonstrated, are being used to create several types of tissues using many different *stimuli*. Analysing the state-of-the-art in bioreactors for TE it is easy to assume that the bioreactors role is to provide not only a stable environment to cells as also the proper *stimulus* to create a specific tissue (Gelinsky *et al*., 2015; Khetani and Bhatia, 2006; Obregón *et al*., 2017; Salehi-Nik *et al*., 2013). A frequent issue in TE is that just one type of *stimulus* when performing the culture of the tissue is not enough to differentiate the cell or the cultivated tissue. Doesn't have the proper mechanical resilience as the natural tissue has or even there aren't enough living cells at the end of the culture to provide a full tissue to implant on the patient (Gelinsky *et al*., 2015; Khetani and Bhatia, 2006; Liu *et al*., 2013; Obregón *et al*., 2017; Salehi-Nik *et al*., 2013).

For these reasons, a novel bioreactor is being developed. A Mechano-Perfusion bioreactor capable of providing the same advantages of a full perfusion bioreactor with the extra condition of also providing a mechanical *stimulus* (Figure 4.1).

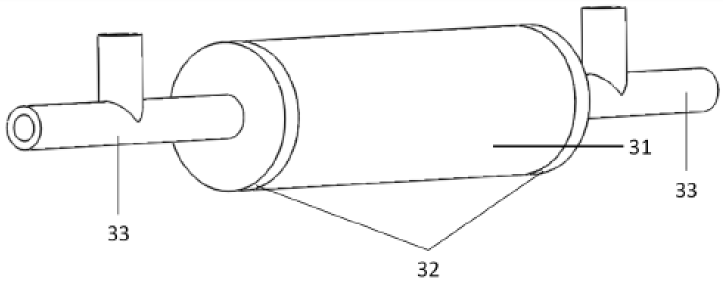

Figura 6

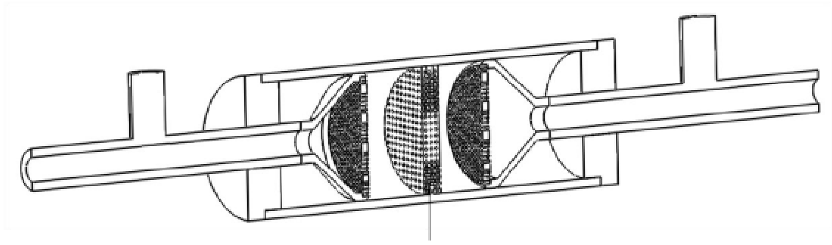

Figure 4.1 Mechano-Perfusion bioreactor design (Freitas *et al*., 2013)

This bioreactor is patented in Portugal with the patent number PT 105176 granted in 2013 (Freitas *et al*., 2013). The perfusion part of this bioreactor will offer excellent control of mass transfer and also will try to correct one of the limitations of the normal perfusion bioreactors, the control of the fluid flow path through the chamber. For that reason, it was developed micro-perforated diffusion membranes (Figure 4.2) with oriented holes to try to redirect the fluid to the necessary parts of the scaffold surface. These oriented holes have three angle configurations, 45º, 0 º and -45º degrees. With these membranes, in theory, there is the potential to create homogenous and heterogeneous tissues. The inlet and outlet are to two mechanical pistons that will move towards and outwards the scaffold providing a compressive *stimulus*.

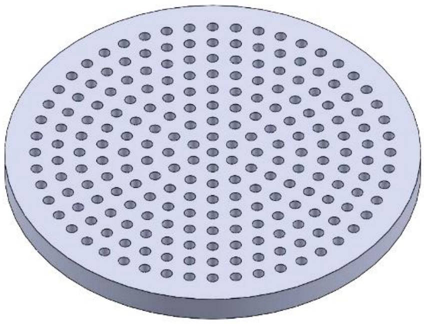

Figure 4.2 Designed micro-perforated diffusion membrane

This combination of Perfusion and Mechanical simulation will, in theory, provide a broader scope of tissues to culture. For instance, a cartilage-like matrix will have their chondrocyte growth, and a mineralised matrix will have the bone cells enhanced both cases due to a direct perfusion bioreactor (Meyer *et al*., 2006; Salehi-Nik *et al*., 2013). Using cartilage as an example once more, a mechanical bioreactor will apply a dynamic compression loading comparable with the natural physiological load applied to real cartilage. With this load the mechanical bioreactor will aid the *in vitro* cartilage to have a higher elastic modulus and a better mass formation very similar to the native cartilage (Elhamian *et al*., 2015; Hoenig *et al*., 2011; Mauck *et al*., 2000; Zhao *et al*., 2016).

One crucial aspect to take into account when designing a novel bioreactor is the microenvironment of the cells. This is one of the factors responsible for the importance of regulating the flow rate of the medium. So, to optimize a bioreactor, specially a mechano-perfusion bioreactor, there must be some balance between the nutrient supply rate, the transport of metabolites off and to the cells, and the proper shear stress effect of the fluid on the cells deposited on the scaffold (Depprich *et al*., 2008; Lovett *et al*., 2010; Salehi-Nik *et al*., 2013; Wendt *et al*., 2008).

To better understand how all of the mentioned physical factors influence the development of the tissues, necessary studies are required to quantify their impact. In order to optimise the physical forces experienced by cells within the bioreactor, computational analysis will be carried on (Salehi-Nik *et al*., 2013; Wendt *et al*., 2008).

4.2 Simulation Parameters

The mechano-perfusion bioreactor was designed, taking into account all the considerations mentioned in the state-of-the-art. The lack of combined *stimulus* has led the design of this novel bioreactor to a mechanical and perfusion combination. In order to optimise this bioreactor, several numerical studies were carried out. The parameters of these numerical simulations include the design of the bioreactor, the scaffold and the fluid properties.

Due to the pertinence of this study and to better understand the fluid behaviour and the stress suffered by the scaffold, and the cells within, it was considered the following sets of numerical simulations:

- 1st phase: CFD simulations without and with a simple scaffold and varying the fluid velocity;
- 2nd phase: Scaffold permeability analysis;
- 3rd phase: CFD and Structural simulations with mimicked scaffold;
- 4th phase: Scaffold degradation CFD and structural analysis.

4.2.1 Perfusion Bioreactor Design

Using Solidworks® CAD software, the bioreactor was modelled with the dimensions described in Figure 4.3. This novel bioreactor has two dynamic hollow pistons in which the fluid flows from inside and is oriented by the perforated membranes and also can promote mechanical compression to the scaffold area.

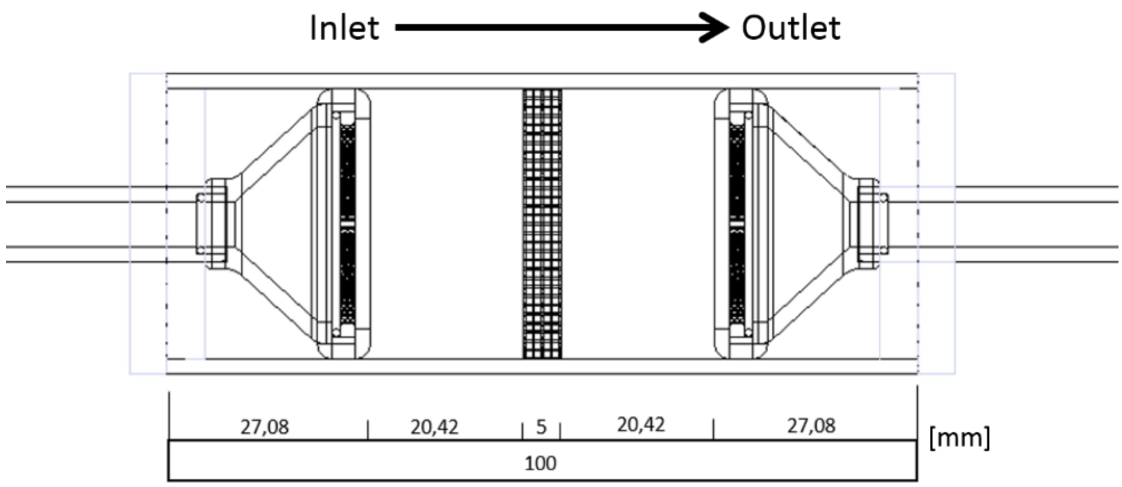

Figure 4.3 Dimensions of the designed mechano-perfusion bioreactor.

The pistons can be used dynamically or stationary and, in the last case, the bioreactor will act as a perfusion system only. The pistons can go closer to the scaffold surface while the fluid is flowing from within the piston. For that reason, it was simulated four scenarios

(Figure 4.4) for the initial approach, taking into account the extreme positions of both pistons. The piston in the Open (O) position is when it is the most distant of the scaffold while the Close (C) position is the opposite when it is closer to the scaffold. With the combination of these two positions it was possible to use four configurations: 1) both pistons in the Open position, OO (Figure 4.4a); 2) Inlet piston (left) Close and the Outlet (right) piston in the Open position, CO (Figure 4.4b); 3) Inlet piston (left) Open and the Outlet (right) piston in the Close position, OC (Figure 4.4c); 4) both pistons in the Close position, CC (Figure 4.4d).

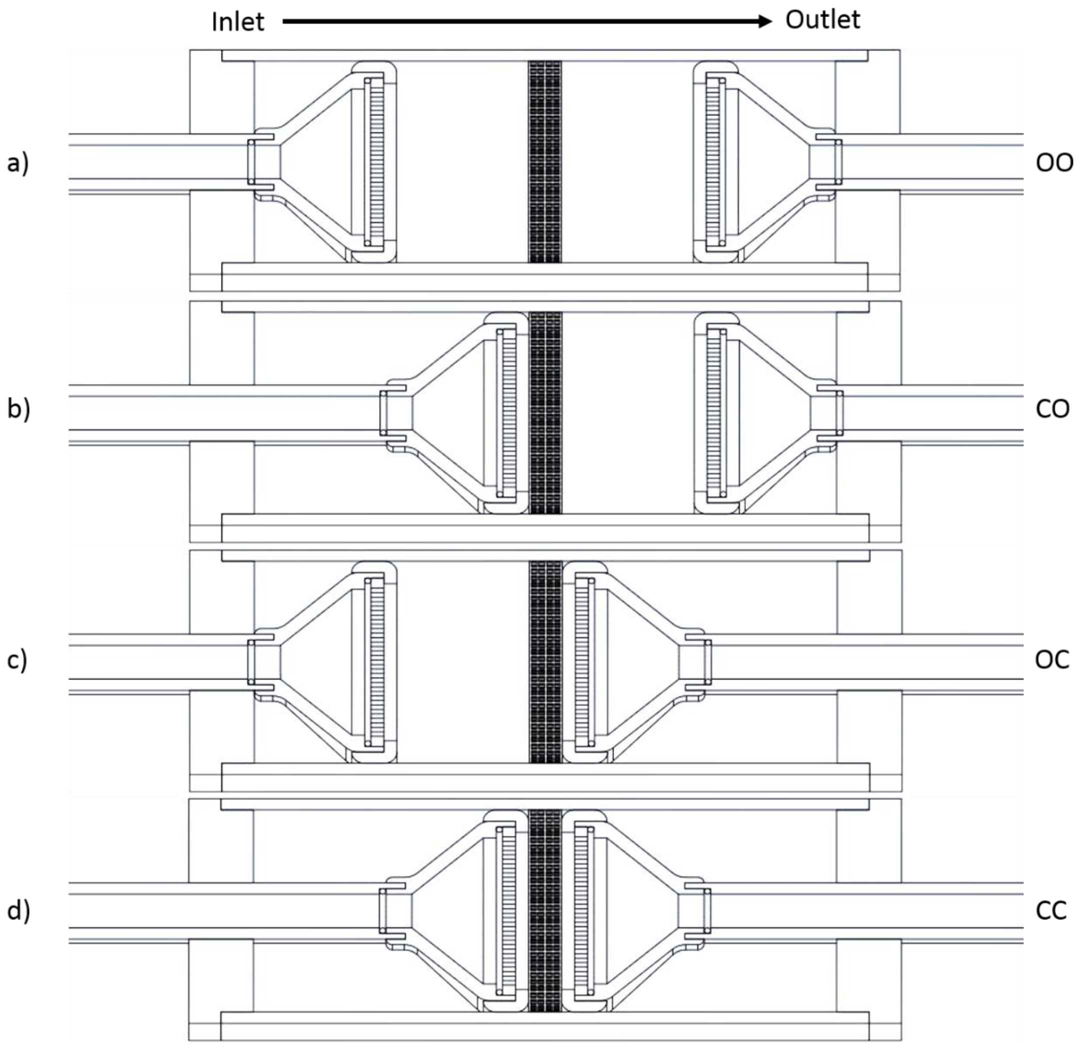

Figure 4.4 Model of the perfusion bioreactor demonstrating the four pistons configurations, a) Open-Open, b) Close-Open, c) Open-Close and d) Close-Close positions.

In general, the fluid in perfusion bioreactors flows directly to the scaffold in a linear way, which originates in most of the cases a uniform distribution of the fluid in the surface of the scaffold. With this flow, depending on its velocity, the impact of the fluid on the scaffold can reach high values of shear stress resulting in cellular necrosis. This novel mechano-perfusion bioreactor intends to solve this issue by using the perforated membranes enabling not only the linear flow of the fluid but also, in a controlled way, different directions for the fluid flow originating different stresses and velocities. With these membranes the intention is to create the optimum levels of *stimulus* to enhance the proliferation of cells and therefore to create homogeneous or heterogeneous tissue.

To better understand the conditions that will be created by these membranes, numerical simulations were carried out with the three different configurations (Figure 4.5): (1) in the first membrane, the fluid flows parallel to the chamber walls (perpendicular to the scaffold surface) denominated as *PF* (Parallel Flow) as seen in Figure 4.5a); (2) in the second membrane configuration (Figure 4.5b), the pores of the membrane redirects the fluid to the centre of the chamber (Inward), referred as *IF* (Inward Flow); (3) in the third and last membrane (Figure 4.5c), the pores of the membrane redirects the fluid towards the walls of the culture chamber, referred as *OF* (Outward Flow).

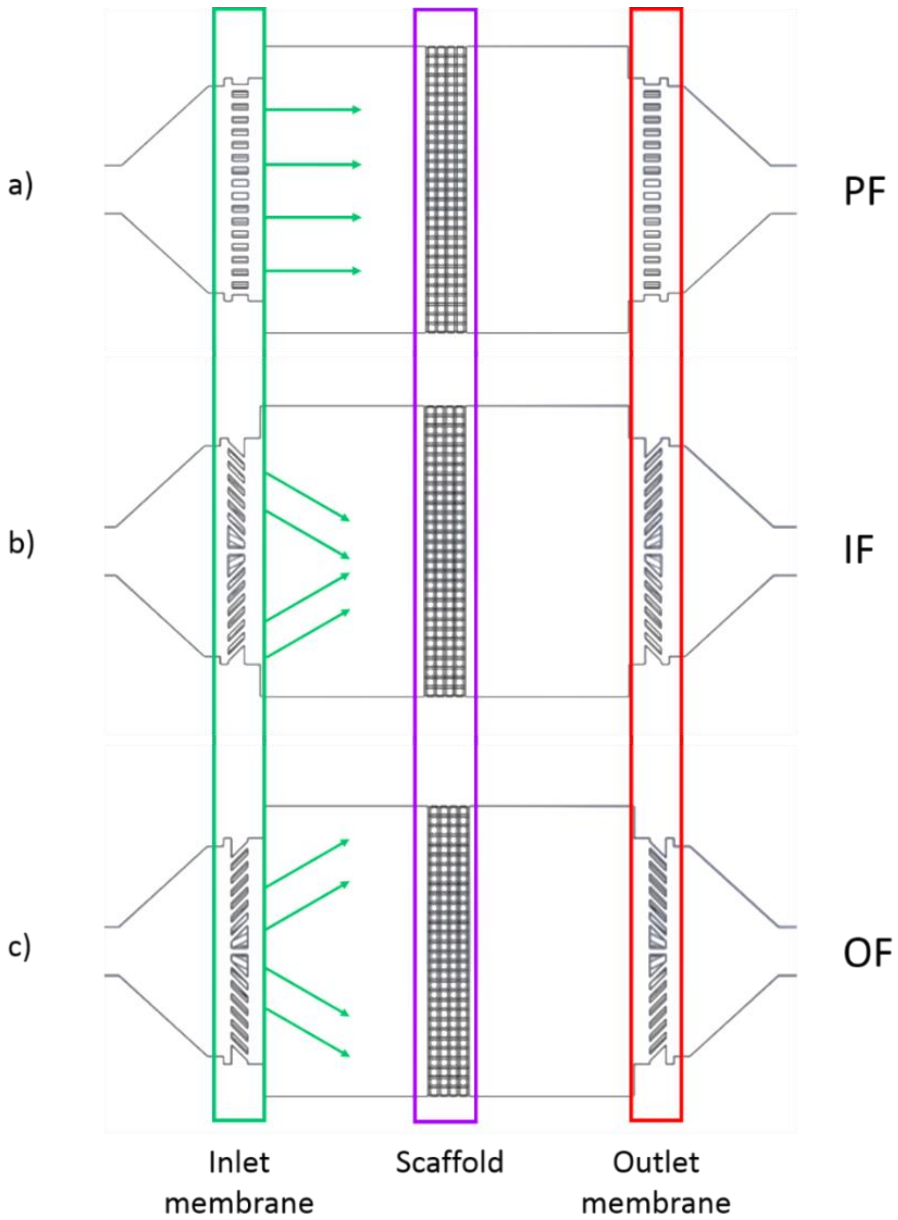

Figure 4.5 Membrane configuration to redirect the fluid flow where a) is the Parallel Flow configuration, b) the Inwards Flow configuration and c) the Outward Flow configuration.

4.2.2 Scaffold Design

For the bioreactor optimisation, it was modelled two scaffolds. One was used for the initial numerical simulations, and it is a simplified model. The second one is an approximation of a real scaffold after being constructed by additive fabrication technologies.

In Figure 4.6 is represented the scaffold used for the initial simulations (1st phase) where it is observed the planar surface of the filaments. It was designed in a cylinder form in order to be fitted in the mechano-perfusion bioreactor chamber with a diameter of 36 mm and 5.1 mm thickness. The filament has a 0.3 mm of edge, a pore size of 0.9 mm and a 0º/90º pattern configuration with approximately 82% of porosity.

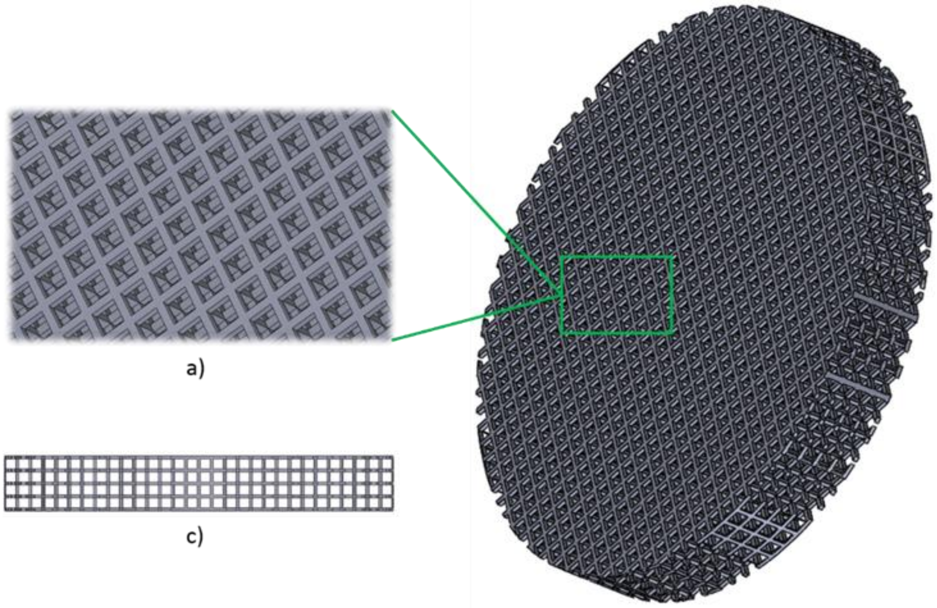

Figure 4.6 Design of the scaffold used in this work, a) detail of the filament pattern; b) lateral view of the scaffold.

For the permeability (2nd phase) study, it was used an eighth of the scaffold described before (Figure 4.7). This was done in order to simplify the numerical calculations.

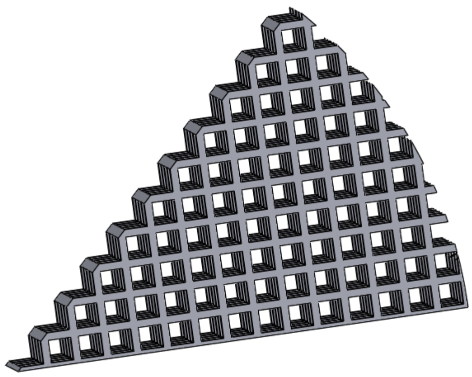

Figure 4.7 1/8th of the scaffold used for the permeability simulations.

For the numerical simulations of the enzymatic degradation (4th phase), it was used the cuboid shape with squared filaments to model the scaffold due to the fact that the scaffold suffers geometric modifications along time and in order to be possible the execution of such numerical simulations was opted for this simplification. The original conditions of the scaffold are 10 mm of edge, a volume of 648 mm^3 and 16 pores in each face with 1 mm of size (Figure 4.8). Then with the degradation process the scaffold will continuously lose its volume till it reaches a 1.2 mm^3 in 340th day of degradation.

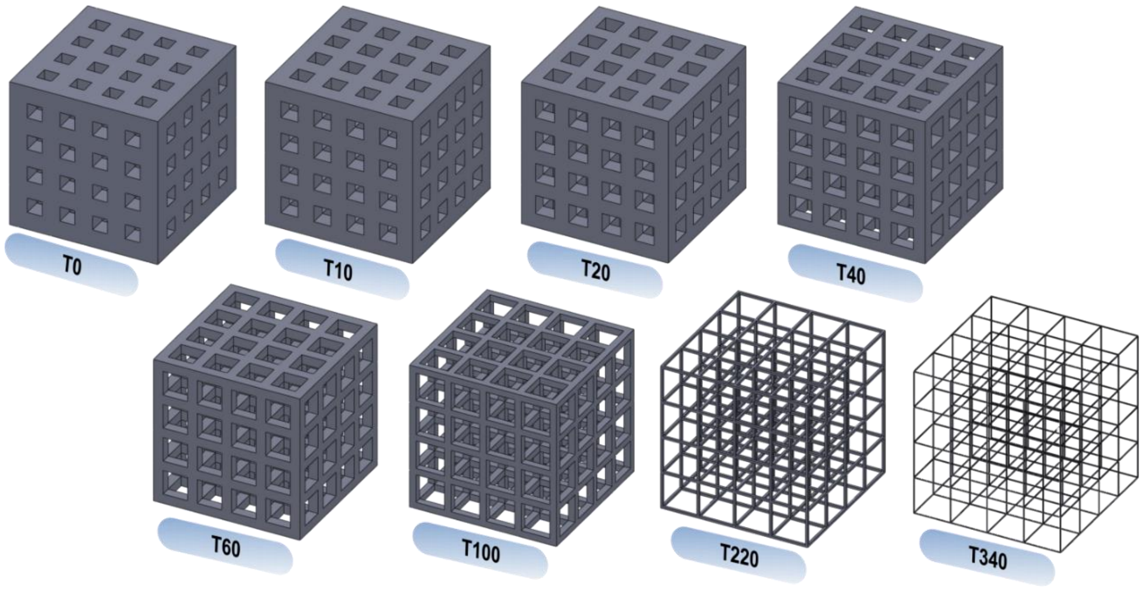

Figure 4.8 Scaffolds used in degradation numerical analysis from Day 0 (T0) until Day 340 (T340) (Almeida *et al*., 2016).

The scaffold designed for the last computational fluid and structural simulation (3rd phase) pretends to mimic the real produced scaffold. Due to the additive manufacturing technique, several parameters have to be taken into account in order to model the scaffold. The strand diameter (*D*) and the horizontal span (*Y*) two parameters that are controllable during the scaffold production. Density is defined by (ρ), and the elastic stress limit will vary according to the material, in which in this case the material used is PCL (Almeida and Bártolo, 2014; Freitas *et al*., 2014a; Li *et al*., 2009; Sanz-Herrera *et al*., 2009). In order to simplify the numerical calculations, a quarter of the scaffold was used (Figure 4.9). The filament diameter has 0.3 mm with a horizontal span of 0.7 mm, a pore size (*Hz*) of 0.255 mm, a pattern configuration of 0º/90º (Θ) and from the geometric model, the porosity, which is defined as the ratio of the void volume to the total volume, is porosity of 63.9%.

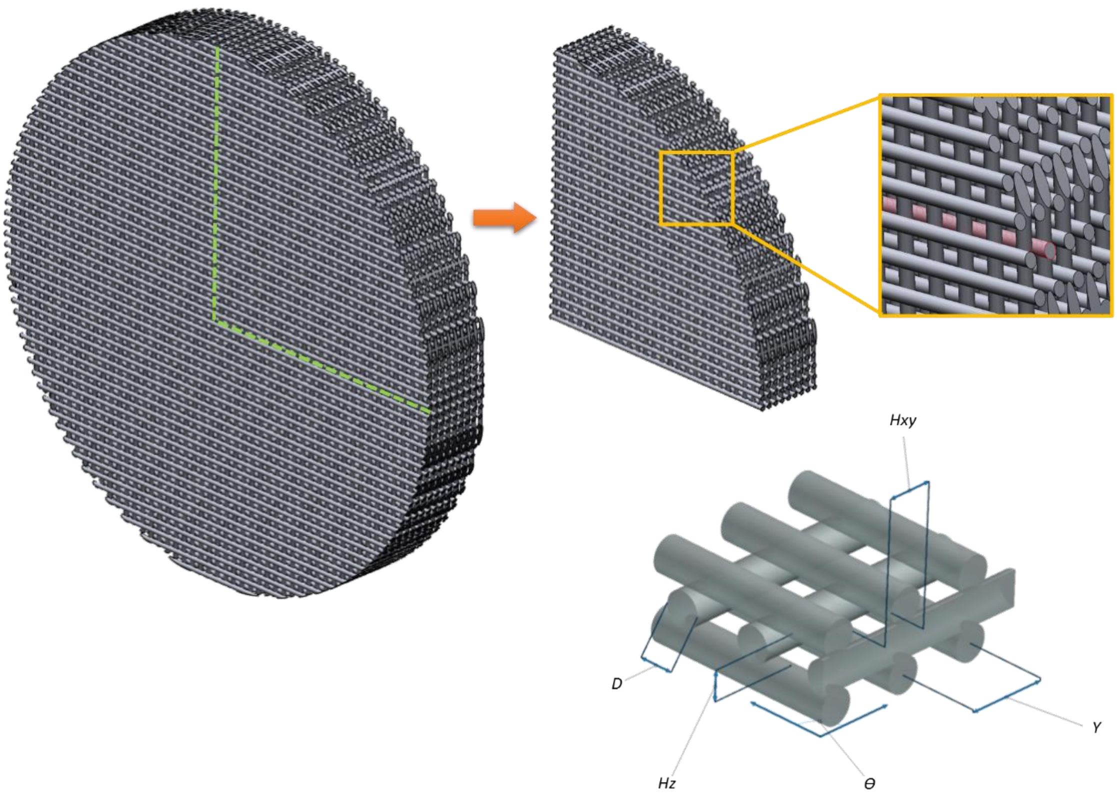

Figure 4.9 One-fourth of the scaffold used in the fluid and structural simulations and designing parameters taking into account.

4.2.3 Simulation Conditions and Settings

In order to perform an optimisation of this novel bioreactor, a full study of the fluid behaviour in the bioreactor was required. Several simulations were performed, and it was considered the conditions of the medium among other parameters described ahead.

For the 1st phase, it was considered twelve combinations of the mechano-perfusion bioreactor (four-piston configurations and the three membranes). The number of finite elements that constitute the mesh and their average size for each configuration can be seen in Table 4.1.

Table 4.1 Mesh conditions used in the 1st phase in the CFD analysis.

Chamber Configuration	Total Elements	Average Elements Size [mm]
PF-OO	3850276	0,825
PF-OC/PF-CO	4313385	0,826
PF-CC	4780823	0,828
IF-OO	3070320	0,817
IF-OC/IF-CO	3382761	0,819
IF-CC	3688855	0,820
OF-OO	3088909	0,818
OF-OC/OF-CO	3416962	0,819
OF-CC	3718000	0,820
Average	**3701143**	**0,821**

In terms of properties of the fluid, it was defined three fluid velocities and the fluid considered has the same properties as the study carried out by Hutmacher and Singh (2008). All the parameters can be seen in Table 4.2 were beside the fluid properties is also displayed the inlet and outlet diameter of the bioreactor.

Table 4.2 Fluid characteristics and chamber properties used in the CFD analysis.

Parameter	Value
Density	1030 Kg/m^3
Dynamic Viscosity	0,0025 Pa/s
Flow velocity	0.1/0.2/0.3 m/s
Pressure	1 atm
Flow regime	Subsonic
Turbulence model	Laminar
Bioreactor in/outlet diameter	8 mm
Bioreactor chamber diameter	50 mm
Bioreactor volume (maximum)	785.71 mL

In order to better understand the behaviour of the fluid within the bioreactor chamber, this 1st phase was separated into two studies, with and without the scaffold. This means that it was carried out twelve simulations for each velocity without scaffold inside the culture chamber. The absence of a scaffold in the simulations is of significant importance to better understand the fluid behaviour along its entire course since the inlet up to the outlet without any constraints in the middle allowing to study the influence of each membrane configuration and each piston position identifying the turbulent effects caused by each of them.

In the 2nd phase, numerical simulations were done using the two extreme configurations of the position of the pistons, the Open-Open (OO) and the Close-Close (CC) (Figure 4.4). With the same fluid properties displayed in Table 4.2 and it was defined the fluid velocity of 0.2 m/s.

After performing the numerical simulations in the 1st phase, velocity plots on the scaffold's surface were obtained, and they were used as the fluid's velocity in these simulations to determine the scaffold's permeability. It was used the previous piston configurations (OO and CC) with the three membrane configurations.

The meshed model was composed of 38866 tetrahedron elements with an average element size of 0.632 mm. The outlet was defined with zero pressure while three different regions of velocity where defined according to the previous results from the velocity plots (Figure 4.10).

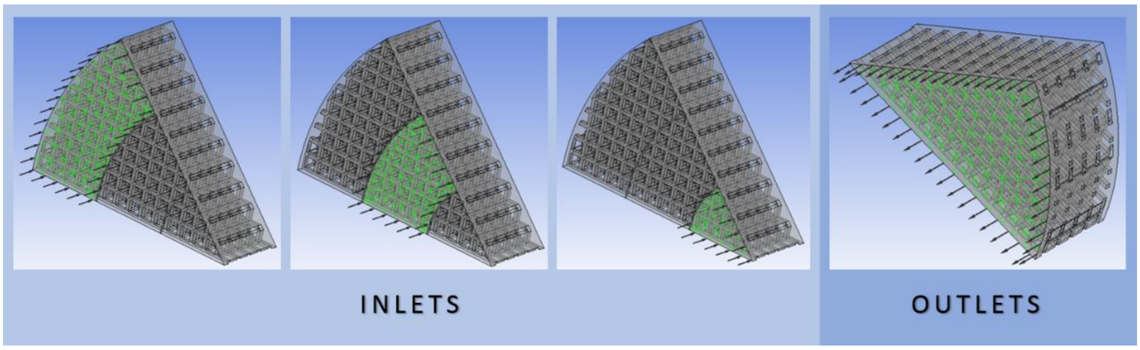

Figure 4.10 Inlets and outlets of the 1/8th of the scaffold used in this phase.

On this phase of simulations (3rd phase) the parameters used to define the boundary conditions, the models of the mechano-bioreactor and scaffold, and the fluid was similar to real conditions. The fluid used for the simulations has the properties of the Human Plasma supplied by Sigma Aldrich (Table 4.3) and its used in many of the TE applications for culturing bone, muscle, skin and vascular tissues (Kakavand *et al.*, 2017; Kwak *et al.*, 2017; Paul *et al.*, 2015; Sadeghi-Ataabadi *et al.*, 2017; Yoo *et al.*, 2009).

Table 4.3 Human plasma properties and CFD definitions.

Parameter	Value
Density	1020.05 Kg/m^3
Dynamic Viscosity	1.3175 Pa/s
Molar Mass	220 Kg/mol
Specific Heat Capacity	3930 J/(Kg·K)
Thermal Conductivity	0.582 W/(m·K)
Flow velocity	0.5 m/s
Pressure	1 atm
Flow regime	Subsonic
Turbulence model	Laminar
Wall property	No Slip Wall
Bioreactor in/outlet diameter	8 mm
Bioreactor chamber diameter	50 mm
Bioreactor volume (maximum)	785.71 mL

Using the Reynolds equation to calculate the turbulence of the fluid within the bioreactor chamber it is possible to observe that the fluid will have a laminar characteristic in both pipes (pistons) of inlet and outlet and also in the chamber. Also, the fluid is considered an uncompressible flow of a Newtonian fluid.

This phase is divided into two parts: (1) fluid analysis and (2) structural analysis. The first part was used to determine the fluid velocity and shear stresses in the scaffold, for that, it was just considered the inlet piston in its extreme positions (Open and Close) and the outlet piston was fixed in the Open position without a membrane. It was created six (6) combinations with the two-piston configurations, OO and CO (Figure 4.11), and the three membranes, Parallel (PF), Inwards (IF) and Outwards (OF). For the second part of the 3rd phase it was used the pressure exerted by the fluid on the scaffold to calculate the deformation and the Equivalent (von-Mises) stress on the scaffold.

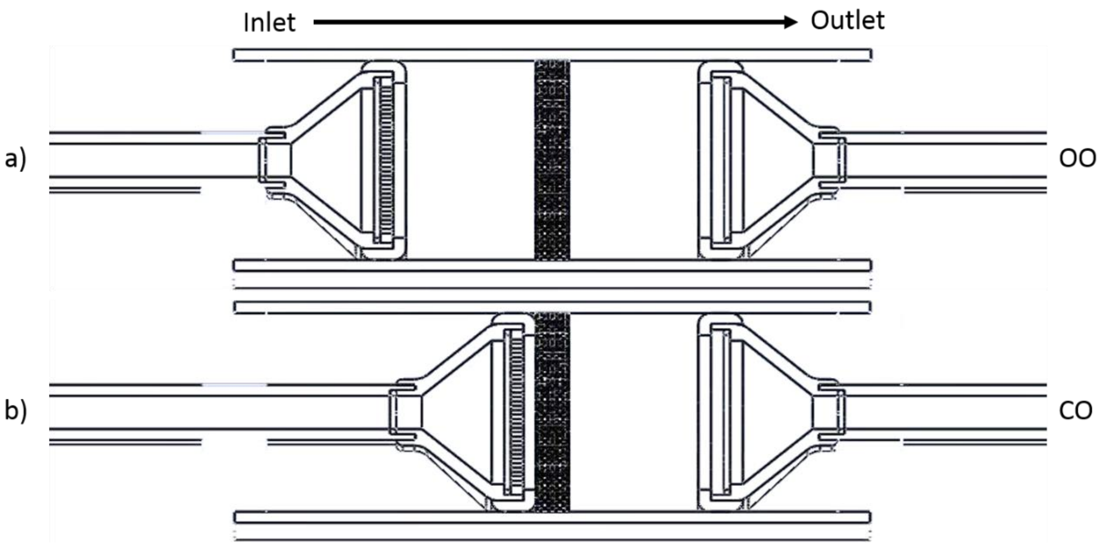

Figure 4.11 The two-piston configurations used in this phase. Only the inlet piston moves and the outlet piston remains in the Open position.

The scaffold was constrained by its rounded facet that is in contact with the interior wall of the bioreactor chamber and the pressure imported from the CFD analysis was applied in all elements.

Taking advantage of the symmetry of the chamber and scaffold, it was possible to simplify the fluid model into 1/4th (Figure 4.12) and this way reducing the computational time.

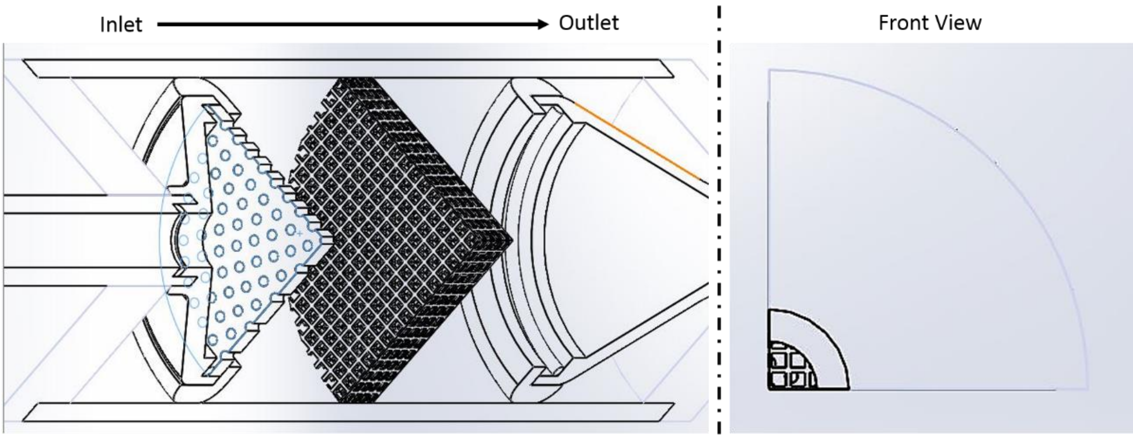

Figure 4.12 Views of the 1/4th of the mechano-perfusion bioreactor chamber used in this phase.

The bioreactor chamber and the scaffold for, CFD and Structural analysis, respectively, were meshed using ANSYS mesh tool, from ANSYS Inc (Figure 4.13). The mesh properties of fluid geometry can be seen in Table 4.4 and Table 4.5. The mesh of the scaffold was created with 7504219 tetrahedrons and with 3.55×10^{-2} of average size of the elements, a skewness of 0.50 and orthogonality of 0.49.

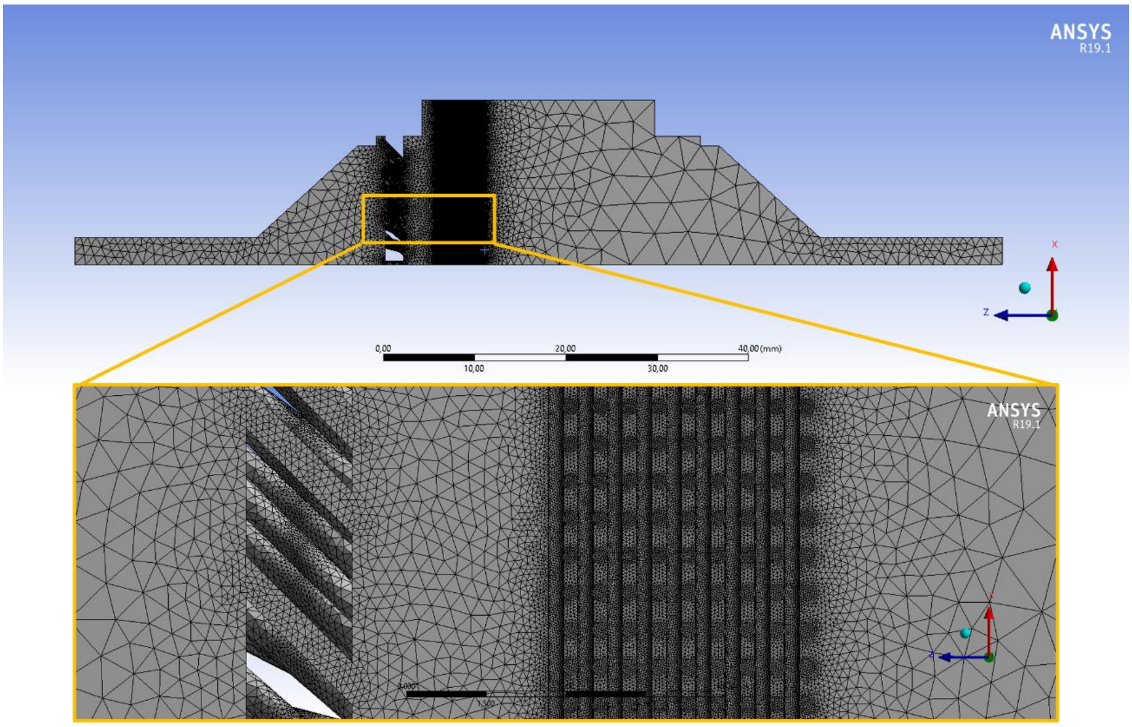

Figure 4.13 Example of a mesh used in the 3rd phase. Mesh from the IF-OO combination with a detail zoom of the membrane and scaffold.

Table 4.4 Mesh properties of the fluid numerical simulations used in the 3rd phase. The average number of elements and size.

Chamber	Total Elements	Average Elements Size [mm]
PF-OO	43500925	4.14x10^{-2}
PF-CC	42546097	4.08x10-^{2}
IF-OO	43563083	4.13x10^{-2}
IF-CC	42638968	4.09x10^{-2}
OF-OO	44032592	4.10x10^{-2}
IF-OO	42884939	4.13x10^{-2}
Average	**43194434**	**4.11x10-^{2}**

Table 4.5 Mesh properties of the geometries used in the 3rd phase in CFD simulations. Focus for Orthogonality, Skewness and Reynolds Number.

Chamber	Orthogonality	Skewness	Reynolds Number
PF-OO	24.7	0.230	9.4525
PF-CC	22.7	0.228	8.1611
IF-OO	25.7	0.231	9.4488
IF-CC	23.9	0.233	8.1552
OF-OO	25.4	0.232	9.4499
IF-OO	23.2	0.229	8.1573
Average	**24.3**	**0.231**	**8.8041**

Numerical simulations in the 4th phase were carried out in order to fully understand the mechanical sustainability of the PCL scaffolds degradation over time. The fluid properties were the same as used in the 1st and 2nd phase just fluctuating the fluid velocity between 0.1 m/s to 1 m/s in increments of 0.1 m/s. The final mesh has 237632 tetrahedron elements with an average element size of 0.612 mm.

The bioreactor chamber used was a simplified perfusion bioreactor due to the fact, mentioned above in the 4.2.2 subsection, of the geometric scaffold variation along time. The perfusion bioreactor as a volume of 250 ml, and 68 mm of diameter and length, with 10 mm of inlet and outlet (Figure 4.14). For purposes of simplifying the simulation, the scaffold was positioned in the centre of the chamber (Figure 4.14), and it was considered a homogenous degradation of the scaffold (Figure 4.8). The scaffold was printed in PCL (PCL CAPA 6500 supplied by Perstorp Holding AB) and the material properties can be observed in Table 4.6. In this phase it was also performed a computational fluid analysis from which resulted the wall shear stresses that were applied in the structural analysis.

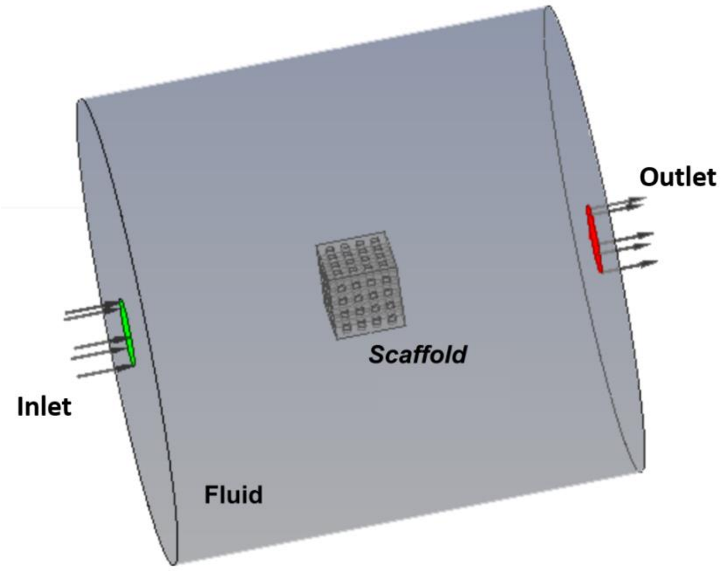

Figure 4.14 Inlet and outlet of the perfusion chamber and the position of the scaffold.

Table 4.6 PCL CAPA 6500 properties.

Parameter	Value
Young's Modulus	4.3×10^{8} Pa
Poisson's Ration	0.33
Bulk Modulus	4.22×10^{13} Pa
Shear Modulus	1.62×10^{14} Pa
Density	1.15×10^{6} kg
Tensile Yield Strength	1.72×10^{7} Pa
Molar Mass	1.14×10^{2} kg/mol
Reference Specific Enthalpy	1.35×10^{5} J/kg
Reference Temperature	6.00×10^{1} °C
Thermal Conductivity	0.25 W/(m·K)
Behaviour	Isotropic

5 Optimisation Results of the Mechano-Perfusion Bioreactor

The results obtained during this research work will be presented in this chapter, as well as a brief discussion of them. The results are divided by the phases mentioned above from the first one until the fourth and final phase.

5.1 1st Phase: Initial CFD Analysis

In this 1st phase, it was carried out two sets of numerical simulations, varying the inlet velocity according to Table 4.1 (0.1/0.2/0.3 m/s). The first set was to analyse the fluid behaviour in the mechano-perfusion bioreactor chamber without the scaffold by analysing the fluid velocity and turbulence generated by the fluid going throughout the diffusion membrane. The second set analyses, again, the velocity and turbulence within the chamber but with the intrusion of the scaffold inside the culture chamber. In this last set it was also analysed the wall shear stress on the scaffold. The results shown through colour map are being demonstrated on a plane located in the middle of the bioreactor (Figure 5.1). The results of this section were published as a book chapter in “Biodental Engineering III” book, and as a journal article in “Procedia Technology” (Freitas *et al.*, 2014b, 2014a)

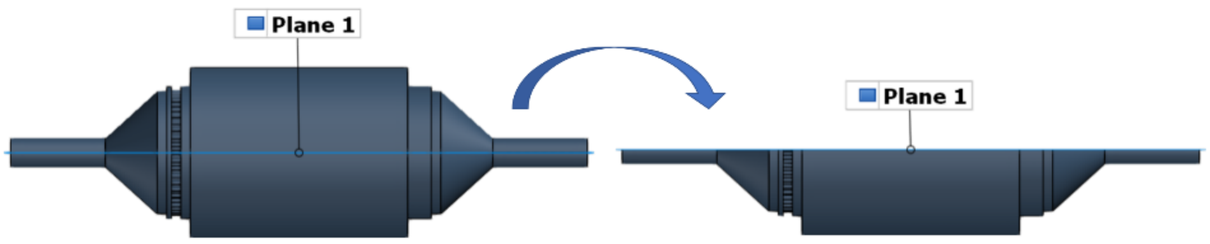

Figure 5.1 Section plane used to demonstrate the results.

5.1.1 Without scaffold

Velocity

In Figure 5.2, it is possible to see the fluid velocity streamlines without the scaffold. The streamlines show the behaviour of the fluid within the scaffold where it is possible to observe that the OO configuration of pistons creates more vortices due to low depression areas. The diffusion membrane successfully redirects the fluid towards the wall (OF) or to the centre (IF). The CC piston configuration due to the small culture chamber space don’t allow the creation of vortices.

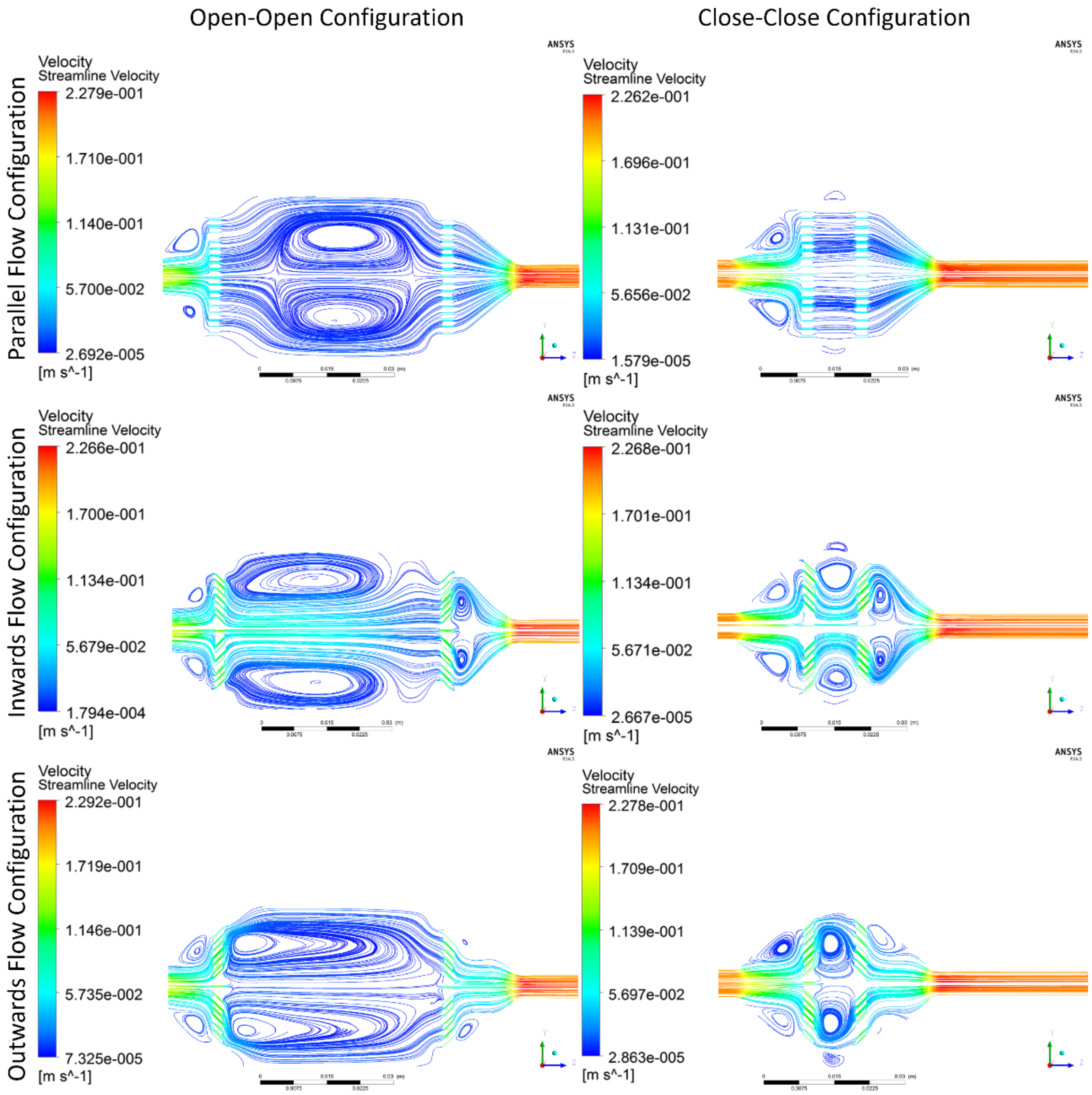

Figure 5.2 Fluid velocity streamlines of the extreme positions for velocity 0.2 m/s.

On the graphics below (Figure 5.3) it is possible to observe that for all the input velocities, the results are almost identical with minor differences as the input velocity increases. In all the input velocities there was a combination with the highest value of velocity, the OF-OC. The low average value was obtained by the IF membrane configuration, although in the velocities 0.2 and 0.3 m/s the PF membrane had the lowest values when combined with the CC piston configuration.

The OF and PF membrane, as the velocity of the fluid rises, tend to increase the velocity just for the OO and OC piston configuration, decreasing abruptly in the CC configuration. This probably occurs due to the small chamber volume in this position of the pistons.

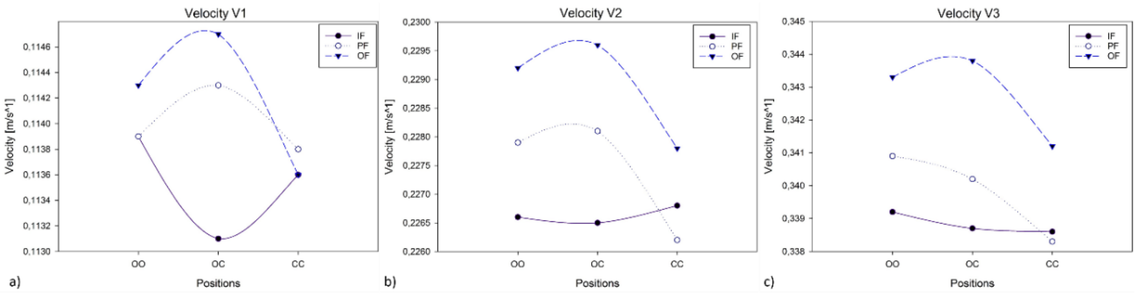

Figure 5.3 Velocity results for the three input velocities without scaffold where, a) is 0.1; b) 0.2; and c) 0.3 m/s.

Turbulence

Analysing the results presented in Figure 5.4, it is possible to see that the IF membrane configuration has the highest value and the PF the lowest. Although at the 0.2 m/s fluid input velocity the combination IF-CC has a significant decrease of turbulence. This may occur due to a small chamber volume created by the outlet piston being in the closed position, approximating the outlet from the scaffold enabling a faster exiting of the fluid.

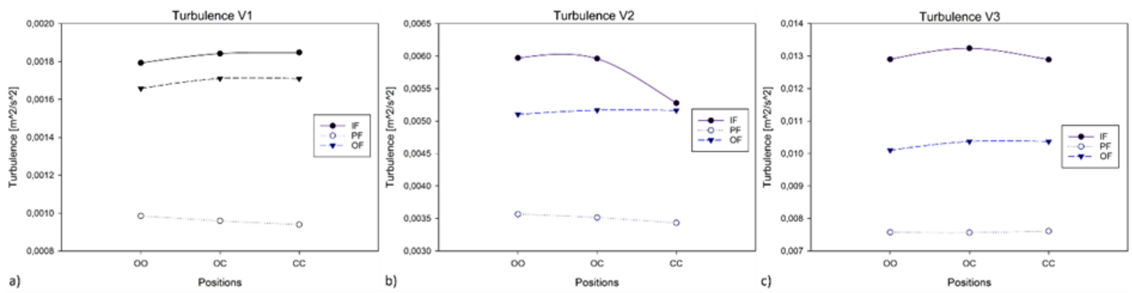

Figure 5.4 Results of all the combinations for the three input velocities in terms of turbulence within the chamber where, a) is 0.1; b) 0.2; and c) 0.3 m/s.

Figure 5.5 shows the comparison between the extreme positions, OO vs CC, in terms of turbulence for the 0.2 m/s input velocity. The directional fluid membranes IF and OF creates higher turbulence respectively in the middle of the chamber and on the wall of the chamber, creating a more heterogeneous flow facing the scaffold.

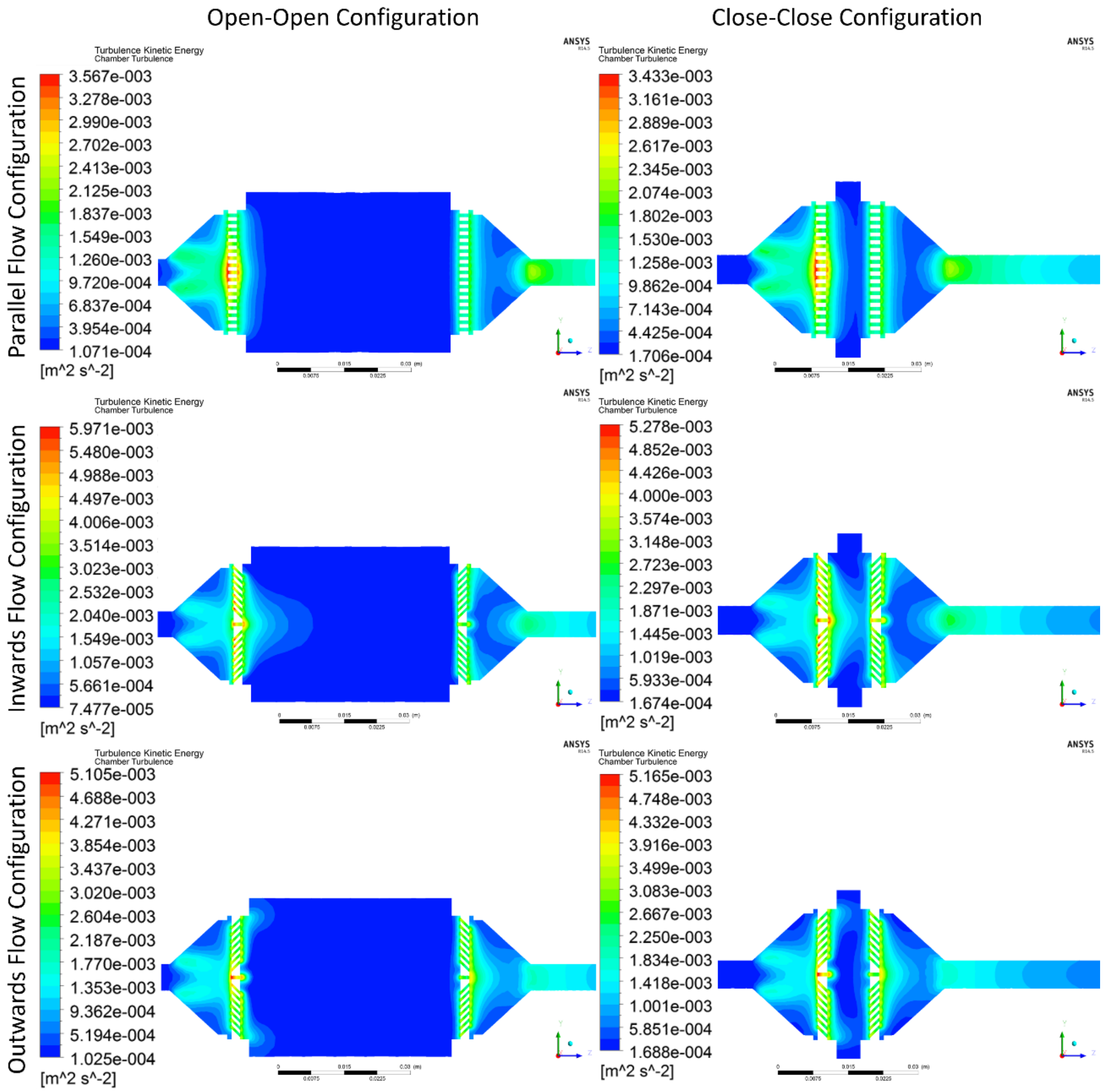

Figure 5.5 Colour map of the turbulence results for 0.2 m/s velocity and for the extreme positions of all the membranes without scaffold.

5.1.2 With scaffold

<u>Velocity</u>

After introducing the scaffold inside the culture chamber, the PF configuration homogenised the fluid, *i.e.*, fluid remains in a direct way and parallel to the chamber without creating any vortices. The OF and IF created vortices due to the fact that they create low-pressure areas and for that reason the vortices are created. With this heterogeneous behaviour of the fluid, different velocities will reach the surface of the scaffold (Figure 5.6).

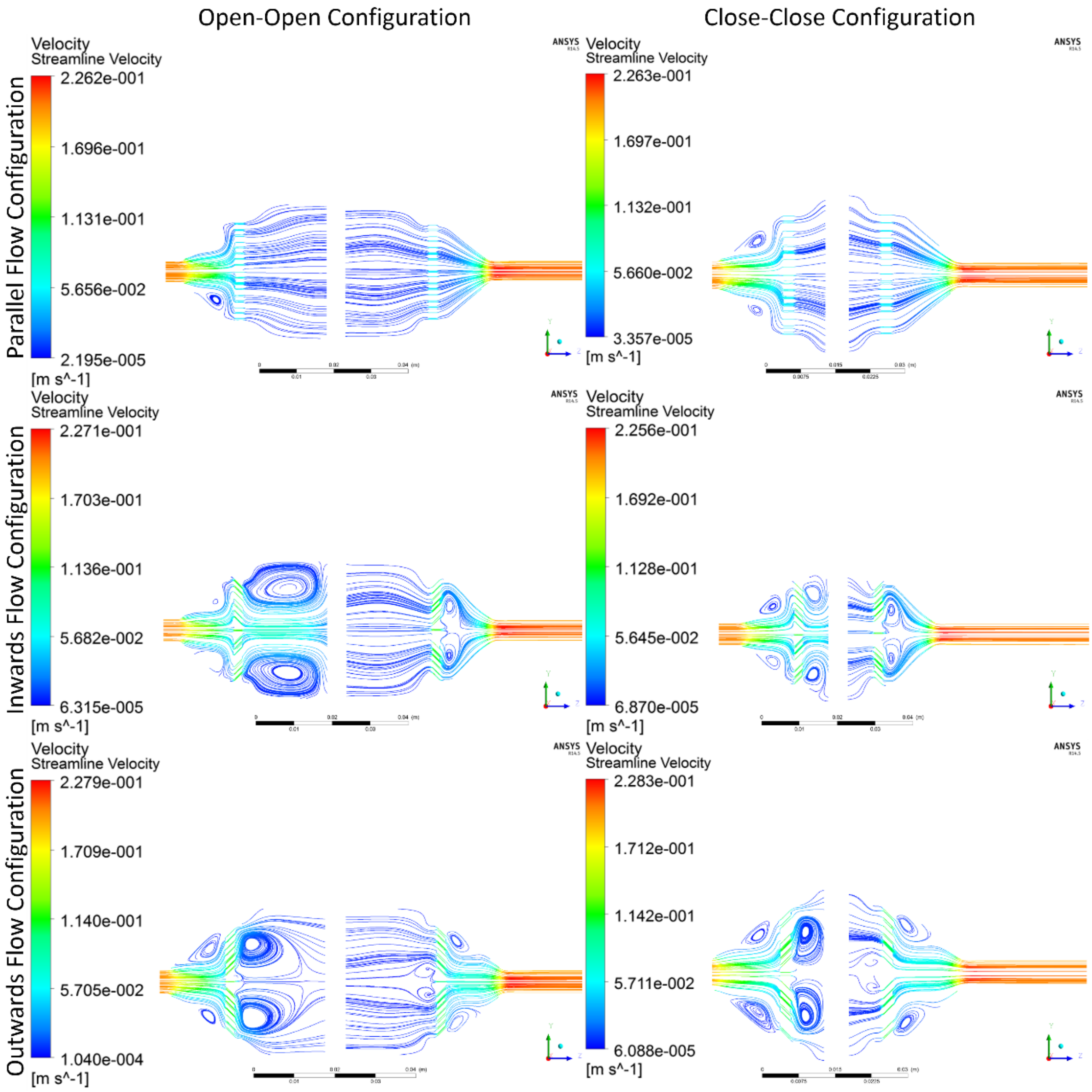

Figure 5.6 Fluid velocity streamlines, for 0.2 m/s, showing the behaviour of the fluid when introducing the scaffold

The velocity results of the simulations with scaffold have a distinct behaviour of the simulations carried out without scaffold (Figure 5.7). For 0.1 m/s, the combination that reaches the highest value of velocity is the OF-CC, being the lowest value the combination PF-OO. In the 0.2 m/s input velocity, it is possible to see that the OF configuration generally has the highest values. Also, the same value was obtained by OF-CC and OF-CO combinations. For the 0.3 m/s input velocity, the configuration OF presents the highest fluid velocity in all the combinations and on the other hand, the IF configuration presents the lowest values in all the configurations.

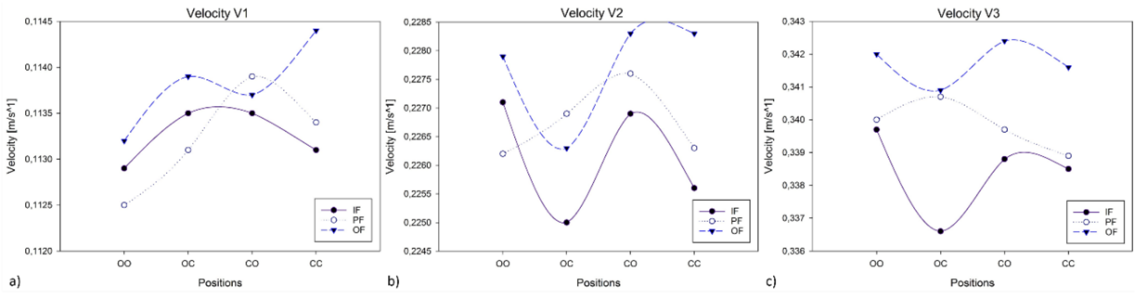

Figure 5.7 Velocity results for the three input velocities with scaffold inside the chamber where, a) is 0.1; b) 0.2; and c) 0.3 m/s.

<u>Turbulence</u>

It is possible to observe the fluid turbulence behaviour within the chamber and in the scaffold. For all the input velocities, it is possible to observe in Figure 5.8 that the IF configuration has the highest value of all the combinations having the IF-OC and IF-CC the highest value. The CC configuration has the smallest volume of fluid, and for that reason the turbulence is slightly lower.

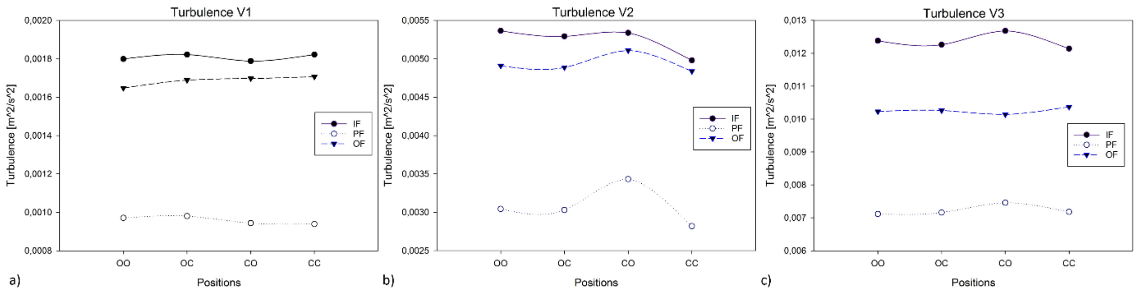

Figure 5.8 Turbulence results for the three input velocities with scaffold inside of the chamber where, a) is 0.1; b) 0.2; and c) 0.3 m/s.

This was reached in the middle of the inlet diffusion membrane exit because it redirects the fluid inwards to the culture chamber creating higher turbulence since it is a point where all the flows from the membrane pores converge. (Figure 5.9)

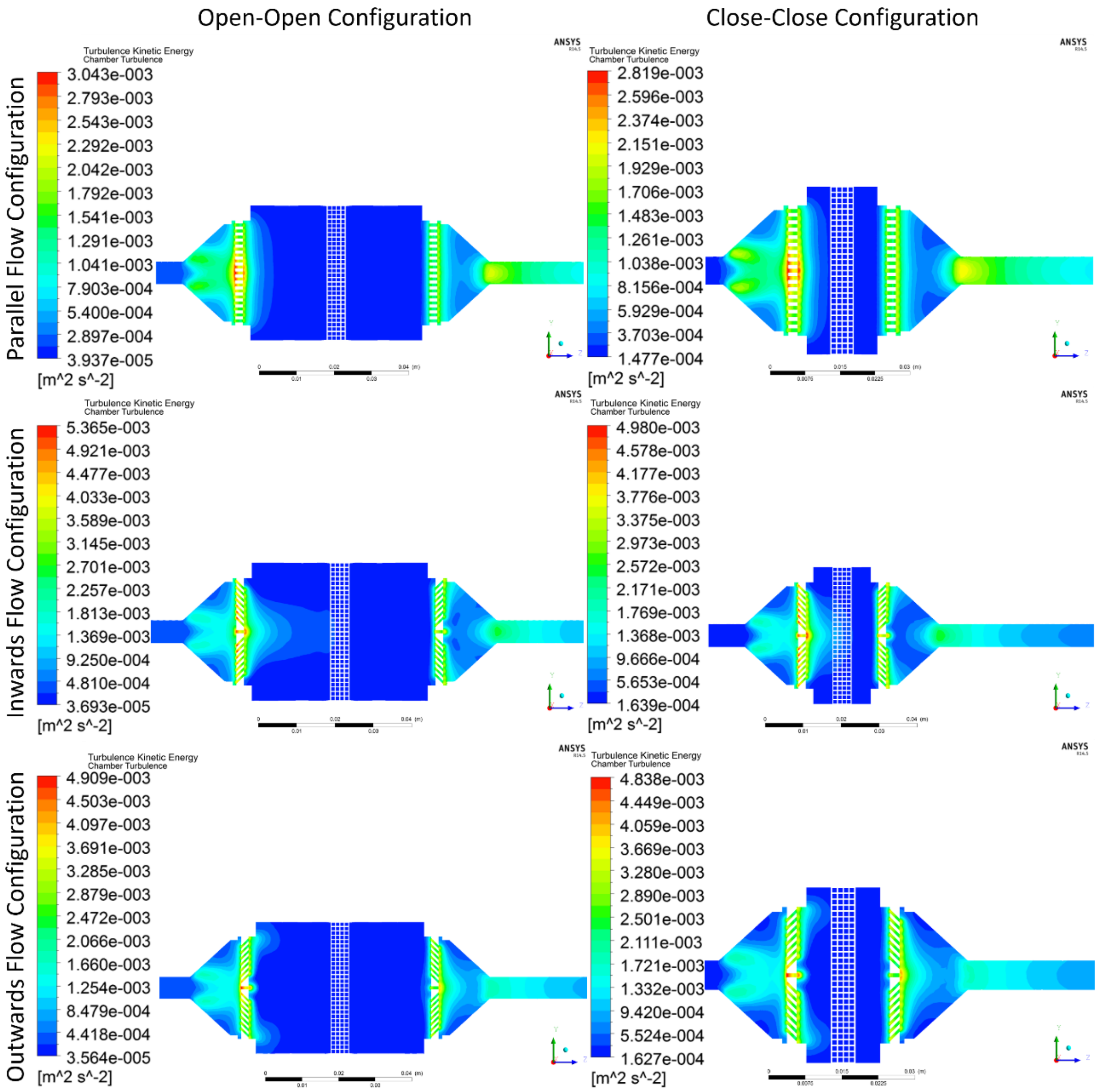

Figure 5.9 Colour map of the turbulence results for 0.2 m/s velocity and for the extreme positions of all the membranes with the scaffold.

<u>Scaffold Velocity</u>

After analysing the behaviour of the fluid flow in the bioreactor chamber, it was also analysed the impact of that fluid in the scaffold. It was analysed the fluid velocity within the scaffold and, as also, the wall shear stress provoked by it.

In Figure 5.10 below, it is possible to observe the effects of the velocity in the scaffold surface and the colour map profile in each extreme position for the three membranes. It is well noted the effect of the membrane over the fluid direction. In the PF configuration the velocities are more homogeneous throughout almost the entire scaffold surface. Analysing both OF and IF membrane configurations it is visible that the redirection of the fluid created a heterogeneous profile of velocities throughout the scaffold. The IF configuration as the outer area of the scaffold with low velocity from the fluid while the centre as a higher fluid velocity, is the opposite true for the OF configuration.

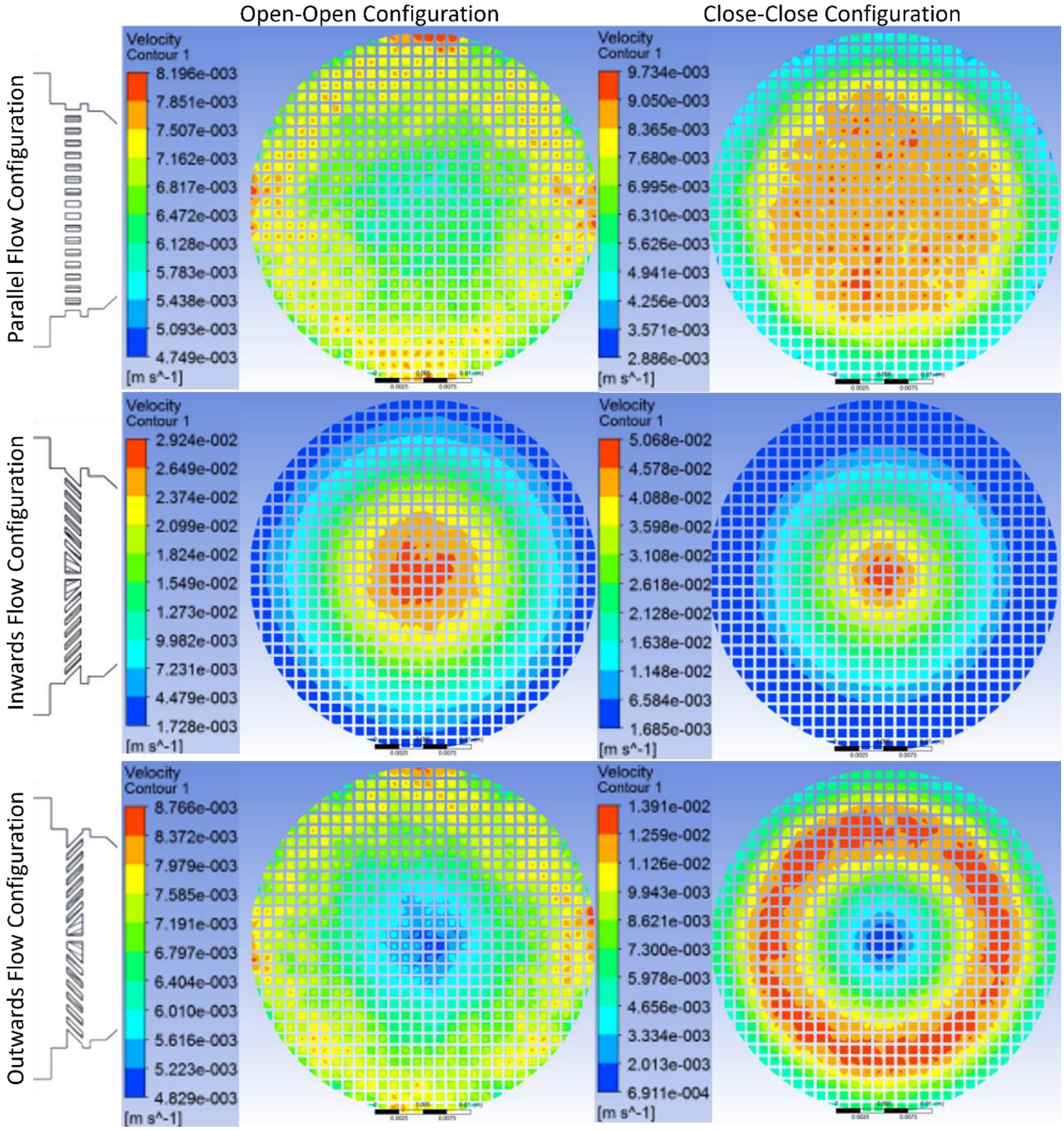

Figure 5.10 Results of the velocity profile for the extreme positions at the scaffold for the 0.2 m/s fluid velocity.

The IF, as seen in Figure 5.11, has the fluid velocity profile for all the three input velocities, where the configuration of pistons with the highest value is the CO. The lowest fluid velocity was obtained by the combination PF-OC for all the velocity inputs.

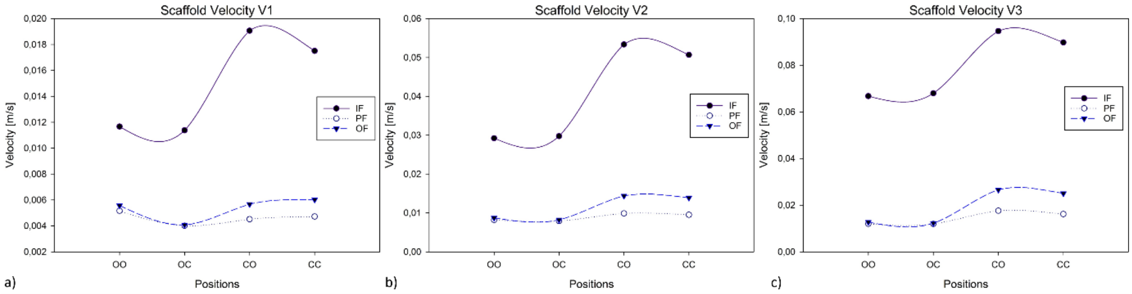

Figure 5.11 Results of the scaffold velocity for a) 0.1; b) 0.2; and c) 0.3 m/s.

<u>Scaffold Wall Shear Stress</u>

The major factor in understanding the optimum parameters of the bioreactor are given by the calculation of the shear stress on the scaffold walls. With this it is possible to foresee if the velocity is too high or if the piston is to close among several other parameters.

Figure 5.12 shows the obtained results for all the input velocities. Comparative to the fluid velocity results, it is possible to deduce a correlation between the velocity of the fluid and wall shear stress behaviour. As in the previous analysis, the IF-CO combination has the highest wall shear stress value and, again, the PF-OC the lowest.

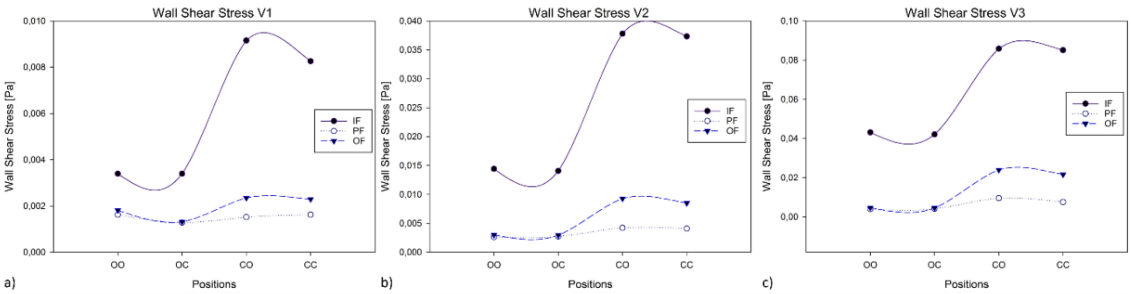

Figure 5.12 Results of the wall shear stress for all the three input velocities where, a) is 0.1; b) 0.2; and c) 0.3 m/s.

Analysing the colour map of the wall shear stress results in Figure 5.13 it is easy to deduce that closer the piston from the scaffold higher will the wall shear stress get for all the combinations, despite that PF configuration just slightly increases in the closed positions.

The redirection of the fluid after passing by the diffusion membrane is seen in the shear stress distribution on the colour map in the figure below. The IF membrane configuration has higher values of wall shear stress in the centre of the scaffold while the OF configuration has higher values in the peripheric region of the scaffold surface.

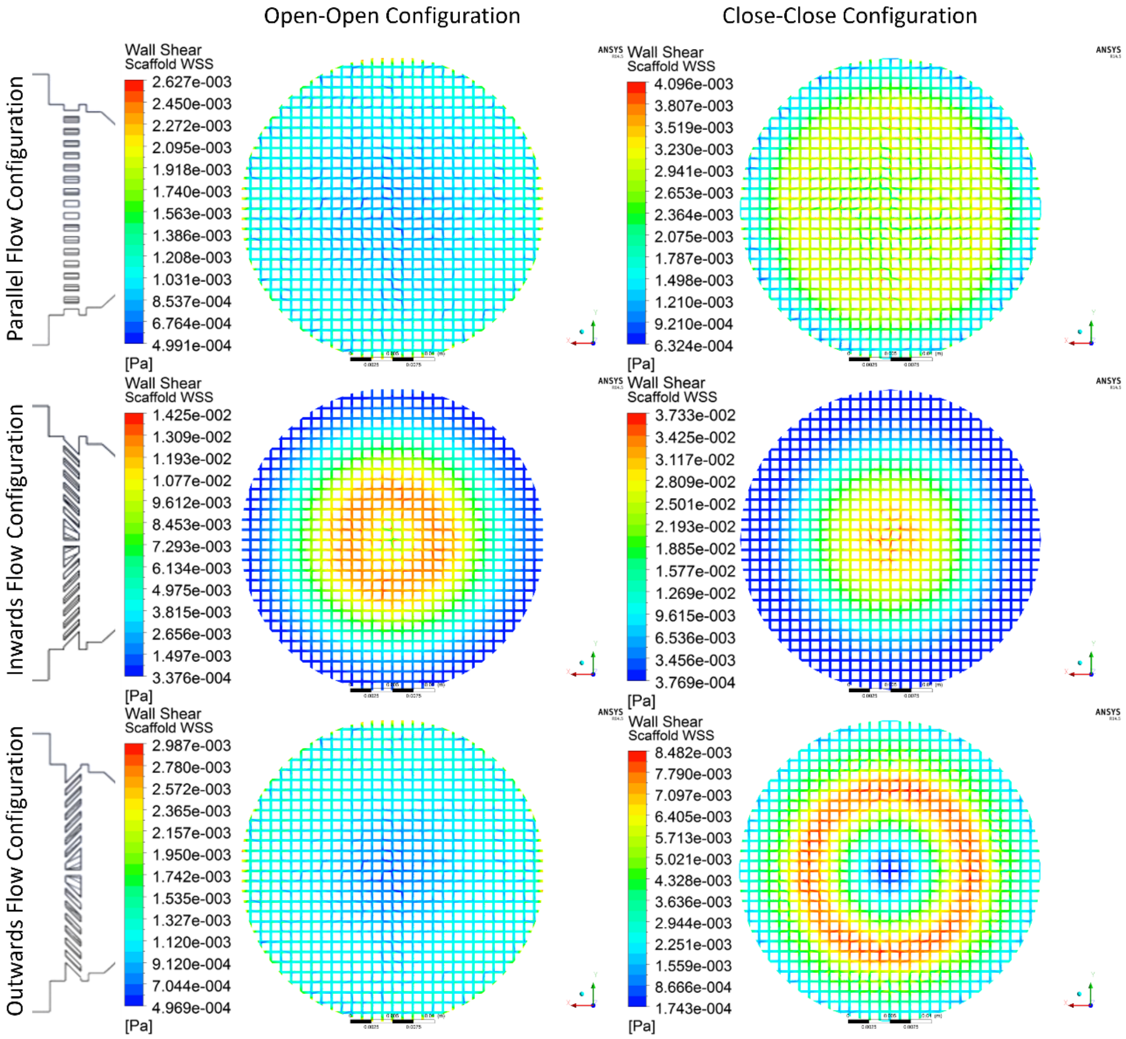

Figure 5.13 Wall shear stress results for the extreme piston positions and the three membrane configurations for 0.2 m/s input velocity.

5.2 2nd Phase: Permeability Study

The numerical analysis of permeability used the velocity results of the 1st phase simulations with the scaffold, as observed in Figure 5.10. For the permeability study it was used only the 0.2 m/s of fluid velocity. The results of this section were published as a book chapter in the book "New Trends in Mechanism and Machine Science" (Freitas *et al.*, 2015a).

The scaffold's permeability numerical calculation allowed obtaining both the total discharge Q (units of volume per time, *e.g.*, m^3/s) and the pressure drop (P_b-P_a). Since the viscosity μ (Pa·s) and the length over which the pressure drop is taking place (m), is already known. Then, for the numerical calculation, Equation 3.13 was applied in order to determine the scaffold's permeability.

As the diffusion of the fluid is forced by the membrane to go from the outer (OF) to the inner (IF) direction, the scaffold's permeability tends to decrease (Figure 5.14). As seen in the scaffold velocity results (Figure 5.10), there are membranes that create a more homogeneous distribution of the velocity on the scaffold, while others present a more heterogeneous distribution. These last cases influence the scaffold's permeability and the stimulation of the cells in terms of proliferation and differentiation.

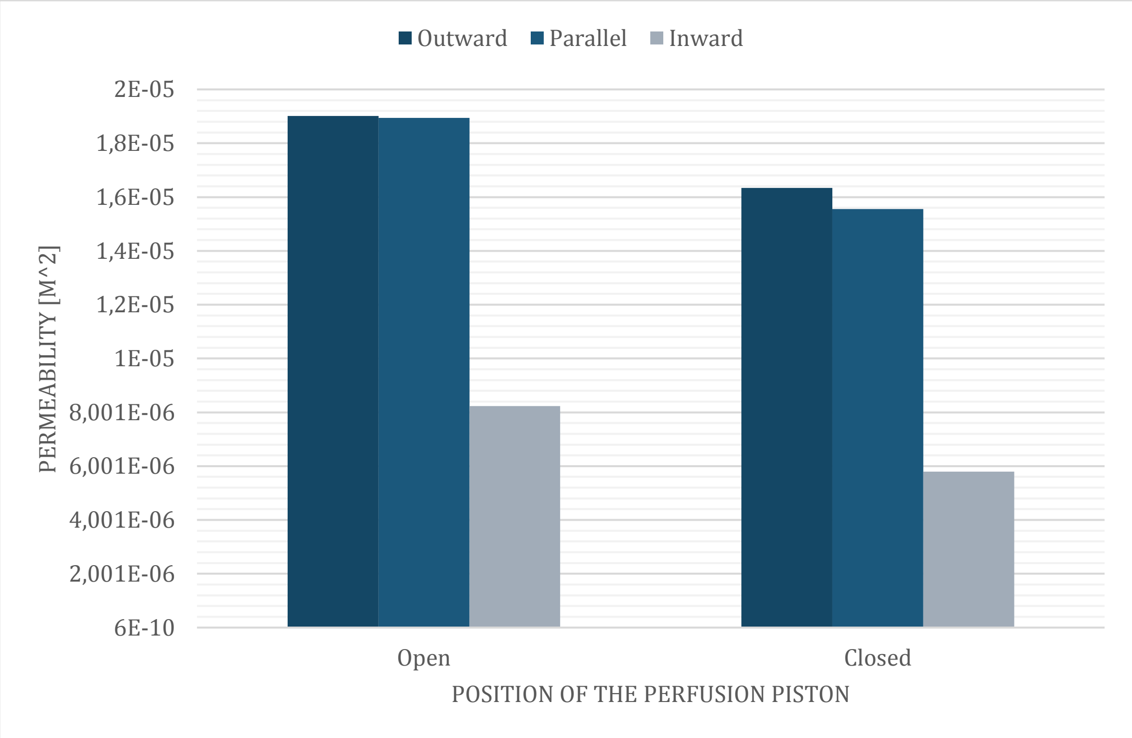

Figure 5.14 Diffusion membrane influence regarding the fluid flow.

Figure 5.15 plots the influence of the proximity of the inlet pistons on the scaffold. Analysing the referred figure is easy to infer that the fluid flow, in the closed positions, is forced and more concentrated in particular sections of the scaffold, creating a more uneven velocity distribution, decreasing the permeability of the scaffold.

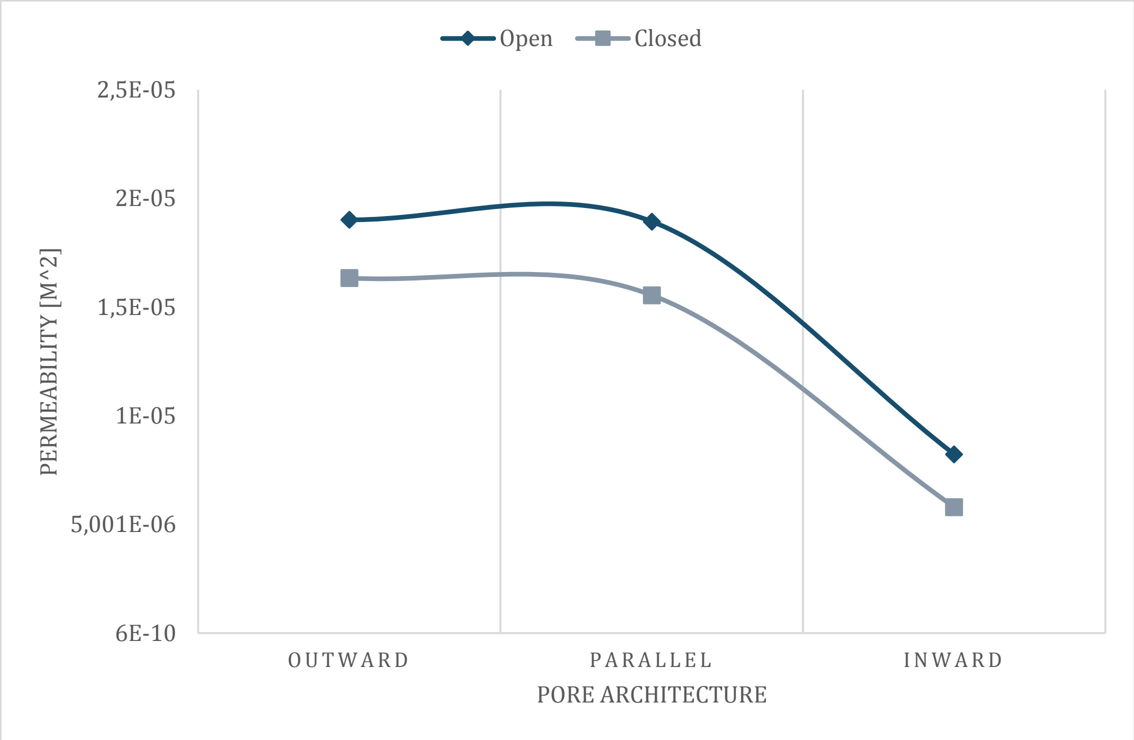

Figure 5.15 Influence of the proximity of the perfusion pistons.

5.3 3rd Phase: CFD and Structural Analysis

In this section, it was performed CFD analysis, and those results were then used to calculate the impact on the scaffold in the initial state (before the degradation process). The scaffold used has the shape of a 3D printed one as mentioned in previous Chapter 4, Section 4.2.2. Also the human plasma fluid properties is the same used in numerous studies (Barckhausen *et al.*, 2016; Chan *et al.*, 2004; Domansky *et al.*, 2010; Fournier, 2017; Malafaya and Reis, 2009; Sarkar *et al.*, 2015; Stamatialis, 2017; Zhang *et al.*, 2016).

The results of this phase were plotted, taking into account the lines in the location of the planes illustrated in Figure 5.16.

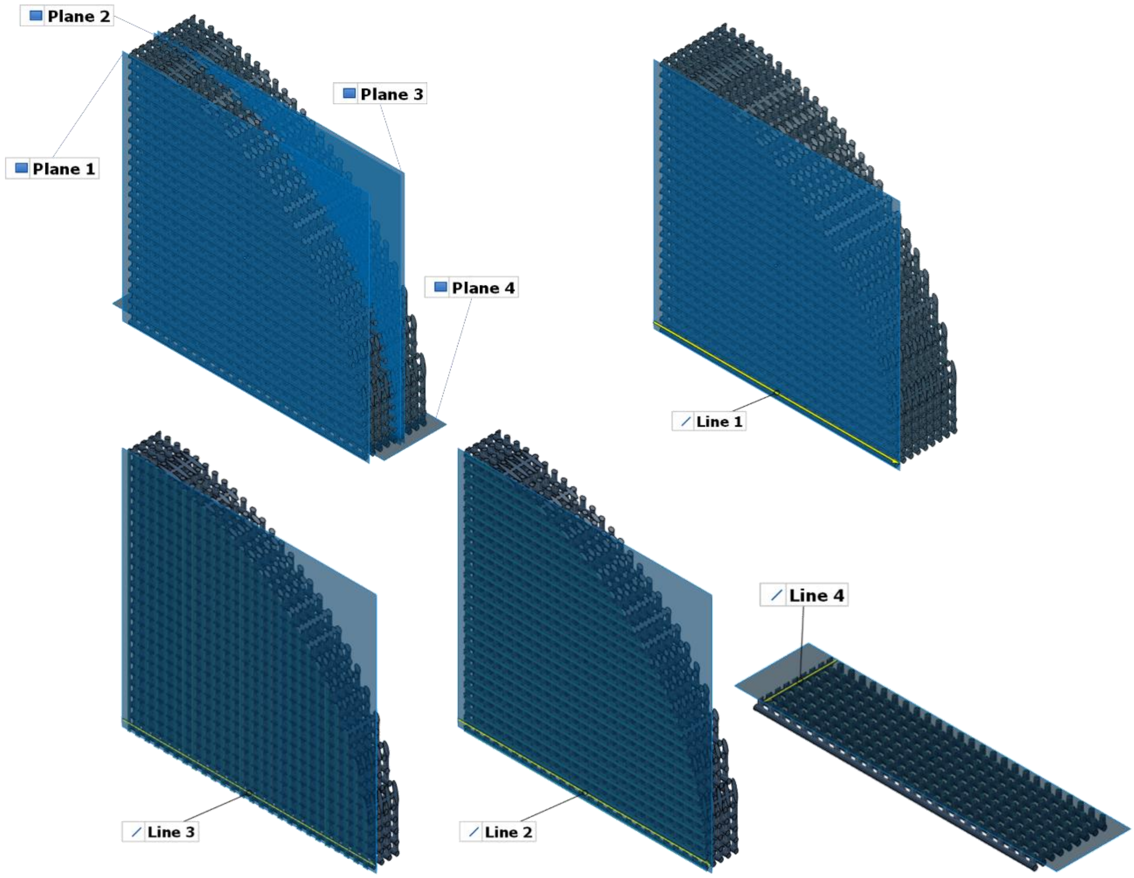

Figure 5.16 The results of this section, 3rd Phase, were plotted in the Lines 1 to 4 and the colour maps were plotted in the Planes 1 to 4.

5.3.1 CFD Analysis

The CFD analysis focused on the velocity and pressure suffered by the scaffold. After calculating the fluid behaviour in the 1st phase, the fluid within the chamber was already analysed therefore it is necessary to see the impact of the optimisation of the mechano-bioreactor on the scaffold and, afterwards, on the cells.

Scaffold Velocity

In terms of velocity within the scaffold, the behaviour for all the bioreactor piston/membrane combinations was more or less the same. Except for the Line 4 was the fluid have a heterogeneous behaviour within the scaffold pores in Z direction. On Line 1 and 3 the behaviour can be described as similar to all the combinations although there is a different behaviour between the Close and Open configuration on Line 1 where the inlet piston after the 14mm, for the Open positions, the velocity goes higher than for the Close position ones (Figure 5.17).

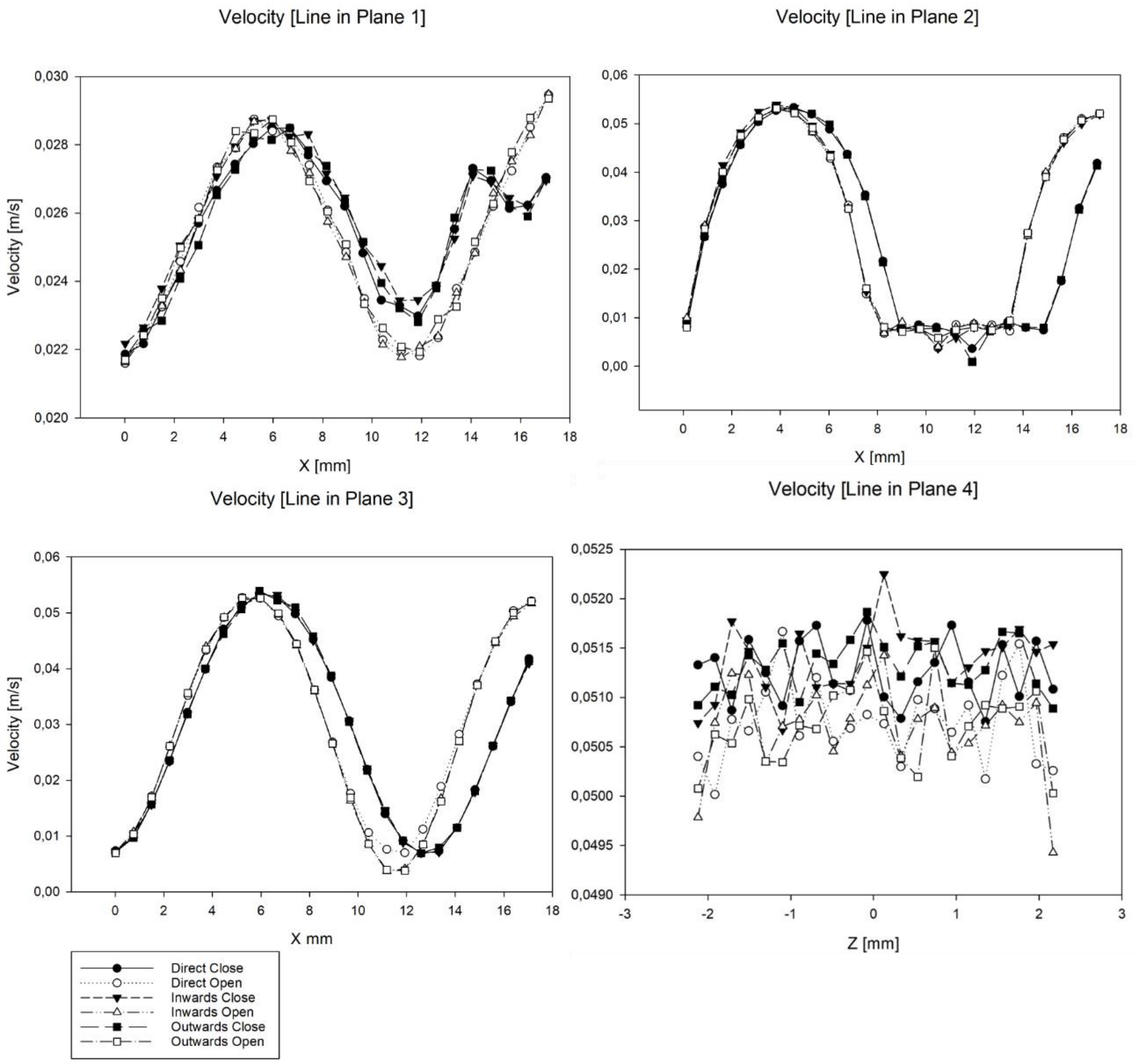

Figure 5.17 Results of the fluid velocity plotted within the scaffold on the lines 1 to 4.

The velocity is higher inside of the scaffold (Planes 2 and 3) than in the Plane 1, and this can be observed by the results obtained in Line 4 and in Figure 5.18 where we can observe a colour plot of the velocity for different combinations. In this figure is also possible to infer that the close positions have more impact in the heterogeneous fluid velocity distribution.

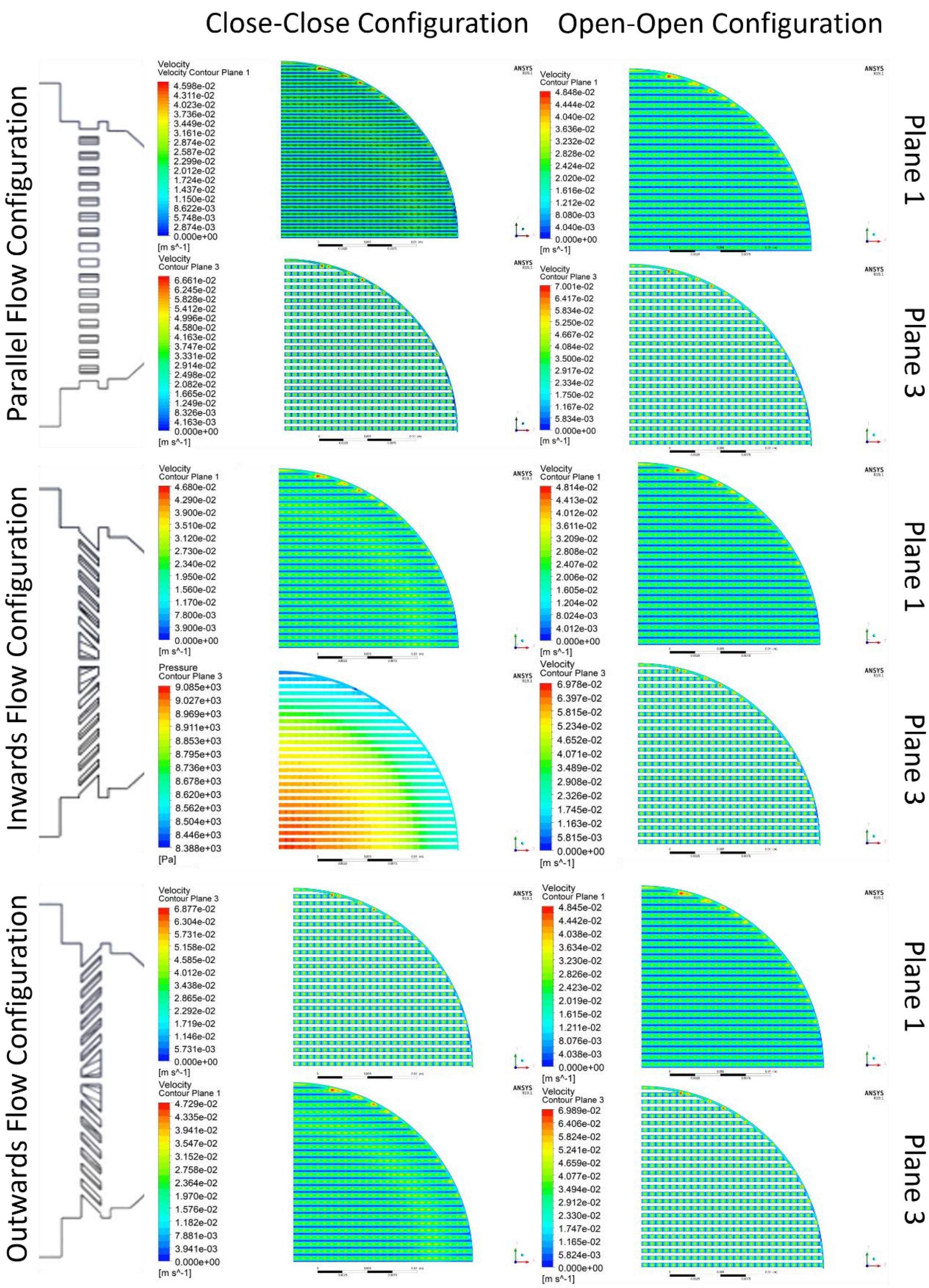

Figure 5.18 Plotted colour results of fluid velocity for Plane 1 and 3 for all the combinations.

Scaffold Pressure

Figure 5.19 shows the pressure results within the scaffold and, as seen, the pressure in the X direction usually is constant opposition to the pressure in Z direction (from inlet to outlet direction) where the pressure rises towards the outlet. In Line 2 there is a small depression in the pressure value due to the low depression caused in that region.

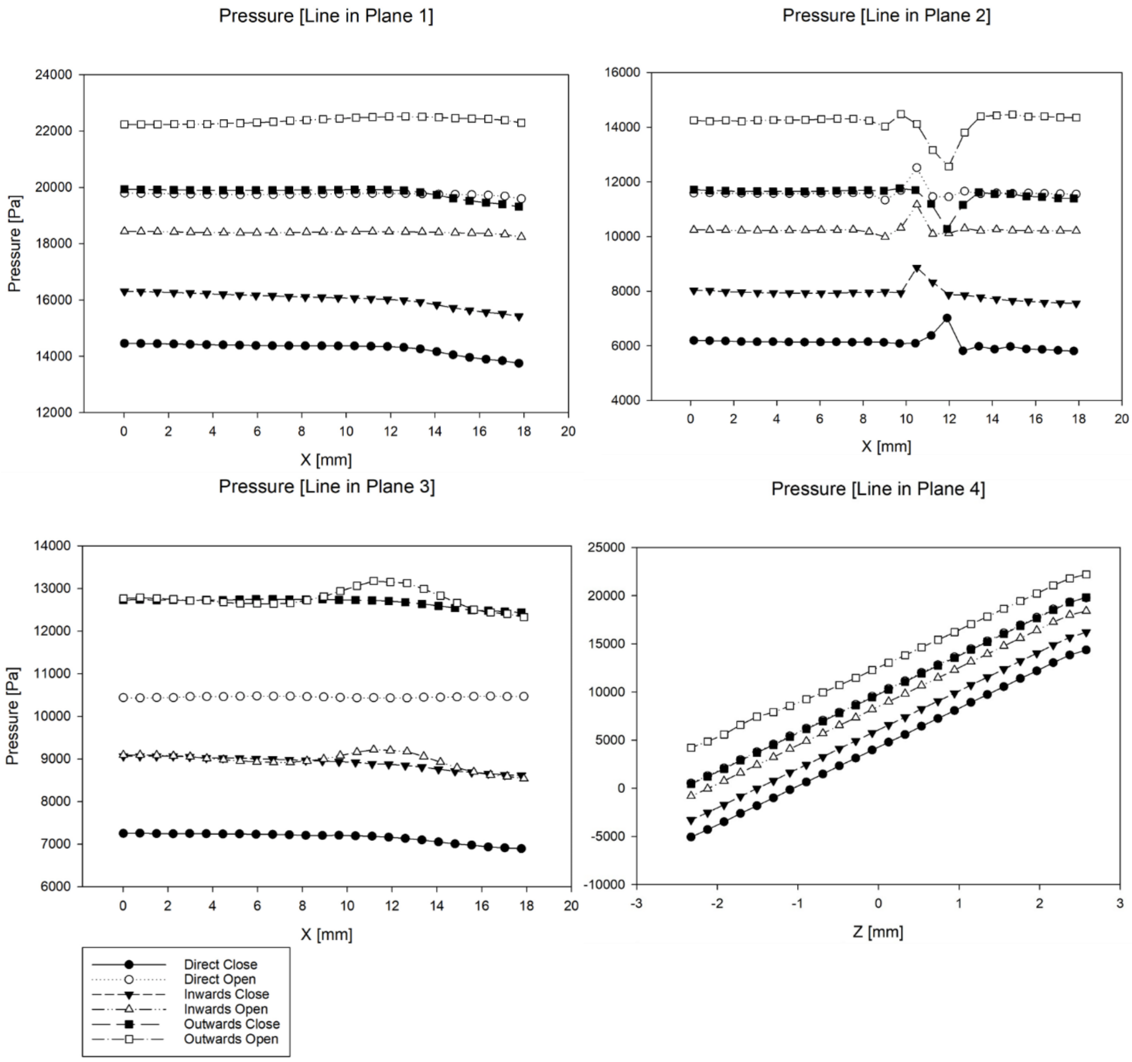

Figure 5.19 Pressure results for all the calculated Lines.

In Figure 5.20 is possible to observe the pressure exerted on Planes 1 and 3 regions. As observed in the previous Figure, the combination with the highest pressure in the X direction is the Outwards-Open (OO), and that can be observed in the colour map. Also, it is possible to see the pressure “ring” created by the diffusion membranes, especially on Plane 3 that is in the centre of the scaffold.

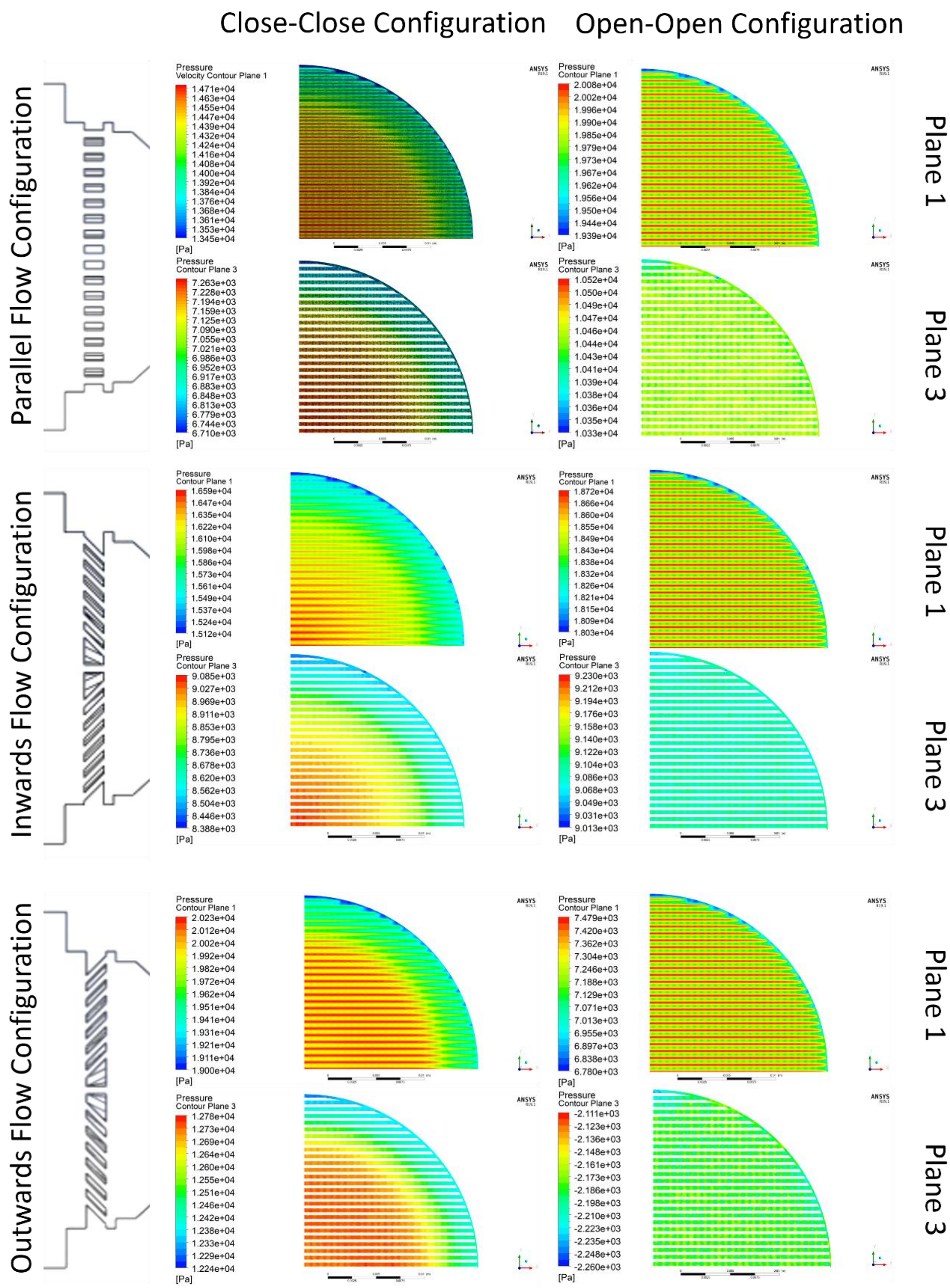

Figure 5.20 Colour plot results of the pressure in Plane 1 and 3 for all the piston and membrane combinations.

<u>Scaffold Wall Shear Stress</u>

The wall shear stress is of most use because it is possible to predict the shear stress values that will occur within the scaffold and therefore if the cells can withstand such stress. Figure 5.21 is plotted the results for each combination. The OO combination has higher shear stress values, while DC has the lowest. The fact that the diffusion membrane is redirecting the fluid to the culture chamber wall creates low depressions regions within the chamber increasing the velocity of the fluid and rising the shear stress.

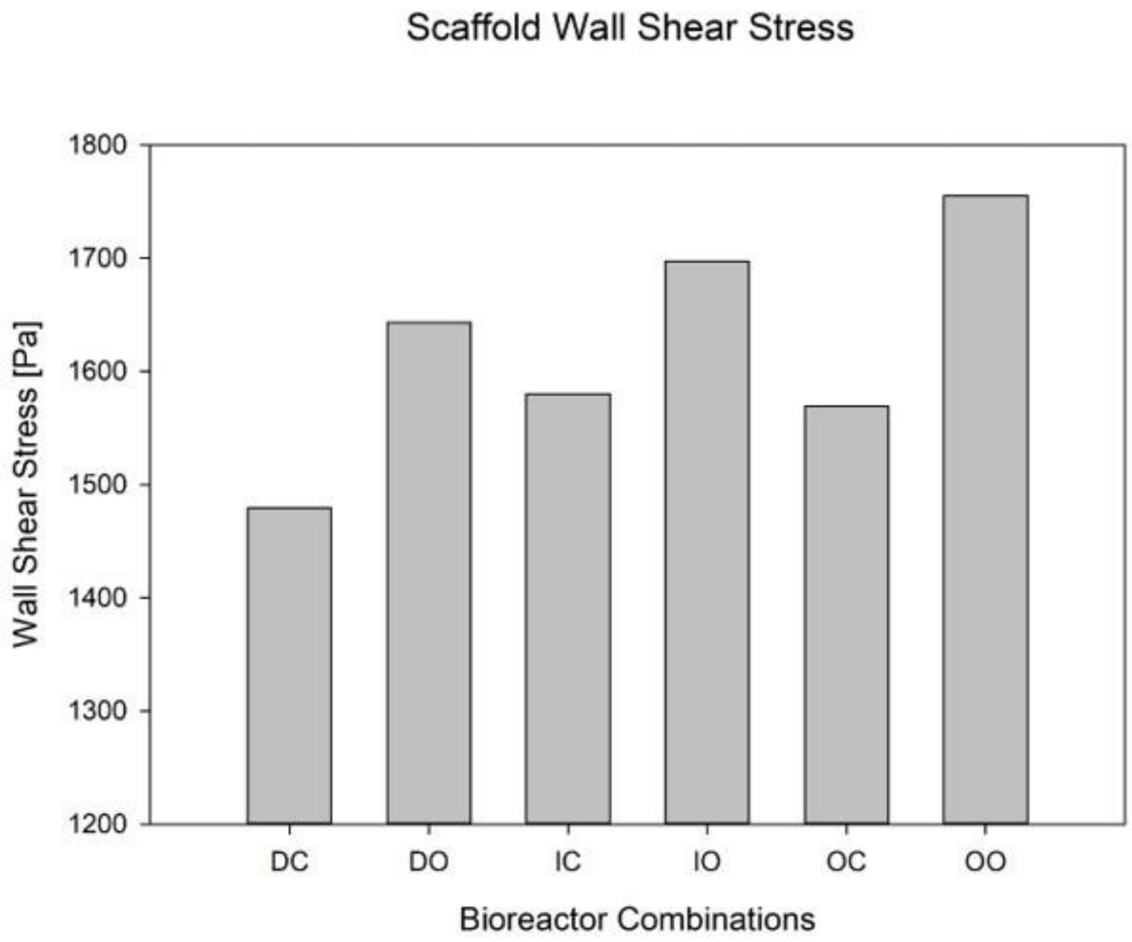

Figure 5.21 Scaffold wall shear stress for each piston/membrane combinations.

In Figure 5.22, it is possible to observe the colour plot on the scaffold surface. It is possible to observe a slightly yellow ring in the Close positions. The values range from 1.569×10^3 Pa from the OO piston/membrane position to 1.479×10^3 from the DC combination. The Open positions have all higher shear stress values than the Close positions.

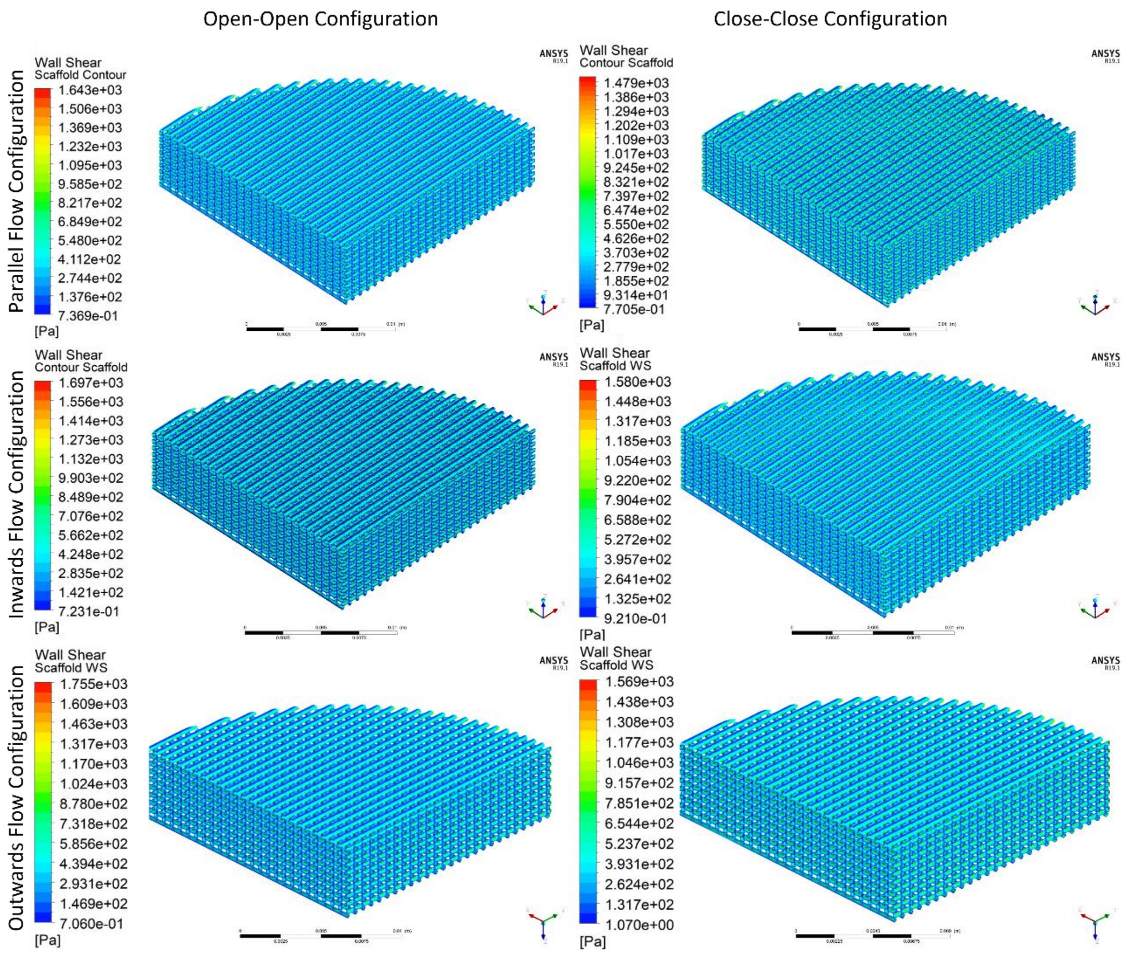

Figure 5.22 Colour plots of the wall shear stress for each combination.

5.3.2 Structural Analysis

By importing the results of the CFD pressure plots to the structural numerical simulation, it was possible to analyse the mechanical performance of the scaffold made of PCL, specifically the deformation and the von Mises stress.

<u>Scaffold Total Deformation</u>

The fluid flow exerts pressure on the scaffold surface that can damage and deform it. The results of the total deformation suffered by the scaffold can be seen in Figure 5.23 where it is visible that the high deformation ratio belongs to the combinations with the pistons in the Open position.

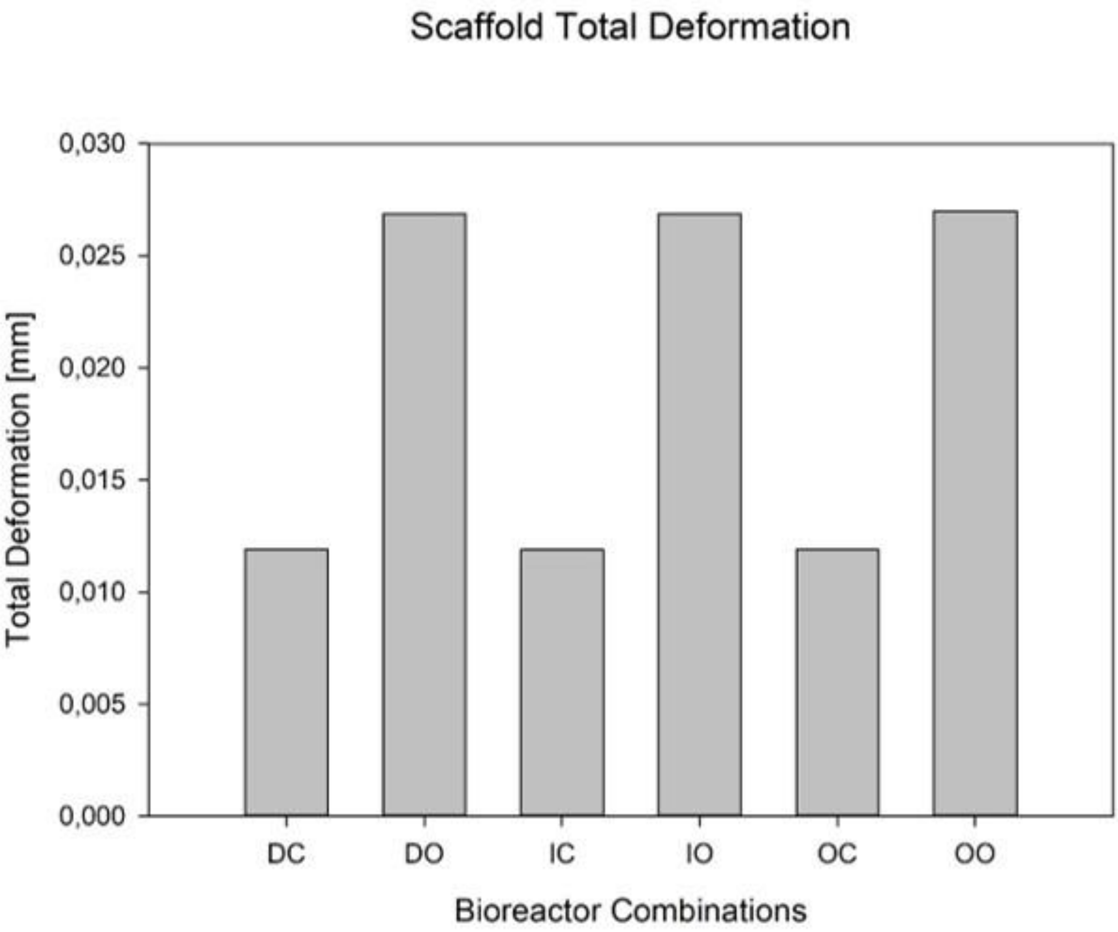

Figure 5.23 Total deformation suffered by the scaffold due to the fluid flow pressure.

The highest value of deformation was reached by the combination OO with 0.026982 mm while the lowest was the IC combination with 0.011881 mm. In fact, the range between the Open configurations is just 0.0001 mm so the results can be said that are very similar, the same happens for the Close position configurations of the piston with an even lower range of deformation of 0.00001 mm. Looking at Figure 5.24, it is possible to observe that because the scaffold is constrained in the perimeter because it is attached to the culture chamber all the deformation is mostly suffered in the centre of the scaffold.

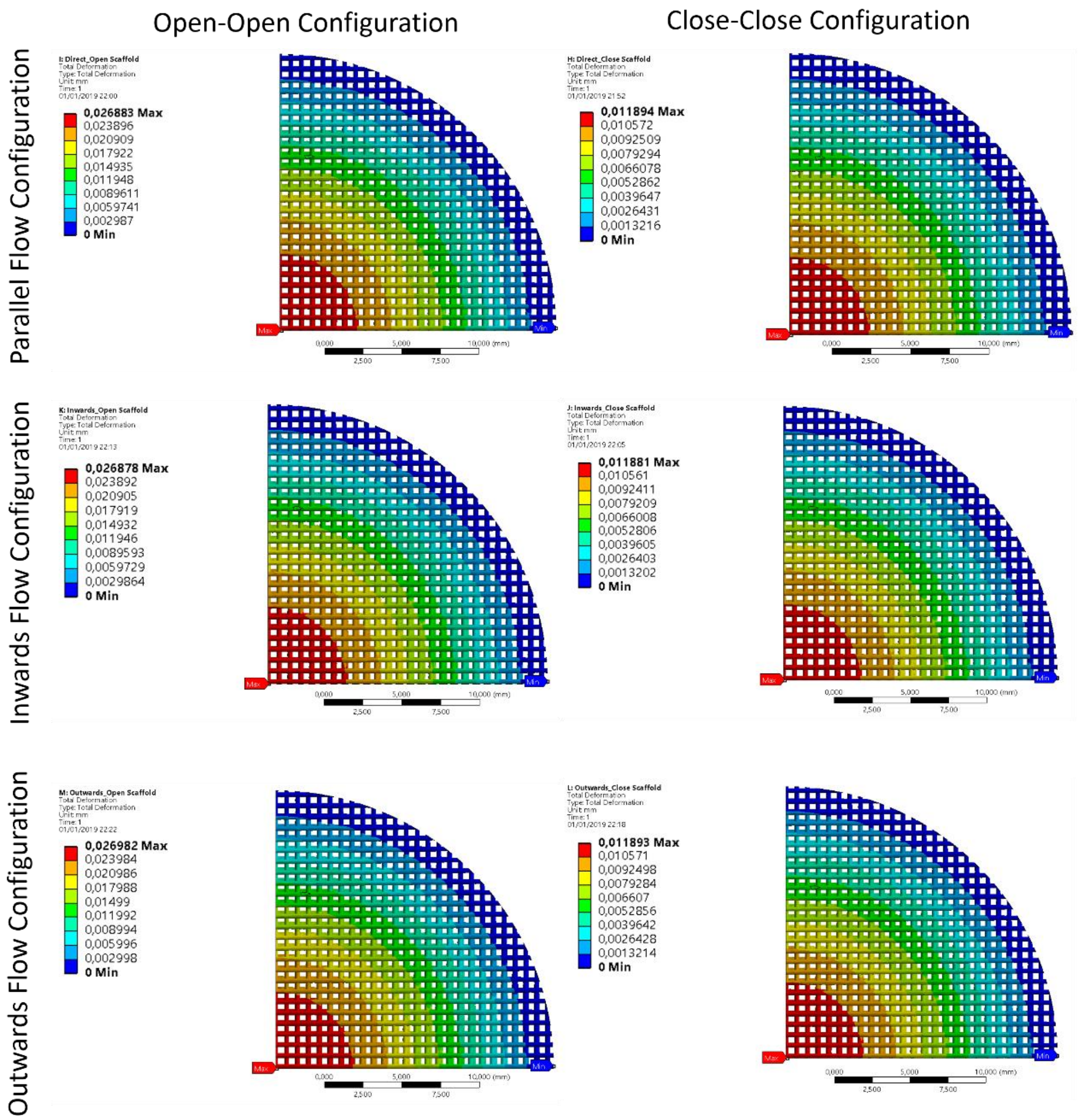

Figure 5.24 Colour plot of the total deformation on the scaffold.

Scaffold von Mises Stress

Analysing the von Mises stress, by observing Figure 5.25, all the calculated values for all the combinations are far from the stress limit of PCL properties. The combinations that hold the higher values of stress were the Open piston configurations with more than the double of the Close configurations stress value.

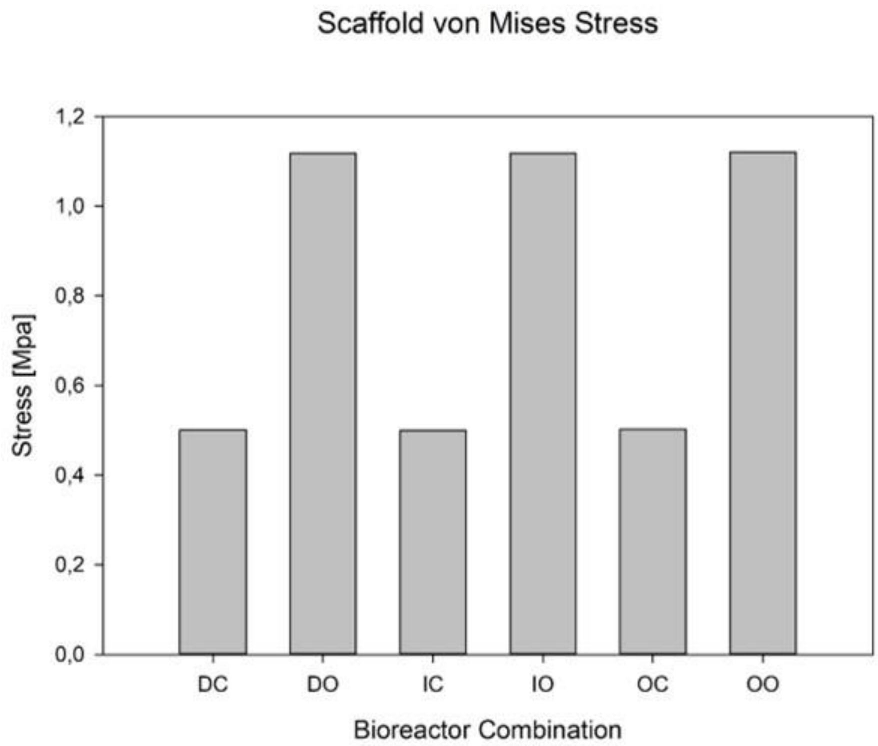

Figure 5.25 Results of the scaffold von Mises stress.

In Figure 5.26, it is possible to observe that the higher stress value is mainly in the constrained area of the scaffold and in the centre of the scaffold. The highest stress value was reached by the OO combination with 1.1201 Mpa, and the lowest was the IC combination with 0.49973 Mpa. The difference in the same piston configurations is little. The Open configuration the difference between the highest and the lowest value is 0.0025 Mpa, the same logic applied to the Close piston configurations, the range is 0.00281 Mpa.

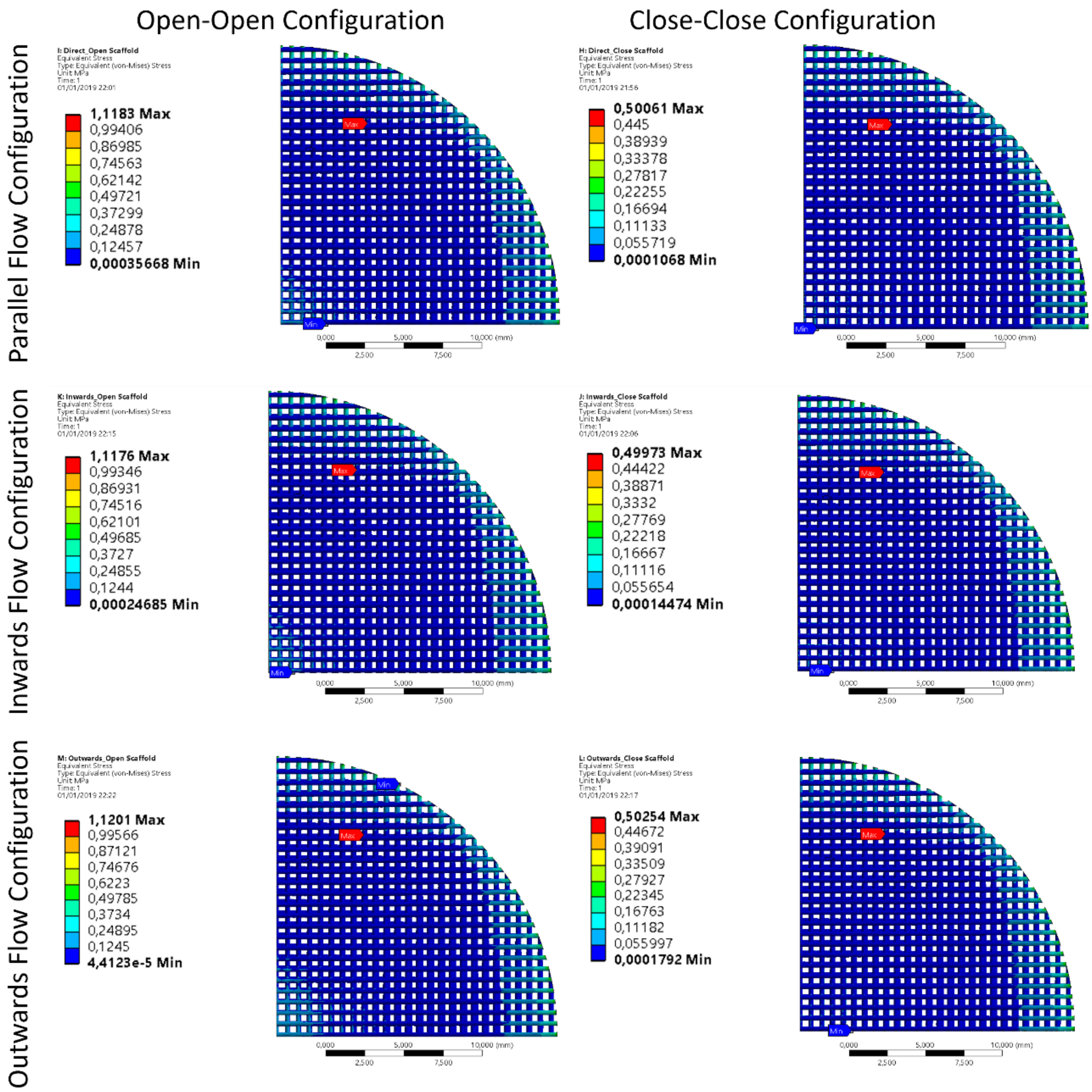

Figure 5.26 Colour map of the von Mises stress on the scaffold.

5.4 4th Phase: Degradation Study

One of the main variables analysed in this research was the wall shear stress in scaffolds. As seen in Chapter 3, Section 3.5 it is possible, through computational simulation, to predict the variation of the wall shear stress in scaffolds during its degradation process and thus to know the effect of the culture conditions on the cells. The results of this section were published as a book chapter in the book “BioMedWomen - Clinical and BioEngineering for Women’s Health” (Almeida *et al.*, 2016).

Figure 5.27 shows the variation of the surface tension along the degradation time for all speed values studied (0.1 m/s to 1.0 m/s). It is possible to infer that between the initial time and 20 days of degradation (between T0 and T20) the wall shear stress decreased from 1.712 Pa to 1.527 Pa. In T40, the wall shear stress rises to 1.686 Pa to decrease again in T60, reaching 1.596 Pa. From this moment, a considerable increase of the wall shear stress until the moment T340, with a maximum value of 2.369 Pa begins.

The lowest wall shear stress always occurs at times of degradation T20 or T60 while the highest tensions occur at T220 or T340. However, the oscillations observed at the initial stages of degradation tends to decrease with the decreasing of the velocity by verifying that similarly, the amplitude of the maximum values of wall shear stresses decreases with the velocity passing from 0.069 Pa to 9.545 Pa when increasing the velocity of 0.1 m/s to 1.0 m/s.

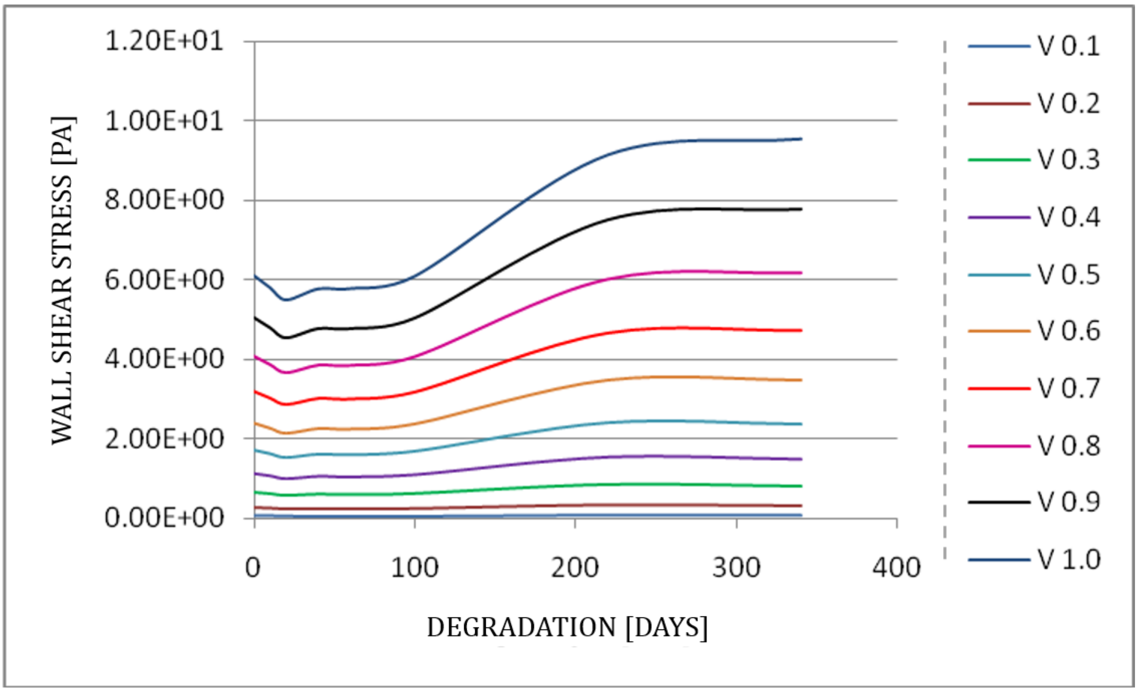

Figure 5.27 Variation of the wall shear stress on the scaffold over degradation time.

Figure 5.28 shows the variation of the wall shear stress in the scaffold along the degradation time, considering an input velocity of 0.5 m / s. It is important to note that, being the forces exerted on the scaffold constant, and decreasing the contact area, the tensions should naturally increase. However, the volume reduction characterising the degradation process translates into an increase in porosity creating less resistance to flow. This effect may be the cause of some observed irregularity in the initial instants.

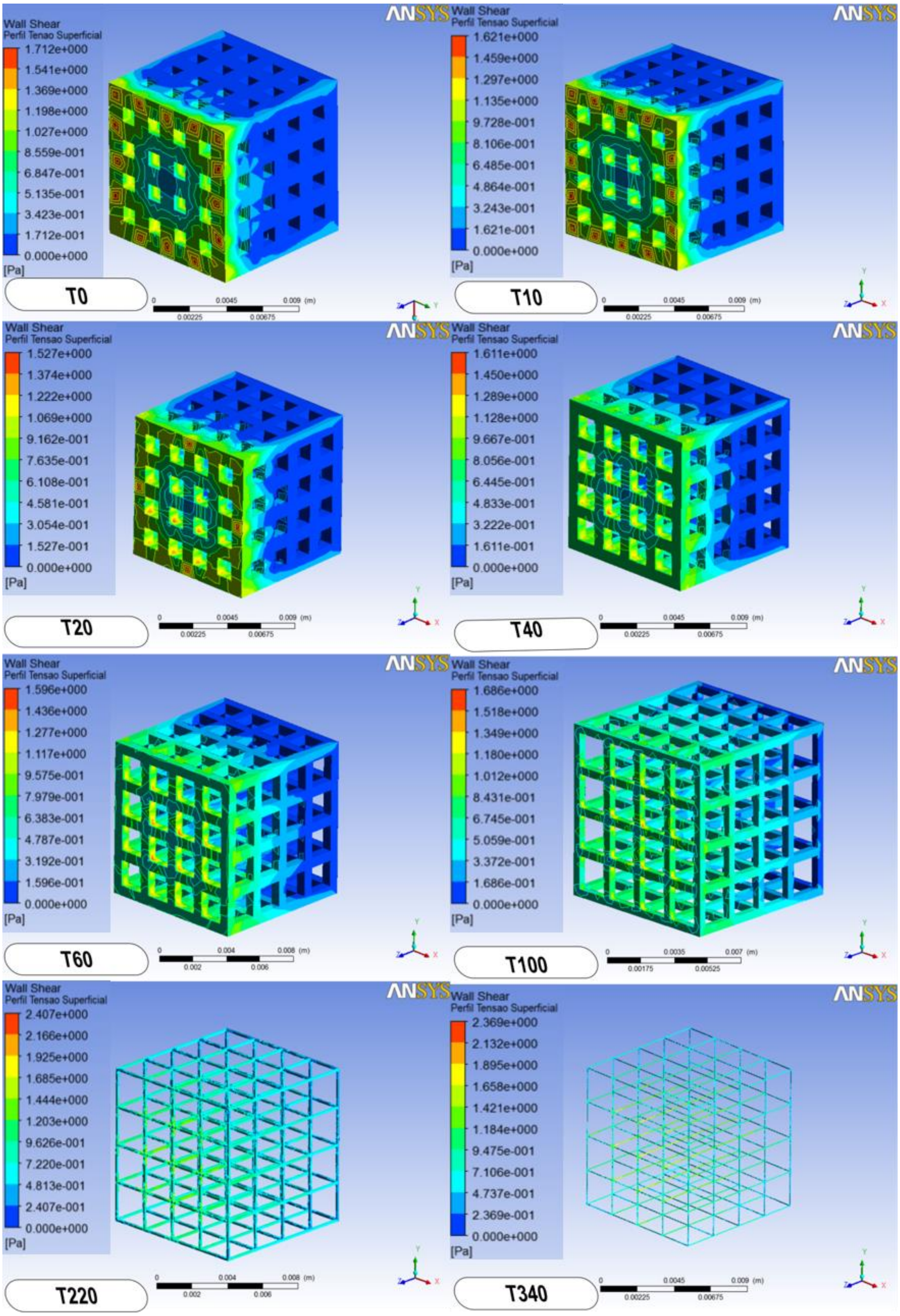

Figure 5.28 Wall shear stress results for the fluid velocity of 0.5 m/s overtime of the scaffold degradation.

In Figure 5.29, we can verify the evolution of the wall shear stress in the scaffold as a function of the flow velocity for all the degradation times. As noted previously, the surface tension increases with speed. For the minimum speed value, the maximum surface tension of 0.054 Pa increases to 5.781 Pa when the speed is maximum.

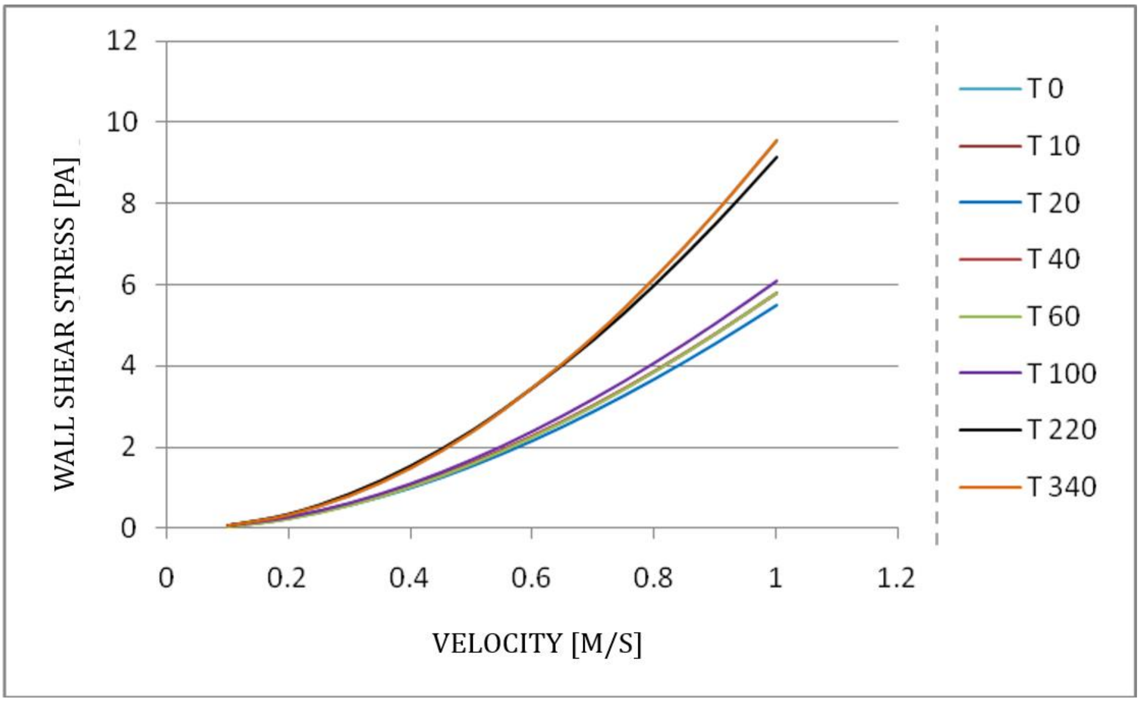

Figure 5.29 Wall shear stress as a function of fluid velocity and degradation time.

Also, structural analysis of the scaffold was performed. Using the results obtained from the CFD analysis, it was then exported the pressure profile to the structural analysis module, and it was calculated the deformation and von Mises stress.

The inlet velocity of 1.0 m/s presented the highest-pressure profiles during the scaffold degradation. Thus, only this input velocity was considered in the structural simulations for each degradation time step. Despite only being considered the velocity of 1.0 m/s, the structural simulations presented low deformation values and von Mises stresses. Figure 5.30 and Figure 5.31 illustrate the variation of the deformation and von Mises respectively, as a function of degradation. It is possible to observe that both the deformation and the von Mises stress tend to have a very slight increase in value until a degradation period of approximately 220 days, after which both increase significantly. In this particular scenario, degradation periods below 220 days has minimal impact on the scaffold's structural performance, after which is highly influenced by the scaffold's degradation.

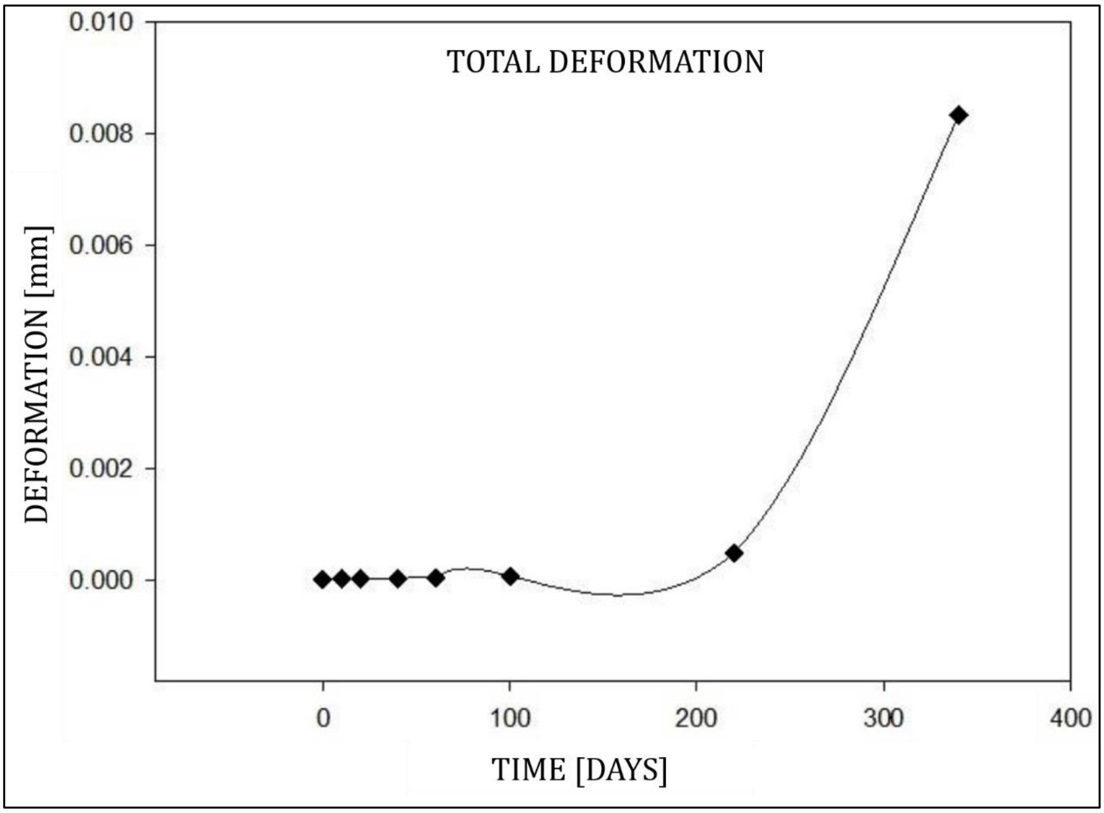

Figure 5.30 Deformation of the scaffold during the degradation time.

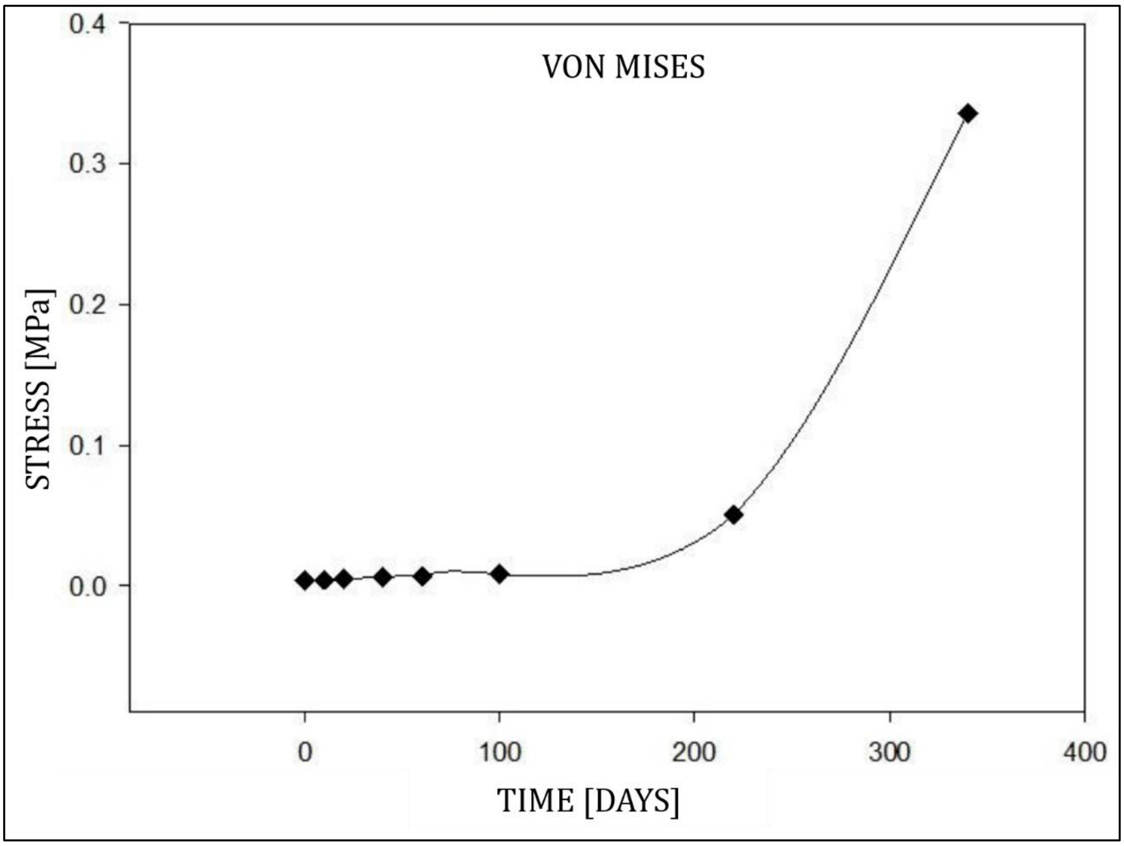

Figure 5.31 von Mises stresses during the degradation process of the scaffold.

6 SUMMARY, CONCLUSIONS AND FUTURE WORKS

In this final chapter will be presented the conclusions of this research work presenting the pros and cons of all the work carried out and in the last subchapter, it is also presented the future works in order to continue improving the field of tissue culture in bioreactors.

6.1 Summary and Conclusions

Tissue culture requires a series of conditions to create an environment suitable for cell culture. For this reason, designing and optimising a Bioreactor for TE is very complex. There are many parameters to be taken into account in order to design the proper culture chamber and create the optimum environment to successful cell culture.

One of the essential characteristics in terms of cell culture is cell stimulation. The proposed mechano-perfusion bioreactor intends to solve the lack of multiple stimulations occurring at the same time during cell cultivation. By means of applying mechanical *stimulus* with the inlet/outlet pistons or using the fluid flow by redirecting it with diffusion membranes and therefore creating a perfusion stimulation.

This study focused on analysing the fluid thoroughly within the culture chamber and on the scaffold. By doing this, the proposed bioreactor was analysed and optimised according to the study of the fluid behaviour in terms of velocity, turbulence, pressure in the culture chamber and, also, by analysing the wall shear stress, deformation and stress limit of the scaffold.

It was concluded that the piston positions and the fluid velocity have a high impact on the wall shear stress while the perforated diffusion membranes have an essential role in the distribution of the shear stress on the scaffold surface.

It was possible to conclude that by using the perfusion membrane, the shear stress distribution is more heterogeneous and therefore the culture of heterogeneous tissues. Also, as the inlet piston is closer to the scaffold (Close position) the velocity tends to be more homogeneous.

The combination that has higher wall shear stress impact on the scaffold is the Outward Flow configuration when both pistons are in the Open position. Using a fluid velocity of 0.5 m/s on the numerical simulations the wall shear stress ranges between 1.479×10^3 Pa to 1.755×10^3 Pa that in theory makes possible the cell culture of tissues such as Osteocytes (bone tissue) and Muscles (Figure 6.1).

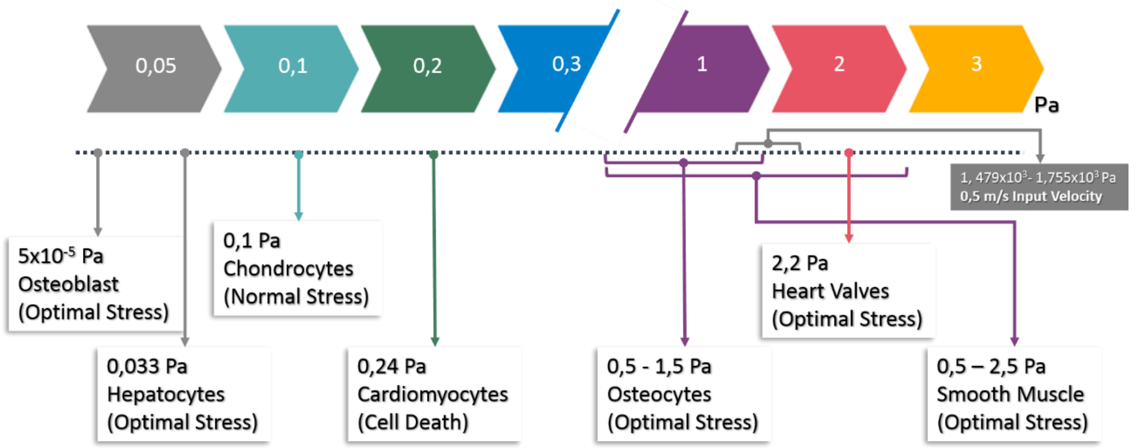

Figure 6.1 Optimum shear stress of common cells and the calculated shear stress of the proposed bioreactor for an input velocity of 0.5 m/s.

Regarding the scaffold degradation and permeability, it is possible to conclude that as the scaffold degrades the wall shear stress reaches critical values that may not help in the cell adhesion during the proliferation and differentiation process. In structural terms, the scaffold after the 220 days of degradation has little impact on the structural performance. In comparison the scaffold is more susceptible to be influenced by the fluid flow stimulations than the structural simulations. The direction of the fluid flow strongly influences the permeability. As the inlet piston gets closer to the scaffold the permeability tends to be higher.

The presented study has as main goal the optimisation of the bioreactor design taking into consideration the fluid behaviour and the applied stimulation on the scaffold. In terms of results it is possible to conclude that this main goal was achieved due to results obtained. The only major reflexion and work that has to be carried on is the construction of this bioreactor to verify these results experimentally.

6.2 Future Works

The future works can be divided into two, experimental work on laboratory and numerical simulations.

Concerning the experimental work;

- Micro-CT images of the degraded scaffolds in order to obtain accurate 3D models;
- Conduct cell tissue culture and compare the results with numerical;
- Construction of the bioreactor and comparison of the simulated data with real data;

Concerning numerical simulation:

- Models of cellular proliferation within this bioreactor;
- Conduct different numerical simulations by varying the angle, diameter and shape of the perfusion membrane holes.

During the time that this work was being carried out, several questions have been answered. Also, new doubts and new research directions have risen.

7 References

Abousleiman RI, Reyes Y, McFetridge P, Sikavitsas V. Tendon tissue engineering using cell-seeded umbilical veins cultured in a mechanical stimulator. Tissue Engineering Part A 2009;15:787–95. doi:10.1089/ten.tea.2008.0102.

Abousleiman RI, Sikavitsas VI. Bioreactors for Tissues of the Musculoskeletal System BT - Tissue Engineering. In: Fisher JP, editor. Tissue Engineering, Boston, MA: Springer US; 2007, p. 243–59.

Akmal M, Anand A, Anand B, Wiseman M, Goodship AE, Bentley G. The culture of articular chondrocytes in hydrogel constructs within a bioreactor enhances cell proliferation and matrix synthesis. The Journal of Bone and Joint Surgery British Volume 2006;88:544–53. doi:10.1302/0301-620X.88B4.16498.

Akter F. Principles of Tissue Engineering. In: Akter Farhana, editor. Tissue Engineering Made Easy, Elsevier; 2016, p. 3–16. doi:10.1016/B978-0-12-805361-4.00002-3.

Aleksieva G, Hollweck T, Thierfelder N, Haas U, Koenig F, Fano C, *et al*. Use of a special bioreactor for the cultivation of a new flexible polyurethane scaffold for aortic valve tissue engineering. Biomedical Engineering Online 2012;11:92. doi:10.1186/1475-925X-11-92.

Almeida HA, Bártolo PJ. Design of tissue engineering scaffolds based on hyperbolic surfaces: Structural numerical evaluation. Medical Engineering & Physics 2014;36:1033–40. doi:10.1016/j.medengphy.2014.05.006.

Almeida SR, Freitas D, Almeida HA, Bártolo PJ. Structural and vascular perfomance of biodegrading scaffolds within bioreactors. In: Natal Jorge R, Mascarenhas T, Duarte JA, Ramos I, Costa ME, Figueiral MH, *et al.*, editors. Biomedwomen, vol. 2, London: CRC Press; 2016, p. 165–71. doi:10.1201/9781315644622.

Altman GH, Lu HH, Horan RL, Calabro T, Ryder D, Kaplan DL, *et al*. Advanced bioreactor with controlled application of multi-dimensional strain for tissue engineering. Journal of Biomechanical Engineering 2002;124:742–9. doi:10.1115/1.1519280.

Amass W, Amass A, Tighe B. A review of biodegradable polymers: uses, current developments in the synthesis and characterization of biodegradable polyesters, blends of biodegradable polymers and recent advances in biodegradation studies. Polymer International 1998;47:89–144. doi:10.1002/(SICI)1097-0126(1998100)47:2<89::AID-PI86>3.0.CO;2-F.

Androjna C, Spragg RK, Derwin KA. Mechanical conditioning of cell-seeded small intestine submucosa: a potential tissue-engineering strategy for tendon repair. Tissue Engineering 2007;13:233–43. doi:10.1089/ten.2006.0050.

Ansys. ANSYS Manual v18 2017.

Ariadna G-P, Marc R, Teresa P, Joaquim C. Optimization of Poli(ε-caprolactone) Scaffolds Suitable for 3D Cancer Cell Culture. Procedia CIRP 2016;49:61–6. doi:10.1016/j.procir.2015.07.031.

Bakker A. The Colorful Fluid Mixing Gallery 2012. http://www.bakker.org/cfm (accessed 17 November 2018).

Baldocchi D. Wind and Turbulence, Surface Boundary Layer: Theory and Principles 2005.

Bancroft GN, Sikavitsas VI, van den Dolder J, Sheffield TL, Ambrose CG, Jansen J a, *et al*. Fluid flow increases mineralized matrix deposition in 3D perfusion culture of marrow stromal osteoblasts in a dose-dependent manner. Proceedings of the National Academy of Sciences of the United States of America 2002;99:12600–5. doi:10.1073/pnas.202296599.

Barckhausen C, Rice B, Baila S, Sensebé L, Schrezenmeier H, Nold P, *et al*. GMP-Compliant Expansion of Clinical-Grade Human Mesenchymal Stromal/Stem Cells Using a Closed Hollow Fiber Bioreactor. In: Gnecchi M, editor., New York, NY: Springer New York; 2016, p. 389–412. doi:10.1007/978-1-4939-3584-0_23.

Bártolo P, Bidanda B. Virtual Prototyping and Bio Manufacturing in Medical Applications. Boston, MA: Springer US; 2008. doi:10.1007/978-0-387-68831-2.

Bartolo P, Kruth J-P, Silva J, Levy G, Malshe A, Rajurkar K, *et al*. Biomedical production of implants by additive electro-chemical and physical processes. CIRP Annals 2012;61:635–55. doi:10.1016/j.cirp.2012.05.005.

Bártolo PJ, Almeida H, Laoui T. Rapid prototyping and manufacturing for tissue engineering scaffolds. International Journal of Computer Applications in Technology 2009a;36:1. doi:10.1504/ijcat.2009.026664.

Bártolo PJ, Almeida HA, Rezende RA, Laoui T, Bidanda B. Advanced Processes to Fabricate Scaffolds for Tissue Engineering. In: Bidanda B, Bártolo P, editors. Virtual Prototyping & Bio Manufacturing in Medical Applications, Boston, MA: Springer US; 2008, p. 149–70. doi:10.1007/978-0-387-68831-2_8.

Bártolo PJ, Chua CK, Almeida HA, Chou SM, Lim ASC. Biomanufacturing for tissue engineering: Present and future trends. Virtual and Physical Prototyping 2009b;4:203–16. doi:10.1080/17452750903476288.

Bedian L, Villalba-Rodríguez AM, Hernández-Vargas G, Parra-Saldivar R, Iqbal HMN. Bio-based materials with novel characteristics for tissue engineering applications – A review. International Journal of Biological Macromolecules 2017;98:837–46. doi:10.1016/j.ijbiomac.2017.02.048.

Begley CM, Kleis SJ. The Fluid Dynamic and Shear Environment in the NASA / JSC. Biotechnol Bioeng 2000;70:32–40.

Belfiore LA, Bonani W, Leoni M, Belfiore CJ. Pressure-sensitive nutrient consumption via dynamic normal stress in rotational bioreactors. Biophysical Chemistry 2009;140:99–107. doi:10.1016/j.bpc.2008.11.015.

Bernhard Rieder. Bioreactors in Tissue Engineering - Part 2. In: Eberli D, editor. Tissue Engineering, InTech; 2018, p. 323–36.

Bhumiratana S, Vunjak-Novakovic G. Concise Review: Personalized Human Bone Grafts for Reconstructing Head and Face. Stem Cells Translational Medicine 2012;1:64–9. doi:10.5966/sctm.2011-0020.

Bilgen B, Chu D, Stefani R, Aaron RK. Design of a biaxial mechanical loading bioreactor for tissue engineering. Journal of Visualized Experiments : JoVE 2013:e50387. doi:10.3791/50387.

Bilgen B, Sucosky P, Neitzel GP, Barabino GA. Flow Characterization of a Wavy-Walled Bioreactor for Cartilage Tissue Engineering. Biotechnology and Bioengineering 2006;95:1009–22. doi:10.1002/bit.

Billiet T, Vandenhaute M, Schelfhout J, Van Vlierberghe S, Dubruel P. A review of trends and limitations in hydrogel-rapid prototyping for tissue engineering. Biomaterials 2012;33:6020–41. doi:10.1016/j.biomaterials.2012.04.050.

Bliem R, Konopitzky K, Katinger H. Industrial Animal Cell Reactor Systems : Aspects of Selection and Evaluation. Advances in Biochemical Engineering Biotechnology 1991;44.

Boontheekul T, Mooney DJ. Protein-based signaling systems in tissue engineering. Current Opinion in Biotechnology 2003;14:559–65.

Brown MA, Rohin K. Iyer, Radisic M. Pulsatile Perfusion Bioreactor for Cardiac Tissue Engineering. Biotechnol Prog 2008:907–20. doi:10.1021/bp.11.

Bueno EM, Bilgen B, Carrier RL, Barabino G a. Increased rate of chondrocyte aggregation in a wavy-walled bioreactor. Biotechnology and Bioengineering 2004;88:767–77. doi:10.1002/bit.20261.

Burkersroda F von, Schedl L, Göpferich A. Why degradable polymers undergo surface erosion or bulk erosion. Biomaterials 2002;23:4221–31. doi:10.1016/S0142-9612(02)00170-9.

Butler DL, Hunter SA, Chokalingam K, Cordray MJ, Shearn J, Juncosa-Melvin N, *et al*. Using functional tissue engineering and bioreactors to mechanically stimulate tissue-engineered constructs. Tissue Engineering Part A 2009;15:741–9. doi:10.1089/ten.tea.2008.0292.

C.I.T. Perfusion bioreactor. Http://CitUnipvIt/Cit/Gallery/MainPhp?G2_itemId=28 2014. http://cit.unipv.it/cit/gallery/main.php?g2_itemId=28 (accessed 12 October 2018).

Cabrita GJM, Ferreira BS, da Silva CL, Gonçalves R, Almeida-Porada G, Cabral JMS. Hematopoietic stem cells: from the bone to the bioreactor. Trends in Biotechnology 2003;21:233–40. doi:10.1016/S0167-7799(03)00076-3.

Candiani G, Raimondi MT, Aurora R, Laganà K, Dubini G. Chondrocyte response to high regimens of cyclic hydrostatic pressure in 3-dimensional engineered constructs. International Journal of Artificial Organs 2008;31:490–9. doi:10.1177/039139880803100604.

Celik IB. Introductory Turbulence Modeling. Univias - Cca 1999.

Chan C, Berthiaume F, Nath BD, Tilles AW, Toner M, Yarmush ML. Hepatic tissue engineering for adjunct and temporary liver support: Critical technologies. Liver Transplantation 2004;10:1331–42. doi:10.1002/lt.20229.

Chen C-L, Rosi NL. Peptide-Based Methods for the Preparation of Nanostructured Inorganic Materials. Angewandte Chemie International Edition 2010;49:1924–42. doi:10.1002/anie.200903572.

Chen CS, Mrksich M, Huang S, Whitesides GM, Ingber DE. Geometric control of cell life and death. Science (New York, NY) 1997;276:1425–8.

Chen H-C, Hu Y-C. Bioreactors for tissue engineering. Biotechnology Letters 2006;28:1415–23. doi:10.1007/s10529-006-9111-x.

Chen H-C, Lee H-P, Sung M-L, Liao C-J, Hu Y-C. A novel rotating-shaft bioreactor for two-phase cultivation of tissue-engineered cartilage. Biotechnology Progress 2004;20:1802–9. doi:10.1021/bp049740s.

Chen H, Cornwell J, Zhang H, Lim T, Resurreccion R, Port T, *et al*. Cardiac-like flow generator for long-term imaging of endothelial cell responses to circulatory pulsatile flow at microscale. Lab on a Chip 2013;13:2999. doi:10.1039/c3lc50123j.

Chen JL, Yin Z, Shen WL, Chen X, Heng BC, Zou XH, *et al*. Efficacy of hESC-MSCs in knitted silk-collagen scaffold for tendon tissue engineering and their roles. Biomaterials 2010;31:9438–51. doi:10.1016/j.biomaterials.2010.08.011.

Chen Y, Zhou S, Li Q. Mathematical modeling of degradation for bulk-erosive polymers: Applications in tissue engineering scaffolds and drug delivery systems. Acta Biomaterialia 2011;7:1140–9. doi:10.1016/j.actbio.2010.09.038.

Chung CA, Chen CP, Lin TH, Tseng CS. A compact computational model for cell construct development in perfusion culture. Biotechnology and Bioengineering 2008;99:1535–41. doi:10.1002/bit.21701.

Chung CA, Chen CW, Chen CP, Tseng CS. Enhancement of cell growth in tissue-engineering constructs under direct perfusion: Modeling and simulation. Biotechnology and Bioengineering 2007;97:1603–16. doi:10.1002/bit.21378.

Chung CA, Yang CW, Chen CW. Analysis of cell growth and diffusion in a scaffold for cartilage tissue engineering. Biotechnology and Bioengineering 2006;94:1138–46. doi:10.1002/bit.20944.

Cimetta E, Flaibani M, Mella M, Serena E, Boldrin L, De Coppi P, *et al*. Enhancement of viability of muscle precursor cells on 3D scaffold in a perfusion bioreactor. The International Journal of Artificial Organs 2007;30:415–28.

Cinbiz MN, Tığlı RS, Beşkardeş IG, Gümüşderelioğlu M, Çolak Ü. Computational fluid dynamics modeling of momentum transport in rotating wall perfused bioreactor for cartilage tissue engineering. Journal of Biotechnology 2010;150:389–95. doi:10.1016/j.jbiotec.2010.09.950.

Cioffi M, Küffer J, Ströbel S, Dubini G, Martin I, Wendt D. Computational evaluation of oxygen and shear stress distributions in 3D perfusion culture systems: Macro-scale and micro-structured models. Journal of Biomechanics 2008;41:2918–25. doi:10.1016/j.jbiomech.2008.07.023.

Coletti F, Macchietto S, Elvassore N. Mathematical Modeling of Three-Dimensional Cell Cultures in Perfusion Bioreactors. Industrial & Engineering Chemistry Research 2006;45:8158–69. doi:10.1021/ie051144v.

Collins PC, Miller WM, Papoutsakis ET. Stirred culture of peripheral and cord blood hematopoietic cells offers advantages over traditional static systems for clinically relevant applications. Biotechnology and Bioengineering 1998;59:534–43. doi:10.1002/(SICI)1097-0290(19980905)59:5<534::AID-BIT2>3.0.CO;2-B.

Cook CA, Huri PY, Ginn BP, Gilbert-Honick J, Somers SM, Temple JP, *et al*. Characterization of a novel bioreactor system for 3D cellular mechanobiology studies. Biotechnology and Bioengineering 2016;113:1825–37. doi:10.1002/bit.25946.

Cooper JA, Li W-J, Bailey LO, Hudson SD, Lin-Gibson S, Anseth KS, *et al*. Encapsulated chondrocyte response in a pulsatile flow bioreactor. Acta Biomaterialia 2007;3:13–21. doi:10.1016/j.actbio.2006.08.010.

Correia C, Pereira AL, Duarte ARC, Frias AM, Pedro AJ, Oliveira JT, *et al*. Dynamic Culturing of Cartilage Tissue: The Significance of Hydrostatic Pressure. Tissue Engineering Part A 2012;18:1979–91. doi:10.1089/ten.tea.2012.0083.

Curcio E, De Bartolo L, Di Maio FP, Khakpour S, Giorno L, Di Renzo A. Oxygen transport in hollow fibre membrane bioreactors for hepatic 3D cell culture: A parametric study. Journal of Membrane Science 2017;544:312–22. doi:10.1016/j.memsci.2017.09.024.

Delafosse A, Collignon M-L, Calvo S, Delvigne F, Crine M, Thonart P, *et al*. CFD-based compartment model for description of mixing in bioreactors. Chemical Engineering Science 2014;106:76–85. doi:10.1016/j.ces.2013.11.033.

Démarteau O, Wendt D, Braccini a, Jakob M, Schäfer D, Heberer M, *et al*. Dynamic compression of cartilage constructs engineered from expanded human articular chondrocytes. Biochemical and Biophysical Research Communications 2003;310:580–8. doi:10.1016/j.bbrc.2003.09.099.

Depprich R, Handschel J, Wiesmann H-P, Jäsche-Meyer J, Meyer U. Use of bioreactors in maxillofacial tissue engineering. British Journal of Oral and Maxillofacial Surgery 2008;46:349–54. doi:10.1016/j.bjoms.2008.01.012.

Derakhshandeh B, Vlassopoulos D, Hatzikiriakos SG. Thixotropy, yielding and ultrasonic Doppler velocimetry in pulp fibre suspensions. Rheologica Acta 2012;51:201–14. doi:10.1007/s00397-011-0577-7.

Dias MR, Fernandes PR, Guedes JM, Hollister SJ. Permeability analysis of scaffolds for bone tissue engineering. Journal of Biomechanics 2012;45:938–44. doi:10.1016/j.jbiomech.2012.01.019.

Diban N, Gómez-Ruiz B, Lázaro-Díez M, Ramos-Vivas J, Ortiz I, Urtiaga A. Factors affecting mass transport properties of poly(ε-caprolactone) membranes for tissue engineering bioreactors. Membranes 2018;8:1–12. doi:10.3390/membranes8030051.

Domansky K, Inman W, Serdy J, Dash A, Lim MHM, Griffith LG. Perfused multiwell plate for 3D liver tissue engineering. Lab Chip 2010;10:51–8. doi:10.1039/B913221J.

Doroski DM, Levenston ME, Temenoff JS. Cyclic Tensile Culture Promotes Fibroblastic Differentiation of Marrow Stromal Cells Encapsulated in Poly(Ethylene Glycol)-Based Hydrogels. Tissue Engineering Part A 2010;16:3457–66. doi:10.1089/ten.tea.2010.0233.

Douglas JF, Gasiorek JM, Swaffield JA, Jack LB. Fluid Mechanics. 5th Editio. Harlow, UK: Pearson Education Limited; 2005.

Eaker S, Abraham E, Allickson J, Brieva TA, Baksh D, Heathman TRJ, *et al*. Bioreactors for cell therapies: Current status and future advances. Cytotherapy 2017;19:9–18. doi:10.1016/j.jcyt.2016.09.011.

Egger D, Fischer M, Clementi A, Ribitsch V, Hansmann J, Kasper C. Development and Characterization of a Parallelizable Perfusion Bioreactor for 3D Cell Culture. Bioengineering 2017;4:51. doi:10.3390/bioengineering4020051.

Elhamian SMM, Alizadeh M, Shokrieh MM, Karimi A. A depth dependent transversely isotropic micromechanic model of articular cartilage. Journal of Materials Science: Materials in Medicine 2015;26:111. doi:10.1007/s10856-015-5449-8.

Eshraghi S, Das S. Mechanical and microstructural properties of polycaprolactone scaffolds with one-dimensional, two-dimensional, and three-dimensional orthogonally oriented porous architectures produced by selective laser sintering. Acta Biomaterialia 2010;6:2467–76. doi:10.1016/j.actbio.2010.02.002.

Fernandes-Platzgummer A, Diogo MM, Baptista RP, da Silva CL, Cabral JMS. Scale-up of mouse embryonic stem cell expansion in stirred bioreactors. Biotechnology Progress 2011;27:1421–32. doi:10.1002/btpr.658.

Fournier RL. Basic Transport Phenomena in Biomedical Engineering, Fourth Edition. 4th Editio. Boca Raton: CRC Press; 2017. doi:10.1201/9781315120478.

Freitas D, Almeida H, Bartolo PJ. Perfusion Bioreactor Fluid Flow Optimization. Procedia Technology 2014a;16:1238–47. doi:10.1016/j.protcy.2014.10.139.

Freitas D, Almeida H, Bartolo PJ. Optimization of a perfusion bioreactor for tissue engineering. In: Jorge R, Campos J, Vaz M, Santos S, Tavares J, editors. Biodental Engineering III, London: CRC Press; 2014b, p. 6. doi:10.1201/b17071.

Freitas D, Almeida HA, Bártolo PJ. Permeability Evaluation of Flow Behaviors Within Perfusion Bioreactors. Mechanisms and Machine Science, vol. 24, 2015a, p. 761–8. doi:10.1007/978-3-319-09411-3_80.

Freitas D, Ciurana J, Almeida HA, Bartolo PJ. Computational analysis of a perfusion bioreactor for Tissue Engineering. The Second CIRP Conference on Biomanufacturing, vol. 00, Elsevier; 2015b, p. 1–7.

Freitas DM, Tojeira AP, Pereira RF, Bártolo PJ, Alves NM, Mendes AL, *et al*. Bioreactor Multifuncional para a Engenharia de Tecidos. Patente de Invenção Nacional No 105176, 2013.

Fu Q, Jia W, Lau GY, Tomsia AP. Strength, toughness, and reliability of a porous glass/biopolymer composite scaffold. Journal of Biomedical Materials Research Part B: Applied Biomaterials 2018;106:1209–17. doi:10.1002/jbm.b.33924.

Fu Q, Saiz E, Rahaman MN, Tomsia AP. Toward Strong and Tough Glass and Ceramic Scaffolds for Bone Repair. Advanced Functional Materials 2013;23:5461–76. doi:10.1002/adfm.201301121.

Fuchs JR, Nasseri BA, Vacanti JP. Tissue engineering: a 21st century solution to surgical reconstruction. The Annals of Thoracic Surgery 2001;72:577–91. doi:https://doi.org/10.1016/S0003-4975(01)02820-X.

Fung YC, Skalak R. Biomechanics. Mechanical Properties of Living Tissues. vol. 49. New York: Springer-Verlag; 2009. doi:10.1115/1.3162171.

García Cruz DM, Salmerón-Sánchez M, Gómez-Ribelles JL. Stirred flow bioreactor modulates chondrocyte growth and extracellular matrix biosynthesis in chitosan scaffolds. Journal of Biomedical Materials Research Part A 2012;100:2330–41. doi:10.1002/jbm.a.34174.

Gaspar DA, Gomide V, Monteiro FJ. The role of perfusion bioreactors in bone tissue engineering. Biomatter 2012;2:167–75. doi:10.4161/biom.22170.

Gelinsky M, Bernhardt A, Milan F. Bioreactors in tissue engineering: Advances in stem cell culture and three-dimensional tissue constructs. Engineering in Life Sciences 2015;15:670–7. doi:10.1002/elsc.201400216.

Gibson I. Rapid Prototyping: a Tool for Product Development. Computer-Aided Design and Applications 2005;2:785–93. doi:10.1080/16864360.2005.10738342.

Godia F, Sola C. Fluidized-bed bioreactors. Biotechnology Progress 1995;11:479–97. doi:10.1021/bp00035a001.

Gomes ME, Reis RL. Biodegradable polymers and composites in biomedical applications: from catgut to tissue engineering. Part 2 Systems for temporary replacement and advanced tissue regeneration. International Materials Reviews 2004;49:274–85. doi:10.1179/095066004225021927.

Goodhart J, Cooper J, Smith R, Williams J, Haggard W, Bumgardner J. Design and Validation of a Cyclic Strain Bioreactor to Condition Spatially-Selective Scaffolds in Dual Strain Regimes. Processes 2014;2:345–60. doi:10.3390/pr2020345.

Göpferich A. Erosion of composite polymer matrices. Biomaterials 1997;18:397–403. doi:10.1016/S0142-9612(96)00151-2.

Grayson WL, Bhumiratana S, Cannizzaro C, Chao P-HG, Lennon DP, Caplan AI, *et al*. Effects of initial seeding density and fluid perfusion rate on formation of tissue-engineered bone. Tissue Engineering Part A 2008;14:1809–20. doi:10.1089/ten.tea.2007.0255.

Grayson WL, Bhumiratana S, Cannizzaro C, Chao PHG, Lennon DP, Caplan AI, *et al*. Effects of initial seeding density and fluid perfusion rate in formation of tiessue-enginereed bone. Tissue Engineering Part A 2009;14:1809–20. doi:10.1089/ten.tea.2007.0255.Effects.

Grayson WL, Marolt D, Bhumiratana S, Fröhlich M, Guo XE, Vunjak-Novakovic G. Optimizing the medium perfusion rate in bone tissue engineering bioreactors. Biotechnology and Bioengineering 2011;108:1159–70. doi:10.1002/bit.23024.

Gross KA, Rodríguez-Lorenzo LM. Biodegradable composite scaffolds with an interconnected spherical network for bone tissue engineering. Biomaterials 2004;25:4955–62. doi:https://doi.org/10.1016/j.biomaterials.2004.01.046.

Guillotin B, Guillemot F. Cell patterning technologies for organotypic tissue fabrication. Trends in Biotechnology 2011;29:183–90. doi:10.1016/j.tibtech.2010.12.008.

El Haj AJ, Wood MA, Thomas P, Yang Y. Controlling cell biomechanics in orthopaedic tissue engineering and repair. Pathologie Biologie 2005;53:581–9. doi:10.1016/j.patbio.2004.12.002.

Halonen KS, Mononen ME, Jurvelin JS, Töyräs J, Salo J, Korhonen RK. Deformation of articular cartilage during static loading of a knee joint--experimental and finite element analysis. Journal of Biomechanics 2014;47:2467–74. doi:10.1016/j.jbiomech.2014.04.013.

Hammond T, Allen P, Birdsall H. Is There a Space-Based Technology Solution to Problems with Preclinical Drug Toxicity Testing? Pharmaceutical Research 2016;33:1545–51. doi:10.1007/s11095-016-1942-0.

Han X, Pan J. Polymer chain scission, oligomer production and diffusion: A two-scale model for degradation of bioresorbable polyesters. Acta Biomaterialia 2011;7:538–47. doi:10.1016/j.actbio.2010.09.005.

Han X, Pan J, Buchanan F, Weir N, Farrar D. Analysis of degradation data of poly(l-lactide–co-l,d-lactide) and poly(l-lactide) obtained at elevated and physiological temperatures using mathematical models. Acta Biomaterialia 2010;6:3882–9. doi:10.1016/j.actbio.2010.05.015.

Hansmann J, Groeber F, Kahlig A, Kleinhans C, Walles H. Bioreactors in tissue engineering-principles, applications and commercial constraints. Biotechnology Journal 2013;8:298–307. doi:10.1002/biot.201200162.

Hao Z, Song Z, Huang J, Huang K, Panetta A, Gu Z, *et al*. The scaffold microenvironment for stem cell based bone tissue engineering. Biomaterials Science 2017;5:1382–92. doi:10.1039/C7BM00146K.

Hirschel M, Gangemi JD, McSharry J, Myers C. Novel Uses for Hollow Bioreactors. Genetic Engineering & Biotechnology News 2011:31(12).

Hoenig E, Winkler T, Mielke G, Paetzold H, Schuettler D, Goepfert C, *et al*. High Amplitude Direct Compressive Strain Enhances Mechanical Properties of Scaffold-Free Tissue-Engineered Cartilage. Tissue Engineering Part A 2011;17:1401–11. doi:10.1089/ten.tea.2010.0395.

Hoesli C a, Luu M, Piret JM. A novel alginate hollow fiber bioreactor process for cellular therapy applications. Biotechnology Progress 2009;25:1740–51. doi:10.1002/btpr.260.

Hoque ME. Robust formulation for the design of tissue engineering scaffolds: A comprehensive study on structural anisotropy, viscoelasticity and degradation of 3D scaffolds fabricated with customized desktop robot based rapid prototyping (DRBRP) system. Materials Science and Engineering: C 2017;72:433–43. doi:10.1016/j.msec.2016.11.019.

Huang B, Caetano G, Vyas C, Blaker J, Diver C, Bártolo P. Polymer-Ceramic Composite Scaffolds: The Effect of Hydroxyapatite and β-tri-Calcium Phosphate. Materials 2018;11:129. doi:10.3390/ma11010129.

Hunter P. One organ at a time: Research has been making much progress to create *in vitro* human tissues for transplantation but laboratory-grown complex organs still remain decades away. EMBO Reports 2014;15:227–30. doi:10.1002/embr.201438528.

Hutmacher DW. Scaffold design and fabrication technologies for engineering tissues — state of the art and future perspectives. Journal of Biomaterials Science, Polymer Edition 2001;12:107–24. doi:10.1163/156856201744489.

Hutmacher DW, Singh H. Computational fluid dynamics for improved bioreactor design and 3D culture. Trends in Biotechnology 2008;26:166–72. doi:10.1016/j.tibtech.2007.11.012.

Hutmacher DW, Teoh SH, Ranawake M, Chong WS, Ting KS, Chua KC, *et al*. Bioreactor for growing cell or tissue cultures. 2006/0019388 A1, 2006.

iData Research. U.S. Orthopedic Biomaterials Market. Dallas, Texas, USA: 2013.

Ishikawa M, Sekine K, Okamura A, Zheng Y-W, Ueno Y, Koike N, *et al*. Reconstitution of hepatic tissue architectures from fetal liver cells obtained from a three-dimensional culture with a rotating wall vessel bioreactor. Journal of Bioscience and Bioengineering 2011;111:711–8. doi:10.1016/j.jbiosc.2011.01.019.

Jaasma MJ, Plunkett N a, O'Brien FJ. Design and validation of a dynamic flow perfusion bioreactor for use with compliant tissue engineering scaffolds. Journal of Biotechnology 2008;133:490–6. doi:10.1016/j.jbiotec.2007.11.010.

Janoušková O. Synthetic polymer scaffolds for soft tissue engineering. Physiological Research 2018;67:S335–48.

Janssen FW, Oostra J, Oorschot A Van, van Blitterswijk C a. A perfusion bioreactor system capable of producing clinically relevant volumes of tissue-engineered bone: *in vivo* bone formation showing proof of concept. Biomaterials 2006;27:315–23. doi:10.1016/j.biomaterials.2005.07.044.

Jeong JH, Kim SW, Park TG. Molecular design of functional polymers for gene therapy. Progress in Polymer Science 2007;32:1239–74. doi:10.1016/j.progpolymsci.2007.05.019.

Jia X, Qi L, Zhang Y, Yang X, Wang H, Zhao F, *et al*. Computational fluid dynamics simulation of a novel bioreactor for sophorolipid production. Chinese Journal of Chemical Engineering 2017;25:732–40. doi:10.1016/j.cjche.2016.09.014.

Juncosa-Melvin N, Shearn JT, Boivin GP, Gooch C, Galloway MT, West JR, *et al*. Effects of mechanical stimulation on the biomechanics and histology of stem cell-collagen sponge constructs for rabbit patellar tendon repair. Tissue Engineering 2006;12:2291–300. doi:10.1089/ten.2006.12.2291.

Jungreuthmayer C, Jaasma MJ, Al-Munajjed AA, Zanghellini J, Kelly DJ, O'Brien FJ. Deformation simulation of cells seeded on a collagen-GAG scaffold in a flow perfusion bioreactor using a sequential 3D CFD-elastostatics model. Medical Engineering & Physics 2009;31:420–7. doi:10.1016/j.medengphy.2008.11.003.

Kakavand M, Yazdanpanah G, Ahmadiani A, Niknejad H. Blood compatibility of human amniotic membrane compared with heparin-coated ePTFE for vascular tissue engineering. Journal of Tissue Engineering and Regenerative Medicine 2017;11:1701–9. doi:10.1002/term.2064.

Kang H, Lu S, Peng J, Yang Q, Liu S, Zhang L, *et al*. *In vivo* construction of tissue-engineered cartilage using adipose-derived stem cells and bioreactor technology. Cell and Tissue Banking 2015;16:123–33. doi:10.1007/s10561-014-9448-7.

Kang Z, Zhang X, Chen Y, Akram MY, Nie J, Zhu X. Preparation of polymer/calcium phosphate porous composite as bone tissue scaffolds. Materials Science and Engineering: C 2017;70:1125–31. doi:10.1016/j.msec.2016.04.008.

Kaul H, Ventikos Y, Cui Z. A computational analysis of the impact of mass transport and shear on three-dimensional stem cell cultures in perfused micro-bioreactors. Chinese Journal of Chemical Engineering 2016;24:163–74. doi:10.1016/j.cjche.2015.11.017.

Khetani SR, Bhatia SN. Engineering tissues for *in vitro* applications. Current Opinion in Biotechnology 2006;17:524–31. doi:10.1016/j.copbio.2006.08.009.

Kim B-S, Mooney DJ. Development of biocompatible synthetic extracellular matrices for tissue engineering. Trends in Biotechnology 1998;16:224–30. doi:10.1016/S0167-7799(98)01191-3.

Kim SS, Penkala R, Abrahimi P. A Perfusion Bioreactor for Intestinal Tissue Engineering. Journal of Surgical Research 2007;142:327–31. doi:10.1016/j.jss.2007.03.039.

Klement BJ, Young QM, George BJ, Nokkaew M. Skeletal tissue growth, differentiation and mineralization in the NASA rotating wall vessel. Bone 2004;34:487–98. doi:10.1016/j.bone.2003.11.015.

Koch MA, Vrij EJ, Engel E, Planell JA, Lacroix D. Perfusion cell seeding on large porous PLA/calcium phosphate composite scaffolds in a perfusion bioreactor system under varying perfusion parameters. Journal of Biomedical Materials Research Part A 2010;95A:1011–8. doi:10.1002/jbm.a.32927.

Korossis A, Bolland F, Kearney N, Fisher J, Ingham E. Bioreactors in Tissue Engineering. In: Ashammakhi N, Reis RL, editors. Topics in Tissue Engineering, 2005.

Kreke MR, Huckle WR, Goldstein AS. Fluid flow stimulates expression of osteopontin and bone sialoprotein by bone marrow stromal cells in a temporally dependent manner. Bone 2005;36:1047–55. doi:10.1016/j.bone.2005.03.008.

Kumar S, Wittmann C, Heinzle E. Minibioreactors. Biotechnology Letters 2004;26:1–10.

Kuppan P, Sethuraman S, Krishnan UM. Tissue engineering interventions for esophageal disorders - Promises and challenges. Biotechnology Advances 2012;30:1481–92. doi:10.1016/j.biotechadv.2012.03.005.

Kwak HS, Nam J, Lee J, Kim HJ, Yoo JJ. Meniscal repair *in vivo* using human chondrocyte-seeded PLGA mesh scaffold pretreated with platelet-rich plasma. Journal of Tissue Engineering and Regenerative Medicine 2017;11:471–80. doi:10.1002/term.1938.

Ladd MR, Lee SJ, Atala A, Yoo JJ. Bioreactor Maintained Living Skin Matrix. Tissue Engineering Part A 2009;15:861–8. doi:10.1089/ten.tea.2008.0195.

Lammi MJ, Inkinen R, Parkkinen JJ, Häkkinen T, Jortikka M, Nelimarkka LO, *et al*. Expression of reduced amounts of structurally altered aggrecan in articular cartilage chondrocytes exposed to high hydrostatic pressure. The Biochemical Journal 1994;304 (Pt 3:723–30.

Langer R. Tissue engineering: a new field and its challenges. Pharmaceutical Research 1997;14:840–1.

Langer R, Vacanti JP. Tissue engineering. Science (New York, NY) 1993;260:920–6.

Lappa M. A CFD level-set method for soft tissue growth: theory and fundamental equations. Journal of Biomechanics 2005;38:185–90. doi:10.1016/j.jbiomech.2004.02.037.

Laurent C, Vaquette C, Martin C, Guedon E, Wu X, Delconte A, *et al*. Towards a Tissue-Engineered Ligament: Design and Preliminary Evaluation of a Dedicated Multi-Chamber Tension-Torsion Bioreactor. Processes 2014;2:167–79. doi:10.3390/pr2010167.

Lei X, Ning L, Cao Y, Liu S, Zhang S, Qiu Z, *et al*. NASA-approved rotary bioreactor enhances proliferation of human epidermal stem cells and supports formation of 3D epidermis-like structure. PloS One 2011;6:e26603. doi:10.1371/journal.pone.0026603.

Lei Y, Ferdous Z. Design considerations and challenges for mechanical stretch bioreactors in tissue engineering. Biotechnology Progress 2016;32:543–53. doi:10.1002/btpr.2256.

Leong K, Chua C, Sudarmadji N, Yeong W. Engineering functionally graded tissue engineering scaffolds. Journal of the Mechanical Behavior of Biomedical Materials 2008;1:140–52. doi:10.1016/j.jmbbm.2007.11.002.

Lewis G. Regenerative Medicine at a Global Level: Current Patterns and Global Trends. In: Webster A, editor. The Global Dynamics of Regenerative Medicine, London: Palgrave Macmillan UK; 2013, p. 18–57. doi:10.1057/9781137026552_2.

Lewis MC, MacArthur BD, Malda J, Pettet G, Please CP. Heterogeneous proliferation within engineered cartilaginous tissue: the role of oxygen tension. Biotechnology and Bioengineering 2005;91:607–15. doi:10.1002/bit.20508.

Li C, Xia J-Y, Chu J, Wang Y-H, Zhuang Y-P, Zhang S-L. CFD analysis of the turbulent flow in baffled shake flasks. Biochemical Engineering Journal 2013;70:140–50. doi:10.1016/j.bej.2012.10.012.

Li MG, Tian XY, Chen XB. Modeling of Flow Rate, Pore Size, and Porosity for the Dispensing-Based Tissue Scaffolds Fabrication. Journal of Manufacturing Science and Engineering 2009;131:034501. doi:10.1115/1.3123331.

Li Z, Cui Z. Three-dimensional perfused cell culture. Biotechnology Advances 2014;32:243–54. doi:10.1016/j.biotechadv.2013.10.006.

Lin C-H, Hsu S, Huang C-E, Cheng W-T, Su J-M. A scaffold-bioreactor system for a tissue-engineered trachea. Biomaterials 2009;30:4117–26.

Liovic P, Sutalo ID, Stewart RP, Glattauer V, Meagher L. Fluid flow and stresses on microcarriers in spinner flask bioreactors. Ninth International Conference on CFD in the Minerals and Process Industries, Melbourne, Australia: CSIRO Australia; 2012.

Liu CZ, Czernuszka JT. Development of biodegradable scaffolds for tissue engineering: a perspective on emerging technology. Materials Science and Technology 2007;23:379–91. doi:10.1179/174328407x177027.

Liu L, Wu W, Tuo X, Geng W, Zhao J, Wei J, *et al*. Novel Strategy to Engineer Trachea Cartilage Graft With Marrow Mesenchymal Stem Cell Macroaggregate and Hydrolyzable Scaffold. Artificial Organs 2010;34:426–33. doi:10.1111/j.1525-1594.2009.00884.x.

Liu M, Liu N, Zang R, Li Y, Yang S-T. Engineering stem cell niches in bioreactors. World Journal of Stem Cells 2013;5:124–35. doi:10.4252/wjsc.v5.i4.124.

Liu Yu, Wang Z-J, Xia J, Haringa C, Liu Ya-ping, Chu J, *et al*. Application of Euler-Lagrange CFD for quantitative evaluating the effect of shear force on Carthamus tinctorius L. cell in a stirred tank bioreactor. Biochemical Engineering Journal 2016;114:209–17. doi:10.1016/j.bej.2016.07.006.

Lovett M, Rockwood D, Baryshyan A, Kaplan DL. Simple Modular Bioreactors for Tissue Engineering: A System for Characterization of Oxygen Gradients, Human Mesenchymal Stem Cell Differentiation, and Prevascularization. Tissue Engineering Part C: Methods 2010;16:1565–73. doi:10.1089/ten.tec.2010.0241.

Lyons E, Pandit A. Design of Bioreactors for Cardiovascular Applications. In: Ashammakhi N, Reis RL, editors. Topics in Tissue Engineering, 2005.

Lysaght MJ, Jaklenec A, Deweerd E. Great Expectations: Private Sector Activity in Tissue Engineering, Regenerative Medicine, and Stem Cell Therapeutics. Tissue Engineering Part A 2008;14:305–15. doi:10.1089/tea.2007.0267.

Mahajan HP. Evaluation of chitosan gelatine complex scaffolds for articular cartilage tissue engineering. Mississipi State University, USA, 2005.

Malafaya PB, Reis RL. Bilayered chitosan-based scaffolds for osteochondral tissue engineering: Influence of hydroxyapatite on *in vitro* cytotoxicity and dynamic bioactivity studies in a specific double-chamber bioreactor. Acta Biomaterialia 2009;5:644–60. doi:10.1016/j.actbio.2008.09.017.

Malda J, Radisic M, Levenberg S, Woodfield T, Oomens C, Baaijens F, *et al*. Cell nutrition. In: Blitterswijk C van, Thomsen P, Lindahl A, Hubbell J, Williams DF, Cancedda R, *et al*., editors. Tissue Engineering, Burlington: Elsevier; 2008, p. 327–62. doi:10.1016/B978-0-12-370869-4.00012-4.

Malda J, Rouwkema J, Martens DE, le Comte EP, Kooy FK, Tramper J, *et al*. Oxygen gradients in tissue-engineered Pegt/Pbt cartilaginous constructs: Measurement and modeling. Biotechnology and Bioengineering 2004;86:9–18. doi:10.1002/bit.20038.

Malda J, Woodfield TBF, van der Vloodt F, Wilson C, Martens DE, Tramper J, *et al*. The effect of PEGT/PBT scaffold architecture on the composition of tissue engineered cartilage. Biomaterials 2005;26:63–72. doi:10.1016/j.biomaterials.2004.02.046.

Martin I, Wendt D, Heberer M. The role of bioreactors in tissue engineering. Trends in Biotechnology 2004;22:80–6. doi:10.1016/j.tibtech.2003.12.001.

Martin Y, Vermette P. Bioreactors for tissue mass culture: design, characterization, and recent advances. Biomaterials 2005;26:7481–503. doi:10.1016/j.biomaterials.2005.05.057.

Matsumoto T, Mooney DJ. Cell Instructive Polymers. In: Lee K, Kaplan D, editors. Tissue Engineering I, Berlin, Heidelberg: Springer Berlin Heidelberg; 2006, p. 113–37. doi:10.1007/b137207.

Mauck RL, Soltz MA, Wang CC, Wong DD, Chao PH, Valhmu WB, *et al*. Functional tissue engineering of articular cartilage through dynamic loading of chondrocyte-seeded agarose gels. Journal of Biomechanical Engineering 2000;122:252. doi:10.1115/1.429656.

McCoy RJ, O’Brien FJ. Influence of Shear Stress in Perfusion Bioreactor Cultures for the Development of Three-Dimensional Bone Tissue Constructs: A Review. Tissue Engineering Part B: Reviews 2010;16:587–601. doi:10.1089/ten.teb.2010.0370.

Mekala NK, Baadhe RR, Parcha SR. Review on bioreactors in tissue engineering. BioTechnology: An Indian Journal 2011;5:246–53.

Melchels FPW, Tonnarelli B, Olivares AL, Martin I, Lacroix D, Feijen J, *et al*. The influence of the scaffold design on the distribution of adhering cells after perfusion cell seeding. Biomaterials 2011;32:2878–84. doi:10.1016/j.biomaterials.2011.01.023.

Meyer U, Büchter A, Nazer N, Wiesmann HP. Design and performance of a bioreactor system for mechanically promoted three-dimensional tissue engineering. British Journal of Oral and Maxillofacial Surgery 2006;44:134–40. doi:10.1016/j.bjoms.2005.05.001.

Minuth WW, Strehl R, Schumacher K. Microreactor Optimisation for Functional Tissue Engineering. In: Chaudhuri J, Al-Rubeai M, editors. Bioreactors for Tissue Engineering, Springer, Dordrecht; 2006, p. 19–45. doi:10.1007/1-4020-3741-4_2.

Mistry AS, Mikos AG. Tissue Engineering Strategies for Bone Regeneration BT - Regenerative Medicine II: Clinical and Preclinical Applications. In: Yannas I V, editor., Berlin, Heidelberg: Springer Berlin Heidelberg; 2005, p. 1–22. doi:10.1007/b99997.

Mizuno S, Tateishi T, Ushida T, Glowacki J. Hydrostatic fluid pressure enhances matrix synthesis and accumulation by bovine chondrocytes in three-dimensional culture. Journal of Cellular Physiology 2002;193:319–27. doi:10.1002/jcp.10180.

Moody LF. Friction Factors for Pipe Flow. Transactions of the American Society of Mechanical Engineers 1944;66:671–81.

Mooney DJ, Cima L, Langer R, Johnson L, Hansen LK, Ingber DE, *et al*. Principles of Tissue Engineering and Reconstruction Using Polymer-Cell Constructs. MRS Proceedings 1991;252:345. doi:10.1557/PROC-252-345.

Mygind T, Stiehler M, Baatrup A, Li H, Zou X, Flyvbjerg A, *et al*. Mesenchymal stem cell ingrowth and differentiation on coralline hydroxyapatite scaffolds. Biomaterials 2007;28:1036–47. doi:10.1016/j.biomaterials.2006.10.003.

Nakamura S, Kubo T, Ijima H. Heparin-conjugated gelatin as a growth factor immobilization scaffold. Journal of Bioscience and Bioengineering 2013;115:562–7. doi:10.1016/j.jbiosc.2012.11.011.

Nazempour A, Wie BJ Van. A flow perfusion bioreactor with controlled mechanical stimulation: Application in cartilage tissue engineering and beyond. Journal of Stem Cell Therapy and Transplantation 2018;1469:015–34. doi:10.29328/journal.jsctt.1001011.

Nesic D, Whiteside R, Brittberg M, Wendt D, Martin I, Mainil-Varlet P. Cartilage tissue engineering for degenerative joint disease. Advanced Drug Delivery Reviews 2006;58:300–22. doi:10.1016/j.addr.2006.01.012.

Nettleship I. Tissue Engineering Using Ceramics and Polymers. Elsevier; 2014. doi:10.1533/9780857097163.2.224.

Nguyen DT, Brotherton JD, Chau PC. Enhancing cell viability with pulsating flow in a hollow fiber bioartificial liver. Biotechnology Letters 2005;27:1511–6. doi:10.1007/s10529-005-1467-9.

Nguyen Q-H, Choi S-B. Optimal Design Methodology of Magnetorheological Fluid Based Mechanisms. Smart Actuation and Sensing Systems - Recent Advances and Future Challenges, InTech; 2012. doi:10.5772/51078.

Nguyen TD, Liang R, Woo SL-Y, Burton SD, Wu C, Almarza A, *et al*. Effects of cell seeding and cyclic stretch on the fiber remodeling in an extracellular matrix-derived bioscaffold. Tissue Engineering Part A 2009;15:957–63. doi:10.1089/ten.tea.2007.0384.

Niklason LE, Gao J, Abbott WM, Hirschi KK, Houser S, Marini R, *et al*. Functional arteries grown *in vitro*. Science 1999;284:489–93.

Nirmalanandhan VS, Shearn JT, Juncosa-Melvin N, Rao M, Gooch C, Jain A, *et al*. Improving linear stiffness of the cell-seeded collagen sponge constructs by varying the components of the mechanical *stimulus*. Tissue Engineering Part A 2008;14:1883–91. doi:10.1089/ten.tea.2007.0125.

Norotte C, Marga FS, Niklason LE, Forgacs G. Scaffold-free vascular tissue engineering using bioprinting. Biomaterials 2009;30:5910–7. doi:10.1016/j.biomaterials.2009.06.034.

O’Dea RD, Waters SL, Byrne HM. A two-fluid model for tissue growth within a dynamic flow environment. European Journal of Applied Mathematics 2008;19:607–34. doi:10.1017/S0956792508007687.

Obregón R, Ramón-Azcón J, Ahadian S. Bioreactors in Tissue Engineering. Tissue Engineering for Artificial Organs, vol. 1–2, Weinheim, Germany: Wiley-VCH Verlag GmbH & Co. KGaA; 2017, p. 169–213. doi:10.1002/9783527689934.ch6.

Oldenburg KR, Holt AB, Weeks RL. Disposable Spinner Flask. US 8,822,209, 2014.

Oragui E, Nannaparaju M, Khan WS. The role of bioreactors in tissue engineering for musculoskeletal applications. The Open Orthopaedics Journal 2011;5 Suppl 2:267–70. doi:10.2174/1874325001105010267.

Orr DE, Burg KJL. Design of a modular bioreactor to incorporate both perfusion flow and hydrostatic compression for tissue engineering applications. Annals of Biomedical Engineering 2008;36:1228–41. doi:10.1007/s10439-008-9505-0.

Paez-Mayorga J, Hernández-Vargas G, Ruiz-Esparza GU, Iqbal HMN, Wang X, Zhang YS, *et al*. Bioreactors for Cardiac Tissue Engineering. Advanced Healthcare Materials 2018;1701504:1701504. doi:10.1002/adhm.201701504.

Park DH, Jeon HJ, Kim MJ, Nguyen XD, Morten K, Go JS. Development of a microfluidic perfusion 3D cell culture system. Journal of Micromechanics and Microengineering 2018;28:045001. doi:10.1088/1361-6439/aaa877.

Pati F, Gantelius J, Svahn HA. 3D Bioprinting of Tissue/Organ Models. Angewandte Chemie International Edition 2016;55:4650–65. doi:10.1002/anie.201505062.

Patrachari AR, Podichetty JT, Madihally S V. Application of computational fluid dynamics in tissue engineering. Journal of Bioscience and Bioengineering 2012;114:123–32. doi:10.1016/j.jbiosc.2012.03.010.

Paul M, Kaur P, Herson M, Cheshire P, Cleland H, Akbarzadeh S. Use of Clotted Human Plasma and Aprotinin in Skin Tissue Engineering: A Novel Approach to Engineering Composite Skin on a Porous Scaffold. Tissue Engineering Part C: Methods 2015;21:1098–104. doi:10.1089/ten.tec.2014.0667.

Paxton ES, Teefey SA, Dahiya N, Keener JD, Yamaguchi K, Galatz LM. Clinical and Radiographic Outcomes of Failed Repairs of Large or Massive Rotator Cuff Tears: Minimum Ten-Year Follow-up. JBJS 2013;95.

Pazzano D, Mercier K a, Moran JM, Fong SS, DiBiasio DD, Rulfs JX, *et al*. Comparison of chondrogensis in static and perfused bioreactor culture. Biotechnology Progress 2000;16:893–6. doi:10.1021/bp000082v.

Pereira RF, Freitas D, Tojeira A, Almeida HA, Alves N, Bártolo PJ. Computer modelling and simulation of a bioreactor for tissue engineering. International Journal of Computer Integrated Manufacturing 2014;27:946–59. doi:10.1080/0951192X.2013.812244.

Pereira RP, Bartolo PJ. 3D Photo-Fabrication for Tissue Engineering and Drug Delivery 2015;1:90. doi:10.15302/j-eng-2015015.

Place ES, George JH, Williams CK, Stevens MM. Synthetic polymer scaffolds for tissue engineering. Chemical Society Reviews 2009;38:1139. doi:10.1039/b811392k.

Plunkett N, O'Brien FJ. Bioreactors in tissue engineering. Studies in Health Technology and Informatics 2010;152:214–30. doi:10.3233/THC-2011-0605.

Pok S, Dhane D V., Madihally S V. Computational simulation modelling of bioreactor configurations for regenerating human bladder. Computer Methods in Biomechanics and Biomedical Engineering 2013;16:840–51. doi:10.1080/10255842.2011.641177.

Porter B, Zauel R, Stockman H, Guldberg R, Fyhrie D. 3-D computational modeling of media flow through scaffolds in a perfusion bioreactor. Journal of Biomechanics 2005;38:543–9. doi:10.1016/j.jbiomech.2004.04.011.

Pörtner R. Characteristics of Mammalian Cells and Requirements for Cultivation. In: Eibl R, Eibl D, Pörtner Ralf, Catapano G, Czermak P, editors., Berlin, Heidelberg: Springer Berlin Heidelberg; 2009, p. 13–53. doi:10.1007/978-3-540-68182-3_2.

Pörtner R, Giese C. An Overview on Bioreactor Design , Prototyping and Process Control for Reproducible Three-Dimensional Tissue Culture. In: Marx U, Sandig V, editors. Drug Testing *In vitro*: Breakthroughs and Trends in Cell Culture Technology, WILEY-VCH Verlag GmbH; 2007, p. 53–78.

Pörtner R, Nagel-Heyer S, Goepfert C, Adamietz P, Meenen NM. Bioreactor design for tissue engineering. Journal of Bioscience and Bioengineering 2005;100:235–45. doi:10.1263/jbb.100.235.

Pozrikidis C. Fluid Dynamics: Theory, Computation and Numerical Simulation. 2nd Editio. New York, USA: Springer; 2009.

Prenosil JE, Kino-oka M. Computer controlled bioreactor for large-scale production of cultured skin grafts. Annals of the New York Academy of Sciences 1999;875:386–97.

Provin C, Takano K, Sakai Y, Fujii T, Shirakashi R. A method for the design of 3D scaffolds for high-density cell attachment and determination of optimum perfusion culture conditions. Journal of Biomechanics 2008;41:1436–49. doi:10.1016/j.jbiomech.2008.02.025.

Qin T-W, Sun Y-L, Thoreson AR, Steinmann SP, Amadio PC, An K-N, *et al*. Effect of mechanical stimulation on bone marrow stromal cell-seeded tendon slice constructs: a potential engineered tendon patch for rotator cuff repair. Biomaterials 2015;51:43–50. doi:10.1016/j.biomaterials.2015.01.070.

Rabionet M, Polonio E, Guerra A, Martin J, Puig T, Ciurana J. Design of a Scaffold Parameter Selection System with Additive Manufacturing for a Biomedical Cell Culture. Materials 2018;11:1427. doi:10.3390/ma11081427.

Radisic M, Marsano A, Maidhof R, Wang Y, Vunjak-Novakovic G. Cardiac tissue engineering using perfusion bioreactor systems. Nature Protocols 2008;3:719–38. doi:10.1038/nprot.2008.40.

Rahbari A, Montazerian H, Davoodi E, Homayoonfar S. Predicting permeability of regular tissue engineering scaffolds: scaling analysis of pore architecture, scaffold length, and fluid flow rate effects. Computer Methods in Biomechanics and Biomedical Engineering 2017;20:231–41. doi:10.1080/10255842.2016.1215436.

Rauh J, Milan F, Günther K-P, Stiehler M. Bioreactor systems for bone tissue engineering. Tissue Engineering Part B, Reviews 2011;17:263–80. doi:10.1089/ten.TEB.2010.0612.

Ravichandran A, Wen F, Lim J, Chong MSK, Chan JKY, Teoh S-H. Biomimetic fetal rotation bioreactor for engineering bone tissues-Effect of cyclic strains on upregulation of osteogenic gene expression. Journal of Tissue Engineering and Regenerative Medicine 2018;12:e2039–50. doi:10.1002/term.2635.

Reddy JN. An Introduction to the Finite Element Method. Third. New York: McGraw-Hill; 2006.

Redondo JM. Topics on Environmental and Physical Geodesy 2014.

Reverchon E, Cardea S. Supercritical fluids in 3-D tissue engineering. The Journal of Supercritical Fluids 2012;69:97–107. doi:10.1016/j.supflu.2012.05.010.

Rijal G, Bathula C, Li W. Application of Synthetic Polymeric Scaffolds in Breast Cancer 3D Tissue Cultures and Animal Tumor Models. International Journal of Biomaterials 2017;2017:1–9. doi:10.1155/2017/8074890.

Riley GP, Harrall RL, Constant CR, Chard MD, Cawston TE, Hazleman BL. Glycosaminoglycans of human rotator cuff tendons: changes with age and in chronic rotator cuff tendinitis. Annals of the Rheumatic Diseases 1994;53:367–76. doi:10.1136/ard.53.6.367.

Risbud M. Tissue engineering: Implications in the treatment of organ and tissue defects. Biogerontology 2001;2:117–25. doi:10.1023/A:1011585117310.

Rolfe P. Sensing in tissue bioreactors. Measurement Science and Technology 2006;17:578–83. doi:10.1088/0957-0233/17/3/S20.

Rose FRAJ, Oreffo ROC. Bone Tissue Engineering: Hope vs Hype. Biochemical and Biophysical Research Communications 2002;292:1–7. doi:10.1006/bbrc.2002.6519.

Rosser J, Thomas DJ. Bioreactor processes for maturation of 3D bioprinted tissue. In: Thomas Daniel J, Jessop ZM, Whitaker ISBT-3D B for RS, editors. 3D Bioprinting for Reconstructive Surgery, Elsevier; 2018, p. 191–215. doi:10.1016/B978-0-08-101103-4.00010-7.

Rouwkema J, Rivron NC, van Blitterswijk C a. Vascularization in tissue engineering. Trends in Biotechnology 2008;26:434–41. doi:10.1016/j.tibtech.2008.04.009.

Saber S, Zhang AY, Ki SH, Lindsey DP, Smith RL, Riboh J, *et al*. Flexor Tendon Tissue Engineering: Bioreactor Cyclic Strain Increases Construct Strength. Tissue Engineering Part A 2010;16:2085–90. doi:10.1089/ten.tea.2010.0032.

Sadeghi-Ataabadi M, Mostafavi-pour Z, Vojdani Z, Sani M, Latifi M, Talaei-Khozani T. Fabrication and characterization of platelet-rich plasma scaffolds for tissue engineering applications. Materials Science and Engineering: C 2017;71:372–80. doi:10.1016/j.msec.2016.10.001.

Sakai S, Mishima H, Ishii T, Akaogi H, Yoshioka T, Ohyabu Y, *et al*. Rotating three-dimensional dynamic culture of adult human bone marrow-derived cells for tissue engineering of hyaline cartilage. Journal of Orthopaedic Research 2009;27:517–21. doi:10.1002/jor.20566.

Salehi-Nik N, Amoabediny G, Pouran B, Tabesh H, Shokrgozar MA, Haghighipour N, *et al*. Engineering Parameters in Bioreactor's Design: A Critical Aspect in Tissue Engineering. BioMed Research International 2013;2013:1–15. doi:10.1155/2013/762132.

Santoro R, Olivares AL, Brans G, Wirz D, Longinotti C, Lacroix D, *et al*. Bioreactor based engineering of large-scale human cartilage grafts for joint resurfacing. Biomaterials 2010;31:8946–52. doi:10.1016/j.biomaterials.2010.08.009.

Sanz-Herrera JA, García-Aznar JM, Doblaré M. On scaffold designing for bone regeneration: A computational multiscale approach. Acta Biomaterialia 2009;5:219–29. doi:10.1016/j.actbio.2008.06.021.

Sarkar U, Rivera-Burgos D, Large EM, Hughes DJ, Ravindra KC, Dyer RL, *et al*. Metabolite Profiling and Pharmacokinetic Evaluation of Hydrocortisone in a Perfused Three-Dimensional Human Liver Bioreactor. Drug Metabolism and Disposition 2015;43:1091–9. doi:10.1124/dmd.115.063495.

Schulz RM, Bader A. Cartilage tissue engineering and bioreactor systems for the cultivation and stimulation of chondrocytes. European Biophysics Journal : EBJ 2007;36:539–68. doi:10.1007/s00249-007-0139-1.

Sengers BG, Van Donkelaar CC, Oomens CWJ, Baaijens FPT. Computational Study of Culture Conditions and Nutrient Supply in Cartilage Tissue Engineering. Biotechnology Progress 2008;21:1252–61. doi:10.1021/bp0500157.

Serra M, Brito C, Leite SB, Gorjup E, von Briesen H, Carrondo MJT, *et al*. Stirred bioreactors for the expansion of adult pancreatic stem cells. Annals of Anatomy 2009;191:104–15. doi:10.1016/j.aanat.2008.09.005.

Seymour P, M. Ecker D. Global Biomanufacturing Trends, Capacity, and Technology Drivers | American Pharmaceutical Review. American Pharmaceutical Review 2017;20.

Shafiee A, Atala A. Printing Technologies for Medical Applications 2016. doi:10.1016/j.molmed.2016.01.003.

Shahin K, Doran PM. Strategies for Enhancing the Accumulation and Retention of Extracellular Matrix in Tissue-Engineered Cartilage Cultured in Bioreactors. PLoS ONE 2011;6:e23119. doi:10.1371/journal.pone.0023119.

Shakeel M. Continuum modelling of cell growth and nutrient transport in a perfusion bioreactor. 2011.

Shakeel M, Raza S. Nonlinear Computational Model of Biological Cell Proliferation and Nutrient Delivery in a Bioreactor. Applied Mathematics 2014;05:2284–98. doi:10.4236/am.2014.515222.

Shangkai C, Naohide T, Koji Y, Yasuji H, Masaaki N, Tomohiro T, *et al*. Transplantation of allogeneic chondrocytes cultured in fibroin sponge and stirring chamber to promote cartilage regeneration. Tissue Engineering 2007;13:483–92. doi:10.1089/ten.2006.0181.

Shi Y. Numerical simulation of global hydro-dynamics in a pulsatile bioreactor for cardiovascular tissue engineering. Journal of Biomechanics 2008;41:953–9. doi:10.1016/j.jbiomech.2008.01.001.

Sikavitsas VI, Bancroft GN, Lemoine JJ, Liebschner MAK, Dauner M, Mikos AG. Flow perfusion enhances the calcified matrix deposition of marrow stromal cells in biodegradable nonwoven fiber mesh scaffolds. Annals of Biomedical Engineering 2005;33:63–70. doi:10.1089/ten.TEC.2010.0241.

Singh H, Ang ES, Lim TT, Hutmacher DW. Flow Modeling in a Novel Non-Perfusion Conical Bioreactor. Biotechnology and Bioengineering 2007;97:1291–9. doi:10.1002/bit.

Skalak R, Fox C. Tissue Engineering. New York: Alan R. Liss, Inc.; 1988.

Skoneczny S, Stryjewski W, Bizon K, Tabiś B. Three-phase fluidized bed bioreactor modelling and simulation. Biochemical Engineering Journal 2017;121:118–30. doi:10.1016/j.bej.2017.01.017.

Song F, Liu T, Song K, Lim M, Shi F, Yan X, *et al*. Numberical simulation of fluid flow and three-dimensional expansion of tissue engineering seed cells in large scale inside a novel rotating wall hollow fiber membrane bioreactor. Bioprocess and Biosystems Engineering 2015;38:1527–40. doi:10.1007/s00449-015-1395-6.

Song L, Zhou Q, Duan P, Guo P, Li D, Xu Y, *et al*. Successful Development of Small Diameter Tissue-Engineering Vascular Vessels by Our Novel Integrally Designed Pulsatile Perfusion-Based Bioreactor. PLoS ONE 2012;7:e42569. doi:10.1371/journal.pone.0042569.

Spencer TJ, Hidalgo-Bastida LA, Cartmell SH, Halliday I, Care CM. In silico multi-scale model of transport and dynamic seeding in a bone tissue engineering perfusion bioreactor. Biotechnology and Bioengineering 2013;110:1221–30. doi:10.1002/bit.24777.

Stamatialis D. Focus issue | Bioartificial organs and tissue engineering. The International Journal of Artificial Organs 2017;40:133–5. doi:10.5301/ijao.5000599.

Stewart M. Fluid flow and pressure drop. In: Stewart MBT-SPO, editor. Surface Production Operations, Boston: Elsevier; 2016, p. 343–470. doi:10.1016/B978-1-85617-808-2.00006-7.

Sucosky P, Osorio DF, Brown JB, Neitzel GP. Fluid mechanics of a spinner-flask bioreactor. Biotechnology and Bioengineering 2004;85:34–46. doi:10.1002/bit.10788.

Sun T, Norton D, Vickers N, L. McArthur S, Neil S Mac, Ryan AJ, *et al*. Development of a bioreactor for evaluating novel nerve conduits. Biotechnology and Bioengineering 2008;99:1250–60. doi:10.1002/bit.21669.

Tabata Y. Recent progress in tissue engineering. Drug Discovery Today 2001;6:483–7. doi:10.1016/S1359-6446(01)01753-6.

Takebe T, Kobayashi S, Kan H, Suzuki H, Yabuki Y, Mizuno M, *et al*. Human Elastic Cartilage Engineering from Cartilage Progenitor Cells Using Rotating Wall Vessel Bioreactor. Transplantation Proceedings 2012;44:1158–61. doi:10.1016/j.transproceed.2012.03.038.

Tamada JA, Langer R. Erosion kinetics of hydrolytically degradable polymers. Proceedings of the National Academy of Sciences 1993;90:552–6. doi:10.1073/pnas.90.2.552.

Tan KH, Chua CK, Leong KF, Cheah CM, Gui WS, Tan WS, *et al*. Selective laser sintering of biocompatible polymers for applications in tissue engineering. Bio-Medical Materials And Engineering 2005;15:113–24.

Tan PS, Teoh SH. Effect of stiffness of polycaprolactone (PCL) membrane on cell proliferation. Materials Science and Engineering: C 2007;27:304–8. doi:10.1016/j.msec.2006.03.010.

Terzaki K, Kissamitaki M, Skarmoutsou A, Fotakis C, Charitidis CA, Farsari M, *et al*. Pre-osteoblastic cell response on three-dimensional, organic-inorganic hybrid material scaffolds for bone tissue engineering. Journal of Biomedical Materials Research Part A 2013;101A:2283–94. doi:10.1002/jbm.a.34516.

Tessmar JK, Göpferich AM. Matrices and scaffolds for protein delivery in tissue engineering. Advanced Drug Delivery Reviews 2007;59:274–91. doi:10.1016/j.addr.2007.03.020.

Thanaphat P, Thunyakitpisal P. Chitosan / Calcium Phosphate Composites Scaffolds Prepared by Membrane Diffusion Process. Journal of Metals, Materials and Minerals 2008;18:67–71.

Tojeira A, Freitas D, Pereira R, Alves N, Capela C, Mendes A, *et al*. Computacional Analysis of a Bioreactor Chamber for Tissue Engineering Applications, 2010.

Toyoda T, Seedhom BB, Yao JQ, Kirkham J, Brookes S, Bonass WA. Hydrostatic Pressure Modulates Proteoglycan Metabolism in Chondrocytes Seeded in Agarose. Arthritis and Rheumatism 2003;48:2865–72. doi:10.1002/art.11250.

Truscello S, Kerckhofs G, Van Bael S, Pyka G, Schrooten J, Van Oosterwyck H. Prediction of permeability of regular scaffolds for skeletal tissue engineering: A combined computational and experimental study. Acta Biomaterialia 2012;8:1648–58. doi:10.1016/j.actbio.2011.12.021.

Valmikinathan CM, Hoffman J, Yu X. Impact of scaffold micro and macro architecture on Schwann cell proliferation under dynamic conditions in a rotating wall vessel bioreactor. Materials Science and Engineering: C 2011;31:22–9. doi:https://doi.org/10.1016/j.msec.2010.04.001.

Vasanthan KS, Subramanian A, Krishnan UM, Sethuraman S. Role of biomaterials, therapeutic molecules and cells for hepatic tissue engineering. Biotechnology Advances 2012;30:742–52. doi:10.1016/j.biotechadv.2012.01.004.

Viana T, Biscaia S, Almeida H a., Bártolo PJ. Permeability Evaluation of Lay-down Patterns and Pore Size of Pcl Scaffolds. Procedia Engineering 2013;59:255–62. doi:10.1016/j.proeng.2013.05.119.

Vickers D, Thomas CK. Some aspects of the turbulence kinetic energy and fluxes above and beneath a tall open pine forest canopy. Agricultural and Forest Meteorology 2013;181:143–51. doi:10.1016/j.agrformet.2013.07.014.

Visscher DO, Farré-Guasch E, Helder MN, van Zuijlen PP, Gibbs S, Wolff J, *et al*. Advances in Bioprinting Technologies for Craniofacial Reconstruction. Trends in Biotechnology 2016;34:700–10. doi:10.1016/j.tibtech.2016.04.001.

Vozzi G, Flaim C, Ahluwalia A, Bhatia S. Fabrication of PLGA scaffolds using soft lithography and microsyringe deposition. Biomaterials 2003;24:2533–40. doi:10.1016/s0142-9612(03)00052-8.

Vunjak-Novakovic G, Obradovic B, Martin I, Bursac PM, Langer R, Freed LE. Dynamic cell seeding of polymer scaffolds for cartilage tissue engineering. Biotechnology Progress 1998;14:193–202. doi:10.1021/bp970120j.

Vyas C, Pereira R, Huang B, Liu F, Wang W, Bartolo P, *et al*. Engineering the vasculature with additive manufacturing. Current Opinion in Biomedical Engineering 2017;2:1–13. doi:10.1016/j.cobme.2017.05.008.

Wang D, Liu W, Han B, Xu R. The bioreactor: a powerful tool for large-scale culture of animal cells. Current Pharmaceutical Biotechnology 2005;6:397–403.

Wang N, Grad S, Stoddart MJ, Niemeyer P, Reising K, Schmal H, *et al*. Particulate cartilage under bioreactor-induced compression and shear. International Orthopaedics 2014;38:1105–11. doi:10.1007/s00264-013-2194-9.

Wang T, Lin Z, Day RE, Gardiner B, Landao-Bassonga E, Rubenson J, *et al*. Programmable mechanical stimulation influences tendon homeostasis in a bioreactor system. Biotechnology and Bioengineering 2013;110:1495–507. doi:10.1002/bit.24809.

Webb K, Hitchcock RW, Smeal RM, Li W, Gray SD, Tresco PA. Cyclic strain increases fibroblast proliferation, matrix accumulation, and elastic modulus of fibroblast-seeded polyurethane constructs. Journal of Biomechanics 2006;39:1136–44. doi:10.1016/j.jbiomech.2004.08.026.

Weinandy S, Rongen L, Schreiber F, Cornelissen C, Flanagan TC, Mahnken A, *et al*. The BioStent: Novel Concept for a Viable Stent Structure. Tissue Engineering Part A 2012;18:1818–26. doi:10.1089/ten.tea.2011.0648.

Wendt D, Marsano A, Jakob M, Heberer M, Martin I. Oscillating perfusion of cell suspensions through three-dimensional scaffolds enhances cell seeding efficiency and uniformity. Biotechnology and Bioengineering 2003;84:205–14. doi:10.1002/bit.10759.

Wendt D, Timmins N, Malda J, Janssen F, Ratcliffe A, Vunjak-Novakovic G, *et al*. Bioreactors for tissue engineering. In: Blitterswijk C van, Thomsen P, Lindahl A, Hubbell J, Williams DF, Cancedda R, *et al*., editors. Tissue Engineering, Burlington: Elsevier; 2008, p. 483–506. doi:10.1016/B978-0-12-370869-4.00016-1.

Whittaker RJ, Booth R, Dyson R, Bailey C, Parsons Chini L, Naire S, *et al*. Mathematical modelling of fibre-enhanced perfusion inside a tissue-engineering bioreactor. Journal of Theoretical Biology 2009;256:533–46. doi:10.1016/j.jtbi.2008.10.013.

Williams K a, Saini S, Wick TM. Computational fluid dynamics modeling of steady-state momentum and mass transport in a bioreactor for cartilage tissue engineering. Biotechnology Progress 2002;18:951–63. doi:10.1021/bp020087n.

Woon CYL, Kraus A, Raghavan SS, Pridgen BC, Megerle K, Pham H, *et al*. Three-Dimensional-Construct Bioreactor Conditioning in Human Tendon Tissue Engineering. Tissue Engineering Part A 2011;17:2561–72. doi:10.1089/ten.tea.2010.0701.

Wu S, Wang Y, Streubel PN, Duan B. Living nanofiber yarn-based woven biotextiles for tendon tissue engineering using cell tri-culture and mechanical stimulation. Acta Biomaterialia 2017;62:102–15. doi:10.1016/j.actbio.2017.08.043.

Xie F, Chen W, Wang J, Liu J. CFD and experimental studies on the hydrodynamic performance of submerged flat-sheet membrane bioreactor equipped with micro-channel turbulence promoters. Chemical Engineering and Processing: Process Intensification 2016;99:72–9. doi:10.1016/j.cep.2015.10.012.

Xie Y, Lu J. Bioreactors for bone tissue engineering. Biomechanics and Biomaterials in Orthopedics, Second Edition 2016;224:115–22. doi:10.1007/978-1-84882-664-9_9.

Yan X, Bergstrom DJ, Chen XB. Modeling of Cell Cultures in Perfusion Bioreactors. IEEE Transactions on Biomedical Engineering 2012;59:2568–75. doi:10.1109/TBME.2012.2206077.

Yan X., Chen XB, Bergstrom DJ. Modeling of the Flow within Scaffolds in Perfusion Bioreactors. American Journal of Biomedical Engineering 2012;1:72–7. doi:10.5923/j.ajbe.20110102.13.

Yeatts AB, Fisher JP. Bone tissue engineering bioreactors: Dynamic culture and the influence of shear stress. Bone 2011;48:171–81. doi:10.1016/j.bone.2010.09.138.

Yoo HS, Kim TG, Park TG. Surface-functionalized electrospun nanofibers for tissue engineering and drug delivery. Advanced Drug Delivery Reviews 2009;61:1033–42. doi:10.1016/j.addr.2009.07.007.

Yoon HH, Bhang SH, Shin J-Y, Shin J, Kim B-S. Enhanced cartilage formation via three-dimensional cell engineering of human adipose-derived stem cells. Tissue Engineering Part A 2012;18:1949–56. doi:10.1089/ten.TEA.2011.0647.

Youngstrom DW, Rajpar I, Kaplan DL, Barrett JG. A bioreactor system for *in vitro* tendon differentiation and tendon tissue engineering. Journal of Orthopaedic Research : Official Publication of the Orthopaedic Research Society 2015;33:911–8. doi:10.1002/jor.22848.

Yu X, Botchwey EA, Levine EM, Pollack SR, Laurencin CT. Bioreactor-based bone tissue engineering: The influence of dynamic flow on osteoblast phenotypic expression and matrix mineralization. Proceedings of the National Academy of Sciences 2004;101:11203–8. doi:10.1073/pnas.0402532101.

Zhang P, Policha A, Tulenko T, DiMuzio P. Autologous human plasma in stem cell culture and cryopreservation in the creation of a tissue-engineered vascular graft. Journal of Vascular Surgery 2016;63:805–14. doi:10.1016/j.jvs.2014.10.015.

Zhang S, Vijayavenkataraman S, Lu WF, Fuh JYH. A review on the use of computational methods to characterize, design, and optimize tissue engineering scaffolds, with a potential in 3D printing fabrication. Journal of Biomedical Materials Research Part B: Applied Biomaterials 2018:1–23. doi:10.1002/jbm.b.34226.

Zhang X, Bürki C-A, Stettler M, De Sanctis D, Perrone M, Discacciati M, *et al*. Efficient oxygen transfer by surface aeration in shaken cylindrical containers for mammalian cell cultivation at volumetric scales up to 1000L. Biochemical Engineering Journal 2009;45:41–7. doi:10.1016/j.bej.2009.02.003.

Zhang YS, Yue K, Aleman J, Mollazadeh-Moghaddam K, Bakht SM, Yang J, *et al*. 3D Bioprinting for Tissue and Organ Fabrication. Annals of Biomedical Engineering 2017;45:148–63. doi:10.1007/s10439-016-1612-8.

Zhang Z-Y, Teoh SH, Chong W-S, Foo T-T, Chng Y-C, Choolani M, *et al*. A biaxial rotating bioreactor for the culture of fetal mesenchymal stem cells for bone tissue engineering. Biomaterials 2009;30:2694–704. doi:10.1016/j.biomaterials.2009.01.028.

Zhang ZY, Teoh SH, Teo EY, Khoon Chong MS, Shin CW, Tien FT, *et al*. A comparison of bioreactors for culture of fetal mesenchymal stem cells for bone tissue engineering. Biomaterials 2010;31:8684–95. doi:10.1016/j.biomaterials.2010.07.097.

Zhao J, Griffin M, Cai J, Li S, Bulter PEM, Kalaskar DM. Bioreactors for tissue engineering: An update. Biochemical Engineering Journal 2016;109:268–81. doi:10.1016/j.bej.2016.01.018.

Zhou S, Ye H, Cui Z. Complexity in Modeling of Cartilage Tissue Engineering. vol. 5. Elsevier; 2011. doi:10.1016/B978-0-08-088504-9.00517-1.

Zienkiewicz OC, Taylor RL, Nithiarasu P. The Finite Element Method for Fluid Dynamics. 6th Editio. Oxford: Elsevier; 2005.

Zienkiewicz OC, Taylor RL, Zhu JZ. The Standard Discrete System and Origins of the Finite Element Method. In: Zienkiewicz OC, Taylor RL, Zhu JZBT-TFEM its B and F (Seventh E, editors. The Finite Element Method: its Basis and Fundamentals, Oxford: Elsevier; 2013, p. 1–20. doi:10.1016/B978-1-85617-633-0.00001-0.

8 APPENDICES

APPENDIX 1 – MECHANO-BIOREACTOR PATENT

inpi instituto nacional da propriedade industrial

(11) Número de Publicação: **PT 105176**

(51) Classificação Internacional:
C12M 3/00 (2006)

(12) **FASCÍCULO DE PATENTE DE INVENÇÃO**

(22) Data de pedido: **2010.06.28**

(30) Prioridade(s):

2011.03.22 20111000022582 PT
2012.05.25 20121000041768 PT

(43) Data de publicação do pedido: **2012.07.20**

(73) Titular(es):

INSTITUTO POLITÉCNICO DE LEIRIA
RUA GENERAL NORTON DE MATOS,
APARTADO 4133
2411-901 LEIRIA PT

(72) Inventor(es):

ANA PATRÍCIA OLIVEIRA TOJEIRA	**PT**
DINO MIGUEL FERNANDES FREITAS	**PT**
RÚBEN FILIPE BRÁS PEREIRA	**PT**
PAULO JORGE DA SILVA BÁRTOLO	**PT**
NUNO MANUEL FERNANDES ALVES	**PT**
AUSENDA LUÍS AVELAR MENDES	**PT**
CARLOS ALEXANDRE BENTO CAPELA	**PT**
HENRIQUE DE AMORIM ALMEIDA	**PT**
MARCO ANDRÉ NEVES DOMINGOS	**PT**

(74) Mandatário:

(54) Epígrafe: **BIOREACTOR MULTI-FUNCIONAL PARA A ENGENHARIA DE TECIDOS**

(57) Resumo: O BIOREACTOR MULTI-FUNCIONAL PARA A ENGENHARIA DE TECIDOS REFERE-SE A UM EQUIPAMENTO QUE SE DESTINA À CULTURA DE CÉLULAS PARA A CONCEPÇÃO DE IMPLANTES. O BIOREACTOR BASEIA-SE NA APLICAÇÃO DE VÁRIOS ESTÍMULOS A CÉLULAS CONTIDAS EM MATRIZES DE SUPORTE BIDIMENSIONAIS (2D) E/OU TRIDIMENSIONAIS (3D). A VARIEDADE DE ESTÍMULOS PASSÍVEIS DE SEREM APLICADOS, EM SIMULTÂNEO, PERMITE MODELAR A PROLIFERAÇÃO E DIFERENCIAÇÃO DE VÁRIOS TIPOS DE CÉLULAS. O EQUIPAMENTO É CONSTITUÍDO POR DIVERSOS SISTEMAS DE CULTURA CELULAR, NOMEADAMENTE, ESTÍMULOS DE ROTAÇÃO, OSCILAÇÃO, PERFUSÃO, ASSIM COMO, COMPRESSÃO E EXTENSÃO MECÂNICA. AS VARIÁVEIS AFECTAS AO PROCESSO DE CULTURA DE CÉLULAS SÃO MONITORIZADAS E CONTROLADAS EM TEMPO REAL ATRAVÉS DE UMA PLACA DE DESENVOLVIMENTO CONECTADA A UM LCD TOUCHSCREEN E, TAMBÉM À DISTÂNCIA, ATRAVÉS DE DISPOSITIVOS MÓVEIS (EX. TELEMÓVEIS, TABLETS). AS CARACTERÍSTICAS INOVADORAS DO EQUIPAMENTO INCLUEM A APLICAÇÃO DE UMA VARIEDADE DE ESTÍMULOS PARA A CULTURA CELULAR, A APLICAÇÃO DE ESTÍMULOS DE PERFUSÃO, COMPRESSÃO MECÂNICA E EXTENSÃO MECÂNICA, ATRAVÉS DE ÊMBOLOS MICROPERFURADOS, E A MONITORIZAÇÃO E CONTROLO REMOTO DAS VARIÁVEIS DO PROCESSO DE CULTURA CELULAR

1

RESUMO

Bioreactor Multi-funcional para a Engenharia de Tecidos

O bioreactor multi-funcional para a Engenharia de Tecidos refere-se a um equipamento que se destina à cultura de células para a concepção de implantes.
O bioreactor baseia-se na aplicação de vários estímulos a células contidas em matrizes de suporte bidimensionais (2D) e/ou tridimensionais (3D). A variedade de estímulos passíveis de serem aplicados, em simultâneo, permite modelar a proliferação e diferenciação de vários tipos de células.
O equipamento é constituído por diversos sistemas de cultura celular, nomeadamente, estímulos de rotação, oscilação, perfusão, assim como, compressão e extensão mecânica.
As variáveis afectas ao processo de cultura de células são monitorizadas e controladas em tempo real através de uma placa de desenvolvimento conectada a um LCD TouchScreen e, também à distância, através de dispositivos móveis (ex. Telemóveis, Tablets).
As características inovadoras do equipamento incluem a aplicação de uma variedade de estímulos para a cultura celular, a aplicação de estímulos de perfusão, compressão mecânica e extensão mecânica, através de êmbolos microperfurados, e a monitorização e controlo remoto das variáveis do processo de cultura celular.

DESCRIÇÃO

Bioreactor Multi-funcional para a Engenharia de Tecidos

Domínio técnico da invenção

A presente invenção encontra-se relacionada com a cultura de células em matrizes de suportes bidimensionais e/ou tridimensionais para aplicações em engenharia de tecidos num bioreactor multi-funcional. O bioreactor foi desenvolvido para permitir modelar a proliferação e diferenciação de vários tipos de tecidos, nomeadamente, tecido ósseo, cartilagem ou pele, com o objectivo de permitir a sua aplicação clínica e consequente implantação em organismos biológicos.

Antecedentes da Invenção

Actualmente, a cultura celular em matrizes de suporte bidimensionais e/ou tridimensionais é ainda considerada uma tarefa complexa, devido à necessidade de controlo de diversos parâmetros de origem biológica e mecânica envolvidos na formação de tecidos *in vitro*. Considerando os vários tipos de células, vários modelos de bioreactores para engenharia de tecidos têm sido propostos ao longo do tempo.
O método mais simples de efectuar a cultura celular é a cultura estática, na qual se destacam os Frascos T, Placas de 12 poços e as caixas de Petri [1], que representam os sistemas de cultura com maior facilidade de utilização, baixo custo e facilidade de esterilização. Contudo, a sua utilização apresenta algumas limitações, nomeadamente, o curto período de tempo de cultura celular, as quantidades celulares limitadas, a baixa reprodutibilidade, a não

Appendix 2 – Structural and Vascular Performance of Biodegradable Scaffolds within Bioreactors

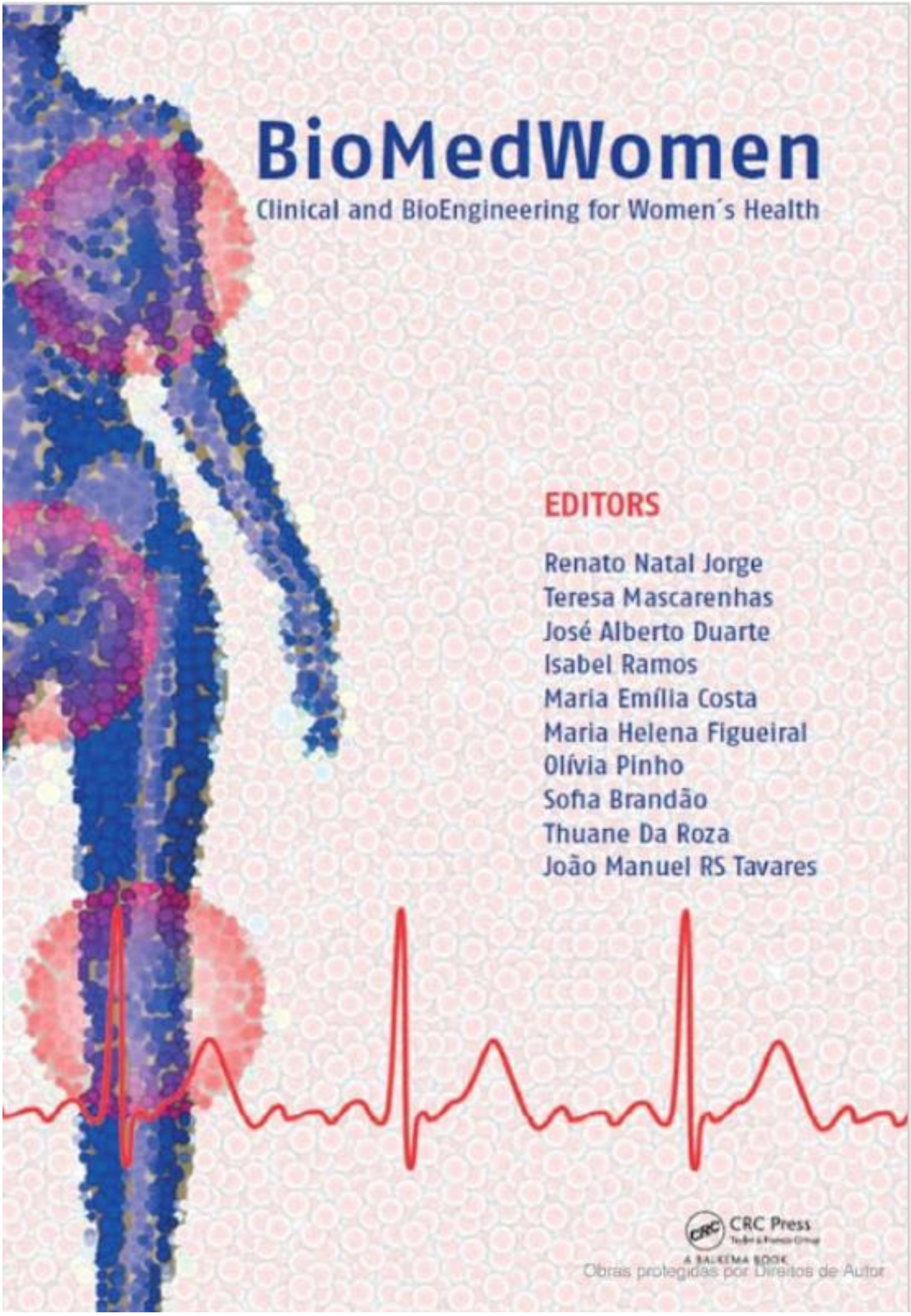

Structural and vascular performance of biodegrading scaffolds within bioreactors

S.R. Almeida

School of Technology and Management, Polytechnic Institute of Leiria, Portugal

D. Freitas

School of Technology and Management, Polytechnic Institute of Leiria, Portugal
School of Mechanical, Aerospace and Civil Engineering, Manchester Biomanufacturing Centre, Manchester Institute of Biotechnology, University of Manchester, UK

H.A. Almeida

School of Technology and Management, Polytechnic Institute of Leiria, Portugal

P.J. Bártolo

School of Mechanical, Aerospace and Civil Engineering, Manchester Biomanufacturing Centre, Manchester Institute of Biotechnology, University of Manchester, UK

ABSTRACT: The organization of tissue engineered cultured cells can be guided by growing them on a 3D substrate known as a scaffold. The cell-seeded scaffold may then be placed in a bioreactor enhancing the cell proliferation and differentiation before implantation. During this process, scaffolds tend to degrade due to enzymatic and/or hydrolytic phenomenon's while the tissue regeneration occurs. Another critical issue during the degradation process is the variation of the scaffold's mechanical properties. With the aid of combined numerical simulations, computational fluid dynamics and structural simulations, this research intends to predict the scaffold's mechanical performance while evaluating its vascular performance in order to optimise the working parameters of bioreactors of biodegrading polymer scaffolds for tissue engineering applications. These parameters are evaluated according to the pressures induced on the scaffolds and their influence on the shear stress caused on the cells which may be stimulated or destroyed on the scaffolds surface.

1 INTRODUCTION

APPENDIX 3 – PERFUSION BIOREACTOR FLUID FLOW OPTIMIZATION

Available online at www.sciencedirect.com

ScienceDirect

Procedia Technology 16 (2014) 1238 – 1247

ELSEVIER

Procedia Technology

CENTERIS 2014 - Conference on ENTERprise Information Systems / ProjMAN 2014 - International Conference on Project MANagement / HCIST 2014 - International Conference on Health and Social Care Information Systems and Technologies

Perfusion bioreactor fluid flow optimization

D. Freitas[a], H.A. Almeida[a,b], P.J. Bártolo[a,c,d]*

[a] *Centre for Rapid and Sustainable Product Development, Polytechnic Institute of Leiria*
[b] *School of Technology and Management, Polytechnic Institute of Leiria*
[c] *Manchester Institute of Biotechnology, University of Manchester, UK*
[d] *School of Mechanical, Aerospace and Civil Engineering, University of Manchester, UK*

Abstract

Tissue engineering aims to repair and regenerate damaged tissues by developing biological substitutes mimicking the natural extracellular matrix. It is evident that scaffolds, being a tri-dimensional matrix, are of extreme importance providing the necessary support for the new tissue. This new tissue is cultivated *in vivo* or *in vitro* in a bioreactor in which is placed the scaffold with cells. In order to control the cell culture process inside of a bioreactor it is essential to know the fluid flow inside and around the scaffold in order to know witch parameters must be controlled in order to obtain optimum conditions to cell culture. The wall shear stress must be adequate to the tissue to be cultivated, i.e., bone, muscle, cartilage and it is known that a proper stimulus is necessary to improve the cell proliferation inside the scaffold.
This study considers a novel multifunctional bioreactor with a perfusion system module and it is intended to optimize the fluid flow within the chamber and the scaffold by assessing the turbulence kinetic energy and the velocity.

Peer-review under responsibility of the Organizing Committee of CENTERIS 2014.

Keywords: Perfusion Bioreactor; Velocity; Turbulence Kinetic Energy; Computational Fluid Dynamics; Tissue Engineering.

* Corresponding author. Tel.: +44 (0) 161 306 4887; fax: +44 (0) 161 200 3723
E-mail address: paulojorge.dasilvabartolo@manchester.ac.uk

Appendix 4 – Optimization of a Perfusion Bioreactor for Tissue Engineering

Biodental Engineering III – Natal Jorge et al. (Eds)
© 2014 Taylor & Francis Group, London, ISBN 978-1-138-02671-1

Optimization of a perfusion bioreactor for tissue engineering

D. Freitas & H.A. Almeida
Centre for Rapid and Sustainable Product Development, Polytechnic Institute of Leiria, Portugal

P. Bártolo
Centre for Rapid and Sustainable Product Development, Polytechnic Institute of Leiria, Portugal
Manchester Institute of Biotechnology, University of Manchester, UK
School of Mechanical, Civil and Aerospace Engineering, University of Manchester, UK

ABSTRACT: Tissue engineering aims to produce artificial tissue in order to create or repair the damage tissue. It is evident that scaffolds are of extreme importance, because they will be the support of the new tissue. This new tissue is cultivated *in vitro* in a bioreactor in which is placed the scaffold. In order to control the cell culture process inside of a bioreactor it is essential to know the fluid flow inside and around the scaffold and the respective wall shear stress. These wall shear stress must be adequate to the tissue to be cultivated, i.e., bone, muscle, cartilage and it is known that a proper stimulus is necessary to improve the cell proliferation inside the scaffold.

This study consider a novel multifunctional bioreactor with a perfusion system module and it is intended to optimize the fluid flow within the scaffold and the respective wall shear stress on the scaffold.

1 INTRODUCTION

The emerging field of tissue engineering represents the combination of concepts and ideas from several disciplinary areas such as biology sciences, engineering, material science and the clinical procedures (Vacanti & Langer, 1999). Different applications are being developed and tested in clinical trials, all of them aiming to restore, maintain or create new tissues to implant on patients suffering of tissue loss or damage (Liu *et al.* 2013). Three main key factors involves the engineering o new tissues, regarding if it is bone, cartilage, blood vessels or liver (Ellis, M. *et al*, 2005).

I. First important factor is the cell source. Although there has been much interest in the use of autologous cells to create new tissue, there was a recently interest in the use of stem cells due to the undifferentiated state of these kind of cells.
II. Second factor is the design of appropriate scaffolds to mimic the behaviour of the extracellular matrix. In order to support cell colonization the scaffold must be biodegradable and biocompatible, possess good mechanical properties and a suitable surface for cell attachment, and must be highly porous to enhance cell proliferation as well allow the transport of nutrients and metabolic waste.
III. Finally, tissue engineering relies on appropriate cell and tissue cultivation methods as. Tissue can be produced *in vivo* or *in vitro*, where the last method relies on techniques and equipment's like a bioreactor (Bártolo *et al.* 2012).

A bioreactor is the general term applied to a closed culture environment that enables control of one or more environmental or operating variables that affect biological processes, in this case tissue culture (Fig. 1).

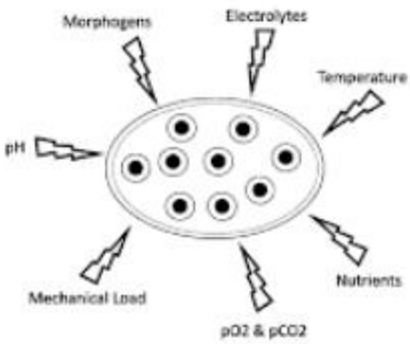

Figure 1. Influence of the multiple factors on functional tissue culture.

145

APPENDIX 5 – PERMEABILITY EVALUATION OF FLOW BEHAVIORS WITHIN PERFUSION BIOREACTORS

Permeability evaluation of flow behaviors within perfusion bioreactors

D. Freitas[1], H.A. Almeida[1], P.J. Bártolo[1,2]

[1] *Centre for Rapid and Sustainable Product Development, Polytechnic Institute of Leiria, Portugal. E-mail: dino.freitas@ipleiria.pt; henrique.almeida@ipleiria.pt*

[2] *Institute of Biotechnology, School of Mechanical, Civil and Aerospace Engineering, University of Manchester, UK. E-mail: paulojorge.dasilvabartolo@manchester.ac.uk*

Abstract. Tissue engineering aims to produce artificial tissue in order to create or repair damaged tissue. It is evident that scaffolds are of extreme importance, because they will be the support structure of the new tissue. This new tissue is cultivated in vitro in a bioreactor in which is placed the scaffold. In order to control the cell culture process inside of a bioreactor, it is essential to know the fluid flow inside the scaffold for an adequate exchange of nutrients and metabolic waste. A novel multifunctional bioreactor with a perfusion system module comprised of three different inlet and outlet membranes is being developed. This research work will evaluate the permeability of the scaffold under the three different inlet and outlet diffusion membranes of the culture chamber.

Key words: Bioreactor Design; Flow Behavior; Permeability; Scaffold; Numerical simulation.

1 Introduction

Scaffold-based strategies represent the most promising approach of Tissue Engineering. Scaffold is the initial tridimensional biomechanical support for cell colonization, migration, growth and differentiation [1]. Tridimensional scaffolds used in conjunction with living cells and biologically active molecules demonstrated promising results for tissue/organ repair and/or regeneration [2-4].

An ideal scaffold must satisfy some requirements, it should be biocompatible and biodegradable at a proper degradation rate matching the regeneration rate of the host tissue. It also should enable the diffusion of cell nutrients and oxygen and the establishment of a suitable mechanical and biological environment for the cells to secrete their own extracellular matrices in an organized way. Architecturally, the porosity, pore size and shape and pore interconnectivity are very important, playing an important role in promoting cellular migration, cellular bridging, vascularisation and new tissue ingrowth. Depending on the application, the optimal porosity and pore size diverge. Scaffolds must provide sufficient mechanical

APPENDIX 6 – COMPUTATIONAL ANALYSIS OF A PERFUSION BIOREACTOR FOR TISSUE ENGINEERING

Available online at www.sciencedirect.com

ScienceDirect

Procedia CIRP 00 (2015) 000–000

www.elsevier.com/locate/procedia

The Second CIRP Conference on Biomanufacturing

Computational analysis of a perfusion bioreactor for Tissue Engineering

Dino Freitas [a,b] , Joaquim Ciurana [b], Henrique A. Almeida[c] *, Paulo J. Bartolo [a,d]

[a] Manchester Biomanufacturing Centre, University of Manchester, UK
[b] Department of Mechanical Engineering and Civil Construction, University of Girona, Spain
[c] School of Technology and Management, Polytechnic Institute of Leiria, Portugal
[d] School of Mechanical, Aerospace and Civil Engineering, University of Manchester, UK

* Corresponding author. Tel.: +351 244 820 300; fax: +351 244 820 310. *E-mail address:* henrique.almeida@ipleiria.pt

Abstract

In order to repair and regenerate tissue, a new medical field that comprises several areas of engineering and expertise has emerged. This new field, namely tissue engineering, aims to repair and regenerate damaged tissues by developing biological substitutes mimicking the natural extracellular matrix. A tri-dimensional scaffold plays a major key-role in providing the necessary support for the new tissues. This new tissue is cultivated either *in vivo* or *in vitro* within a bioreactor after the scaffold being seeded with cells.
To control the cell culture process within a bioreactor, it is essential to know the fluid flow inside and around the scaffold in order to know which parameters must be controlled in order to obtain optimum conditions to promote cell culture. The wall shear stress must be adequate to the tissue being cultivated, *i.e.*, bone, muscle, cartilage and it is known that a proper stimulus is necessary to allow cell proliferation. In order to understand the ideal conditions and working parameters of the bioreactor upon the cells on the scaffold, a computational study to optimize a new perfusion bioreactor was performed.

Peer-review under responsibility of the scientific committee of The Second CIRP Conference on Biomanufacturing.

Keywords: Perfusion Bioreactor, Scaffold, Computational Fluid Dynamics, Tissue Engineering

1. Introduction

In spite of the continuous advance of modern medicine there is a huge necessity for the regeneration of damaged tissues [1]. Tissue engineering is the combination of biological sciences and engineering in order to fill that necessity to restore, improve or maintain the tissue function [2,3].

In Tissue Engineering (TE), cell culture plays a major role in the construction of tissue replacement [4]. Normally cells are harvested from embryonic tissue being these type of cells used in primary cultures because they have an enormous potential to differentiate and grow into different types of tissues [5,6]. In TE there are three major biological key factors to consider in order to create new tissues (Fig. 1) [7].

- First factor relates do designing an appropriate scaffold mimicking the behaviour of the extracellular matrix and holding the cells together. This structure most possess an adequate porosity enhancing cell proliferation, provide the transport of nutrients and metabolic waste, have optimum mechanical properties and be biodegradable and biocompatible [8].
- Second factor concerns the cell source. While the use of autologous cells was of great use to create new tissue, recently, there was an increasing interest in the use of stem cells due to their un-differentiation state.
- Third factor depend on the proper signals to perform tissue cultivation, *i.e.* mechanical and chemical signals that direct the cells to prompt the wanted tissue [9].

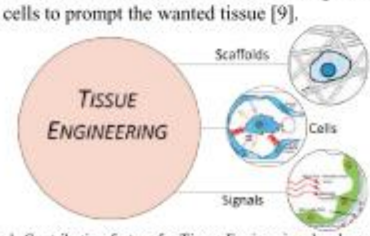

Fig. 1. Contributing factors for Tissue Engineering development [10]

2212-8271 © 2015 The Authors. Published by Elsevier B.V.
Peer-review under responsibility of the scientific committee of The Second CIRP Conference on Biomanufacturing.

APPENDIX 7 – COMPUTER MODELLING AND SIMULATION OF A BIOREACTOR FOR TISSUE ENGINEERING

International Journal of Computer Integrated Manufacturing, 2014
Vol. 27, No. 10, 946–959, http://dx.doi.org/10.1080/0951192X.2013.812244

Taylor & Francis
Taylor & Francis Group

Computer modelling and simulation of a bioreactor for tissue engineering

Rúben F. Pereira, Dino Freitas, Ana Tojeira, Henrique A. Almeida, Nuno Alves and Paulo J. Bártolo*

Centre for Rapid and Sustainable Product Development, Polytechnic Institute of Leiria, Leiria, Portugal

(*Received 4 October 2012; final version received 16 May 2013*)

A conventional approach to tissue engineering involves the implantation of porous, biodegradable and biocompatible scaffolds seeded with cells into the defect site. In some strategies, tissue engineering requires the *in vitro* culture of tissue-engineering constructs for implantation later. In this case, bioreactors are used to grow 3D tissues under controlled and monitored conditions. However, the quality of the resulting 3D tissue is highly dependent on the design and dimensions of the bioreactor, as well on the operating conditions. In this work, a computational fluid dynamic software package was used to investigate the influence of cylindrical bioreactor dimensions (length and diameter) on the fluid flow and scaffold shear stress. Computer simulations were performed using three different rotational movements (horizontal, vertical and biaxial rotation) and appropriate boundary conditions. Results show that the effect of the bioreactor length on the scaffold shear stress is more important than the diameter, while high length is associated to low scaffold shear stress. On the other hand, the fluid flows within the bioreactor and scaffold shear stresses are dependent on the rotational movement, being more uniform in the biaxial rotation due to the combination of rotational movements.

Keywords: tissue engineering; bioreactor; scaffold; computational fluid dynamics

1. Introduction

Despite recent advances in medicine and biology, the development of cost-effective approaches for the regeneration of damaged tissues remains a huge challenge. Currently, the most common treatments include the implantation of prosthesis, surgical reconstructions by transferring a healthy tissue to the damaged site in the same patient or organ transplantation from a donor (Bártolo et al. 2012; Bártolo, Domingos, Gloria et al. 2011). However, several drawbacks of these clinical treatments (e.g. shortage of donors, chronic rejection or transmission of diseases) motivated the development of novel approaches.

Tissue engineering is an interdisciplinary field involving the use of biological sciences and engineering towards the development of biological substitutes that restore, maintain or improve tissue function (Bártolo, Domingos, Patrício et al. 2011). In tissue engineering, the biological substitutes can be engineered using two main strategies, namely the bottom-up approach and the top-down approach (Bártolo, Domingos, Patrício et al. 2011; Nichol and Khademhosseini 2009).

The bottom-up or scaffold less approach is based on the principle of fusion and self-ability of cells to synthesise their own extracellular matrix (ECM), representing an emerging method for the creation of complex 3D biomimetic tissues (Melchels et al. 2012; Bártolo, Domingos, Patrício et al. 2011). This approach employs techniques such as self-assembled aggregation, microfabrication of cell-laden hydrogels or direct printing to produce modular tissues that can be assembled into larger tissues (Nichol and Khademhosseini 2009). The top-down or scaffold-based approach, the most commonly used, involves the use of porous, biocompatible and biodegradable scaffolds made of natural and/or synthetic materials that act as a temporary support for the seeded cells (autologous or allogeneic) to proliferate, differentiate and synthesise their own ECM (Melchels et al. 2012; Almeida and Bártolo 2010; Bártolo et al. 2009; Bártolo, Domingos, Patrício et al. 2011; Chen and Hu 2006). The success of this approach is strongly dependent on biomaterials, cells, signalling molecules and manufacturing processes. Some strategies involve the culture of constructs outside the body towards the creation of functional tissue-engineering constructs for implantation later. The *in vitro* culture can be performed under either static or dynamic conditions.

The static culture of 3D cellular scaffolds is performed in T-flasks, well plates or petri dishes, without the mixing or circulation of the culture medium (Gaspar, Gomide, and Monteiro 2012; Porter et al. 2005). This method limits the supply of oxygen and nutrients to the scaffold surface, which generally leads to cell death at the centre of the construct (Gaspar, Gomide, and Monteiro 2012; Yeatts and Fisher 2011; Porter et al. 2005; Martin, Wendt, and Heberer 2004; Cabrita et al. 2003). The major problems of static culture of 3D cellular scaffolds can be caused by the limited dimensions of the scaffolds, insufficient mass transfer, non-homogeneous cell distribution and the

*Corresponding author. Email: paulo.bartolo@ipleiria.pt